AN ABSTRACT OF THE THESIS OF

SHAHROKH GHAFFAIR NEYZARI for the degree of DOCTOR OF PHILOSOPHY in CHEMISTRY presented on November 9, 1984

Title: DESIGN AND APPLICATION OF A MICROCOMPUTER AUTOMATED MULTIELEMENT FLAME ATOMIC FLUORESCENCE INSTRUMENT

Redacted for Privacy

Abstract approved: J. D. Ingle, Jr.

An automated multielement flame atomic fluorescence (AF) spectrometer based on microcomputer control was constructed to determine four elements simultaneously. The instrument employs a multiple exit slit monochromator where the light from various exit slits is directed to a single detector with a mirrored funnel. Each element is excited to fluoresce with a single element hollow cathode lamp (HCL) and a time multiplex mode is used for pulsing the HCL's and data acquisition.

A SYM-1 microcomputer is the center of the system and controls the pulsing of HCL's, sample introduction into the flame, data acquisition, and other electronic components. Values for the experimental variables such as the HCL pulse rate, peak current, and pulse width are selected at the computer's terminal.

The HCL and background signals for each element are integrated for equal periods of time selected from 0.5 to 250 ms. The integrated background (lamp off) signal is subtracted from the HCL (lamp on) signal to correct for the non-lamp related portion of the

signal.

For most measurements, an air/H_2 flame sheathed with Ar was the atomizer. Numerous experimental variables were optimized including HCL current and fuel and oxidant flow rates.

For single element flame AF under optimum conditions, the following detection limits (in ng/mL) were obtained: Au, 2.2 x 10^2; Cd, 4.8; Co, 26; Cu, 3; Fe, 50; Mg, 0.8; Mn, 7; Ni, 36; Pb, 1.0 x 10^3; Zn, 21. For multielement flame AF under compromise conditions, the following detection limits (in ng/mL) were obtained: Cd, 10; Cu, 4; Mg, 1.5 x 10^2; Zn, 1.1 x 10^2.

With a sheathed air/C_2H_2 flame in the multielement mode, the following detection limits (in ng/mL) were obtained: Cd, 7.7 x 10^2; Cu, 1.3 x 10^2; Mg, 18; Zn, 4.3 x 10^3. The higher flame background emission noise degraded detection limits compared to the air/H_2 flame.

The system was studied briefly in a nondispersive multielement AF mode with a set of filters installed directly in front of the detector window. The following detection limits (in ng/mL) were obtained under multielement flame AF conditions with an air/H_2 flame: Cu, 33; Mg, 16; Mn, 76.

The relative standard deviation of measurements for single and multiple element determinations was typically 1% or better for concentrations well above the detection limit.

Design and Application of a Microcomputer Automated Multielement Flame Atomic Fluorescence Instrument

by

Shahrokh Ghaffari Neyzari

A THESIS

submitted to

Oregon State University

in partial fulfillment of
the requirement for the
degree of

Doctor of Philosophy

Completed November 9, 1984

Commencement June 1985

APPROVED:

Redacted for Privacy

Professor of Chemistry in charge of major

Redacted for Privacy

Chairman of Department of Chemistry

Redacted for Privacy

Dean of Graduate School

Date thesis is presented November 9, 1984

Typed by Marcy Brown for Shahrokh Graffari Neyzari

DEDICATED TO

my wife

Gisla (Ghaemi) Ghaffari

Whom I $(X)^{\infty}$ the most,

With special thanks to

Dr. James D. Ingle, my thesis advisor, whose encouragement and advice helped me throughout this work,

Dr. Edward H. Piepmeier, who was always ready to help me during the research, especially when my circuits were mixed up,

Dr. James H. Krueger, Dr. Joseph W. Nibler, and Dr. Max Deinzer, who served on my doctoral advisory committee, and their invaluable assistance and understanding,

and my parents, who provided moral and monetary security.

Finally, I wish to express my gratitude to the graduate students of the chemistry department-analytical division-for their encouragement during my graduate work.

TABLE OF CONTENTS

LIST OF FIGURES

LIST OF TABLES

DESIGN AND APPLICATION OF A MICROCOMPUTER AUTOMATED MULTIELEMENT FLAME ATOMIC FLUORESCENCE INSTRUMENT

INTRODUCTION

Instrumentation which allows simultaneous determination of several elements provides important advantages compared to instruments which allow determination of only one element at a time in a sequential manner. These advantages include reduction of the sample size required and increased speed of analysis. These benefits can increase the simplicity, reliability, and cost effectiveness for analyses requiring determination of several elements in clinical, metallurgical, biological, industrial, and environmental samples.

Automation is an important attribute of modern analytical instrumentation. The availability of microcomputers has spurred the development of automated instruments. Automation with microcomputers enhances the basic advantages of multielement instrumentation. The amount of data produced per unit time is greater with a multielement instrument. Automated rather than manual data acquisition and manipulation frees the operator from tedious tasks. This reduces post analysis time and increases the overall sample throughput. The use of microcomputers also makes it easier to implement automated sample introduction and to control and to optimize the experimental variables.

Many methods for multielement analysis have been developed based on x-ray, nuclear, chromatographic and electrochemical methods of ana-

lysis. Single element spectrometric techniques have been proved to be easily adapted to multielement techniques. Most multielement spectrometric techniques are based on atomic spectrometric methods involving the formation of an atomic vapor of the analyte in the sample and the excitation of this atomic vapor. These techniques can be divided into three major categories: (a) atomic emission (AE), (b) atomic absorption (AA), and (c) atomic fluorescence (AF). At this time, AE is the most popular method for multielement analysis and the least popular method is AA. In AF, the subject of this thesis, photons from an excitation light source are absorbed by the atomic vapor and excited atomic states are produced. The photons emitted from these excited states are measured at 90 degrees to the excitation beam.

The multielement system that has been developed in our laboratory by Salin (1) is capable of flame AA or flame AF measurements. The research in this thesis is concerned with the improvement of this instrument with many modifications including incorporation of a microcomputer.

The instrument built by Salin is a time multiplex multiple slit (TMMS) system which employs a multiple exit slit array in the focal plane that is manufactured from one piece and the position of each slit is selected to correspond to the resonance wavelength of one element. The light exiting from all slits is directed to a single detector with a mirrored light funnel. For each element being determined, a separate single element HCL is used to excite analyte fluorescence, and the different HCL's are sequentially pulsed (time multiplex arrangement).

For the work in this thesis, the instrument was modified only for use in the AF mode. Compared to the AA mode, the AF mode is simpler, requires fewer optical components and is easier to optically align. Moreover, manufacturing of the exit slit array is much simpler compared to the ones made for the AA system (1) because much larger slit widths are employed. Also, excess light problems are less severe than for the AA mode. Excess light is light from other HCL's that passes through the slit for the element of interest. In the AF mode, this arises only for wavelengths which are a resonance wavelength for another element and not for non-resonance lines from the HCL's if scattering is not significant. This problem of excess light can be eliminated or minimized by using a filter in front of a given slit to block unwanted wavelengths or an inteference calibration curve can be made for correction of measured analytical signal.

Lamp pulsing and data acquisition were controlled by a hard wired digital circuitry in the Salin instrument. A major step in the improvement of the Salin instrument was incorporation of a single board SYM-1 microcomputer to control the operations available on the Salin instrument and also to provide many new options. These options allow the user to control by input at a terminal various HCL parameters (pulse rate, pulse width, peak current), data acquisition parameters (delay times, number of data points per pulse, and number of pulses averaged), and sample (blank and analyte solution) introduction into the flame.

To utilize the microcomputer, various electronic circuits were modified including the circuitry for pulsing the HCL's. Several new

circuits such as an analog-to-digital converter (ADC), and a digital-to-analog convertere (DAC), power supplies, a two byte multiplexed up-down counter, and an automated start switch were built. Non-electronic hardware modifications include construction of an annular shaped HCL mount, expansion of the burner gas control system, addition of two telescopic tubes to shield room light and construction of two burner heads--capillary and Meker--for insertion into a Jarrell-Ash nebulizer. Additionally, provision was made for water cooling of the burners and gas sheathing of the flame, and a computer controlled automated sampler for introduction of sample into the flame was built.

Extensive software was also developed. The software coordinates the timing of the various operations such as lamp pulsing and data acquisition. Additionally, the software allows the user to communicate with the instrument and to change the magnitude of experimental variables. Data manipulation options include calculation of the mean and standard deviation of blank and analyte signals, and calculation of detection limits, shot noise, and signal to noise ratios (S/N). Data from standards are fitted to provide a calibration curve and automated reporting of the analyte concentration in unknowns.

The system was studied in the single element AF mode. All determinations in the single element mode were made with an air/H_2 flame sheathed by Ar gas and Meker type of burner head. For each element the instrument was optimized for maximum S/N. Variables optimized include wavelength, burner head position (x, y, and z axes), oxidant and fuel flow rates, Ar flow rate (sheathing gas), HCL peak current,

HCL position with respect to the flame, data acquisition parameters and HCL pulse rate and pulse width.

Calibration curves are linear over three orders of magnitude. Higher lamp current does not significantly degrade the linearity of the calibration curves at the higher concentrations in most cases.

Precision curves (plots of relative standard deviation (RSD) vs analyte concentration) show 1% or better precision for single element AF measurements at concentrations well above the detection limit. The detection limits obtained for ten elements, compared to those reported by Salin (1), are lower by factor of 3 to 7, except for Mg, for which the detection limit is lower by factor of 50.

For simultaneous multielement measurements, four elements, Cd, Cu, Mg, and Zn, were selected from the ten elements studied in single element mode. A sheathed air/H_2 flame with a Meker type of burner head were used for this part of the study. The same variables which were optimized for single element measurements were also considered in multielement optimization procedure. Optimum conditions for multielement measurements are not necessarily the optimum condition for any one of those elements; but in fact, the optimum conditions are a set of compromise optimum conditions. The detection limits obtained under compromise multielement conditions were within a factor of 2-5 of those obtained in a single element mode except for Mg. A RSD of 1% or better was obtained for all elements at higher concentrations.

These same elements were measured in the multielement mode with a sheathed air/C_2H_2 flame. The detection limits obtained were well above those obtained with a sheathed air/H_2 flame due to the increase

of flame background noise.

The multielement AF instrument was briefly studied in a time multiplex nondispersive mode. The modification from a dispersive to a nondispersive system involves replacing the monochromator with a set of interference filters in front of the single detector. This system is much simpler to work with and less expensive to manufacture. The detection limits compared to those obtained by dispersive system are higher because the interference filters used in nondispersive system have a larger bandpass which significantly increases the flame background emission and scattering signals and noises. THese decrease the range of linearity of calibration curves and compared to those obtained with the dispersive system. Measurement precision is as good as with the dispersive system for concentrations well above the detection limit.

HISTORICAL

In this section multielement atomic spectrometric techniques are discussed since the TMMS AF multielement instrument developed for this thesis research falls into this category of techniques. Atomic spectrometric techniques are based on atomization of the elements in a sample with a flame, plasma, or electrothermal atomizer. The emission, absorption, or fluorescence in the UV-visible region from the atomic vapor is then measured. Multielement atomic spectrometric instruments vary in design based on the optical phenomenon (emission, absorption, or fluorescence) that is measured and on the method that is used to distinguish and measure the optical signal from each element which is encoded at a particular wavelength.

The general characteristics of atomic multielement spectrometric measurements are first reviewed. Then recent developments in multielement atomic absorption, atomic emission, and atomic fluorescence instruments are discussed in turn. The Historical section concludes with a more detailed description of the TMMS AF instrument built by Salin since it represents the starting point for this research.

General Characteristics of Multielement Atomic Spectrometric Systems

The difference between multielement atomic spectroscopy and single element spectroscopy is not the atomization cell or light source, but the methods by which the optical information is selected and directed. The optical signal from each element at a different

wavelength must be distinguished. Winefordner et. al. (2) provide a superb discussion of the approaches used in multielement atomic spectroscopy which can first be classified by their optics as either dispersive or nondispersive. Dispersive techniques employing monochromators, polychromators, or spectrographs are most commonly used. In dispersive systems, the radiation from the source is focused on the entrance slit, collimated, and then directed to the dispersion device, a prism or a grating. The dispersed radiation is incident upon a focal plane where radiation over a small wavelength is selected and observed by an exit slit-detector combination or a small detector element. Nondispersive systems do not use monochromators but rather use filters or some form of spectral or time-based encoding to give element selectivity.

Dispersive systems can be temporal, spatial, or multiplex. Temporal devices use one single detector. Therefore the information collection is "sequential" or only one spectral element falls on the detector at any given time. Spatial systems employ multiple detectors or a multichannel detector. The spectral information from each spectral element falls on a separate detector or a different element of a multichannel detector simultaneously and independently (in a parallel fashion). The most common spatial detection system is a direct reader. They are used in arc and spark emission spectrographs as the replacement for photoplates and film. Direct readers are monochromators with many slits on the focal plane and a separate photomultiplier tube (PMT) behind each slit.

With multiplex systems one detector receives signals from

different spectral components of the spectrum. These signals are encoded in such a way that the signals corresponding to different spectral elements (e.g. wavelengths) can be distinguished. The signal from each spectral element can be encoded with respect to time (time multiplex) or different frequencies (frequency multiplex). Fourier transform spectroscopy (FTS) or dispersive Hadamard transform spectroscopy (HTS) (3) methods are frequency multiplex techniques. FTS is a nondispersive technique in which an interferometer is used to encode the wavelength information.

The PMT has become the primary photoelectric detector since its inception. A wide selection of tubes is now available to cover different zones of the spectrum (200 to 900 nm) with good amplification which makes it the detector of choice in most UV-visible optical spectrometers.

The image dissector photomultiplier tube (IDT) has been designed to overcome the limitations of the PMT as a detector device in multichannel systems (2, 4-8). An IDT is very much similar to PMT except it has a magnetic focusing circuitry that focuses photoelectrons from any point on the photocathode onto an aperture that directs the electrons to the dynodes. The IDT is placed in the focal plane of a spectrograph so that the spectrum is dispersed across the photocathode. Thus the signal from different areas of the photocathode and different wavelengths can be sequentially read.

Imaging devices, such as photodiode arrays and Vidicon target tubes are truly multichannel detectors. They consist of a series of discrete miniature photosensitive elements which each intercept at a

different small wavelength range when put in the focal plane of a spectrograph. The number of electrons-hole pairs generated by the photons impingent on detector elements is interrogated sequentially after a selected integration time. This is done with an electron beam in a SIT and with direct coupling and switches in a diode array (9). Both systems have been widely used in multielement atomic spectroscopy instruments (8, 10-17). These devices suffer from low S/N for low light levels because they have no internal gain and a relatively large electronic readout noise (2). The introduction of silicon intensified target (SIT) Vidicons has reduced the S/N problem by providing internal gain. The gain of the SIT is due to the acceleration of single photoelectrons before they strike the detector elements. Microchannel plate intensifiers have been placed in front of diode arrays to improve the S/N. Multichannel detectors are quite expensive when intensified and both Vidicons and diode arrays require a computer to process the great amount of information produced.

There are two types of excitation sources for multielement AAS and AFS, line sources and continuum sources. Hollow cathode lamps (HCL) and electrodeless discharge lamps (EDL) are the most commonly used line excitation sources. The xenon arc lamp is the primary continum excitation source used for AAS and AFS. It has high intensity over a wide wavelength range.

A high resolution echelle monochromator (18-21) is required for AA with a continuum source to isolate a wavelength band as small as an absorption profile. Also they are useful for plasma emission system to isolate analyte narrow emission lines from other lines that can

cause spectral interference.

The concept of the echelle grating was developed in the late 1940's by Harrison and coworkers (7). An echelle monochromator has a very high dispersion and resolution. An echelle grating is used to disperse the spectrum in the horizontal direction and another cross-dispersion element, which can be either a prism or another grating, is used to disperse the spectrum into a two-dimensional format. Cross dispersion is required because the echelle grating is used with high orders which results in a small free spectral range. The disadvantage of the echelle system is a nonuniform spectral format when a prism used as a cross-dispersion element.

Multielement atomic absorption techniques

A primary concern in a multielement atomic absorption spectroscopy (AAS) system is alignment of several single element lamps to allow the radiation from all sources to be focused and directed down the same optical axis through the atomizer (e.g. a flame). This is difficult for a large number of sources and thus limits the number of elements that can be determined simultaneously. This problem was somewhat circumvented by combining radiation from different angles into one beam (1, 22-23) or by use of multielement HCL's (7, 24, 26) or a single continuum excitation source (27-29). In spite of being the most suitable instrument for single element analyses, AA still remains the least favorable technique for multielement analysis.

To overcome this alignment problem, Mavrodneau (21) used a grating to combine the radiation from different light sources and

directed the combined beams through a flame into a direct reader.

Rawson (23) used fiber optics to combine the light from five different HCL's into a single quartz tube called an integrator and directed the combined beam into a flame. Unfortunately the tube was short and caused incomplete mixing of radiation from the lamps inside the tube. He also used rectangular fiber optics as exit slits to direct the desired resonance lines into the PMT's of his direct reader.

Butler et. al. (24) used a multielement HCL as their light source with a direct reader configured with four moveable slits. Flame atomization was employed.

The application of rapid scanning spectrometers (RSS) to AAS analysis was studied by Rose (26, 30) and Dawson (31). An instrument of this type can scan a selected wavelength window or region on a time scale ranging from a few microseconds to several seconds.

Rose et. al. (26) modified an oscillating mirror rapid scanning spectrometer as a detector for a rapid simultaneous multielement AA system with electrothermal atomization. They used a zinc, cadmium, lead and copper multielement HCL as an excitation source and a PMT as the detector device. No data were reported for zinc due to the presence of zinc in their deionized water and the problems associated with Zn determinations by furnace AA. The detection limits in ng/mL obtained with this system using a carbon furnance atomizer were Cd (0.3), Pb (7), and Cu (5).

Dawson et. al. (31) demonstrated the potential of a RSS which utilized an oscillating diffraction grating as the scanning mechanism.

Coupled to an automatic sampler, the instrument was applied to simultaneous multielement analyses of clinical samples. With an air/C_2H_2 flame, Na and K were determined by AE and Ca and Mg by AA. The detection limits in μg/mL were Na (0.06), K (0.4), Ca (0.08), and Mg (0.02). The analytical precision was approximately 3%.

Felkel and Pardue (7) studied the performance of an IDT coupled to an echelle grating spectrometer for simultaneous multielement AA measurements. The detector system and monchromator were computer controlled. The detection limits reported in μg/mL were Cr (0.024), Cu (0.022), Fe (0.160), Mn (0.019), Ni (0.13), Co (0.52). Data reported were obtained with a multielement HCL containing Cr, Cu, Fe, Mn, Ni, and Co with an air/C_2H_2 flame as the atomizer source.

Horlick (10, 14) used a diode array in his multielement flame AAS for detecting two elements at time. He used a small array (256 elements, 0.25 in.) which enabled him to view a larger spectral range for additional elements. The report does not present AA sensitivities or detection limits.

Salin (1) developed a time multiplex multiple slit (TMMS) instrument for multielement AA measurements. He used single element HCL's in a pulsed mode of operation. The radiation from the HCL's is directed through the flame along one optical axis by using the beam splitters. The detection limits in ng/mL obtained for flame AA measurements were Au (50), Cd (8), Co (300), Cu (5), Fe (60), Mg (20), Mn (5), Ni (50), Pb (50), and Zn (20), and using carbon rod atomizer were Cd (0.2), Mn (2), Pb (8).

O'Haver et. al. (18) used a continuum source AAS with echelle

monochromator. The monochromator was modified for wavelength modulation with a quartz refractor plate to correct for nonanalyte absorbance at all wavelengths. A 200 W Hg-Xe arc and a 150 W Eimac Xe arc lamp were used as the continuum sources. A PMT was used as the detector device with an air/C_2H_2 flame. Linearity of the standard curves and detection limits compare well with standard curves for background corrected AAS with a line source. Sensitivities were poorer by a factor of 2-5.

This same system was modified to demonstrate its capability for correcting all major types of spectral interferences and for simultaneous multielement AA measurements (19). The modified instrument was computer controlled. Detection limits in μg/mL were Mn (0.006), Zn (0.06), Fe (0.06), Cu (0.01), Ni (0.4), Cr (0.01), V (0.4), Co (0.08), Sn (33), Mg (0.0003), Ca (0.003), Na (0.003), K (0.2).

Codding et. al. (15) evaluated a self-scanned linear photodiode array as a multichannel detector for a flame AAS. Electronic readout noise was the dominant noise source under all experimental conditions. All measurements were made with an air/C_2H_2 flame atomizer. A beam splitter was used to combine the radiation from single element HCL's. Simultaneous multielement determinations were performed with Mn and Mg as analytes and with Cu and Ag as analytes. Reported detection limits in μg/mL for a 1 s integration time were Ag (0.081), Cu (0.097), Mg (0.006), and Mn (0.046), and for 5 s integration time, were Ag (0.023), Cu (0.022), Mg (0.001), and Mn (0.011).

The Perkin-Elmer Co. has developed an automated sequential AA/AE system (32). The Perkin-Elmer Model 5000 conjuction with it automated

sequential multielement sample-handling system has the ability to analyze many samples for many elements. This system is essentially a highly automated single element AAS and is computer controlled. The wavelength, flame conditions, and the HCL position and current are selected for a given element and the absorbance is measured. This sequence of selection of measurement condition and measurements is automatically performed for all elements selected. This system can use both flame or furnace atomizer.

Lundberg and Johansson (25) developed a non-flame AAS. The system utilized a set of fixed exit slits corresponding to the elements of interest. A disc with suitable sections removed, rotated behind the set of slits and sequentially blocked and unblocked the different slits at a high rate. This allowed only one slit to be open at a time. A multielement HCL was used as an excitation line source. The background nonanalyte absorption was corrected by a hydrogen continuum lamp. Twenty background and analyte line measurements were made for each element per second. The detection limits are reported in pg for 2 μL sample size as follows: Mn (2.0), Co (20), and Cu (8.0). Also they claimed their multislit spectrometer has somewhat better sensitivities compared to Varian Techtron AA6, but detection limits are higher by factor of 2-4.

Multielement atomic emission techniques

One can date the beginning of simultaneous multielement analysis by atomic emission spectroscopy (AES) back to the development of emission spectrometers with photoelectric detection in the 1940's.

Emission spectrometry is inherently the measurement mode most easily adaptable to multielement measurements since an external excitation source is not required. The atomizer is also the excitation source so that it is only necessary to distinquish and detect the emission at different wavelengths corresponding to different elements.

During the past decade, the inductively coupled plasma (ICP), direct coupled plasma (DCP), and microwave inductively coupled plasma (MIP) have replaced the flame or arc and sparks as the most popular emission excitation sources (8, 33-37). The high temperature plasmas provide efficient atomization and excitation of most elements at the expense of high background emission. Different techniques are available to reduce this background problem (38, 39).

Many of the commercial ICP systems in use today are direct reading polychromators (fixed wavelength) for simultaneous determination of 20-40 elements (33). These systems are not economically feasible when only a few elements are to be determined in each run. Computerized scanning monochromators for sequential reading are useful alternative to expensive and inflexible direct reading systems (33, 36). High resolution echelle monochromators are also employed in the ICP systems with a PMT for simultaneous analyses (34) or with multichannel detectors (18).

Berman and McLaren (34) assembled an ICP emission spectrometer for simultaneous multielement analysis. They used an echelle monochromator and made an extensive study of line/background ratios of atom and ion lines as a function of observation height, power, and aerosol Ar flow rate for several elements. No detection limits were

presented.

Fricke et. al. (35) compared several microwave cavities with Ar/He or He plasmas for the simultaneous determination of As, Ge, Sb, and Sn. The microwave induced plasma involves capacitatively coupling microwave energy into a flowing gas within a quartz tube (2). A polychromator configured as a direct reader was used with a 25 m entrance slit and 75 μm exit slits. They concluded that a Beenaker cavity using a pure He plasma is the easiest to tune and to operate and provides the most reproducible results. The detection limits reported in ng/mL were As (2.0), Sb (1.9), Ge (1.5), and Sn (2.0).

Rose et. al. (37) used their modified RSS for simultaneous microwave induced AES determination. The reported detection limits in μg/mL were Zn (0.07), Bi (0.7), Cd (0.02), Mn (0.04), Mg (0.02), and Cu (0.09).

Pardue and Felkel (8) interfaced an echelle spectrometer to a SIT and IDT for multielement determination with a DCP excitation source. Spectral resolutions obtained varied from 0.4 to 0.9 Å or the Vidicon system and 0.2 to 0.7 Å with the IDT system. They extensively studied interelement effects, sensitivity, and S/N's for both systems. The detection limits obtained with IDT in μg/mL were Li (0.27), Na (0.027), K (0.15), Mg (2.7), Ca (0.023), Sr (0.039), and Ba (0.076).

Caruso et. al. (35) compared a commercial ICP direct reader system (Jarrell-Ash Model 1160 Plasma Atomcomp) to a laboratory constructed ICP sequential detection system based on a computer controlled scanning monochromator system. The precision of the polychromator system is slightly better to that obtained with the

sequential slew scanning system. Detection limits reported in μg/g for the polychromator system were Cd (0.004), Cu (0.003), Fe (0.003), Mg (0.0008), Mn (0.002), Mo (0.004), P (0.02), and Zn (0.005) and for sequential system were Cd (0.002), Cu (0.002), Fe (0.003), Mg (0.0002), Mn (0.0009), Mo (0.06), P (0.2), and Zn (0.007).

Olsson et. al. (36) studied a computerized sequential reading monochromator system for AES with an ICP as excitation source. The computer controls the grating rotation in the 200 to 430 nm wavelength range. Data acquisition, sample changing calibration, and background correction all are controlled by computer. No detection limits are reported.

Winefordner et. al. (29) developed a computer controlled AF/AE spectrometer for simultaneous multielement analysis. The system consists of a slewed scan monochromator with a PMT as the detector. For the AF mode of operation, a xenon arc (EIMAC) lamp is used. A quartz refractor plate-torque motor assembly is mounted behind the entrance slit of the monochromator and modulates the wavelength. A synchronous photon counting system is employed for detection. This arrangement provides a net signal consisting of emission plus fluorescence, continuous background emission correction, and correction for scatter from the continuum source. The detection limits for 19 elements in the N_2 separated air/C_2H_2 flame and for 6 elements in the N_2 separated N_2O/C_2H_2 flame are reported for all three modes of operation: AF, AE, and AE/AF. The detection limits ranged from 3×10^{-4} mg/mL for Na (AE/AF mode) up to 12 mg/mL for Pb (AE mode).

Busch et. al. (16) developed a multielement emission spectro-

meter based on a SIT. To overcome the limited wavelength coverage associated with a one dimensional system, a multiple entrance slit was constructed from an aluminum plate with a horizontal row of 1.588 mm diameter holes spaced on 4 mm centers. This produced 29 holes across the 12 cm exit port opening. Then each hole was masked from behind the plate with two pieces of black tape to form an entrance slit 1.6 mm high. Polyvinylchloride fiber optic light guides were chosen to direct the light from the N_2O/C_2H_2 excitation source to the individual entrance slits. The diameter of the fiber optic light guides was selected so that each fiber optic strand could plugged into each one of the 29 possible holes. The input end of each fiber optic was fitted with a lens which was mounted on a vertical slotted plate to permit individual adjustment vertically from 3 to 40 mm above the burner head. Detection limits obtained in g/mL were Mn (0.46), Cr (0.56), Sr (0.041), Ba (0.50), Li (0.013), and K (0.84).

Korba and Yeung (40) used a scanning Fabry-Perot interferometer for multielement flame emission analysis. A PMT was used as the detector and a total consumption burner with a H_2/O_2 flame as the excitation source. Reported detection limits in ng/mL were Mn (65), K (24), Rb (60), Ca (19), Cr (220), In (12), Sr (160), Ba (550), Na (0.7), and Li (45).

Multielement atomic fluorescence techniques

Atomic fluorescence spectroscopy (AFS) has received considerable attention as the basis for multielement analysis systems. AFS offers several distinct analytical advantages over the other methods, espe-

cially AAS (41). Compared to AAS, AFS can provide lower detection limits for some elements and calibration curves linear over a much larger concentration range. Also alignment of the excitation sources is much simpler since the emission and excitation optical axes are independent. AF spectra have fewer lines than AE spectra which enable lower resolution monochromators to be employed (2).

Since the AF intensity depends linearily on the source intensity, the ideal experimental set up for AFS employs a high intensity excitation source. Also a high efficiency atomization system with low background is critical (42). Tunable dye lasers are excellent excitation sources for single element AFS analysis (43-45). High intensity laser radiation can result in near saturation of upper energy level involved in the fluorescence transition. Operating at saturation is advantageous because the fluorescence radiance does not depend on the source intensity or the quantum effeciency of the transition (46-48).

Unfortunately, the cost of using many lasers tuned to different excitation wavelengths in a multielement AF system is cost prohibitive. A single dye laser can be used in a sequential multielement system although the wavelength range of tuning and the ease of tuning are restrictive. Winefordner et. al. (49) recently used a frequency-doubled, flashlamp-pumped, tunable dye laser for determination of nickel and tin in a nitrogen-separated air/C_2H_2 flame. They used the non-resonance nickel fluorescence line near 340 nm and tin fluorescence line at 317.5 nm with a 0.1 m monochromator and a PMT modified for pulsed, high current operation. The lowest detection limits obtained for nickel was 0.5 ng/mL and for tin was 3 ng/mL.

HCL's and EDL's are the most commonly used line excitation sources used for AF. HCL's do not have high enough output intensity for AF unless they are operated in a pulsed mode. There have been several interesting studies on pulsed HCL's (50-57) and comparisons of pulsed to DC current operation (42, 57). The pulsed HCL technique was applied originally by Mitchell and Johansson (58) to AFS measurements. Also this xenon arc lamp is used as a continuum excitation source for AFS (5, 26-29, 59).

Recently Winefordner et. al. (60, 61) used an ICP as an excitation source for flame AFS. A low resolution monochromator coupled with PMT as the detection device was used. The solution used for excitation of analyte emission from the ICP contained 10 to 20 mg/mL of the analyte. Several analytical flames are employed in this study. The effect of interferent contamination in the excitation solution is discussed. They reported an analytical precision of 1-2% at high concentrations and discussed the capability of an ICP excitation source for multielement analysis.

West and co-workers published a series of papers (62-67) on a sequential AFS system utilizing a wavelength scanning monochromator with dual element EDL's as light sources. Four elements could be scanned in about 1.5 min. The detection limits obtained by air/C_2H_2 in g/mL were Co (0.02), Ni (0.02), Cd (0.002), and Zn (0.003).

A slewed-scan (programed scan) dispersive system that utilizes computer control can save considerable analysis time and provide greater versatility over a linear scan system. Here the monochromator scans very fast between the analytical wavelengths of interest.

Malmstadt and co-workers (55, 68-70) used the programmed rapid scan approach with pulsed HCL's as light sources. A pre-mixed air/C_2H_2 or an Ar/H_2 diffusion air or oxygen flame were used for atomization. The detection limits obtained with the H_2/O_2 flame (68) in ng/mL were Cu (0.001), Cd (0.05), Cr (0.5), Fe (0.05), Mg (0.001), Ni (0.07), and Zn (0.02). Later the AE mode was added to their instrument and they were able to determine up to 8 elements by AFS and up to 25 elements by AES (69, 70). They employed a quartz refractor plate for background correction. The gain of the PMT was automatically adjusted for each element under computer control. This instrument was used to analyze a variety of clinical samples.

Winefordner and his co-workers also used the previously explained slewed-scan monochromator approach with a xenon arc lamp as an excitation source multielement for AE/AF (29).

Brinkman et. al. (71) used a slew-scan AF spectrometer with a xenon arc lamp for both AE and AF measurements with no background correction. The instrument was used to analyze oil samples using a standard addition procedure. Reported detection limits in μg/mL for the air/C_2H_2 flame were Cd (0.3), Cr (0.4), Fe (0.7), Mg (0.02), Ni (0.8), Pb (1.0).

As previously mentioned, AFS does not require a high resolution monochromator. In fact, some multielement AFS systems do not use monochromators (non-dispersive).

Mitchell and Johansson (58, 72) used modulated HCL's and AC detection to electronically distinguish the analyte AF signal from the flame background emission signal. A rotating wheel containing four

interference filters was used for sequential wavelength selection. This four-element AFS instrument evolved into the Technicon's AFS 6 (9). Their instrument used four HCL's which were pulsed on-off in synchronization with placement of the appropriate interference filter in the emission optical path. The detection limits in μg/mL were Ca (0.003), Cd (0.03), Co (0.06), Cr (0.02), Fe (0.03), Mg (0.005), Ni (0.08), Pb (0.07) in an air/C_2H_2 flame.

A non-dispersive multielement AF spectrometer using pulsed HCL's and computer control system was developed by Palermo et. al. (73). They used a "solar blind" PMT with a photocathode which is sensitive only in the UV region. HCL's were pulsing sequentially. Therefore the fluorescence signals were also pulsed and each detected pulse was associated with a different HCL (element). The detected pulses were multiplexed in the time domain. Duration of the "on" pulses was 2-10 ms, depending on the atomizer (flame or electrothermal) used. The delay time before the next lamp was turned on was about three times the "on" time. Each cycle was repeated about 20 times in order to improve the S/N. The reported detection limits in μg/mL with sheathed air/H_2 were Cd (0.02), Hg (2.0), Pb (50), and Zn (0.2), and with a Pt-loop atomizer, were Cd (0.005), Hg (0.5), and Zn (2.0).

More recently Thamssen et. al. (74) described a multielement time multiplex AF system for direct analysis of air filters which is very similar to that just described, except no computer was used. A modified Perkin-Elmer graphite furnace was used to ash and volatilize the filter. The volatiles were directed into an air/C_2H_2 flame. They used 4 HCL's or EDL's as the light sources.

In 1981 Baird[a] introduced a HCL-ICP-AFS spectrometer, which is called the Plasma/AFS spectrometer (75-77). In this system an ICP is the atomization source and a separate wavelength selection and detector module is used for each element. Each module consists of one HCL, one PMT, an optical interference filter, and lenses. The modules are arranged around the plasma. Radiation from the HCL in a given module is directed into the plasma and the AF radiation generated in the plasma is passed through the optical interference filter to be detected by a PMT of the same element module. The instrument is a non-dispersive and operates in a rapid time division multiplex mode. HCL's are pulsed sequentially and at any given time, only one AF signal is being produced and detected. They claimed less spectral overlap interference was observed with HCL-ICP-AFS than with flame AAS, except for the nickel interference on antimony. The detection limits for 32 elements are reported, and compared with two other methods, flame AAS and ICP-AES. For most elements, detection limits are very comparable except for the refractory elements which are worse up to more than 2 orders of magnitude in some cases. They obtained a linear ranges of about 5 orders of magnitude for Ca and Ag.

Up to date, no one has used a photodiode array as a detector in multielement AFS. Chester et. al. (13) have evaluated the use of a SIT tube for multielement combined AE/AFS system. For multielement determinations, the monochromator has to be slewed 8 times to cover most of the analytical useful wavelength region (200-500 nm) in sec-

---

[a]Baird Corporation, 125 Middlesex Turnpike, Bedford, MA 01730

tions. Detection limits in μg/mL in air/C_2H_2 were Cd (1), Co (1), Cr (0.04), Fe (0.7), Mg (0.006), Ni (8), Pb (1), and Zn (>1000).

Time Multiplex Multiple Slit AF Spectrometer

The instrumentation to be described later in this thesis is a modification of a multielement flame AF Spectrometer constructed in this laboratory by Eric Salin (1). Therefore, this previous instrument will be described in some detail to provide a foundation for later discussion. This previous instrument was designed for both multielement AA and AF operation, although only the multielement AF mode of operation is described here.

The time multiplex multiple slit (TMMS) multielement flame AF spectrometer described by Salin (1) is based on the use of a multiple exit slit (MS) monochromator with a single detector and a time multiplex (TM) mode of pulsing for the HCL's and data acquisition. A "boxcar" type up-down integration technique previously described (69) is employed to process the signals.

The general operation of the instrument is illustrated by Figures 1 and 2. Much of the instrument is similar to a common single-element AF; however, the radiation from two or more lamps (one single element lamp for each element to be determined) is directed through the flame. The normal single slit in the focal plane of the monochromator is replaced by a multiple slit array such that the appropriate AF resonance radiation line from each element passes through the appropriate exit slit. The radiation passing through all the slits is directed to a single photomultiplier tube (PMT) with a mirrored light funnel. The

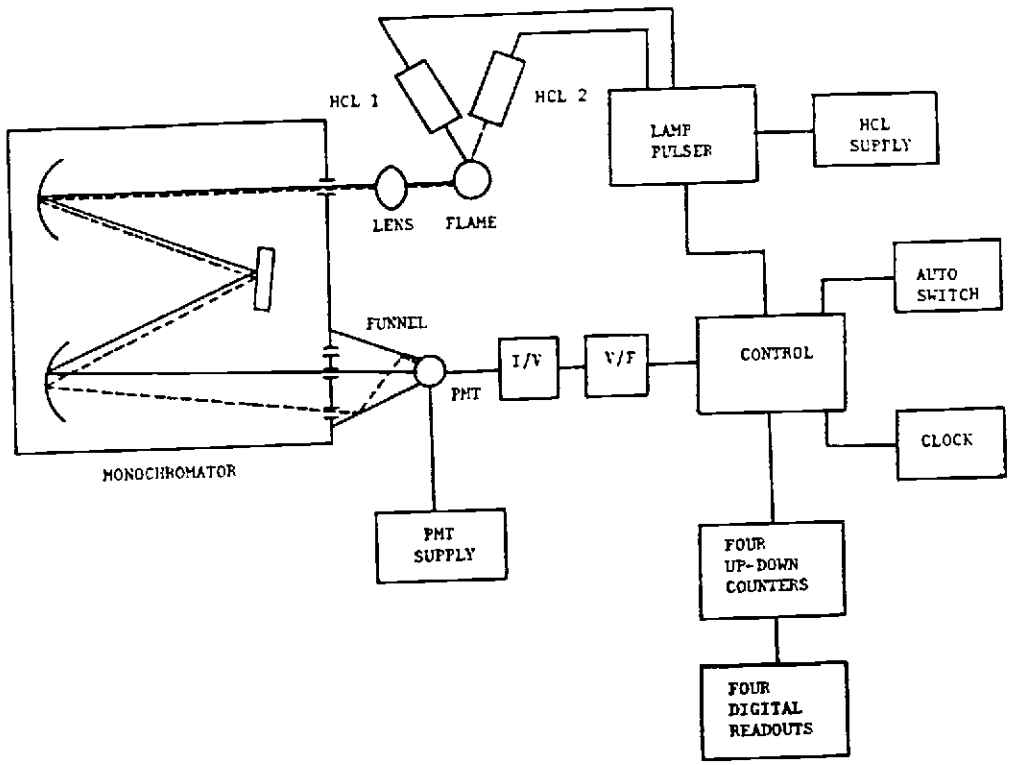

Figure 1. TMMS system schematic in the AF configuration.

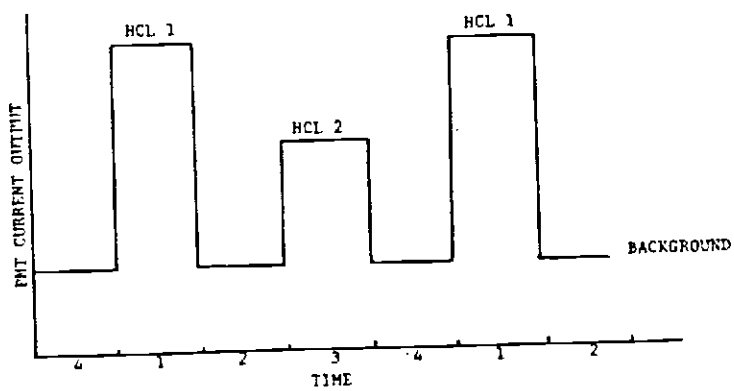

Figure 2. TMMS PMT output.

anodic current from the PMT is converted to a voltage with an operational amplifier (OA) current-to-voltage (I/V) converter and then to a frequency with a voltage-to-frequency (V/F) converter. Thus the spectral signals are processed as frequencies proportional to the PMT signal by further circuitry. The signals for each element are distinguished with a time multiplex approach. With a clock and central control circuit, each element's HCL is pulsed at the same frequency but only one is turned on at a time in a sequential manner. The duty cycle (% time that a given lamp is on) is considerably less than typical 50%.

The same clock and control circuit controls the data acquisition and directs the PMT related V/F signal to a separate data acquisition channel which consists of essentially an up-down counters for each element. When a given lamp is pulsed on, the PMT signal is integrated for a specified time. This integration is accomplished digitally by counting the number of pulses output from the V/F converter for a given length of time with the up-down counter in the count mode. This integrated "lamp on" signal is proportional to the AF signal and the scattering signal and any signal due to the PMT dark current of flame background emission. To correct for the non-lamp related portion of the signal, the PMT signal is integrated for the same time period after the lamp is turned off. This signal is subtracted from the first lamp on integrated signal. This is accomplished by subtracting the number of V/F pulses in the "lamp off" period from the counts accumulated during the "lamp on" period by using the up-down counter in the count down mode. This integration addition-subtraction or

up-down counting can be carried out separately for each lamp for any number of lamp pulses.

For simplicity in the following discussion, a two element (2 HCL) system will be considered although the system was designed to determine four elements simultaneously with the same principle.

At time 1 (see Figure 2), HCL 1 is pulsed on (solid line in Figure 1) for one clock period (typically 10 ms). The light from this HCL goes through the flame and excites atomic fluorescence. An image of the flame is focused on the entrance slit of the monochromator and the light is dispersed by the grating in the focal plane such that the resonance AF radiation passes through its exit slit. The resonance radiation and any flame background emission over the spectral band pass is then reflected down a mirrored funnel into a PMT. The current from the PMT anode is converted to a voltage and then a frequency. After a brief delay (typically 0.7 ms) to allow for the lamp rise time, the signal is integrated (counted up) for 9.3 ms. Time 2 then begins. HCL 1 is turned off and after the same brief delay, the background signal is integrated for 9.3 ms and the result is subtracted from the previously stored signal in counter 1 by counting down during time period 2. At time 3, HCL 2 is pulsed on for 10 ms and the same procedure is again initiated except that the resonance radiation (dotted line in Figure 1) is passed through another exit slit and the signal in time interval 4 is subtracted from the result in counter 2.

Another cycle then begins after each 40 ms (in this example). Each complete cyle is called a lap and normally 100 laps are run for

signal averaging.

The detection limits obtained by Salin (1) in the multielement AF mode are (in ng/mL) Cd (90), Cu (50), Mg (100), and Zn (200). The single element AF detection limits reported are (in ng/mL) Au (200), Cd (20), Co (30), Cu (7), Fe (300), Mg (40), Mn (50), Ni (100), Pb (7,000), and Zn (30).

EXPERIMENTAL

The TMMS AF instrument designed by Salin (1) and described in the Historical section, was modified in two stages. In the first stage, a number of modifications were made to the instrument to improve the performance and the operating characteristics of the non-computerized instrument. In the second stage, the instrument was computerized by addition of a microcomputer system. These two stages of instrumental development will be described in turn. This section ends with a description of solution preparation procedures.

Non-Computerized TMMS AF Spectrometer

A block diagram of the non-computerized instrument is shown in Figure 1. Most components are the same as described by Salin (1) and the modifications or additions are described below.

The V/F converter, four-5 decade up-down counter boards, HCL power supply, and 5 V supply for the control, clock, up-down counter boards, and digital readout, and PMT supply were identical to that used by Salin. The I/V converter board was similar except an Analog Devices AD540JH OA was used in place of AD380J OA, and the OA feedback resistors and feedback capacitors were mounted on a printed circuit (PC) instead of a Vector board. The new electronic, optical, and burner instrumentation constructed is described below.

HCL pulsing system

Salin used the circuit illustrated in Figure 3A to pulse the HCL's. This circuit was slightly modified in this research as

shown in Figure 3B. In both cases, there are actually four identical circuits for the four HCL's. The timing for lamp pulsing is controlled by the outputs from lamp demultiplexer and buffer circuitry on the control circuit board to be discussed later. This control board circuitry outputs a 10 ms logic 1 (+5 V) pulse every 20 ms in a sequential manner to the base of each of the four control transistors (T_2 Figure 3) corresponding to each of the HCL's. These transistors are in the common collector configuration and are used simply as an on/off switch capable of high current throughput. When the control transistor receives a logic 1 signal, it is turned on and provides a current to the base of the power transistor (T_1 Figure 3). This current turns on the power transistor and allows current to flow through the HCL. In Figure 3A, the current through HCL is limited and controlled by the load resistor R_L and will be denoted the resistor control configuration. This system of controlling current is inconvenient. First, to adjust the current, the power to the lamp pulsing circuit must be turned off to allow a different load resistor to be substituted. Second, the choice of lamp current is limited by the resistances of the high wattage resistors available. The HCL high voltage supply voltage can also be changed to alter the lamp current but this will affect the current to all lamps since only one supply is used. Third, the load resistance required for a given lamp current must be calculated beforehand.

To eliminate these problems, it was decided to control the lamp current through the HCL by controlling the base current into the power

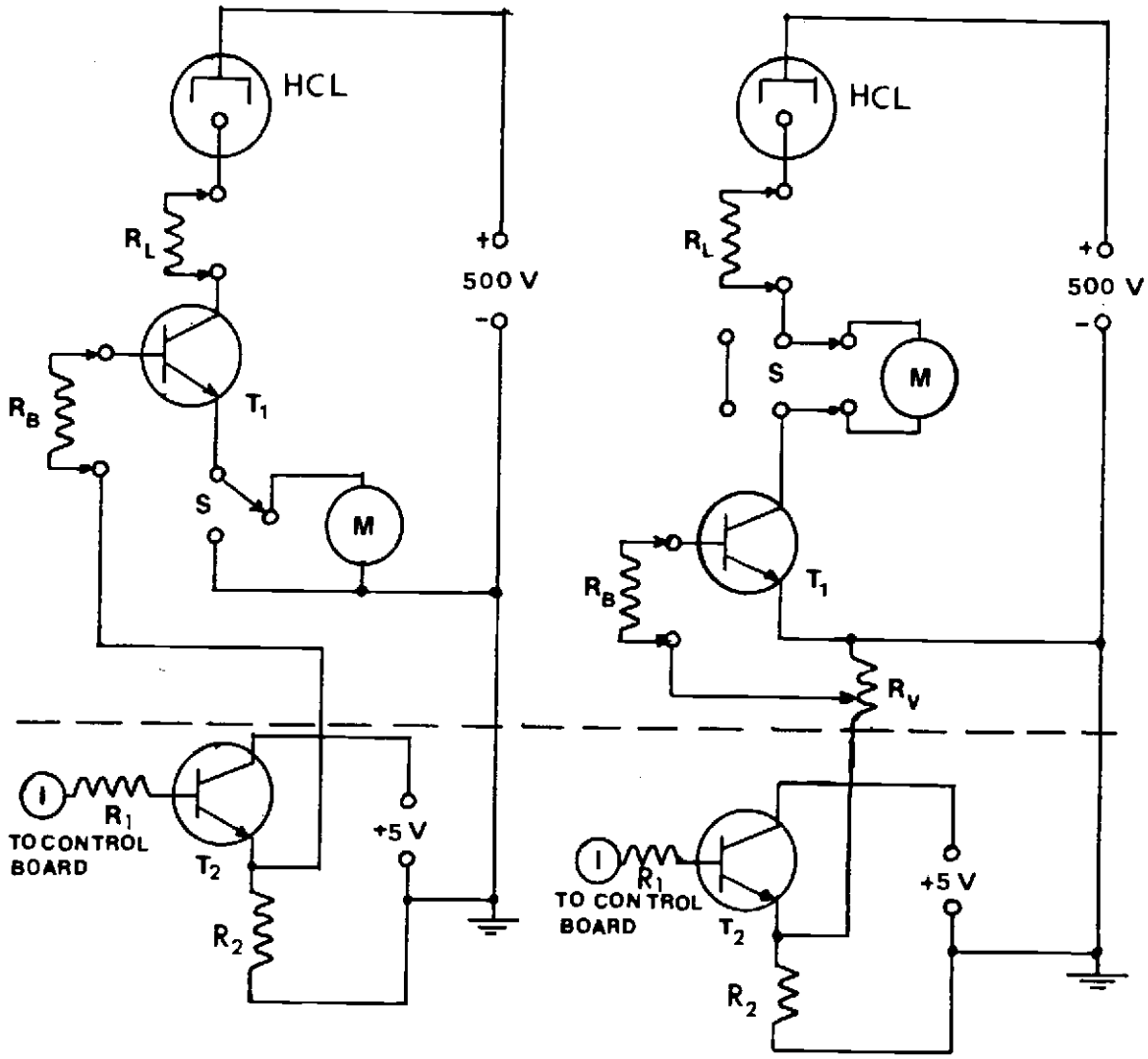

Figure 3. Non-computerized HCL pulsing circuitry. Components below the dotted line are mounted on PC board and above are mounted on the front panel of the electronic case. T1, SK3111, NPN power transistor; T2, 2N3416, NPN transistor; M, 20 mA DC, ammeter; R_L, 5W resistor; R_B, R_1, and R_2 are 100 Ω, 1.5 kΩ, and 18 kΩ, resistors, respectively; R_V is a 3 kΩ potentiometer; S, DPDT switch.

resistor (52). The base current and hence the lamp current is controlled by a variable resistor R_V, installed between R_B and T_1 as shown in Figure 3B. The knobs controlling the potentiometer R_V for each of the four lamps are installed on the front panel of the electronics case for easy access.

The resistor and current control modes of operation were compared. It was found that the noise and drift in the HCL signals were equivalent in both modes of operation.

As shown in Figure 3A, the ammeter (M) could be placed between the T_1 and ground of the original circuit to measure the average lamp current for one HCL at a time. However, even when the HCL current was zero, a residual signal of about 2.2 mA registered on M due to current passing from the base to the emitter of the power transistor. Therefore, the ammeter was relocated between R_L and T_1 as shown in Figure 3B. Four DPDT switches were installed on the front panel, which allow the operator to put the ammeter in any one of four HCL pulsing circuits. A rotary selector switch on the front panel is used in conjunction with the above switches to choose for which of the four HCL circuits the current meter is inserted. This prevents the accidental usage of ammeter by two HCL pulsing circuits.

Control board

The control board schematic shown in Figure 4 is identical to that described by Salin (1) except for a few modifications. The operation of the control board revolves around the use of demultiplexer IC's. One demultiplexer [15] controls the pulsing of

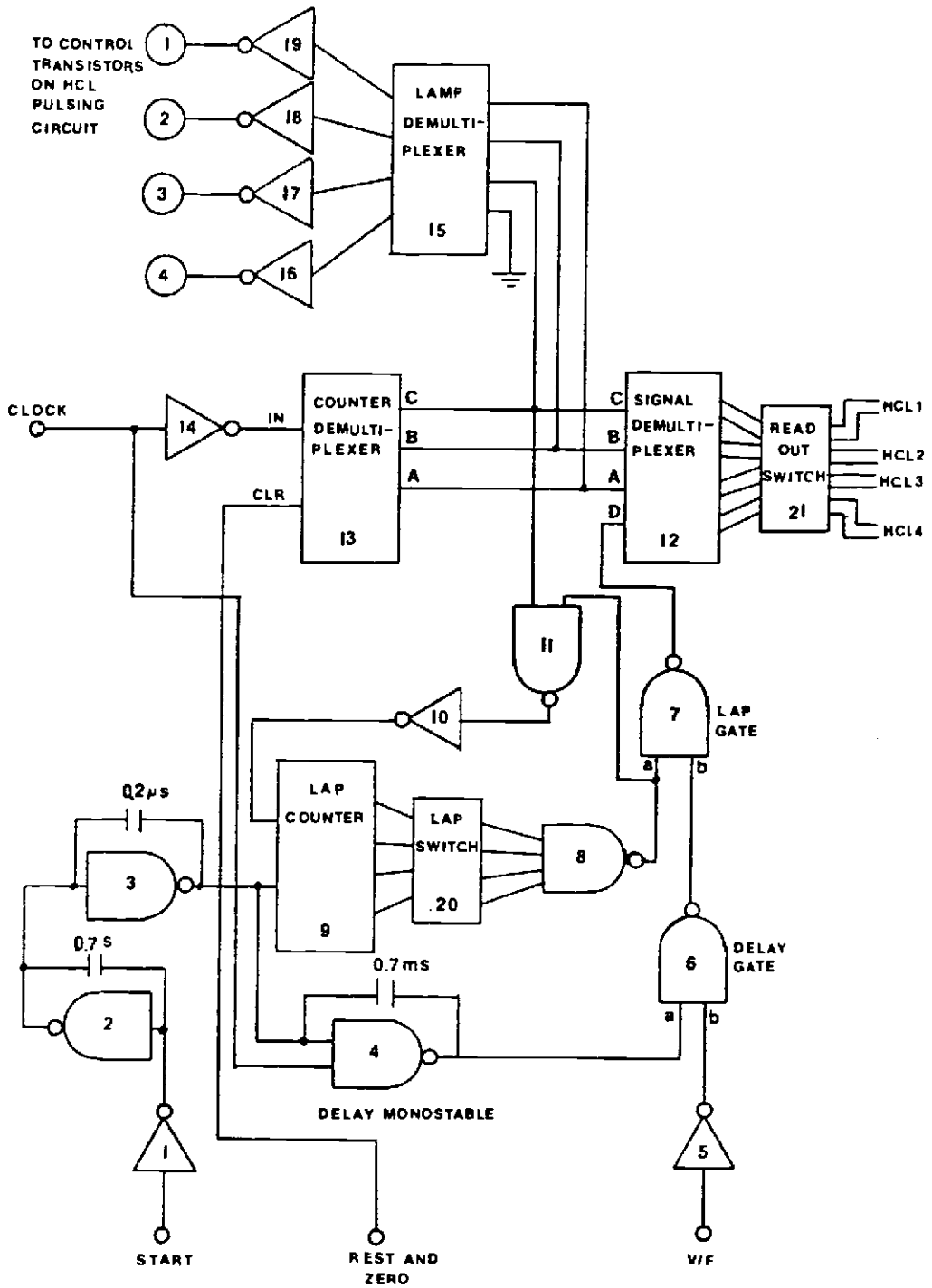

Figure 4. Simplified control electronics schematic.

the HCL's, and the other [12] controls the sequential channeling of the V/F pulse train to the appropriate up-down counter. The pulsing of the lamps and data acquisition are perfectly synchronized since they are triggered off the same clock signal.

The data acquisition is initiated with a logic 0 start pulse from the auto start circuit to be described later. This start pulse triggers monostables ([2], [3]) to produce a 0.2 μs pulse which clears the lap counter and the demultiplexer counter, sets the up-down counters outputs to zero and resets the clock. The demultiplexer counter [13] starts to trigger on the logic 0 to 1 transitions from the clock after the starting pulse. The BCD outputs of this counter (A, B, C) are decoded by the lamp demultiplexer to cause sequential pulsing of the HCL's and by the signal demultiplexer to cause the pulse train from the V/F converter directed sequentially to the appropriate up-down counter.

The lap counter [9] receives one pulse from the output of demultiplexer counter after every eight clock pulses (one lap). After a preselected number of laps, the output of gate 8 is driven to logic 0 which blocks any more data acquisition via gate 7 and stops the lap counter. At this time, the lamps continue to be pulsed, and the same data acquisition cycle is repeated by activating with another start pulse.

The control board used by Salin was a prototype wired on a SK-10 bread board, and this was replaced with a PC board. Additional switches were added to the control board to allow easy selection of different operating conditions. The readout switch [21] (two 8 SPST

switches) allows the V/F signal due to any one HCL to be sent to two (rather than one) up-down counters and their respective readouts. This is useful for testing the readout systems. The lap switch [20] (two 8 SPST switches) is used to select the number of laps (1 to 324) to be used in a measurement. The schematic for the control board as well as coding for the switches is given in Appendix I.

Digital readout

The original instrument used two 5-digit and two 4-digit decimal readouts to read to BCD outputs of the four 5-decade up-down counter boards. The 4-digit readouts were bulky Nixie tube readout modules installed in a Heath EU-801-15 analog digital designer. An added disadvantage of the 4-digit counters was that only the upper four digits of the up-down counters could be monitored thus resulting in loss of one digit of resolution. To make the instrument more compact and to provide full resolution for all four signal channels, two more 5-digit decimal readouts with appropriate decoding were constructed and the details are found in Appendix II.

Crystal clock board

The crystal clock board provides the system clock signal which is input to the control board which in turn controls the timing for HCL pulsing and data acquisition. Previously, a Heath Model EU-800-KC crystal clock board was employed which did not conveniently fit into a Vector PC card cage or allow convenient switching of the clock frequency. A crystal clock circuit was constructed on a PC board. The board is based on a standard design (78), using a 1 MHz crystal, and

provides switch selectable TTL clock frequencies from 10 Hz - 1 MHz in 1 decade steps. Details are given in Appendix III.

Automated start switch

In the previous instrument, each measurement cycle (given number of laps) was initiated with a manually controlled SPDT switch. To make repetitive measurements more convenient, an automated start switch circuit was constructed on a PC board to trigger the control circuit at preselected time intervals. The circuit provides a pulse train with a pulse width of 5 ms with a period adjustable between 2 s and 56 s. Normally the period is chosen to be about 12 s longer than the time to complete the chosen number of laps to provide enough time for reading the data off the digital displays. Details of the circuit and operation are found in Appendix IV.

Optical instrumentation

The optical configuration for AF was the same as used by Salin except for a few changes. The photofunnel and PMT were identical to before. The only modification to the monochromator was moving the wavelength selection dial to the opposite side for convenience. The entrance slit is 1.2 mm wide and 13 mm high and the slits on the exit slit array are manufactured to the same size to yield a 4.2 nm spectral bandpass. The construction of the slit array is simple. A quartz slide is placed on top of the AA slit mask slide (1) which defines the wavelength positions for ten elements. Pieces of silver tape (Leitz silver tape for binding slides) were placed on the slide using the same center to center distances used for AA. The 1.2 x 13

mm gaps between pieces of silver tape define the slits. Separate slits were made for Zn, Co, Fe, Au, Mn, and Cu. The Ni and Cd, and Mg and Pb lines pairs were so close that a single 1.2 mm slit width was used for each pair. The slit array slide is placed in a slide holder and held by electrical tape; the holder is secured to the focal plane in a predetermined position as described by Salin (1).

The Mg 285.2 nm line is used as a standard or reference line for alignment of the slit array holder because it is an intense and easy to find line which can be isolated with an interference filter. Also, this line appears in the middle of the slit array pattern.

Two telescopic tubes (3 to 6 in. extension) of 1 inch diameter were constructed (one from gray PVC plastic [D] and the other one from anodized aluminum [B]). The PVC tube is placed between the entrance lens and the entrance slit [E]. The aluminum tube is placed on the other side of the entrance lens and pointed down the optical axis toward the flame [A]. Both tubes are screwed to entrance lens holder [C] as shown in Figure 5. These tubes block room light from entering the monochromator.

Also, a new HCL mount was constructed ([F] in Figure 5). It has an annular shape and is made from one-fourth inch thick aluminum. The mount encompasses three-fourths of a circle and is 3/4 inch wide with a 10 inch internal diameter. Twenty-three evenly spaced one-fourth inch tapped holes are drilled around the ring mount. The ring mount is attached to the optical rail on which the burner and entrance lens are mounted with a rod and optical rail carrier mount. The HCL's are secured in "V" shaped aluminum HC holders [G] with four plastic screws

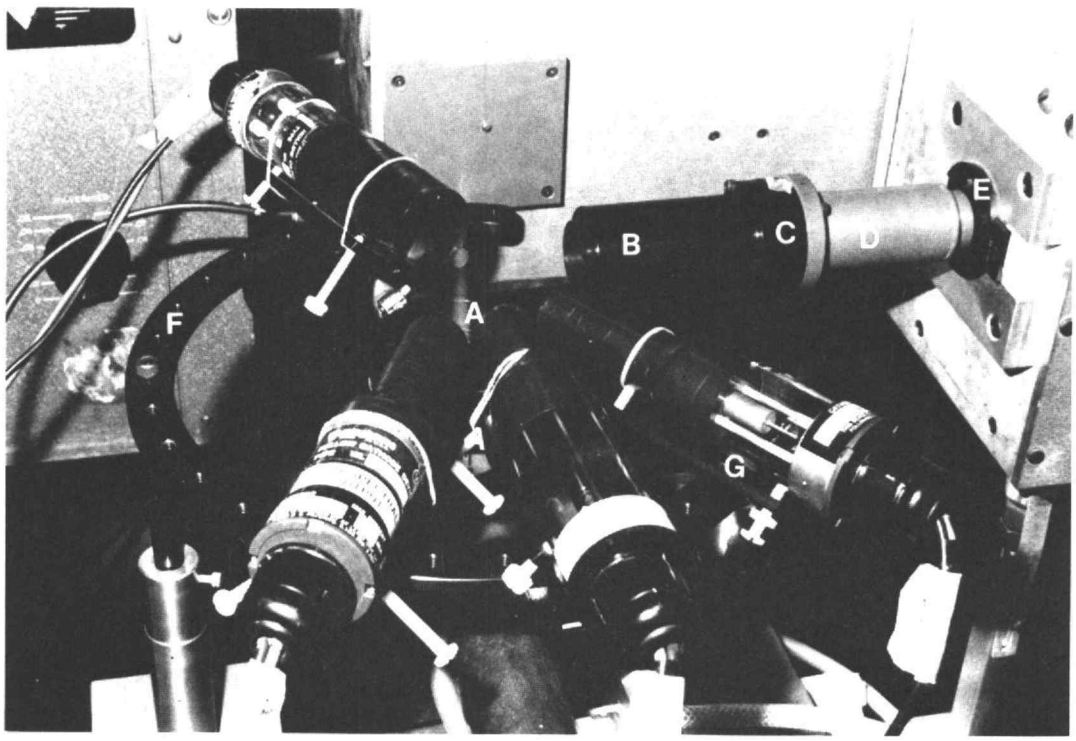

Figure 5. HCL mounting assembly and optical tubes. A, flame; B, aluminum tube; C, entrance lense holder; D, PVC plastic tube; E, entrance slit of monochromator; F, HCL mount; G, "V" shaped aluminum HCL holder.

which can also be used to adjust the HCL beam position. These HCL holders can be screwed into any of the twenty-three holes on the HCL mounting ring. All aluminum parts are anodized black to minimize light reflection. The HCL mounting ring and the HCL holders are shown in Figure 5.

Burner instrumentation

Two burner heads were constructed for insertion into a Jarrell-Ash (82-835) nebulizer-chamber assembly. One is a capillary (79) burner head which consists of a stainless steel cylindrical body (1 in. diameter and 1.5 in. length) with a 0.5 in. diameter hole drilled through the center. A bundle of 0.5 in. long and 0.027 in. ID diameter stainless steel hypodermic tubes were packed in 0.5 in. hole and the space between the tubes at the top was filled with high temperature resistant Savereisen 1800 cement. The capillary tubes extend approximately 1/5 inch above the level of the burner head to prevent overheating of the stainless steel head as shown in Figure 6A.

The second burner head is of a Meker design and is made from a cylindrical piece of stainless steel (1 in. diameter and 1.5 in. length). An 0.7 in. hole is drilled in one end of the cylinder to leave an 0.1 in. thick cap. A 16-hole pattern of 0.040 in. uniformly spaced holes is drilled into the cap in a circular area of 0.5 in. diameter as shown in Figure 6B.

The Meker burner head used by Salin (1) has a safety plug and was not designed to be used with water cooling and gas shielding accessories. Therefore, the new burner heads were made to fit into a

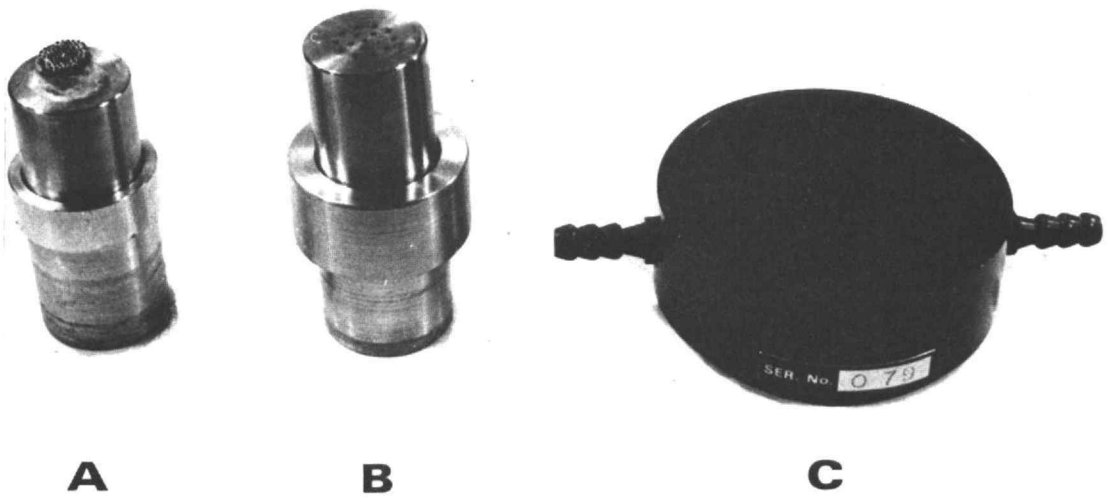

Figure 6. Burner heads and flame sheathing. A, capillary burner head; B, Meker burner head; C, Varian Techtron circular flame separator for inert gas sheathing and water cooling jacket.

Varian Techtron circular flame separator (SER. No. 076) (Figure 6C). It is an annular shaped metal device which slips over the burner head. The sheath gas is brought into a gas port on the side and exits through two circular concentric orifices on the top to form a gas sheath around the flame. Two more ports on the side are used for circulation of water through the separator to cool the burner head.

The Jarrell-Ash nebulizer-chamber assembly with the desired burner head was mounted on a micrometer bushing translation stage to provide precise positioning capability in the Y axis (perpendicular to optical axis). The nebulizer-chamber assembly already had X axis (along the optical rail) and Z axis (flame height) positioning capability. The HCL mount, telescopic tubes, and burner translation stage all are mounted on previously described optical rail (K) which is perpendicular to monochromator face (entrance slit) (Figure 7).

The burner gas control system was expanded over that used by Salin (1). All gas control components were mounted on a panel as shown in Figure 7. The three flowmeters (Roger Gilmont No. 3) and three 2-way (on-off) valves Whitney B-43XS4) are used to control the flow rates of the fuel (H_2 or C_2H_2), oxidant (air), and sheath gas (Ar). An additional 3-way ball valve (Whitey SS-43X54) is used to switch between H_2 and C_2H_2. Also, a flash arrestor (Matheson No. 6103) was installed between the burner and fuel flowmeter to prevent any flashback through the system.

Nondispersive AF instrumentation

The TMMS AF spectrometer was converted for some studies to a non-

Figure 7. TMMS flame AF configuration.

A. Electronic Cage (PC boards, digital displays, power supplies, ADC, DAC, V/F, I/V, and HCL current system)

B. SYM-1 microcomputer system

C. PMT power supply

D. HCL power supply

E. Monochromator

F. Entrance lens holder and telescopic tubes

G. Gas flow system control

H. Automated sampler

I. HCL's and burner assembly

K. Optical rail

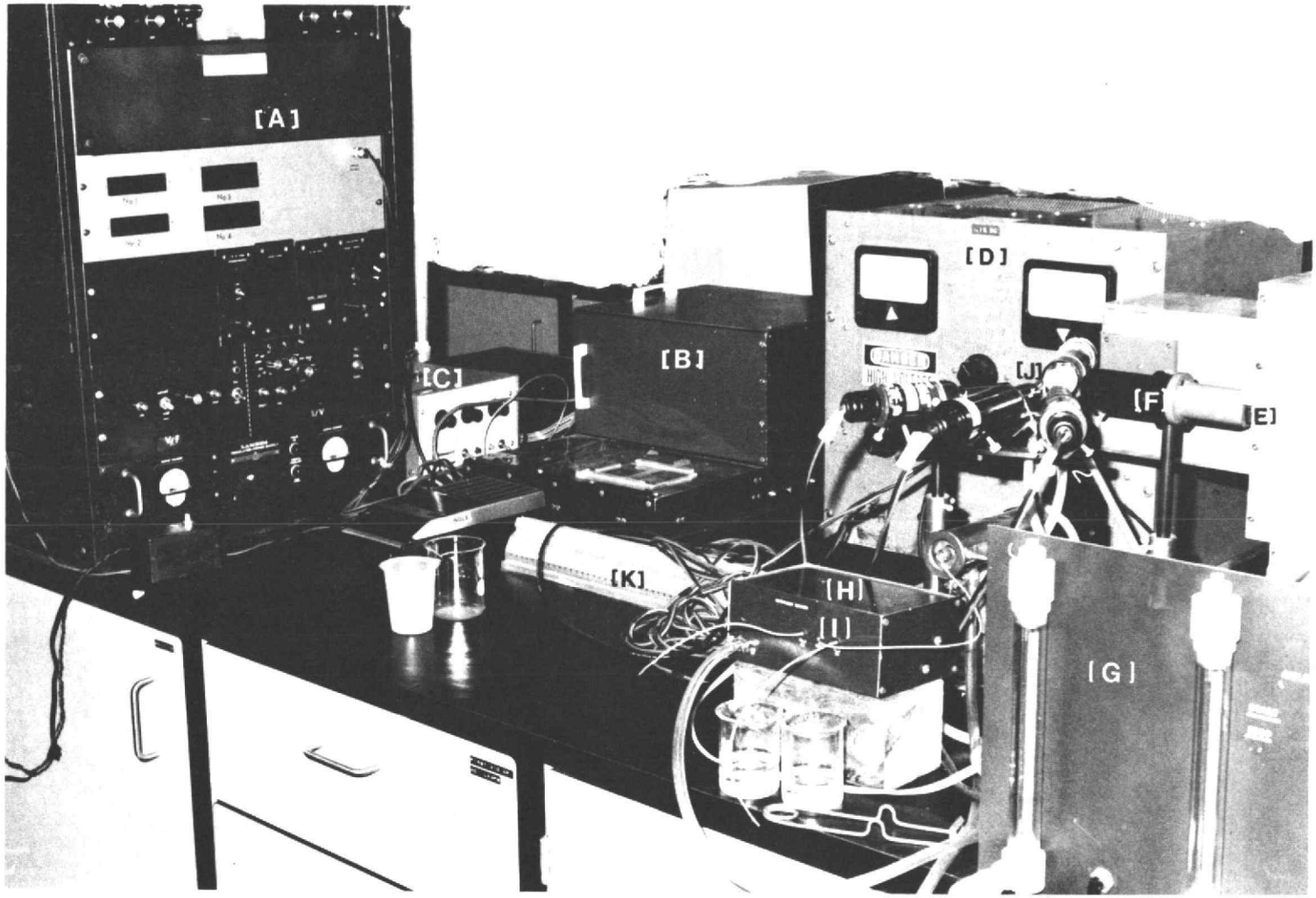

Figure 7.

dispersive configuration by using filters instead of a monochromator for wavelength selection. Thus, this instrument configuration is based on the use of a time multiplex (TM) mode of operation and multiple filter (MF) window with a single detector. All electronic and optical instrumentation is the same as for the dispersive TMMS AF instrument except the monochromator and photon funnel-PMT assembly are replaced by PMT-filter assembly and mount. As shown in Figure 8, the PMT-filter assembly consists of a commercial PMT housing [A] (Model 3150, Pacific Precision Instruments) containing a RCA-1P28A PMT to which two filters [B] are taped across the PMT housing window, and all the open holes between filters are covered with black electrical tape. Because only a small portion of the PMT housing window is exposed to the radiation coming from the flame, a small square of a 0.5 inch side length was cut from the middle of a black piece of cardboard (2 x 2.5 in.) and was placed in front of filters.

The filters used in this assembly are 1-inch diameter circular interference filters from the Corion Instrument Corporation with the specifications shown in Table I. A circular lens holder [C] is placed in front of the filters and the cardboard aperture and is taped to PMT housing in order to block room light such that the filters are exposed only to the light which passes through the lens (one inch diameter with a focal length of 3 in.). A black painted paper tube (1 in. diameter and 1.5 in. length) is placed and taped to the other side of the lens holder. The tube [D] is located around the optical axis between the entrance lens and the flame.

The PMT housing filter assembly is taped to a "V" shaped piece

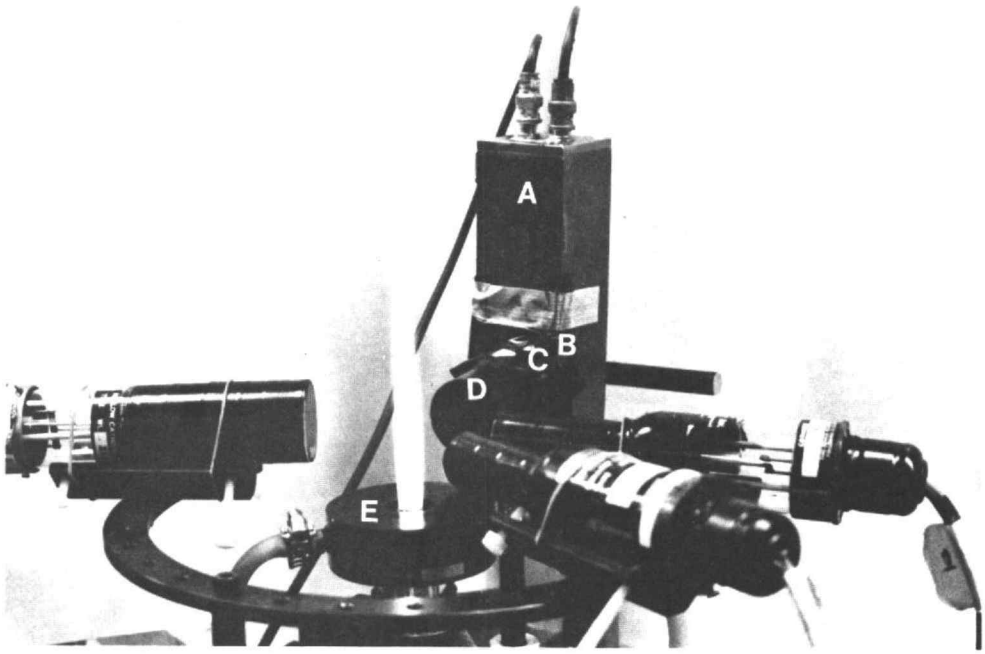

Figure 8. TMMF flame AF configuration. A, PMT housing; B, filters; C, entrance lense; D, paper tube; E, flame assembly.

of aluminum which is screwed to the rod of a base carrier. To fit the PMT housing filter assembly and its lens holder on the optical axis, the entrance lens holder and optical tubes from TMMS AF set up must be removed to create enough room for TMMF AF set up. The burner assembly, HCL mount, PMT housing-filter assembly and entrance lens holder are all mounted on the same optical rail as shown in Figure 8.

Table I. Specifications for Filters Used in TMMF PMT Filter-Assembly

Filter No.	Half Width (nm)	Wavelength of Max. Transmittance (nm)	Maximum % T	Elements(s) Used For
772178	12	285.2	13	Mg, Mn
3228-9602177-c	10	322.5	21	Cu

Computerized TMMS AF Spectrometer

The second stage of modification centered around the use of a microcomputer for control and data acquisition to allow the operator the versatility of software modification of the AF experiments and to permit instant "on line" data processing.

Introduction

In the computerized system (Figure 9) a microcomputer (SYM-1) is the heart of the system and controls various operations. The optical system and arrangement in this system is the same as the conventional TMMS AF system (Figure 1).

The computerized AF instrument was contructed to provide three different modes of operation which are switch selectable. In all three modes of operation, the AF signals, encoded as photoanodic currents, are converted to a voltage by the I/V converter. Mode 1 is the manual mode described in the previous section with the control board and four digital displays. In mode 2 the voltage is converted to a frequency by the V/F converter and the frequency is counted by a 2-byte up-down counter. For mode 3, the analog voltage is converted to a digital number with an ADC. In both modes 2 and 3, the data acquisition (control of counter or ADC) is controlled by the microcomputer and data are stored in memory for later manipulation. User communication to the microcomputer and display of data, calculations, and the messages is accomplished with a teletype (TTY). The microcomputer also controls the lamp pulsing system and sample introduction into the flame. In the following sections the computer system and interfacing

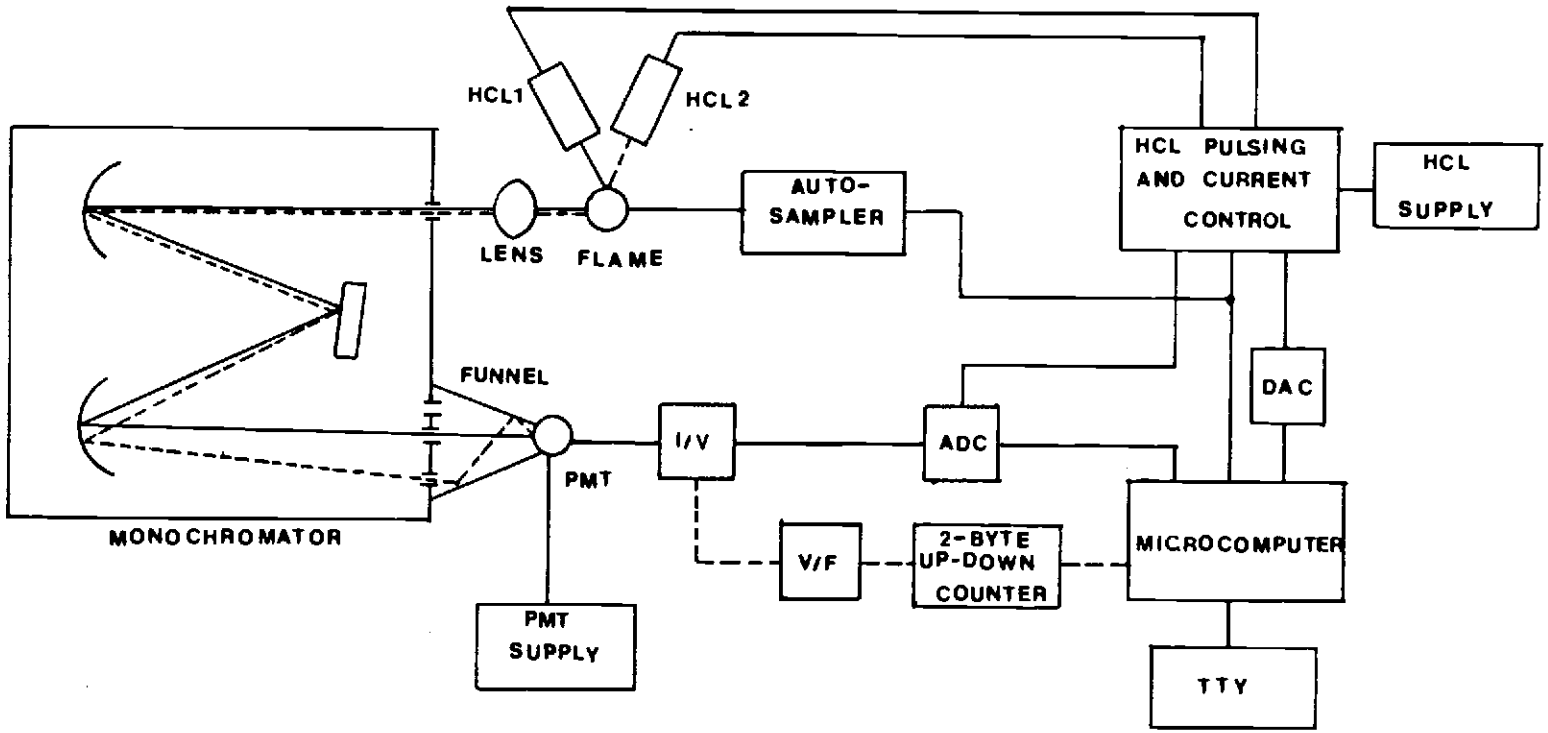

Figure 9. TMMS microcomputer control system schematic. Mode 2 involves using the V/F and 2-byte up-down counter for digitization of the signal. Mode 3 involves using the ADC instead of the V/F and counter.

hardware are described in detail. This is followed by an overview of the software.

The SYM-1 single board microcomputer

The single board SYM-1 microcomputer (μC) used in this research is based on the 6502 microprocessor (μP), and it is produced by Synertek System Corporation. The 6502 has a set of 56 instructions with 13 addressing modes. The features and operation of this computer are documented in detail in several manuals (80).

The SYM-1 is an 8-bit μC which is equipped with 1) 4K of on-board static RAM, 2) a system monitor (supermon) which is stored in 4K of ROM, 3) three exteral sockets to install additional ROM or EPROM chips, 4) a cassette tape interface with monitor control for program and/or data storage, 5) a 20 mA 110 baud rate current loop teletype (TTY) interface, 6) an RS-232 serial interface (baud rates of 110, 300, 600, 1200, 2400, and 4800), 7) 30 I/O lines provided by three 6522 and one 6532 chips that are bidirectional and individually programmable. An extra 6522 was inserted into an on- board socket to provide 16 more I/O lines. The 6522 versatile interface adapter (VIA) chips each provide 16 I/O lines plus 2 timers. A few changes were made on the SYM board (Appendix V) to provide a total of 50 I/O lines, 8) a HEX keyboard and HEX LED display are included on the SYM-1 board which is often sufficient for interaction with the μC.

The buss structure of the SYM-1 consists of 1) a unidirectional 16-bit address buss (e.g. 64K of addressable memory), 2) an 8-bit bidirectional data buss, 3) a control buss which includes two

interrupt input lines (Interrupt Request ($\overline{IRQ}$) and a Non-Maskable Interrupt ($\overline{NMI}$), a 1.0 MHz system clock line, a ready/write (R/W) line, a reset ($\overline{RES}$) line, and a ready (RDY) line.

The address, data, and control buss lines as well as I/O and TTY, RS-232, and cassette interface lines are brought out to edge connectors which include the application connector (AC), the expansion connector (EC), the auxiliary application connector (AAC), the power connector (PC), the terminal connector (TC), and the key board connector (KC). All these connectors provide +5 V and ground (GND), and the AC provides some of I/O lines, audio, TTY, and keyboard lines. All the 6532 chip's functions such as RDY, $\overline{IRQ}$, $\overline{NMI}$, R/W, data, address, clocks, and some I/O lines are available at EC. The AAC provides mostly I/O lines from 6522 chips. The PC's lines are all +5 V and GND. The TC provides RS-232, TTY, audio, and audio remote lines and the KC provides two RS-232 lines.

A number of jumpers on the SYM were changed or added to increase I/O lines availability, to add basic ROM chips, to provide automatic log-on (80), and to provide better tape reliability (81) (see Appendix V).

Two-4KX8-ROMs containing a 8K BASIC by Synertek and designed to run with the Supermon monitor, were installed in sockets U21 (ROM #02-0019-01), and U22 (ROM #02-0020-01).

The SYM microcomputer system

The SYM was connected to a motherboard which provides additional memory and allows a 16K RAM board and 16K EPROM board to be connected

to the SYM buss. The SYM and motherboard were housed in a metal and plexiglas box with a fan. The motherboard, RAM board, and EPROM board are described in more detail later.

Various connectors, switches, and cables were attached to the box to allow selection of option and connection to external devices as shown in Figure 10A. Connections were provided in the form of 4-sets of DB25 Amphenol female connectors for I/O port lines. Each connector is attached to the appropriate pins of a 6522 (three) or 6532 (one) on the SYM such that each connector provides two eight-bit I/O ports, 2 chip selection lines, and ground. The upper port is called PB and lower port is called PA (Figure 10B). The I/O port connections are indicated in Appendix VI. Two ports are required for ADC, two for the DAC, one port for the up-down counter, and 2 ports for the auto sampler and HCL pulsing circuit.

The in, out audio tape lines from the SYM TC connector were each brought out on a separate cable fitted with an Amphenol jack phone connectors to plug into a portable tape recorder (Panasonic, Model RQ-2133). The remote control circuitry on the SYM-1 allows the cassette recorder to be used under software control (Supermon audio cassette interface program (80)). This allows the computer to start the tape recorder when a program is to be loaded or saved and to stop the recorder when the process is completed. Details of remote control connection and usage is found in SYM-1 manual (80).

The TTY lines from the SYM TC connector pins 9, 10, 11, and 12 were brought out on a cable fitted with a 7 pin Amphenol connector.

As Figure 10A indicates, a BNC male connector is brought out and

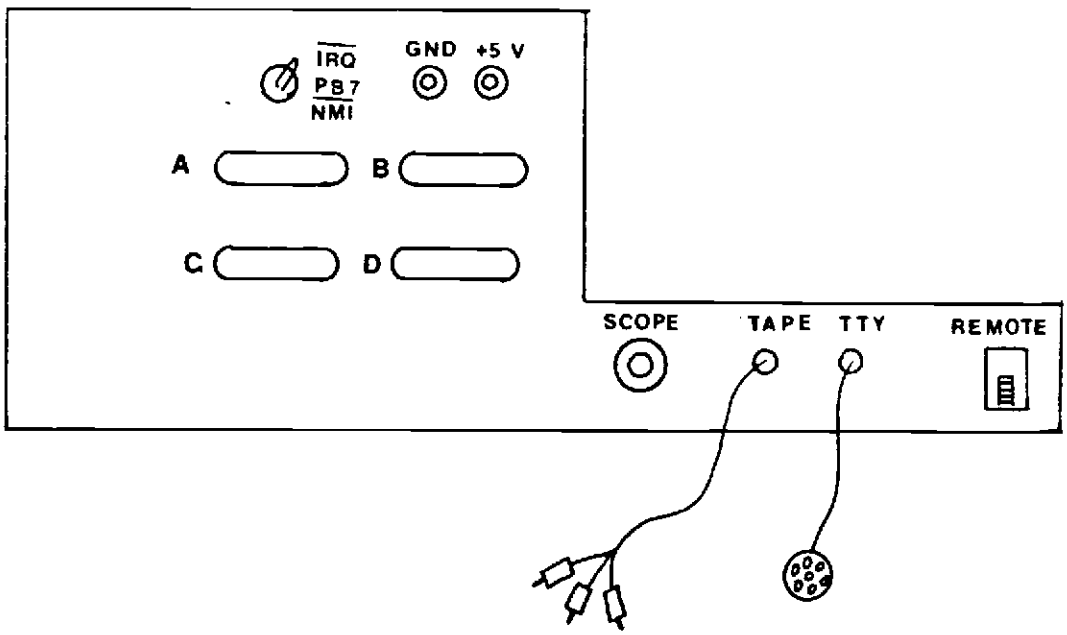

Figure 10A. Physical configuration of left side of computer box. Connector A is from AAC (A800 and A801), Connector B is from AC (A000 and A001), Connector C is from AAC (AC00 and AC01), Connector D is from AC (A400, A4001), and SCOPE, TAPE, TTY, and REMOTE are from TC.

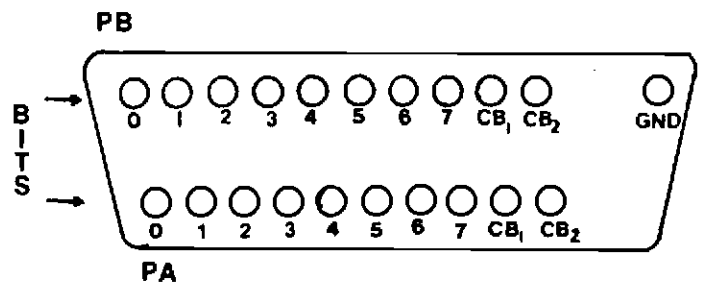

Figure 10B. A typical I/O connector.

connected to the scope line on the SYM TC connector. It allows an oscilloscope to be used as a one line monitor.

The +5 V and GND connections in the form of female banana jack plugs provide power for a logic test probe and other low current testing tools.

Whenever an interrupt is to be used, $\overline{IRQ}$ or $\overline{NMI}$ has to be connected externally to PA7 I/O line of the 6532 at A400. A SPDT on-off-on switch is installed to connect PA7 to $\overline{NMI}$ or $\overline{IRQ}$ line from the SYM EC connector when required. When the switch is in the off position, PA7 acts as a I/O line.

The Little Buffered Mother board (LBM) (Seawell Marketing, Inc.) mates directly to the SYM-1's AC, EC, and PC connectors. The LBM provides 1) sockets for 4K of additional RAM which were filled, 2) four 44-pin female edge connectors which allow the boards to be plugged into the SYM buss, 3) three voltage regulators that convert unregulated +8, +16, and -16 V to +5, +12, and -12 V, respectively, 4) 3 LED's indicating power on or off and the status of the $\overline{IRQ}$, and $\overline{NMI}$ lines. There are 10 switches on the LBM board used to properly configure the memory space. The switch positions used are indicated in Appendix V. Two wires are brought through the back of the computer box and connected to the power connector (PC) on the LBM. The other ends of the wires are terminated with male banana plugs and connected to the ground and +8 V terminals of an unregulated power supply.

To expand the memory of the system a SEAWELL SEA-16 (Seawell Marketing, Inc.) memory expansion board was inserted in one slot of the LBM board. The SEA-16 board is a 16K x 8 static N-MOS RAM board.

It has two equivalent 8K x 8 sections of memory, and each section is addressable separately to any desired 8K block through switches as detailed in Appendix V. This RAM was located from 2000 to 4000 as shown in the memory map (Figure 11).

An EPROM PC board was constructed. This board has space for eight 2K 2516 EPROM chips and thus 16K total of EPROM can be used, and the address lines are buffered. Each of two 8K EPROM blocks can be addressed separately to any 8K block in the memory map with switches located on top right corner of the EPROM board. The switch positions are described in Appendix V.

To expand the exsisting 8K BASIC interpreter a BROWN'S BASIC ENHANCEMENT software package was purchased from SYM-1 Users' Group. This package provides a powerful set of tools to assist in construction and development of BASIC programs. The use of this package is described in detail in its manual (82). It provides 1) a super terminal control patch that includes a versatile collection of control code editing and absolute and relative cursor addressing commands, 2) Save/Load extensions which allow all the tape files, whether program, variable, or memory block, to be identified by means of a quoted label ("ID (a hex ID, a decimal ID, or a BASIC arithmetic expression ID)"), 3) an ultra renumber patch which provides a fast four parameter renumbering commands.

This enhancement program was burned on to two 2K EPROM's which were installed into the EPROM board. The original program was written to start at location 0200. An image of this program was burned on EPROM's with a base address of 6000. This method of storing program

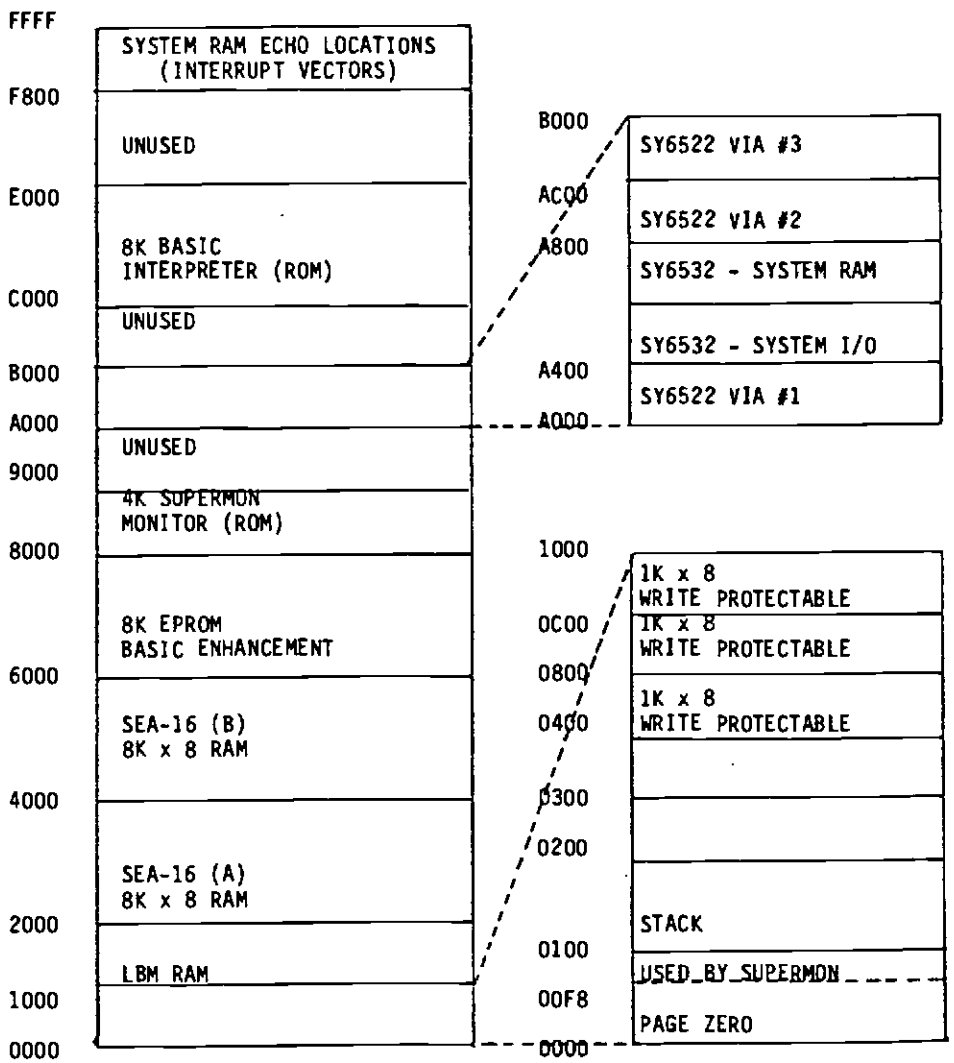

Figure 11. SYM-1 memory map.

is necessary because the EPROM board is addressed in 8K blocks. Therefore to locate it at 0200 would require the EPROM's base address to be 0000. This would result in an address conflict with the computer use of R/W memory in pages 0 and 1. To overcome this problem a short mover program was burned into EPROM just above the image of the enhancement program. To use the enhancement program with BASIC, the user executes the mover program with a G 6B00 [CR] command. This copies an image of the enhancement program into R/W memory starting at 0200. The last instruction of the mover program is a jump to 0200 which initializes the enhancement program and establishes links to the BASIC program, and BASIC responds with a cold start prompt. A listing to the mover program is given in Appendix VIII.

For interaction between the operator and the μC, an inexpensive, small keyboard (No. 753, George Risk Industries, Inc.) and hard copy unit (Ser. No. EUY-IOEOIIL U Panasonic) was constructed (83) and connected to the TTY 20 mA current loop serial interface. This device is a UART (Universal Asynchronous Receive and Transmit) based "TTY" which employs a commercially available keyboard and electrostatic printer and driver as previously described (83). It did not initially work reliably with the SYM-1 microcomputer because of the sensitivity of the SYM-1 to variations and drifts in the baud rate determined by the 555 time clock circuit in the keyboard-printer. To alleviate this problem, a baud rate generator PC board (Appendix VIII) was constructed to replace the 555 timer circuit (Figure 24, (83)). The stability of the crystal controlled oscillator ensures reliable operation.

The break key on the keyboard is connected to $\overline{NMI}$ pin of the EC connector of the LBM board. This pin is normally high (+5 V) and each time that the break key is pushed, a short logic 0 pulse is generated which causes a $\overline{NMI}$. This allows an exit from BASIC to the monitor without resetting the μC.

2-Byte multiplexed up-down counter

In mode 2, the PMT anodic currents are converted to a voltage, and then directed to the V/F for conversion to a pulse train. Binary counters are used to count the number of pulses in a preselected time. This converts the signal data into the binary form which can be directly transferred to μC memory through I/O lines.

A 2-byte (16 bit) multiplexed up-down counter was constructed from four cascaded 4-bit binary up-down counters (Appendix IX) for this purpose. This counter is connected to μC via 13 I/O lines. Eight I/O lines are used to transfer the data from the counter outputs to the SYM-1. The 16 output lines of the counters are TRI-STATE'd to 8 I/O lines such that the data in lower 8 bits and upper 8 bits can be transferred in two steps. The other 5 I/O lines are used to control the counter. The control lines are used to clear the counter, to gate in the V/F pulse train for a selected time, to control the counting mode (up or down), and to control the transfer of data to the SYM.

HCL pulser

During the time which μC is performing calculations or printing the results, it can not control the lamp pulsing system through software. Therefore a simple HCL pulse circuit was designed to pulse

the lamps when the computer is busy and allow the computer under software control to pulse the lamps during data acquisition. Details are presented in Appendix X.

Automated sampler

To allow automated introduction of the samples into the flame in AF experiments, an automated sampler was designed (Figure 12). Through software control, one can switch between the blank and an analyte solution.

A SPDT relay switch is used to turn on and off the AC power to the 3-way solenoid valve. The solid state relay is controlled by one I/O line which goes through a TRI-STATE buffer before going to the control input of the relay. A logic 1 signal on the I/O line switches the relay on and hence the solenoid valve which directs air (40 PSI) to a 3-way slide valve. This causes the output of the slide valve to be connected to input 1 (blank). The output of the valve is connected to the burner nebulizer with 0.5 mm ID tubing. When a logic 0 signal is connected to the control input, the output of the solenoid valve is connected to the atmosphere and the output of the slide valve is connected to position 2 (sample) through the action of a spring.

The TRI-STATE buffer is installed on the HCL pulser board to eliminate an extra PC board. The buffer output is brought out to a BNC male connector on the right side of the front panel of the electronics cage just below the PC boards' cage.

8-12 bit ADC

In mode 3 the signal voltage from the I/V converter is connected

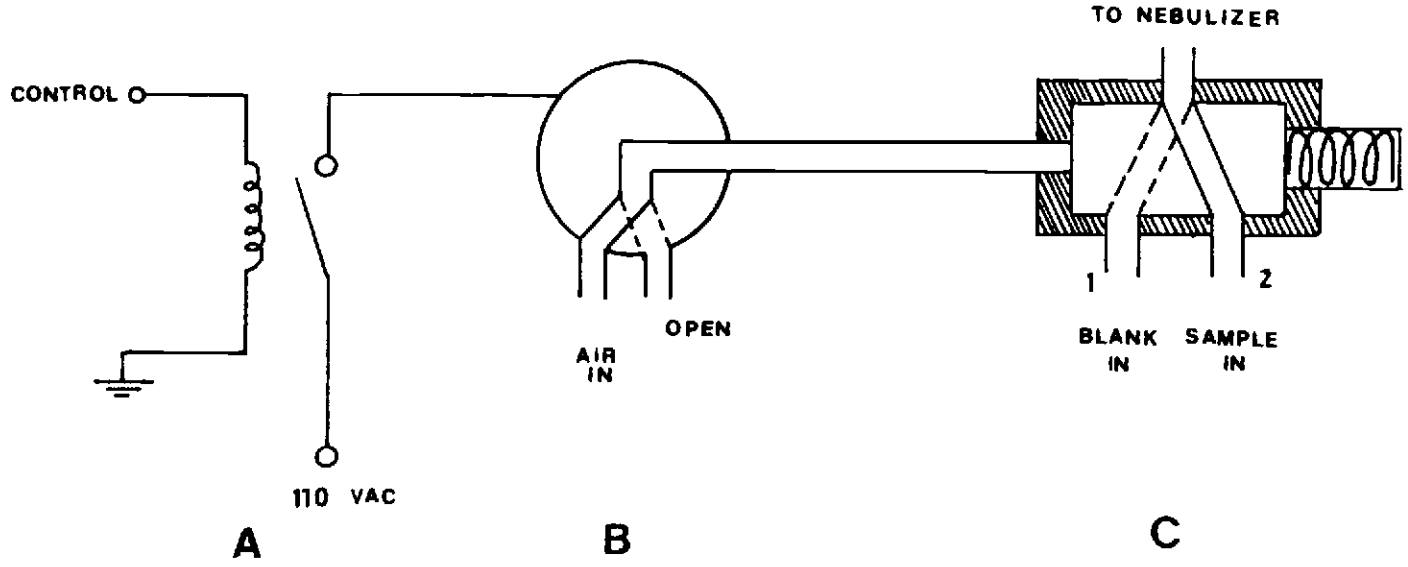

Figure 12. Automated sampler schematic components. A, SPST microcube solid state relay switch (Grayhill); B, 3-way solenoid valve (ser. no. H02-726 Skinner Precision Industries, Inc.; C, 3-way slide valve (Dionex).

to ADC. The ADC module constructed is based on a previous design and is documented in detail elsewhere (83). It is reviewed in briefly here. The ADC PC board is based on an Analog Devices AD7501 one of eight analog multiplexer and an Analog Devices AD574 eight or twelve bit ADC. The device is capable of 1) selecting one of eight analog channals for digitization, 2) performing an eight bit converson in 16 s or a 12 bit conversion in 25 s, and 3) transferring the resulting data in two steps into the SYM-1 using eight I/O lines. The ADC board in mounted in a box and placed inside of a Vector rack mountable strut cage which is mounted in the electronics cage. The board's 22 pin male edge connector protrudes through the back of the box and inserts into a 22 pin female edge connector, screwed to the back of the cage. All the input and output connections to or from ADC are connected to this 22 pin female connector.

12 bit latched DAC

The microcomputer controlled HCL pulsing circuit requires a digital to analog conversion. For this purpose a DAC PC board was constructed and placed in a vector box and installed in the electronics cage. An eight pole DIP switch was installed on front of box for range selection, and other connections are at the back of box. The design of the DAC PC board is identical to that previously described (83) except an OA in the voltage follower configuration was installed on the output as shown in Appendix XI. This allows the DAC to output a higher current and prevents damage to the DAC.

HCL pulsing circuitry system with power supply current regulator

HCL's pulsed at high currents provide excellent high intensity sources for atomic fluorescence spectrometry. The power supply must provide very reproducible current pulses to ensure stable light output from the lamp.

The current through the lamp can change if the lamp resistance changes. For this reason a current-regulator system was designed. The current-regulator system, which is basically a feedback control system, is based on the null comparision concept. The HCL's, and power supply are in the feedback loop of an operational amplifier (OA). This allows the lamp current to be continually compared to a reference current set by the user.

Figure 13 presents the modified HCL pulsing circuit. In the following description only two HCL's are considered even though the circuit is actually used for 4 HCL's. When a logic 1 pulse is generated from the HCL pulser circuit (Appendix X) (software or free running mode) for input 1, transistor T1 is turned on and T2 is turned off so that point A is at +15 V which turns FET switch AS1 on. This allows the voltage applied to point C from the DAC (or +5 V power supply) to pass through AS1 (the 250 kΩ variable resistor is turned completely clockwise for zero resistance) to the non-inverting input of control amplifier (OA1). The output voltage of OA1 is controlled to be the same as non-inverting input voltage. Transistor T5 passes the OA output signal to FET's AS3 and AS4. At this time, only AS3 passes the signal because point F is connected to point A (+15 V) and Point G is connected to point B (0 V). The signal passed by AS3 turns

Figure 13. HCL pulsing circuitry system with power supply current regulator.

Component	Identification No. or Valve	Description
T1-T5	2N3416	NPN transistor
T6, T7	SK3111	NPN power transistor
AS1-AS4	CD4016	FET - analog switch
OA1	TL081	Operational amplifier
R1-R6	100 Ω	Resistor
R7-R12	1 kΩ	Resistor
R13, R14	250 kΩ	Variable resistor
R15, R16	1 MΩ	Resistor
R17	5 kΩ	Potentiometer
R18	18 kΩ	Resistor
R19	400 kΩ	Resistor
R_{Sense}	15 - 3Ω	Resistor
M	10 mA DC	Current meter
S1, S2	DPDT	Switch
C1	100 pF	Capacitor
SS	Two-QPDT	Rotatory switch

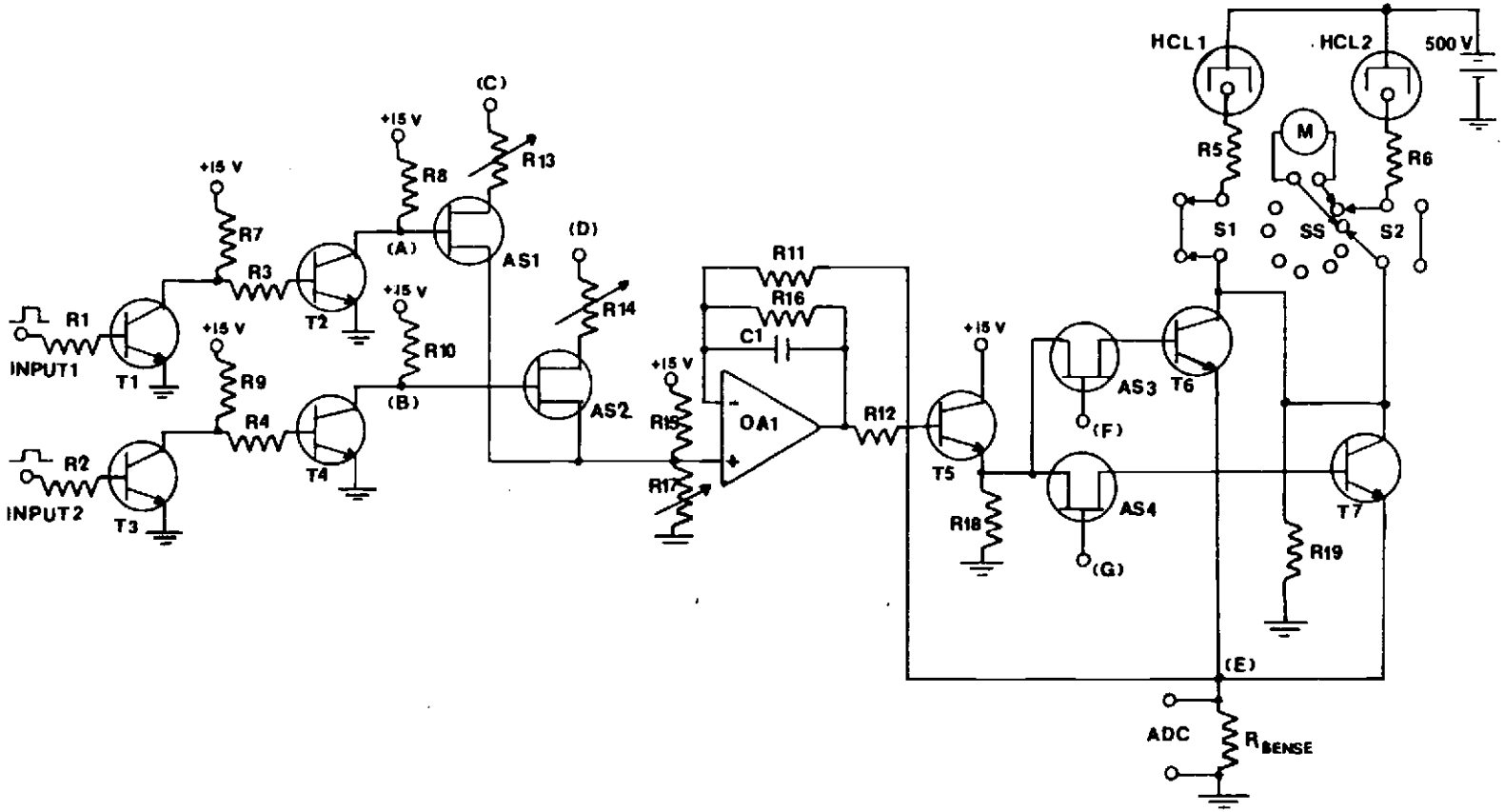
HCL1
HCL2
500 V
M
R5
R6
S1
SS
S2
(C)
+15 V
R8
R13
(D)
+15 V
R7
R3
(A)
AS1
R14
R11
R16
C1
+15 V
R10
T2
+15 V
R1
INPUT1
T1
+15 V
R9
R4
(B)
AS2
+15 V
R15
OA1
R12
+15 V
AS3
T6
(F)
R2
INPUT2
T3
T4
R17
T5
AS4
T7
R18
R19
(G)
(E)
ADC
R SENSE

Figure 13.

Table II. HCL Pulsing Circuitry System Pin Configuration

Pin	Description
A	To HCL #2 - Control Resistor (250 kΩ variable)
B	To HCL #3 - Control Resistor (250 kΩ variable)
C	To HCL #4 - Control Resistor (250 kΩ variable)
D	To HCL #1 - Control Resistor (250 kΩ variable)
E	HCL #1 - Control Pulse in (from HCL pulser board Pin P)
F	HCL #2 - Control Pulse in (from HCL pulser board Pin M)
H	HCL #3 - Control Pulse in (from HCL pulser board Pin U)
J	HCL #4 - Control Pulse in (from HCL pulser board Pin S)
K-S	N.C.
T	To the power transistor emitters
U	+15 V
V	HCL #1 - Control pulse out (to the power transistor base)
W	HCL #2 - Control pulse out (to the power transistor base)
X	HCL #3 - Control pulse out (to the power transistor base)
Y	HCL #4 - Control pulse out (to the power transistor base)
Z	-15 V
1-22	GND

the power transistor T6 on and allows current to flow through the HCL1 and turn it on for the period of time that input 1 is at logic level 1. When the lamp is on, current flows through load resistor R5, transistor T6, and R_{sense}. The voltage drop across R_{sense} is E_{sense} and is given by equation 1.

$$E_{sense} = (i_{HCL}) (R_{sense}) \quad (1)$$

This positive voltage at point E is applied to the inverting input of control amplifier OA1. The current through the HCL1 quickly assumes the value such that the voltage at point E (E_{sense}) equals the voltage at non-inverting input. By the same reasoning, any fluctuation in the lamp circuit (e.g. lamp resistance), which causes non-equality between the inverting and non-inverting inputs of the OA1, causes the output of OA1 to assume value to maintain E_{sense} and hence i_{HCL} to a constant level. The above process is repeated for each HCL. For HCL2, the lamp is turned on when the input 2 and T3 is high and AS4 and T7 are turned on.

If the system is controlled by the μC, lamp currents are selected by the user at the TTY terminal. The software calculates the digital signal to feed to the input of the DAC which produces the necessary DAC output voltage to produce a selected i_{HCL}. This calculation is based on R_{sense} value, experimental constants, and other variables to provide the selected i_{HCL}.

When the μC is not interfaced, a constant voltage (+5 V) is applied to points C and D instead of the DAC output. The current i_{HCL} is adjusted with the 250 kΩ variable resistor. During this adjustment, the ammeter (M) is switched into the appropriate HCL

current path, first by selector switch SS, then by switching S1 (for HCL1) or S2 (for HCL2) to the "M" position. The two-switch system is used to prevent any accidental damage to the ammeter or HCL by connecting two HCL's to the same ammeter.

The voltage at point E (E_{sense}) is connected to the one channel of the ADC to convert the voltage to digital form for input to the computer. This digital signal is used by the computer to calculate i_{HCL} which is displayed at the computer terminal. This provides the user with conformation that the desired i_{HCL} has been selected.

Mode selection

A switch box was designed which allows easy selection of the three modes of operation. These switches are installed on front panel of the electronics cage and described in Appendix XII.

PC board arrangement in vector card cage

The PC boards are placed in a Vector card cage (type CCK13-Vector) which is mounted in a rack. The locations of the boards are shown in Figure 14. The letters correspond to the standard card rail locations on the Vector card cage.

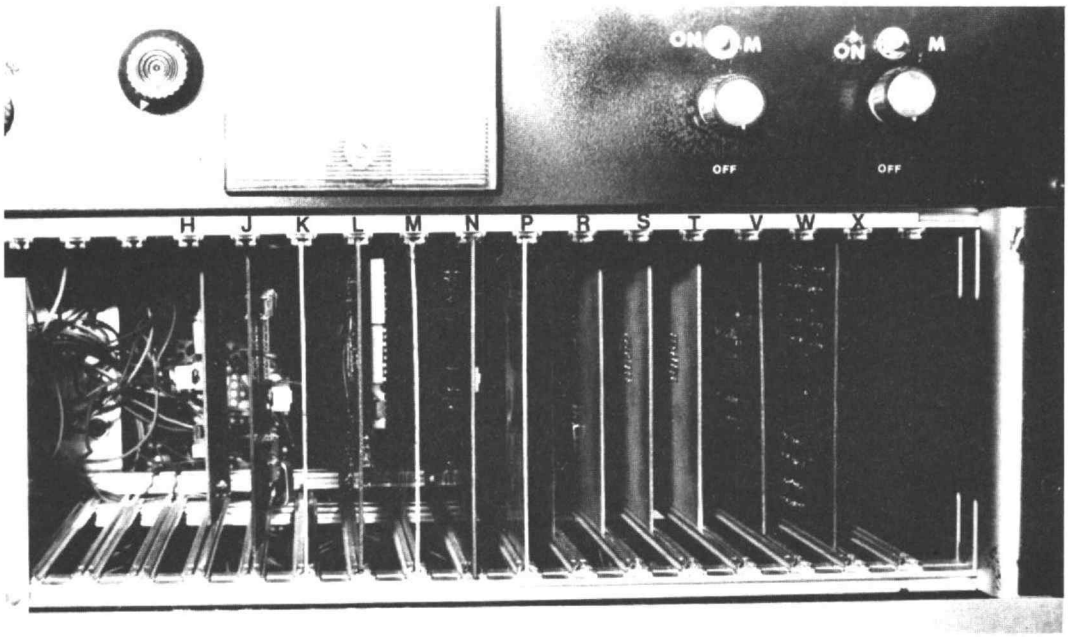

Figure 14. PC board locations in Vector card cage. H, automated start switch; J, 1 MHz crystal clock; K, aluminum shield; L, control board; M, aluminum shield; N, HCL pulse control and current feedback circuit; P, aluminum shield; R, up-down counter #1; S, up-down counter #2; T, up-down counter #3; V, up-down counter #4; W, HCL pulser; X, 2-byte multiplexed up-down counter.

Operation and Software for Computerized TMMS AF Spectrometer

In this section, the variables that are important in computerizing the operation of the instrument are first defined. Also the calculations necessary to extract signal and S/N information from the raw data are reviewed. Next the software is described from an operational point of view. This includes a discussion of the operator input of experimental parameters and the control, calculation, and output functions performed by the software.

Definitions of lamp and data acquisition parameters

The variables relating to the pulsing of the HCL's and to data acquisition are identified and briefly described below and in Figure 15.

1) HCL peak current (i_p): The maximum HCL current during the time the lamp is on, typically 70 to 1000 mA.
2) HCL pulse width (t_p): The length of time the HCL is pulsed on, typically 1 to 10 ms.
3) Lap (cycle) time (t_L): The total time for all the HCL's used (up to 4) to be pulsed on and off one time. Typically the signals from 10 to 100 laps are added together in one measurement to produce one data point.
4) Percent duty cycle (%DC): The percent time that given HCL is on during one lap (cycle) or

$$\%DC = 100\ (t_p/t_L) \qquad (2)$$

Typically %DC is 1-12.5.

5) HCL rms current (i_{rms}): The average HCL current over the period of one lap.

$$i_{rms} = i_p \times \%DC/100 \quad (3)$$

6) Delay time (t_d): The period of time from the moment that lamp goes on (or off) until data acquisition begins. Normally the delay time is adjusted to be about five times the time constant (τ) of the I/V converter feedback network to allow the electronics to respond fully.

7) Data collection time (t_c): The period of time over which the data are acquired for the rest of the pulse after the delay or

$$t_c = t_p - t_d \quad (4)$$

For background corrected measurements, an identical delay and data collection time occur after the pulse to yield the lamp off signal which may be subtracted from the previous lamp on signal.

In mode 2, the V/F counter integrates for the signal the rest of the pulse width for time t_c. For mode 3, one or more data acquisitions are made and summed per pulse. The number of data acquisitions (q) is determined by the data collection time to t_c and the time to make one data acquisition and store the result in memory (t_a). Thus q is equal to t_c/t_a rounded up to the closest integer value. Since t_a is 200 s, q is 48 for a pulse width of 10 ms and 3 for a pulse width of 1 ms for a fixed t_d of 0.5 ms.

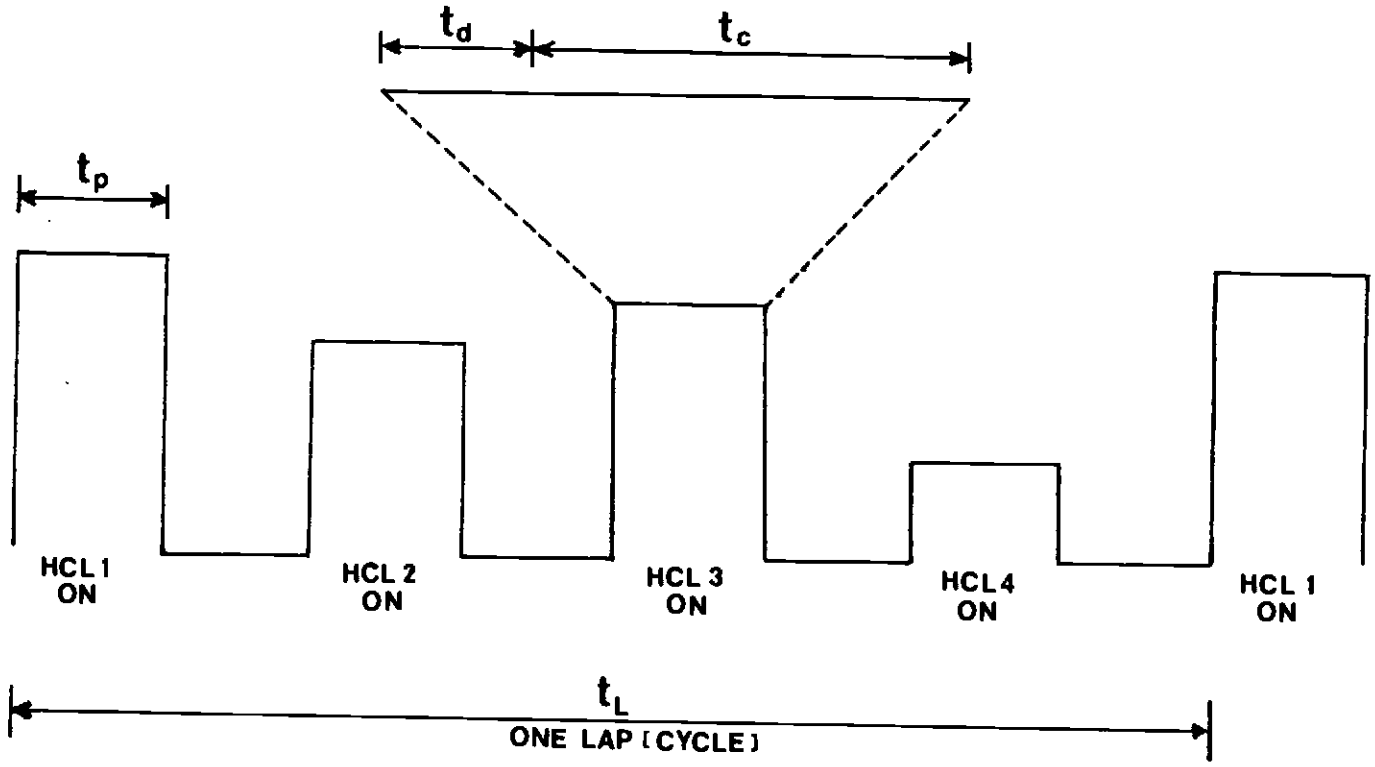

Figure 15. TMMS AF variables timing diagram. t_p = pulse width, t_d = delay time, t_c = data collection time, t_L = lap time.

Signal information and resolution considerations

In mode 2, the signals for ℓ laps are summed together and presented as one data point. Equation 5 shows how the signal reported by the computer (N) is related to input peak voltage to V/F counter.

$$N = \ell K E_p t_c \quad (5)$$

N = number of counts

K = V/F conversion factor (100 kHz/V)

E_p = peak signal voltage, V

t_c = data collection time per pulse, s

ℓ = number of laps

In mode 3, each data point is normalized by dividing it by the number of readings per pulse. The stored digital number (D') acquired by the ADC during one reading is proportional to the voltage input to the 12-bit ADC. Thus during one pulse with q readings, the summed signal is qD'. The final digital signal acquired by summing the results for ℓ laps is ℓqD'. This is normalized by dividing by q to yield a data point (D) equal to ℓD'. This value is reported as the sum of the mV readings from ℓ pulses (E_{sum}) by multipling D by (10,000/4095) (10,000 mV is equivalent to 4095 for 12-bit ADC or DAC). Thus in mode 3, one data point is calculated as

$$E_{sum} = 10{,}000D/4095 \quad (6)$$

The peak voltage E_p in volts can be calculated from E_{sum} with equation 7.

$$E_p = E_{sum}/1000\ell \quad (7)$$

The resolution of the V/F converter is 1 count per lap. The relative resolution per lap (N^{-1}) and absolute voltage resolution per

lap $(Kt)^{-1}$ depends on the integration time and thus the pulse width. The relative resolution for ℓ laps is $\ell^{1/2}/N$ if the contribution from quantization noise is limiting. In contrast, the resolution of the ADC is determined by the least significant bit and is independent of pulse width. For one data acquisition, the absolute resolution is 2.4 mV and the relative resolution is $(2.4 \times 10^{-3})/E_p$. For q acquisitions and ℓ laps, the relative resolution is $(2.4 \times 10^{-3})/(E_p(q\ell)^{1/2})$.

Table III shows the effect of the HCL pulse height and width on the resolution for both the ADC and V/F converter. The peak voltage varies from 10 to 0.01 V for a dynamic range of 3 orders of magnitude.

Table III. Resolution Considerations[a]

		V/F			ADC[b]		
E_p	t_p	Counts	Rel. Res.	Abs. Res.	D	Rel. Res.	Abs. Res.
(V)	(ms)	(N)	(N^{-1})	(mV)		(D^{-1})	(mV)
10	10	10^4_2	10^{-4}	1	4095	2.4×10^{-4}	2.4
0.1	10	10^2_1	10^{-2}	1	40.9	2.4×10^{-2}	2.4
0.01	10	10^1_3	10^{-1}	1	4	2.4×10^{-1}	2.4
10	1	10^3_1	10^{-3}	10	4095	2.4×10^{-4}	2.4
0.1	1	10^1	10^{-1}	10	40.9	2.4×10^{-2}	2.4
0.01	1	1	1	10	4	2.4×10^{-1}	2.4

[a]Calculations for one lap. Delay time t_d assumed to be 0 ms.

[b]One data acquisition per lap (q = 1).

For a 10 ms pulse, the resolution of the V/F converter (mode 2) is about a factor of 2.5 better. However, for a 1 ms pulse width, the resolution of the ADC (mode 3) is superior by about a factor of 4. This occurs because 10 times less counts are accumulated by the counter with the V/F when the integration time is reduced by a factor

of ten. Table III shows that if measurements are limited by resolution rather than noise, mode 3 is superior for pulse widths less than about 4 ms. The contribution of quantization error to the relative uncertainty of noise decreases in mode 3 in proportion to $q^{1/2}$.

Extraction of signal and noise information

The signals and noise observed are composed of various component signals and noise from different sources. These different signal and noise components can be extracted from measurements made under different sets of conditions. The general procedure and terminology used follows the work of Bower and Ingle (84).

Data are acquired during the lamp pulse (or when the lamp would be pulsed on if the lamp is blocked or off) and for an equal time after the lamp pulse. In the corrected mode, the lamp off data are subtracted from the lamp on data for each lap. This corrected signal is related only to signals dependent on the lamp intensity (i.e. analyte and background fluorescence and scattering). The average signal for non-lamp related signals (e.g. background and analyte emission, dark current) is zero because these are DC signals that are present all the time. In the uncorrected mode, the total or uncorrected lamp on signal is obtained by not subtracting the lamp off signal from the lamp-on signal. If the lamp is off or blocked, this uncorrected measurement yields the magnitude of the lamp off signal.

To calculate the mean signal and noise under different sets of conditions, n data points (N's or E_{sum}'s) (typically 20) are taken and the computer calculates the mean, the rms noise or standard deviation

(SD), and the signal-to-noise ratio (S/N). This complete process is called a run, and often the results of a few runs are used to calculate the average mean, SD and S/N.

The signal (mean) and rms noise (SD) calculated from n data points have units of counts in mode 2 or millivolts in mode 3. These can be converted to units of volts with equations 5, 6, and 7 and are symbolized below as E and σ, for the mean signal and rms noise, respectively, of the peak signals in V.

Repetitive measurements are made in the corrected signal mode with the entrance slit covered. This yields E_{dt} and σ_{dt}, the dark current signal and rms noise, respectively. With the flame and lamps off, the same measurements can be made in the corrected mode with the entrance slit uncovered to determine if stray light from the room causes significant noise.

With the lamps off and a blank aspirating, E_{bet} and σ_{bet} are obtained from n repetitive measurements in the corrected mode and are the total background emission signal and rms noise, respectively.

The above dark current and total background emission measurements can be used to determine the noise contribution with synchronous detection due to background emission from the flame (σ_{be}) from equation 8.

$$\sigma_{bet} = (\sigma_{be}^{2} + \sigma_{dt}^{2})^{1/2} \qquad (8)$$

The above dark current and total background emission measurements can also be made in the uncorrected mode to determine the magnitude of the DC signals, E_{dt} and E_{bet}, from which the DC background emission signal from the flame (E_{be}) can be calculated from equation 9.

$$E_{bet} = E_{be} + E_{dt} \quad (9)$$

Under corrected conditions, the noise magnitudes may be less than in the uncorrected mode if flicker noise limits measurements.

With the flame and lamp on and a blank aspirating, n measurements are made in the corrected mode to estimate E_{bft} and σ_{bft}, the total fluorescence background signal and noise, respectively. Note that σ_{bft} is the blank noise that limits the detection limit. Comparison of σ_{bft} to σ_{bet} (corrected mode) indicates if scattering or background fluorescence noise is significant.

With an analyte solution aspirating, n measurements are made in the corrected mode to obtain the total analyte fluorescence signal E_{ft} and its rms noise, σ_{ft}. From these measurements and the blank measurements, the analyte fluorescence signal (E_f) and the rms noise (σ_F) for making a paired fluorescence measurement (i.e. sample and blank) are calculated with equations 10 and 11.

$$E_f = E_{ft} - E_{bft} \quad (10)$$

$$\sigma_F = (\sigma_{ft}^2 + \sigma_{bft}^2)^{1/2} \quad (11)$$

With the lamps off and an analyte solution aspirating, E_{et} and σ_{et} are obtained with the uncorrected or the corrected modes from n repetitive measurements and are the total analyte emission signal and rms noise, respectively.

In the corrected mode E_e averages to zero and the contribution of analyte emission noise (σ_e) to fluorescence measurements is calculated from σ_{et} and equation 12

$$\sigma_e = (\sigma_{et}^2 - \sigma_{bet}^2)^{1/2} \quad (12)$$

where σ_{bet} is measured in the corrected mode. The noise due to

analyte fluorescence (σ_f) is calculated from equation 13.

$$\sigma_f = (\sigma_{ft}^2 - \sigma_{bft}^2 - \sigma_e^2)^{1/2} \quad (13)$$

In the uncorrected mode, the analyte emission signal is obtained from equation 14.

$$E_e = E_{et} - E_{bet} \quad (14)$$

The computer calculates several quantities from the acquired mean signals and noise magnitudes (SD's) in the sample (total fluorescence) and blank measurements. The net analyte fluorescence signal (E_f) is calculated from equation 10. The S/N for making an AF measurement is calculated from equation 15

$$S/N = E_f/\sigma_F \quad (15)$$

where σ_F is calculated from equation 11. Equation 16 is used to calculated the blank noise limited S/N ($(S/N)_{bk}$).

$$(S/N)_{bk} = E_f/\sigma_{bft} \quad (16)$$

The detection limit (DL) is obtained from equation 17

$$DL = 2\,\sigma_{bft}/(\text{slope}) \quad (17)$$

where the slope is calculated from E_f/c and the value for c has previously been input to the computer.

The fundamental rms shot noise in the analyte fluorescence signal, $(\sigma_f)_s$, is calculated from equations 18-21.

$$(\sigma_f)_s = (mR_fKE_f)^{1/2} \quad (18)$$

$$K = 2e\Delta f\,(1 + \alpha) \quad (19)$$

$$\delta = 10^{(\log m)/9} \quad (20)$$

$$\alpha = (\delta - 1)^{-1} \quad (21)$$

m = PMT gain

R_f = feedback resistance, Ω

K = noise bandpass constant, A

Δf = noise equivalent bandpass, s^{-1}

α = secondary emission factor, dimensionless

δ = gain per dynode stage of PMT, dimensionless

$e = 1.6 \times 10^{-19}$ C

For a DC signal in mode 2, $\Delta f = (2t)^{-1}$, where t is the integration time (t_c).

The above equations normally apply to measurements on DC signals. For TMMS measurements, the lamp is pulsed so E_f in equation 18 represents the peak value or total analyte fluorescence signal during the lamp pulse. The total observation time for the fluorescence signal of one element in one run of ℓ laps is ℓt_c and

$$\Delta f = (2\ell t_c)^{-1} \qquad (22)$$

For mode 3 with q = 1, the time constant of the I/V converter limits the noise equivalent bandpass of $\Delta f = (4\tau)^{-1}$ where τ is the time constant. Since q points are taken per pulse every 2τ (τ = 0.1 ms, t_a = 0.2 ms), mode 3 effectively performs an integration over the data observation time t_c. This signal averaging provided by taking q points per pulse for ℓ laps reduces Δf calculated from τ by $\sim (1/q\ell)$ such that the Δf from equation 22 provides a good estimate for Δf in mode 3.

In the program, the shot noise is the analyte fluorescence signal is calculated from equation 18. The user inputs the values R_f, C_f, ℓ, and the PMT bias voltage E_{PMT}. The PMT gain (m) is determined from the bias voltage applied to the PMT and RCA 1P28 calibration graph (84). The computer program has a look up table of m values for

voltages from 400 - 1000 V in 100 volt intervals. Next δ and α are calculated from equations 20 and 21 and the value of m. The value of Δf is calculated from equations 4 and 22 and the known values of t_p, t_d, and ℓ. This value of Δf is then used to determine K with equation 19. Finally the analyte fluorescence shot noise is calculated from equation 18 and the known calculated values of m, R_f, and K.

For mode 2, E_f is taken as the difference in total counts accumulated (N) for the sample and blank measurements divided by $Kt_c\ell$ so that the shot noise is reported in volts. For mode 3, E_f is taken as the difference in E_{sum} for the total sample and blank measurements and divided by 1000 and reported as the shot noise in volts. From equation 7 and 18, the shot noise in volts is the shot noise reported divided by $\ell^{1/2}$.

In many cases it was useful to calculate manually the analyte fluorescence photocathodic peak current (i_f) from equation 23. The

$$i_f = E_f/mR_f \tag{23}$$

rms photocathodic current in amperes is calculated from equation 24.

$$(i_f)_{rms} = i_f t_p/t_L = i_f(\%DC) \tag{24}$$

Operation and software considerations

Before starting the program, the operator selects R_{sense}, E_{PMT}, the HCL load resistors, the proper slit mask, R_f, C_f, the burner and the oxidant, fuel and the sheath gas flow rates. The monochromator wavelength drive is used to align the system based on the 285.2 nm line from the Mg HCL.

BASIC and machine language programs were developed for modes 2 and 3 and the listings are given in Appendix XIII. Figure 16 shows a

flow chart for the programs. The operator first loads the appropriate BASIC and assembly language programs for the mode to be used. After typing RUN, the program first, through TTY communication, requests input information from the user about the magnitude of experimental variables. The operator then chooses between two basic options, the operator analysis or characterization. Depending on the option selected, the operator is guided by prompts to choose the types of measurements to be made (dark, blank, or sample) or to input other data. Once the correct information is input, the user signals the start of data acquisition. After data acquisition, various calculations are performed and printed out with the data. The assembly language routines perform most of the control functions. After input of parameters and bookkeeping calculations performed in BASIC for any particular measurement (calibration, dark, blank, or sample), the assembly part of the program takes over and starts to pulse the HCL's and collect data. The assembly program configures the I/O lines properly (input or output), controls the HCL's pulsing and currents, collects data, and stores the data in reserved memory blocks. It also controls the operations of the ADC, the DAC, or the 2-byte up-down counter and keeps track of the number of laps and data points. Finally it controls the clock and all other timing functions. The data stored are later pulled out of memory by BASIC and calculations are performed in BASIC. The use of the program is described now in more detail.

The program starts in BASIC, and asks the operator to input the HCL's pulse width in milliseconds, then percent duty cycle, the

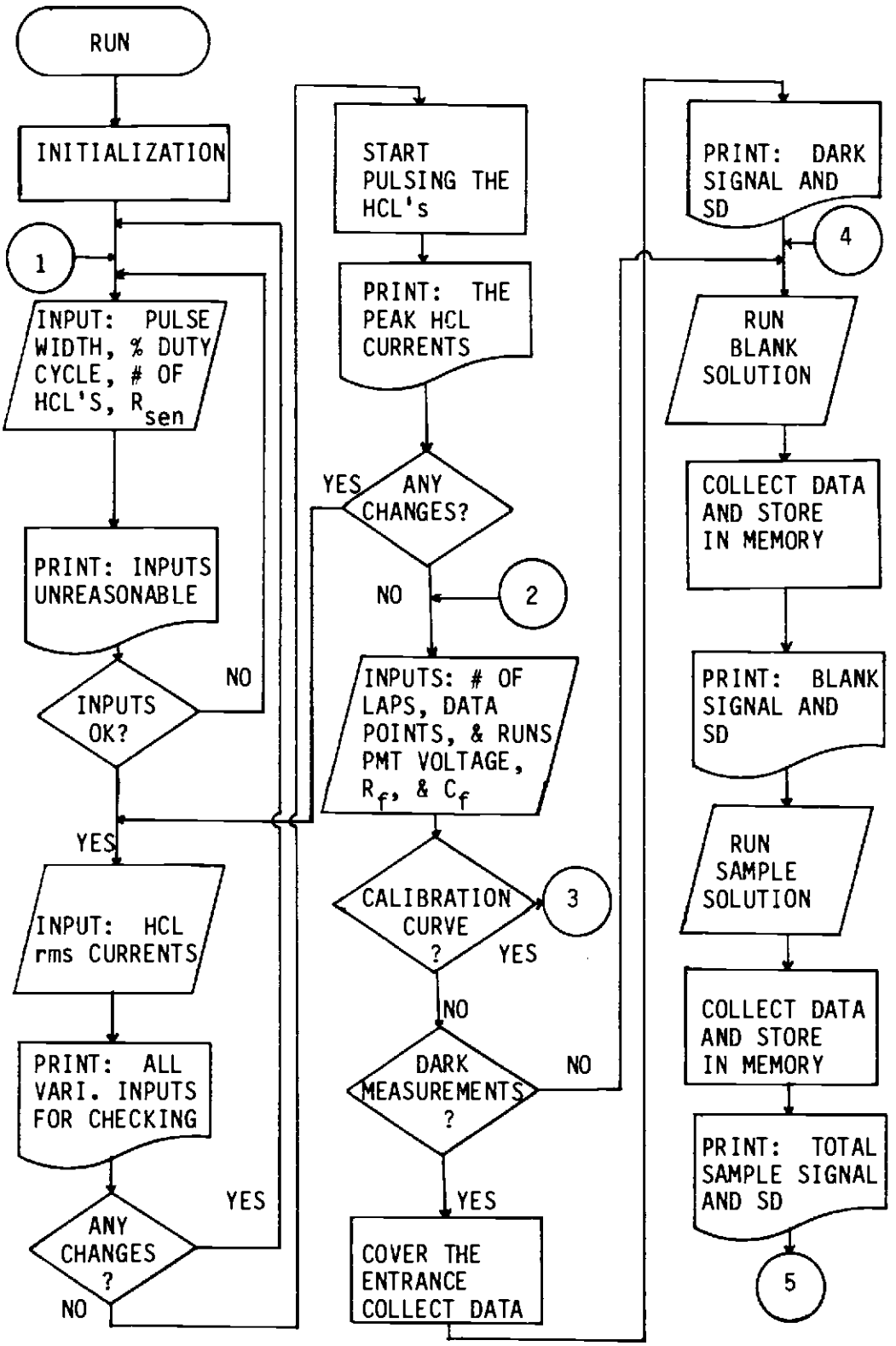

Figure 16. Simplified computer program flowchart.

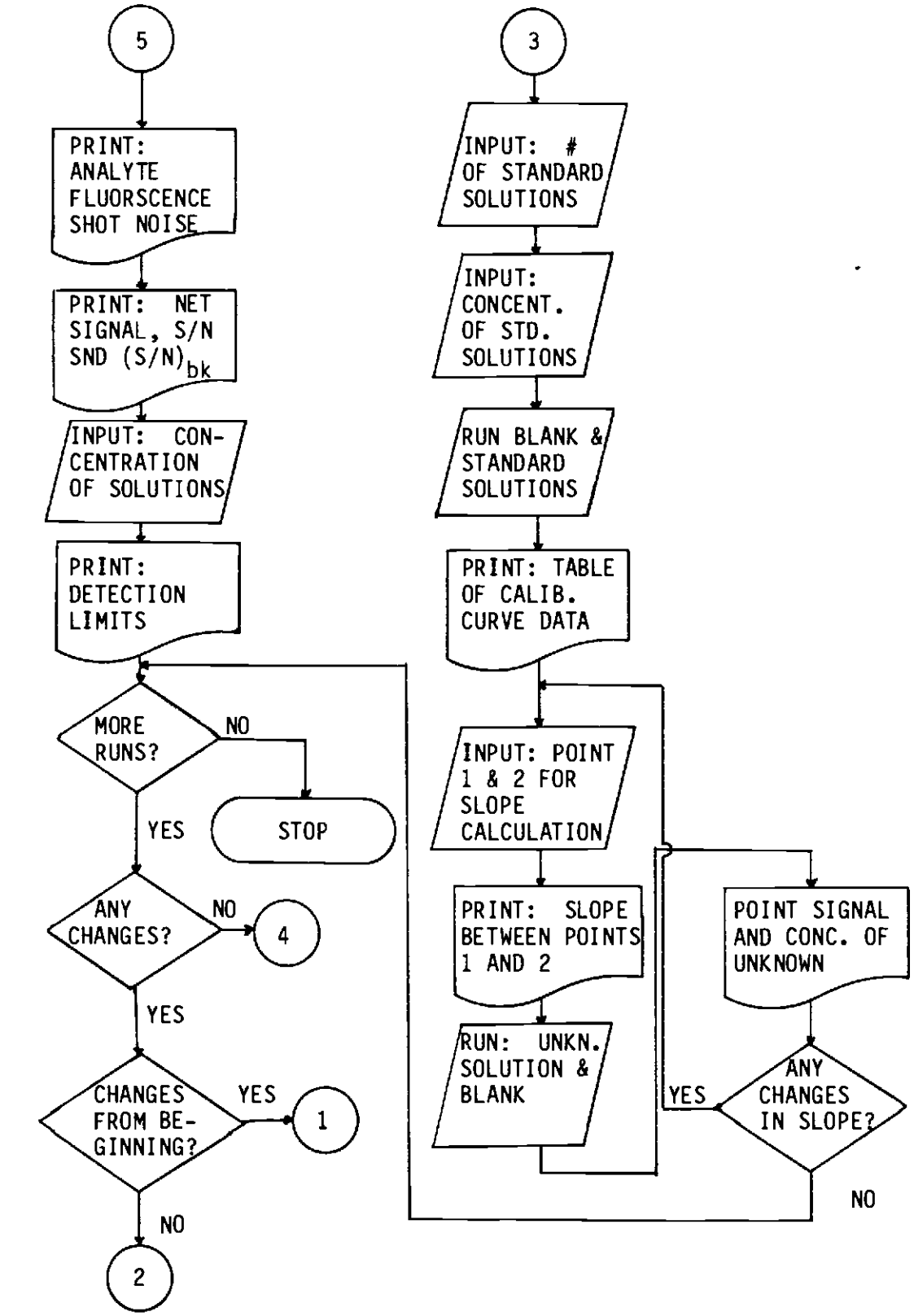

Figure 16. continued.

number of HCL's to be used, and the R_{sense} value in ohms. The off time is calculated for the given percent duty cycle and the number of HCL's, and if the off time is smaller than the selected HCL pulse width (the product of percent duty cycle and number of lamps greater than 50%), an error message is printed and new inputs are requested. Next the rms HCL currents are input sequentially. These values are converted to appropriate digital numbers and checked against the DAC capacity (not larger than 4095). If the DAC capacity is exceeded, an error message is printed which indicates that the HCL current or R_{sense} should be changed.

Before pulsing the HCL's, all the input values are printed for final checking and if no changes needed, the pulsing starts. The ADC reads the voltage at the sense resistor and calculates the peak HCL current from equation 1 and R_{sense} for each HCL and prints i_p for HCL. If the currents are acceptable, the program proceeds to the next step. If not, new HCL currents values are input. Once the HCL currents are acceptable, the program asks for the number of laps, the number of data points per run, the values of R_f in M ohms and C_f in p Farads (I/V converter feedback resistor and capacitor), the number of runs, and the PMT voltage in volts. At this point the program calculates the delay time t_d as $5R_fC_f$. The delay time and pulse width (t_p) are then used to calculate the data collection time with equation 4. For later shot noise calculations, Δf, δ, and K are calculated with equation 22, 20 and 19, respectively.

Next the operator chooses between two of the basic options, analysis or characterization. If the characterization option is chosen

(a no answer (0) to calibration curve question), the program asks if a dark current measurement is needed. If so the operator is requested to cover the entrance slit. On a signal (CR) from the operator, the data are taken in the uncorrected mode and the mean and SD in the dark signal are calculated and printed for each HCL chosen. The operator is given the choice of printing out the n dark signals obtained in the run.

After the dark current measurement or if no dark current measurement is requested, the program indicates a blank run is to be made. The program switches the auto sampler to the blank position and after a CR, the blank data are taken in the corrected mode, and the blank mean signal (E_{bft}) and SD (σ_{bft}) are printed for each element chosen. Again the data for each point in the run can be printed out if desired. If the above measurements are taken with the lamp blocked, then the mean and SD in the total background emission signal are obtained.

After the blank measurement, the program tells the operator that an analyte solution is to be measured. The program switches the autosampler to the sample position, and the user inserts the sample capillary tube from the autosampler into the desired solution. After a CR, the data are collected and the mean (E_{bft}) and SD (σ_{ft}) of the total signal are calculated and printed for each element chosen. The data for all runs can be printed out if desired. Next the analyte fluorescence shot noise ($(\sigma_f)_s$ from equation 18), the net analyte fluorescence mean signal (E_f from equation 10), $(S/N)_{bk}$ (from equation 16), and S/N (from equation 15) for each element are printed

out.

The operator is requested to input the concentration of the analyte solutions run in mg/L. The detection limits are calculated (from equation 17) and printed in mg/L.

If the above blank and analyte measurements are made the HCL's blocked, data are obtained about the analyte emission noise (the same section of the program which does the dark measurements is used for emission measurements).

If more than one run was requested at the beginning of the sequence, the program goes through the dark, blank, and sample measurement scheme for the number of runs requested. After this the operator can request more runs with the same experimental parameters, change the experimental parameters before more runs, or end the experiment. A sample printout for a characterization run is shown in Figure 17.

If the calibration curve option is chosen, the operator is asked to input the number of standards to be run and the concentration of standards in mg/L for each element. On a signal from the operator (CR), the program obtains a blank measurement and then a sample measurement through control of the autosampler. This is repeated for each standard solution. After all the standards have been run, a calibration data table is printed out which indicates, for each element and standard, the net fluorescence signal and the corresponding standard solution concentration in mg/L. Also other information such as the blank signal and SD, and the total signal and SD, are printed out after each sample (blank or standard) is run.

Figure 17. MULTI-AD computer program sample output.

```
RUN

HC#1
HC#2
HC#3
HC#4

TIME ON
T1=10

% TIME ON
PC=12.5

# OF LAMP
LM=4

RESISTOR VALUE
R=6.7

H.C. AVE. MAMP CURRENTS

H.C. #1 CURRENT
C1=13

H.C.#2 CURRENT
C2=14

H.C.#3 CURRENT
C3=15

H.C.#4 CURRENT
C4=15

T1=10     PC=12.5     LM=4      R=6.7
C1=13     C2=14       C3=15     C4=15

ARE THESE VALUES CORRECT?  YES=1, NO=0
ANS=1

READY TO READ CURRENT!  PUSH (CR).

PEAK TO PEAK CURRENTS

H.C.#1 CURRENT=110 MAMP
H.C.#2 CURRENT=118 MAMP
H.C.#3 CURRENT=127 MAMP
H.C.#4 CURRENT=127 MAMP
```

Figure 17. continued

```
READ MORE YES=1, NO=0
ANS=0

# OF LAPS
LP=100

# OF POINT
PT=20

RF VALUE (M-OHM)
RF=1

CF VALUE (P-F)
CF=100

# OF RUNS
RN=1

PMT VOLTAGE
PM=1000

CALIBRATION CURVE YES=1, NO=0
ANS=0

DO YOU WANT DARK DATA?  YES=1, NO=0
DK=1

COVER ENTRANCE SLIT & PUSH (CR).

DARK DATA

DARK AVE & STD DIV.

4         2         4         8
6.81      6.20      5.36      5.74

PRINT DATA YES=1, NO=0
ANS=0

RUN BLANK PUSH (CR) TO START.

BLANK DATA

BLANK AVE & STD DIV.

26        66        875       2828
14.59     11.68     14.77     18.07
```

Figure 17. continued

```
PRINT DATA YES=1, NO=0
ANS=0

RUN SAMPLE PUSH (CR) TO START.

SAMPLE DATA

TOTAL SIG AVER & STD DIV.

410        2196       1074       11383
16.30      29.04      19.83      63.67

PRINT DATA YES=1, NO=0
ANS=0

RMS SHOT NOISE (VOLTAGE)

4.2113728E-04     2.2556523E-03     1.1031742E-03     1.1692209E-02

NET SIGNAL

384     2130     199     8555

NET SIGNAL/BLANK STD DIV.

26.3     182.4     13.5     473.4

NET SIGNAL/TOTAL NOISE

17.5     68.0     8.0     129.3

CONC. OF SOLN. #1 (PPM)
G1=1

CONC. OF SOLN. #2 (PPM)
G2=1

CONC. OF SOLN. #3 (PPM)
G3=1

CONC. OF SOLN. #4 (PPM)
G4=1

DETECTION LIMITS (PPM)

76.0     11.0     148.0     4.0
```

Figure 17. continued

```
EXTRA RUN YES=1, NO=0
ANS=0
```

Next the operator inputs the numbers of two standards to calculate the slopes in signal units per mg/L for each element upon a signal from the operator, the signals for the blank and unknown solutions are obtained and the blank signal and SD, the unknown total signal and SD, and the net signal for the unknown are printed out during the measuring process. The concentration of each element in the unknown is calculated from the ratio of the net unknown signal and appropriate slope and printed.

At this point, the operator can choose different standards for the slope calculations. In this case the program recalculates the slopes and the concentration of each element in the previously run unknown.

The above process is repeated for the number of runs chosen. After this, the operator can stop or make more runs with the same or new parameters. Figure 18 shows a copy of a typical output for a calibration run from the point a calibration run is chosen.

Solution Preparation

Ten elements, Au, Cd, Co, Cu, Fe, Mg, Mn, Ni, Pb, and Zn, were selected to be used in different experimental studies. Standard stock solutions of approximately 1000 μg/mL of these elements were prepared by dissolving a suitable amount of a primary standard of each element in a proper solvent such as an acid or deionized distilled water. The primary standards used were the pure metals for Au, Co, Cu, Fe, Ni, and Zn, and the compounds CdO, MgO, $MnSO_4 \cdot H_2O$, and $Pb(NO_3)_2$, for Cd, Mg, Mn, and Pb, respectively. Typically 500 mL of stock solution were

Figure 18. Computer program sample output for calibration curve measurements.

```
CALIBRATION CURVE YES=1, NO=0
ANS=1

# OF STANDARDS
SD=3

INTER THE CONCENTRATION OF STANDARDS.

1     1
2     2.5
3     10

# OF RUNS PER SAMPLE
RN=1

CALIBRATION CURVE DATA
----------

DO YOU WANT DARK DATA?  YES=1, NO=0
DK=0

RUN BLANK PUSH (CR) TO START.

BLANK DATA
----------

BLANK AVE & STD DIV.

110       46       702       388
66.12     61.5     59.09     70.27

RUN SAMPLE PUSH (CR) TO START

SAMPLE DATA
----------

TOTAL SIG AVER & STD DIV.

198       1103      923       3821
69.25     75.03     78.27     107.32

DO YOU WANT DARK DATA?  YES=1, NO=0
DK=0

RUN BLANK PUSH (CR) TO START.
```

Figure 18. continued

BLANK DATA

BLANK AVE & STD DIV.

64	22	717	355
65.45	47.26	72.98	48.23

RUN SAMPLE PUSH (CR) TO START.

SAMPLE DATA

TOTAL SIG AVER & STD DIV.

502	2490	1208	9086
148.88	86.87	97.44	218.07

DO YOU WANT DARK DATA? YES=1, NO=0
DK=0

RUN BLANK PUSH (CR) TO START.

BLANK DATA

BLANK AVE & STD DIV.

60	10	693	361
59.28	55.58	72.66	73.33

RUN SAMPLE PUSH (CR) TO START.

SAMPLE DATA

TOTAL SIG AVER & STD DIV.

1561	7601	3012	32859
265	155.85	164.58	656.85

CONC.	NET AVE. SIGNAL.			
1	88	1057	221	3433
2.5	438	2468	491	8731
10	1501	7591	2319	32498

Figure 18. continued

```
WHAT ARE THE 1ST & 2ND POINTS FOR THE SLOPE CALC.

1ST=1
2ND=3

SLOPE OF CALIB. CURVES

157      726      233      3229

DO YOU RUN UNKNOWN YES=1, NO=0
ANS=1

DO YOU WANT DARK DATA?  YES=1, NO=0
DK=0

RUN BLANK PUSH (CR) TO START.

BLANK DATA

BLANK AVE & STD DIV.

69         28         713        353
64.41      54.17      52.79      62.52

RUN SAMPLE PUSH (CR) TO START

SAMPLE DATA

TOTAL SIG AVER & STD DIV.

436        201        1275       2375
121.73     69.41      90.32      100.30

NET UNK. SIGNAL.

367      173      562      2022

CONCENTRATION OF UNK.

2.34      0.24      2.41      0.63

CALCULATE THE SLOPE AGAIN YES=1, NO=0
ANS=0

EXTRA RUN YES=1, NO=0
ANS=0
```

prepared and about 10 mL of concentrated nitric acid was added before dilution to make the solution 2% (v/v) in nitric acid. Addition of nitric acid to each standard solution prevents the loss of analyte by adsorption on the walls of its storage container.

From these stock solutions, a series of lower concentration standard solutions were prepared by dilution to be approximately 0.1, 2.5, 5, 10, 25, 50, 100, 250, 500, and 750 μg/mL in each element. Multiple element standard solutions were prepared in a similar way by dilution of stock solutions. These solutions were preserved by the previously described method and stored in available glass or polyethylene bottles.

All the glassware including storage bottles were soaked in 50% nitric acid and rinsed with deionized distilled water each time before use.

RESULTS AND DISCUSSION

Introduction

To evaluate the capabilities and limitations of the automated multielement TMMS AF instrument, an extensive experimental study was conducted and the results of these studies are presented in this section. The first subsection is concerned with the optimization of critical variables in the single element AF mode. The second subsection presents the results for single element AF measurements of 10 elements under optimized conditions. The results are presented in the form of calibration curves, S/N curves and detection limits. The third subsection deals with measurements of four elements in the multielement AF mode in two types of flames. Nondispersive AF multielement measurements are discussed in the final section.

In all these studies, mode 2 or 3 was used. In these modes, the microcomputer is used for control of experimental variables and data acquisition. This allows the operator to change conveniently the magnitude of experimental variables with software rather than through time consuming hardware changes. Computer controlled data acquisition and calculation saves a considerable amount of the operator's time by reducing post-measurement calculation time.

Optimization Studies

Effect of type of lamp pulsing circuit

In the instrumental section, two configurations were presented for pulsing the HCL's. In the unregulated configuration (Figure 3B), the lamp current is determined by a ballast resistor and the

resistance of the lamp. In the regulated configuration (Figure 13), a feedback circuit is used to maintain the lamp current constant even if the lamp resistance varies.

To compare these two configurations, the radiation from the Cu HCL was focused with the entrance lens directly on the entrance slit and pulsed with a 10 ms pulse width and 12.5% duty cycle. Each data point is the sum of 100 laps (8 s total acquisition time). Twenty data points were collected for each configuration and the mean signal, SD, and S/N were automatically calculated and reported by the microcomputer. The relative standard deviation (RSD) is calculated from the inverse of the S/N. The means and RSD's from ten such runs were averaged. This whole experiment was repeated on two separate occasions and the results are reported in Table IV.

Table IV. Effect of Lamp Pulsing Configuration on Precision[a]

	With Feedback Circuit		Without Feedback Circuit	
Experiment No.	Mean Signal[b]	%RSD	Mean Signal[b]	%RSD
1	25	0.15	22	1.5
2	18	0.18	18	1.3

[a]The experiments were performed in mode 3 under the following conditions: R_f, 1 MΩ; $(i_{rms})_{HCL}$, 4 mA; ℓ, 100; PMT voltage, 400 V; t_p, 10 ms; t_d, 0.2 ms; , 0.1 ms; %DC, 12.5; wavelength, 325 nm.

[b]peak photocathodic current x 10^{11} A.

The results in Table IV indicate that the feedback configuration increases the lamp output stability by about a factor of ten compared to operation without current feedback. Therefore the feedback configuration was used for all further studies, unless otherwise noted. Signal shot noise is insignificant in that the %RSD would be less than 0.01% if signal shot noise was limiting.

Effect of data acquisition mode

In mode 2, the V/F converter (Figure 9, dashed line) is used for data acquisition and the signal is integrated over the whole lamp pulse except during the delay time t_d. An ADC is used for data acquisition in mode 3 (Figure 9, solid line) where the number of data points acquired during a lamp pulse is determined by the pulse width (t_p) chosen and t_d.

The radiation from the Co HCL was focused with the entrance lens on the entrance slit. A beam splitter was placed between the HCL and the lens to reduce the lamp signal so measurements would be resolution limited. For each mode, 20 data points were collected where each data point represents the sum of the signals from 100 laps. The mean signal, SD, and S/N from the 20 data points were calculated and reported by the computer. The RSD was calculated from the S/N. The experiment was performed for low and high lamp currents as well as with 10 and 1 ms pulse widths. The delay time was 0.5 ms for both modes. For mode 3, 48 data acquisitions were made collected during a given 10 ms pulse and 3 data acquisitions were made acquired during a 1 ms pulse. For each condition, 6 runs of 20 data points were made

and the average mean signal and RSD of these runs are reported in Table V.

Table V. Comparison Between Modes 2 and 3[a]

t_p (ms)	$(i_p)_{HCL}$ (mA)	ADC			V/F		
		Mean Signal[d]	%RSD	%Rel. Res.[e]	Mean Signal[d]	%RSD	%Rel. Res.[f]
10[b]	27	4.7	0.36	0.15	5.7	0.7	0.38
1[b]	27	4.7	1.7	0.60	6.2	6.4	6.5
1[c]	295	210	0.37	0.01	270	0.39	0.15

[a]PMT voltage, 1000 V; R_f, 1 MΩ; τ, 0.1 ms; wavelength, 241 nm; $(i_{rms})_{HCL}$, 3 mA; t_d, 0.5 ms; ℓ, 100.

[b]%DC, 12.5.

[c]%DC, 1.

[d]peak photocathodic current x 10^{15} A.

[e]calculated from $(2.4 \times 10^{-3})/(E_p(q\ell)^{1/2})$

[f]calculated from $\ell^{1/2}/N$.

The results in Table V indicate that a significant difference between the two systems appears only for a small pulse width in combination with a low HCL peak current. The results from this study are in harmony with the conclusions from Table III about the resolution limitations of mode 2 for small pulse widths.

The calculated relative resolution for both modes is also shown in Table V. These agree reasonably well with the experimental RSD's. Because the light levels measured were low, the signal shot noise is on the order of the readout resolution. Mode 3 was used for all

other studies, unless otherwise noted, because of the resolution limitations of mode 2 for small lamp pulse widths.

Delay Time and Time Constant

When current is applied to a HCL, it takes a finite time for the I/V converter output to reach its maximum value due to time constant of the I/V converter, the response time of HCL pulsing circuit and the response time of HCL. The delay time (t_d) before data acquisition should be long enough that the signal reaches near its maximum value. However, t_d should not be too long as this restricts the data collection period (t_c). In mode 3 of operation, it takes about 0.2 ms to acquire and store a data point. For short pulse widths, a long delay time, significantly limits the number of readings per pulse.

The effect of the I/V time constant (τ) and t_d was evaluated by making measurements with the radiation from the Zn HCL focused on the entrance slit with the entrance lens. Table VI show how mean and the S/N of the HCL signal depends upon τ where t_d is adjusted to a constant value of 0.15 ms. Four readings were taken during each 1.0 ms pulse. The mean signal and S/N reported are the average from 3 runs of 20 data points.

The data indicate that the larger τ causes about a 3% decrease in signal and about a 50% improvement in S/N. The signal decreases with a larger τ because the lamp signal has not reached its maximum value when the data collection starts. The S/N improves because the noise equivalent bandpass is reduced with a larger τ. This reduces the noise observed by the ADC.

Table VI. Effect of Time Constant[a]

τ (ms)	Mean Signal[b]	S/N[c]
0.03	37	23
0.1	36	36

[a]rms HCL current, 5 mA; t_p, 1 ms; %DC, 12.5; ℓ, 100; R_f, 1 MΩ; PMT voltage, 1000 V.

[b]Mean peak photocathodic current x 10^{16} A.

[c]Mean signal divided by standard deviation.

The effect of delay time on the mean signal and S/N is shown in Table VII. The conditions are the same as in the previous experiment (Table VI) except is kept constant at 0.1 ms and t_d and the number of readings per pulse are varied.

Table VII. Effect of Delay Time

Delay Time (ms)	# of Readings	Mean Signal[a]	S/N
0.3	4	36	31
0.5	3	37	31

[a]Mean peak photocathodic current x 10^{16} A.

Table VII shows that increasing t_d from 0.3 to 0.5 ms reduces the number of readings per pulse from 4 to 3 and increases the mean signal by about 4% because the lamp signal reaches its maximum before data collection starts. The S/N does not change significantly. Theoretically the noise should increase by a factor of $(4/3)^{1/2}$ due to

the decreased number of readings. This is not observed because of the uncertainty in measuring the S/N and the slight increase in the signal. For all further measurements, a τ of 0.1 ms and a t_d of 0.5 ms were employed, unless otherwise noted.

Effect of HCL peak current on the lamp signal

In AF measurements, high intensity sources are employed to achieve better detection limits. In this and other research, HCL's are operated in a short pulse width, high peak current mode to produce a large radiant intensity during the pulse. Pulsed HCL's have been shown (42,57) to produce better S/N's than DC operated lamps in AF measurements because the total noise observed from the flame is reduced by acquiring data only during the HCL pulse.

To determine the effect of the HCL peak current on the radiant power output, a 1 ms pulse width was chosen. This is the minimum t_p provided by the software written which uses a microcomputer timer to generate the pulses. The radiation from the HCL's was focused on the entrance slit with the entrance lens. Five data points were collected for each HCL peak current, and each data point consists of 1 lap. The maximum HCL rms current chosen was 10 mA which is 2/3 of maximum rms current allowed for the HCL's used. The minimum duty cycle allowed by the program is 1% which yield a maximum peak HCL peak current of about 1000 mA or 1 A. Higher HCL currents can damage the HCL load resistor (Figure 3) or the HCL. The HCL peak current can be changed two ways as shown in equation 3. Either the percent duty cycle (%DC) can be varied with a constant rms HCL current ($(i_{rms})_{HCL}$) or $(i_{rms})_{HCL}$ can be changed with a constant %DC.

Figures 19 and 20 show the dependence of lamp intensity on HCL peak current. For the data in Figure 19, $(i_{rms})_{HCL}$ was kept constant at 10 mA and the peak HCL current was changed by changing the duty cycle from 1 to 12.5% for the Co and Cu HCL's. In the case of Figure 20, the %DC was kept constant at 1% and $(i_{rms})_{HCL}$ was varied from 1 to 10 mA to change the HCL peak current for the Co, Zn, and Cu HCL's.

In both experiments, the log-log plots are linear with slopes of 1.06 - 1.47 over most of the HCL current range studied. A negative deviation in the plots is observed for the Zn HCL at about 900 mA and for the Co HCL at about 700 mA. This negative deviation could be due to self-absorption and self reversal. Self-absorption in HCL's occurs when photons emitted by excited atoms within the emitting volume are reabsorbed by other ground state atoms before escaping. This is more likely to occur at higher currents because a larger or denser cloud of atoms is produced at the surface of the cathode. Self-reversal occurs when the radiation from the center of the emission line of the atoms in the center of emitting volume is absorbed to a greater extent then radiation in the wings of the emission profile (50, 52-53).

Piepmeier (50, 52-53) observed line profile changes during the application of current pulses to HCL's due to self-reversal and self-absorption. The results of one study (52) showed that, for a given HCL and current, the amount of self-absorption decreases with decreasing modulation frequency; the best line profile shape is obtained at a pulse duration of about 1 ms; and for a given frequency, self-reversal increases with increasing peak HCL current.

No significant difference was observed between the two modes of

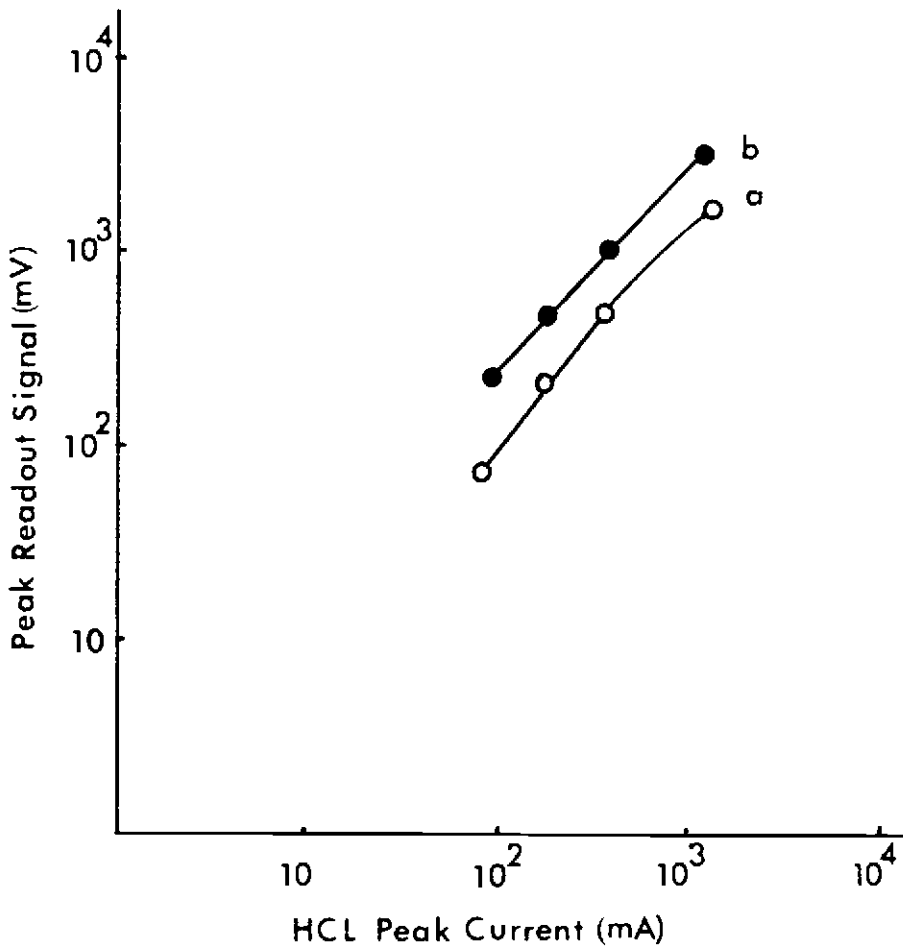

Figure 19. Dependence of the HCL signal on peak HCL current with a variable duty cycle. a, Co HCL (λ = 241 nm); b, Cu HCL (λ = 325 nm); R_f, 1 MΩ; τ, 0.1 ms; t_d, 0.5 ms; ℓ, 1; PMT voltage, 400 V; $(i_{rms})_{HCL}$, 10 mA; t_p, 1 ms; # of readings per pulse, 3.

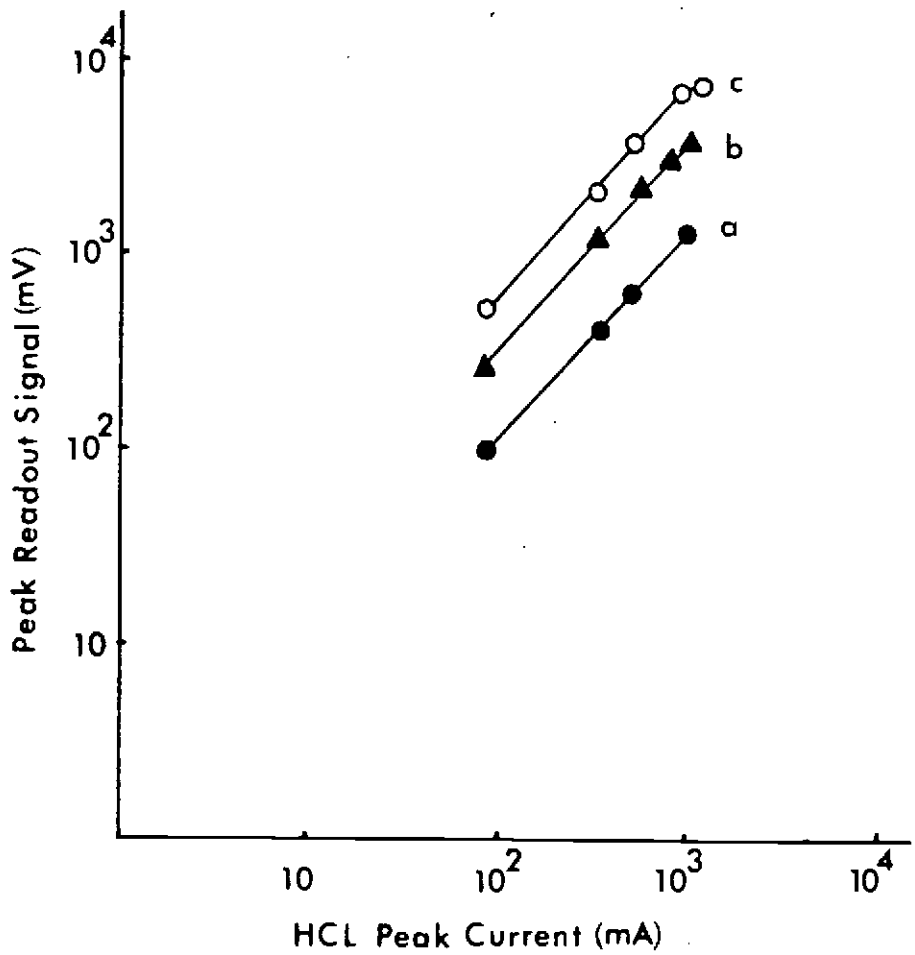

Figure 20. Dependence of HCL signal on HCL peak current with a constant duty cycle. a, Cd HCL (λ = 224 nm); b, Cu HCL (λ = 325 nm); c, Zn HCL (λ = 214 nm); conditions same as Figure 19 except %DC = 1.

varying the HCL peak current. Both modes yield the same log-log slope for the Cu HCL. Mode 1 (variable %DC) was used to vary the HCL peak current in most further studies.

Burner head comparison

The three burner heads available were compared under identical conditions with Co as the analyte (10 mg/L) to choose the burner head to use for the rest of the study. Table VIII show the results of the this study.

Table VIII. Burner Head Comparison[a]

Burner Head	Signal[b]	$(S/N)_{bk}$	S/N
Meker with safety collar	4.2	150	36
capillary	2.6	52	23
Meker	3.5	91	27

[a]The means and S/N's reported are the means for two runs of 20 data points; ℓ, 100; $(i_{rms})_{HCL}$, 10 mA; %DC, 12.5; burner height, 2.8 cm; H_2 flow rate, 4.4 L/min; air flow rate, 5.6 L/min; t_p, 10 ms; R_f, 1 MΩ; PMT voltage, 1000 V; wavelength, 241 nm.

[b]peak photocathodic analyte fluorescence signal x 10^{15} A.

The Meker burner with the safety plug provides the best S/N's while the capillary burner yields the worst S/N's. The Meker burner (without a safety collar) was chosen for all further studies because

it provides reasonable S/N's and be used with the water cooling and argon gas sheathing. Water cooling maintains the burner head at lower temperature during long operation times and reduces the possibility of combustion of gases inside of the burner head. Argon gas sheathing increases the S/N as discussed in a later section.

The capillary burner head can also be used with Ar gas sheathing and is safe with respect to flashback. The long capillary tubes in the capillary burner head do not allow the flame to burn back into the nebulizer chamber if the burning velocity exceeds the gas supply velocity. However, the loss in S/N with this burner is significant.

Burner height

The burner height is defined as the distance from the top of the burner head to the optical axis as defined by the center of the entrance slit of the monochromator. It must be optimized for the best S/N for each element and set of experimental conditions. An initial burner height optimization study was conducted with copper (10 mg/L) and the Meker burner head to establish the general region of optimum burner height. Later on in single element studies, it is shown that there is not a significant difference in the optimum region of burner height for most elements.

Figures 21, 22, and 23 show plots of S, S/N, and $(S/N)_{bk}$ vs burner height for two different H_2 flow rates. Figure 21 indicates that the maximum signal is obtained for burner height values in the 1.5 - 2.5 cm region. The signal is larger with a larger H_2 flow rate. As Figure 22 shows, the best S/N is obtained at lower burner

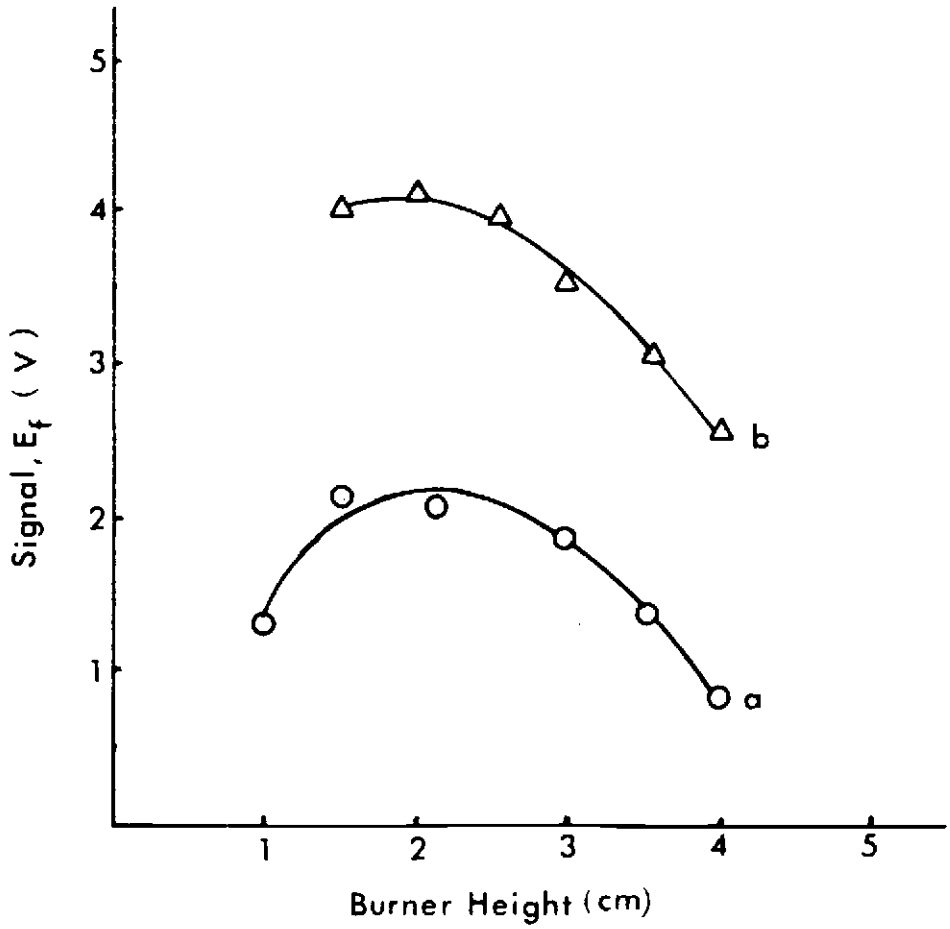

Figure 21. Dependence of signal on burner height. a, H_2 flow rate = 0.8 L/min; b, H_2 flow rate = 2.8 L/min; t_p, 10 ms; $(i_{rms})_{HCL}$, 10 mA; %DC, 12.5; number of data points, 10; ℓ, 25; air flow rate, 4.6 L/min; 10 mg/L Cu solution; R_f, 1 MΩ; E_{PMT}, 1000 V; number of runs, 1; t_d, 0.5 ms; λ, 325 nm.

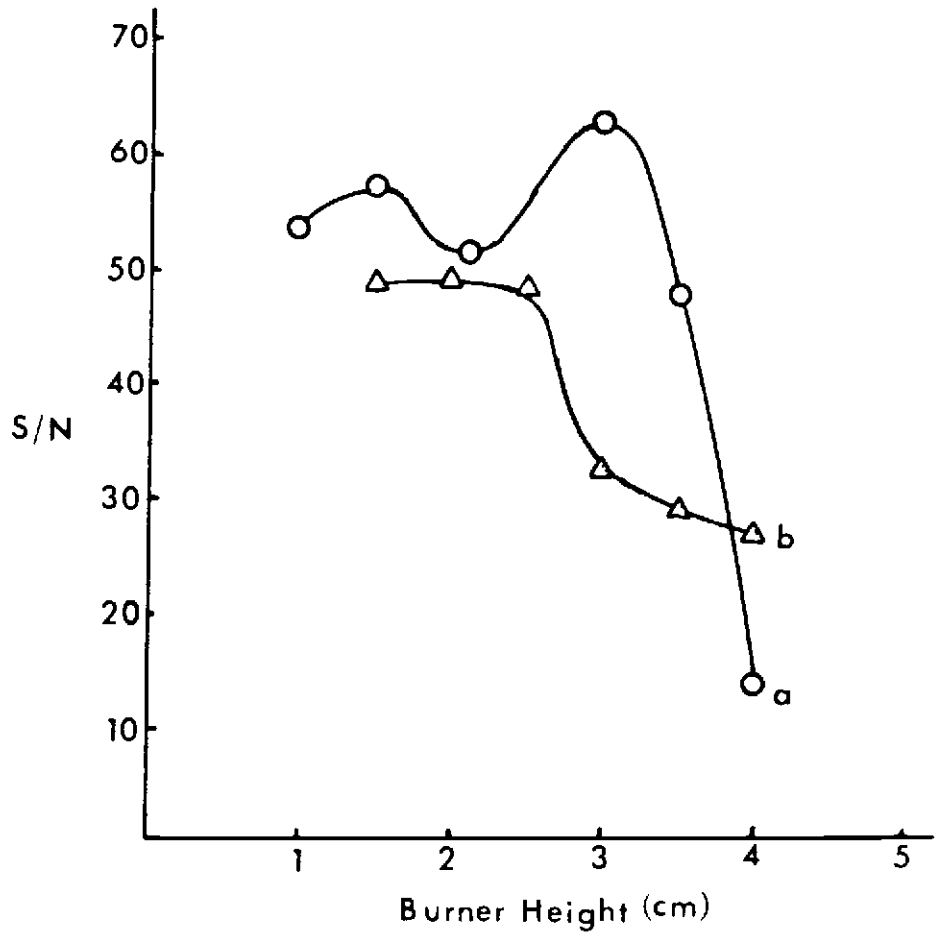

Figure 22. Dependence of S/N on burner height. a, H_2 flow rate = 0.8 L/min; b, H_2 flow rate = 2.8 L/min; other experimental conditions are the same as Figure 21.

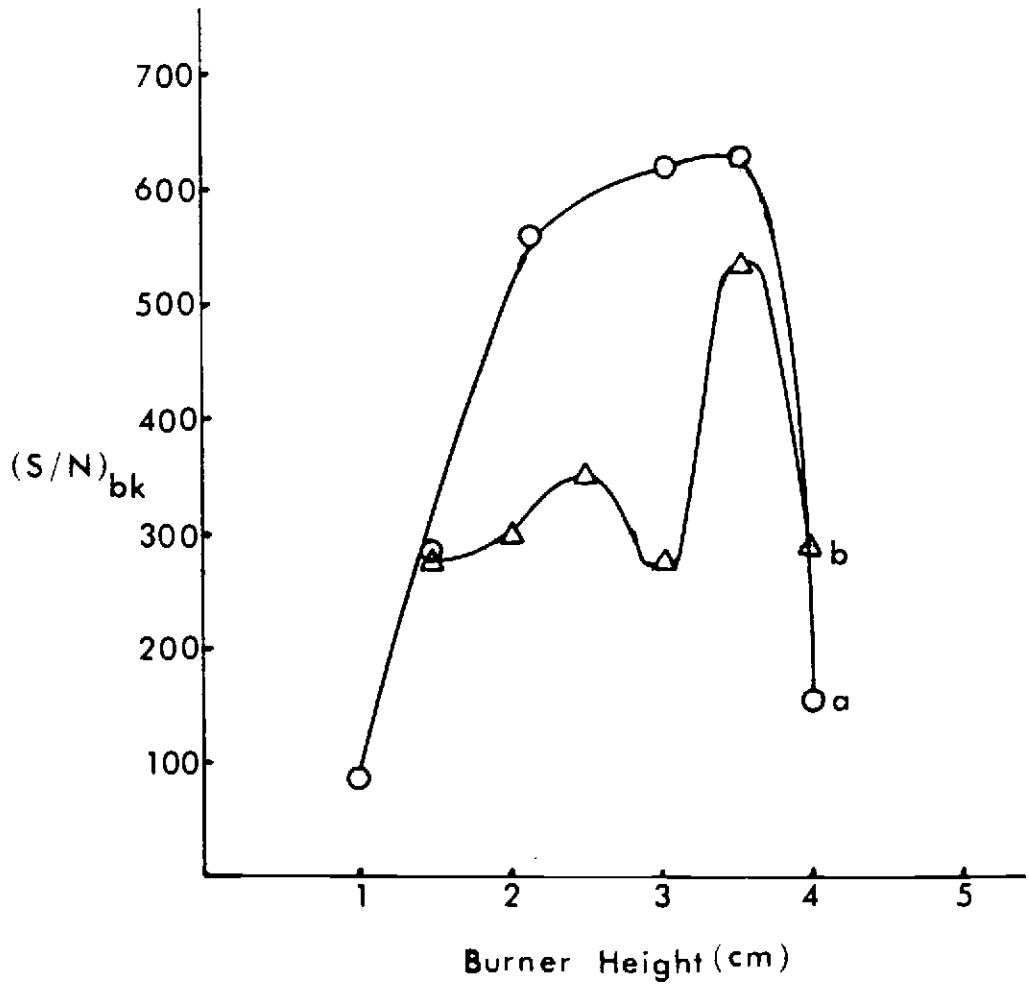

Figure 23. Dependence of $(S/N)_{bk}$ on burner height. a, H_2 flow rate = 0.8 L/min; b, H_2 flow rate = 2.8 L/min; other experimental conditions are the same as Figure 21.

heights (1.5 - 3 cm). This occurs because the signal is greater at lower burner heights but the noise (σ_F) is fairly independent of burner height. The S/N is better at the lower H_2 flow rate. The noise increases slightly with burner height at the higher H_2 flow rate and decreases slightly with burner height for the lower H_2 flow rate.

The plots of $(S/N)_{bk}$ versus burner height (Figure 23) show a broad optimum between 2 and 3.5 cm for the lower H_2 flow rate. The S/N optimum is at a larger burner height than the signal optimum because the background noise (σ_{bft}) decreases with increasing burner height as the background signal decreases. The magnitude of $(S/N)_{bk}$ is generally lower with the larger H_2 flow rate because of increased background signal and noise. For further studies, a burner height of 2.0 - 3.5 cm was used as this range provides the best S/N's.

Air flow rate

It was decided to optimize the air flow rate first since it controls the solution nebulization rate. The hydrogen flow rate was later varied to optimized the flame stoichiometry. Argon gas sheathing was employed in this and further studies to reduce the flame background emission signal and noise. Table IX show the effect of air flow rate on the solution flow rate. As expected the solution flow rate increases with increasing air flow rate.

The effect of the air flow rate on the S/N and $(S/N)_{bk}$ for Cu and Mg is show in Figure 24. Both S/N's are best at an air flow rate of 4.6 - 4.8 L/min for both elements and this air flow rate range was used for further studies. The blank noise (σ_{bft}) is relatively

Table IX. Effect of Air Flow Rate on Solution Flow Rate

Air Flow Rate (L/min)	Solution Flow Rate (mL/min)
1.9	0
3.2	1.3
4.0	3
4.8	4
5.7	6

independent of the air flow rate so that the increase in $(S/N)_{bk}$ with increasing flow rate is due primarily to an increase in the AF signal with flow rate. The decrease in $(S/N)_{bk}$ at the highest air flow rate is due to an increase in σ_{bft}.

H_2 flow rate

The H_2 flow rate is a critical variable to optimize. For a constant air flow rate, the H_2 flow rate affects the flame stoichiometry which in turn affects the atomization efficiency and background emission signal and noise. The dependence of the AF signal, S/N, and $(S/N)_{bk}$ on the H_2 flow rate over the 0.8 - 5.6 L/min range was studied for Ni, Co, Fe, Mn, Mg, Cu, Au, Pb, Zn, and Cd.

One goal of this study was to determine the optimum H_2 flow rate for each of the test elements. Another goal was to determine what set of elements could be measured under near optimum conditions in a multielement mode with the same H_2 flow rate.

For the elements Au, Zn, Cd, and Cu, the AF signals are relatively independent (within a factor of 2) of the H_2 flow rate. For the other six elements, plots of the AF signal vs H_2 flow rate

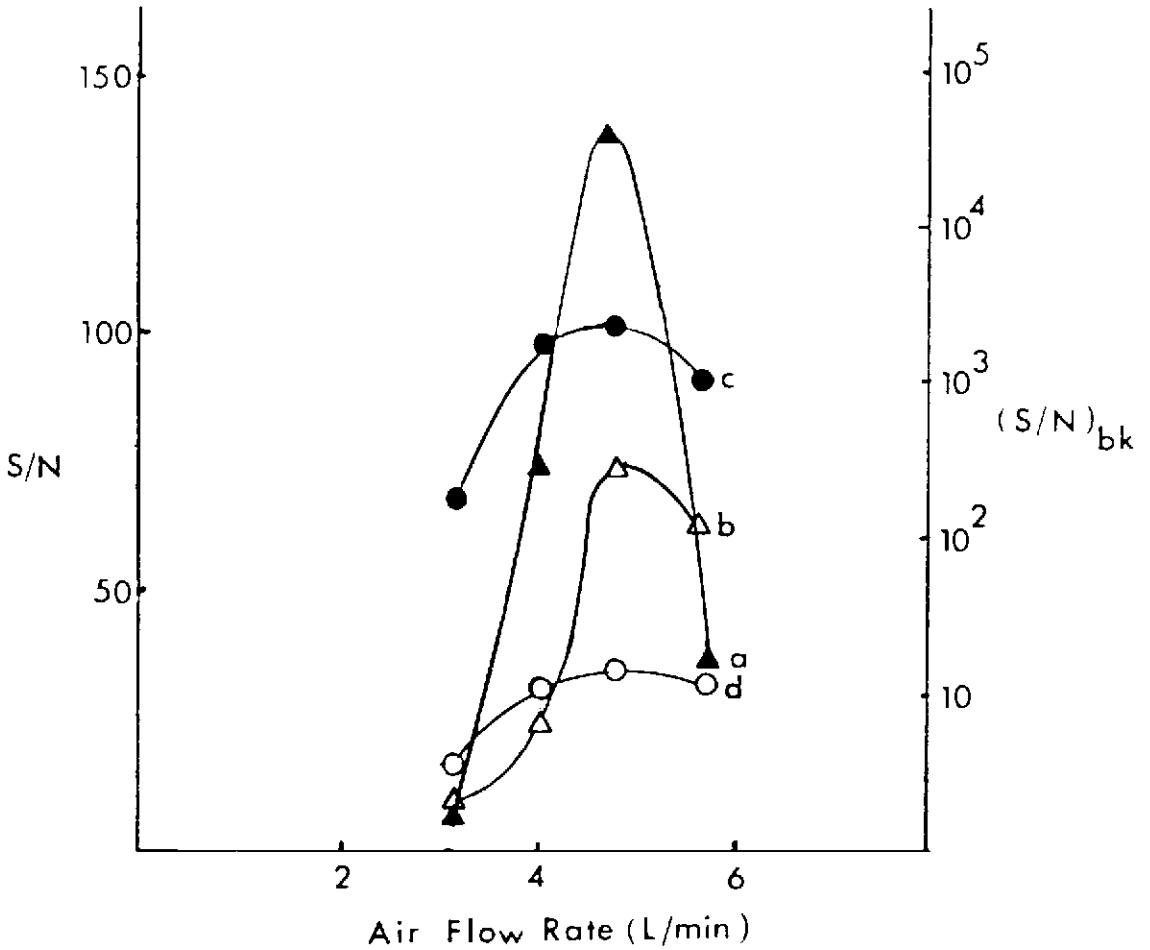

Figure 24. Dependence of S/N and $(S/N)_{bk}$ on air flow rate. a, S/N for Mg; b, S/N for Cu; c, $(S/N)_{bk}$ for Mg; d, $(S/N)_{bk}$ for Cu; $(i_{rms})_{HCL}$, 15 mA; H_2 flow rate, 3.7 L/min; Argon flow rate, 4.4 L/min; number of data points, 30; ℓ, 100; burner height, 2 cm; %DC, 12.5; R_f, 1 MΩ; E_{PMT}, 1000 V; concentrations, 10 mg/L; number of runs, 1; wavelengths (in nm), Mg (285), Cu (325); t_p, 1 ms.

show an initial dramatic increase in the AF signal up to a point followed by a plateau region. For Co, Pb, and Ni, the AF signal is relatively constant above a H_2 flow rate of about 2.5 L/min, while for Mg, Mn, and Fe, the plateau region does occur until about 3.5 L/min. Apparently a fuel rich flame is required for more complete atomization of these latter 6 elements. Figure 25 show the dependence of the AF signal for Mg on H_2 flow rate which is typical of the elements that are more difficult to atomize.

For the elements that are easier to atomize (Au, Zn, Cd, and Cu), the $(S/N)_{bk}$ is independent of H_2 flow rate within a factor of two for Cd and Zn. For Au and Cu, the $(S/N)_{bk}$ and hence detection limits, are better by a factor of 2 - 3 at low H_2 flow rates (e.g., 1 L/min) because the background emission noise is less in a leaner flame.

In the case of elements that are more difficult to atomize (Ni, Co, Fe, Mn, Pb, and Mg), the blank noise (σ_{bft}) is relatively independent of the H_2 flow rate. Therefore the dependence of the $(S/N)_{bk}$ on H_2 flow rate tracks the dependence of the AF signal. The $(S/N)_{bk}$ becomes relatively independent of the H_2 flow rate above 2.5 - 3.5 L/min. This type of dependence is also illustrated in Figure 25 for Mg.

Based on the air flow rate, the oxygen flow rate is about 1 L/min. Thus a 2 L/min H_2 flow rate should be required for a stoichiometric flame. For the elements more difficult to atomize, the flame must significantly fuel rich for the best results.

Argon flow rate

Argon (Ar) gas was used as sheathing gas to reduce the

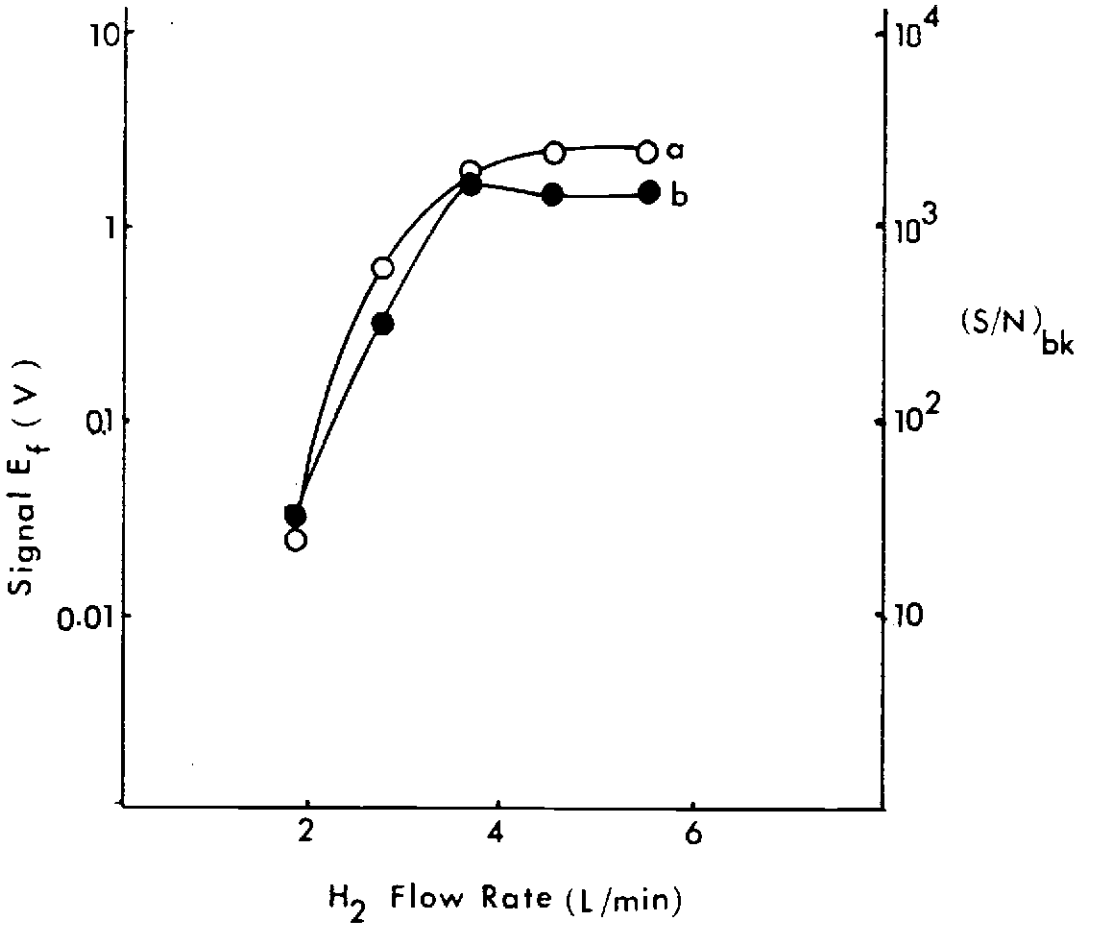

Figure 25. Dependence of AF signal and $(S/N)_{bk}$ on H_2 flow rate for Mg. a, peak fluorescence signal in V; b, $(S/N)_{bk} = E_f/\sigma_{bft}$; air flow rate, 4.8 L/min; Ar flow rate, 4.0 L/min; t_p, 1 ms, $(i_{rms})_{HCL}$, 8 mA; %DC, 12.5; number of data points, 20; ℓ, 100; 5 mg/L Mg solution, R_f, 1 MΩ; E_{PMT}, 1000 V; number of runs, 1; burner height, 2.8 cm; λ, 285 nm.

concentration of quenchers in the flame which decrease the AF signal and to reduce the flame background emission signal and noise by preventing entrainment of air. The AF signal and $(S/N)_{bk}$ for Cu, Mg, Cd, and Zn (0.5 mg/L) were determined with Ar flow rates of 0, 2.2, and 3.8 L/min with low and high H_2 flow rates and the results are shown in Table X. A 1 ms pulse width, 12.5% duty cycle, and 2.5 cm burner height were used.

Table X. Dependence of AF Signal, Blank Noise, and $(S/N)_{bk}$ on Ar Flow Rate[a]

Ar Flow Rate (L/min)	Element	H_2 Flow Rate, 0.80 L/min			H_2 Flow Rate, 4.6 L/min		
		E_f (mV)	σ_{bft} (mV)	$(S/N)_{bk}$	E_f (mV)	σ_{bft} (mV)	$(S/N)_{bk}$
0	Cd	16	0.64	25	15	4.4	3.3
2.2	Cd	18	0.76	24	17	3.2	5.1
3.8	Cd	19	0.86	22	15	1.9	7.7
0	Cu	19	0.76	25	45	4.2	11
2.2	Cu	39	0.82	47	49	3.6	13
3.8	Cu	43	1.0	42	49	1.7	29
0	Mg	--	0.75	--	410	4.1	99
2.2	Mg	--	0.72	--	650	3.0	220
3.8	Mg	--	0.80	--	800	1.8	430
0	Zn	1.3	0.59	2.3	--	4.3	--
2.2	Zn	2.4	0.50	4.8	--	3.4	--
3.8	Zn	3.3	0.53	6.2	--	1.9	--

[a]Number of runs, 1; number of data points, 20; ℓ, 100; E_{PMT}, 1000 V; R_f, 1 MΩ; wavelengths (in nm), Cd (229), Cu (325), Mg 285, Zn (214); rms HCL currents (in mA), Cd (14), Cu (14), Mg (14), Zn (13).

At the lower H_2 flow rate (0.8 L/min), the signal for Mg was insignificant as expected in a lean flame. The blank noise is primarily dark current noise so that the Ar flow rate has little effect

on σ_{bft}. For Cd, the Af signal and S/N are independent of Ar flow rate. For Zn and Cu, the AF signal and $(S/N)_{bk}$ increase about a factor of 2.5 as the flow rate is increased from 0 to 3.8 L/min.

With a higher H_2 flow rate (4.6 L/min), the blank noise increases a factor of 2 - 8 depending on the element due to the more luminous nature of the flame. The blank noise is primarily due to flame background emission noise. The Zn AF signal was too small to measure reliably at the concentration tested. The use of a 3.8 L/min Ar flow rate relative to no sheathing improves the $(S/N)_{bk}$ for Cd and Cu by a factor of 2 and 3, respectively, due to a reduction in background emission noise. For Mg, the $(S/N)_{bk}$ is enhanced by about a factor of 4 due to both an increase in signal and reduction of noise. The increase in the Mg AF signal may be due in part to a richer flame in the absence of air entrainment.

For all further studies, Ar sheathing at 3.8 L/min or slightly higher was employed. Although the effect of sheathing in negligible for some elements, improvements of a factor of 2 - 4 in $(S/N)_{bk}$ and detection limits are realized for some elements.

Dependence of AF signals on HCL peak current

A previous study in this section indicated that the HCL signal increases in a near linear fashion with respect to HCL peak current except near peak currents of 1 A. At higher HCL peak currents, the source line profile may be significantly broadened or exhibit self-absorption effects. Under these conditions, the AF signal is not expected to be proportional to the HCL signal since the fraction of

the source radiation absorbed decreases with significant line broadening.

To provide information to optimize the HCL peak current, the dependence of the AF signal on peak HCL current was measured at one concentration for each of the test elements with a 1 ms pulse width. The HCL peak current was increased by decreasing the %DC (typically from 12.5 to 1.25%) with a constant HCL rms current. The results are shown in Figures 26 and 27. The conditions for these measurements and important characteristics of these plots are presented in Table XI.

Table XI. Conditions and Characteristics for Plots of the[a] AF Calibration Sensitivity versus HCL Peak Current

Element	Conc. (mg/L)	λ (nm)	H_2 Flow Rate (L/min)	$(i_{rms})_{HCL}$ (mA)	Slope[b]	Critical $(i_p)_{HCL}$[c] (mA)
Au	5	267	1.5	12	0.35	(2)
Cd	2.5	224	0.8	8	0.75	150
Co	5	241	3.7	12	1.0	(1)
Cu	5	325	0.8	13	1.1	400
Fe	11	248	3.7	15	1.0	(1)
Mg	2	285	3.7	8	0.25	(2)
Mn	10	279	5	16	1.0	(1)
Ni	2	232	3.7	15	0.90	(1)
Pb	50	283	0.8	6	0.45	(2)
Zn	2.5	214	2.8	13	0.25	(2)

[a] air flow rate, 4.8 L/min; flame height, 2.8 cm; E_{PMT}, 1000 V; R_f, 1 MΩ; # of runs, 1; # of data points, 20; t_p, 1 ms; ℓ, 100.

[b] log-log slope for linear curves or for lower portion of non-linear curves.

[c] approximate peak HCL current where log-log slope is less than 0.5; (1) and (2) indicate that the slope is greater or less than 0.5, respectively, over whole HCL peak current range studied.

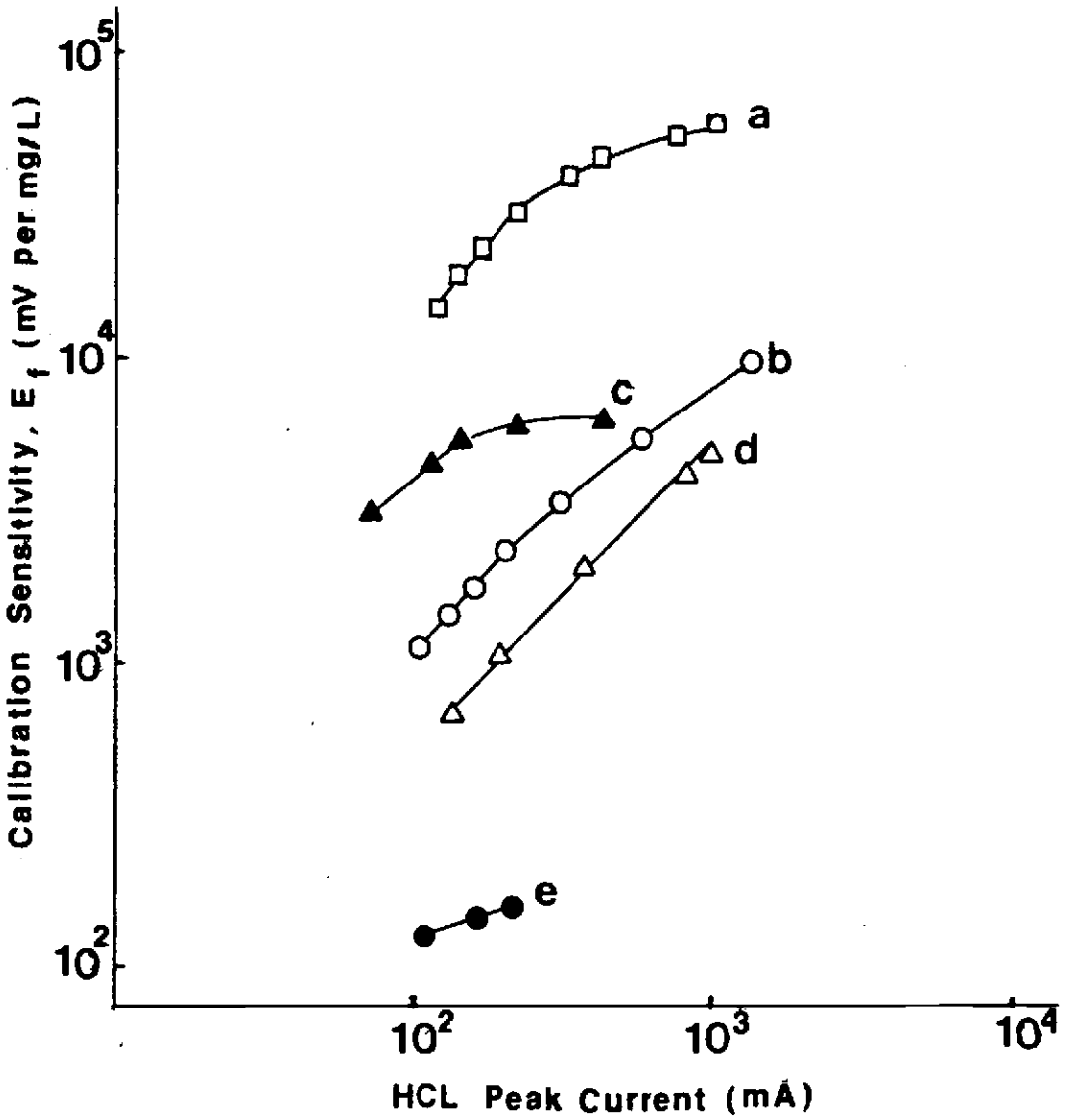

Figure 26. Dependence of calibration sensitivity on HCL peak current for Au, Cd, Co, Cu, Fe. a, Cu; b, Co; c, Cd; d, Fe; e, Au; see Table XI for experimental conditions.

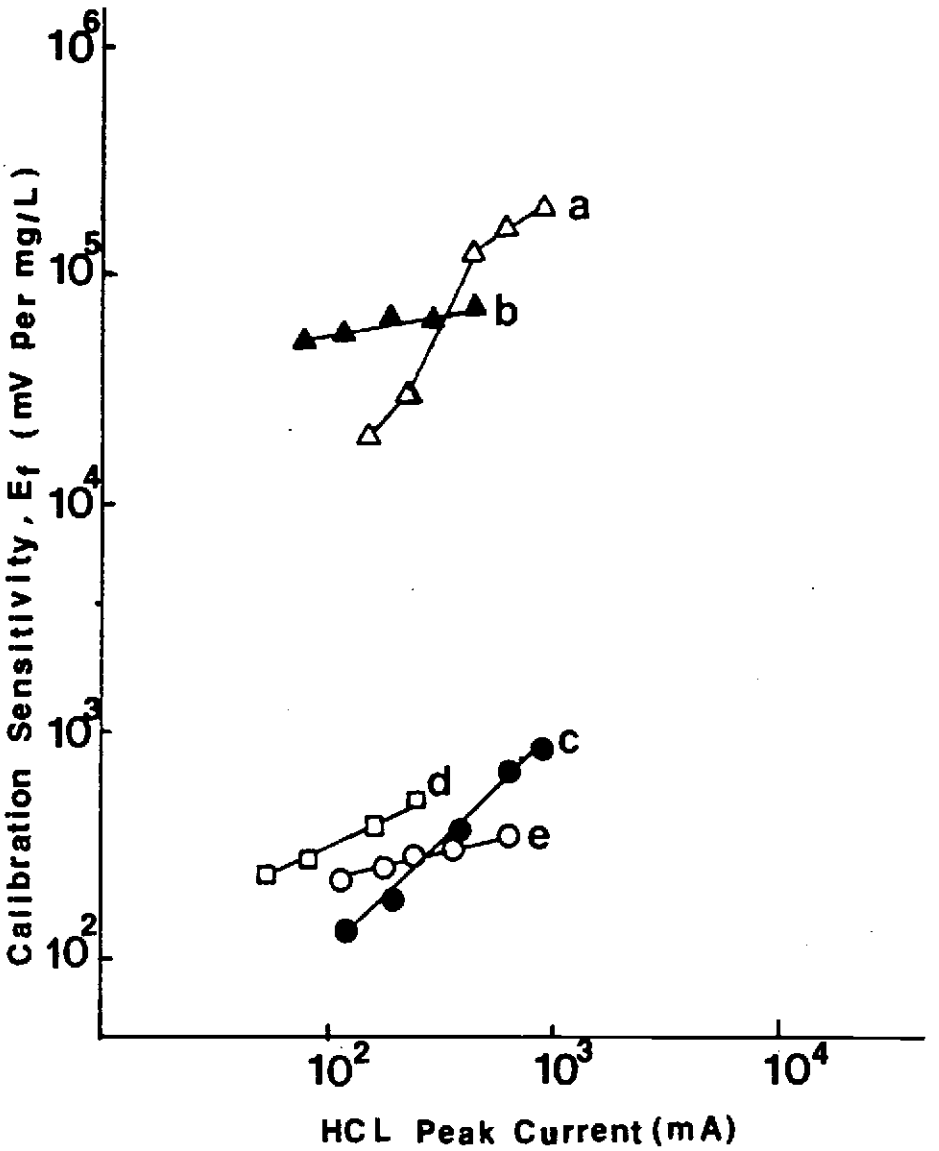

Figure 27. Dependence of calibration sensitivity on HCL peak current. a, Mn; b, Mg; c, Ni; d, Pb; e, Zn; see Table XI for experimental conditions.

Note that plots of $(S/N)_{bk}$ versus $(ip)_{HCL}$ show the same dependence as the curves in Figure 26 and 27 since the background noise is constant with a constant HCL pulse width. For a given pulse width, the highest allowable HCL peak current provides the largest peak AF signal and hence $(S/N)_{bk}$.

To optimize the $(S/N)_{bk}$, and hence the detection limit which is inversely proportional to $(S/N)_{bk}$, one must also consider the total time for a data collection run which is the product of the lap time and number of laps ($t_L \ell$). To keep total lap measurement constant, then ratio $\%DC/t_p$ must be kept constant (equation 2). Thus with a larger pulse width, the %DC must be corresponding larger. For a constant HCL rms current, an increased %DC requires that the peak HCL current be reduced (equation 3). Under these conditions (constant measurement time and HCL rms current) the smallest pulse width and largest possible HCL peak current do not necessarily provide the best $(S/N)_{bk}$.

The $(S/N)_{bk}$ is calculated from equation 16 as E_f/σ_{bft}. For white noise, σ_{bft} is proportional to $(t_p)^{-1/2}$ because the averaging time increases with pulse width (i.e. $\sigma_{bft} \propto \Delta f^{1/2} \propto t^{-1/2}$). The peak signal E_f decreases with increasing t_p (for a given HCL rms current and lap time) but the exact relationship depends on the element.

Consider the case where t_p is decreased from 10 to 1 ms with a corresponding decrease in %DC from 12.5 to 1.25% and factor of ten increase in peak HCL current. The background noise increases by a factor of $(10)^{1/2}$. If there is a linear relationship between the AF peak signal (E_f) and peak HCL current, the peak AF signal is ten times

larger at a 1 ms pulse width providing an improvement in $(S/N)_{bk}$ of $(10)^{1/2}$. However, if the peak AF signal is only larger by a factor of $(10)^{1/2}$ or less at the smaller t_p, the $(S/N)_{bk}$ is the same or worse than with a 10 ms pulse width.

The data in Figures 26 and 27 can be used to pick the optimum HCL peak current and pulse width for a given lap time. For elements (Co, Fe, Mn, Ni) for which the log-log slope is greater than 1/2 (see Table XI) over the whole current range studied, the optimum current is the highest value and a small pulse width and large %DC should be used. For Au, Mg, Pb, and Zn, the slope is less than 1/2 over the whole current range studied and the lowest peak current and large t_p and %DC provides the best $(S/N)_{bk}$. With Cd and Cu the critical peak current specified in Table XI should be used because above this HCL peak current, the log-log slope is less than 1/2 and $(S/N)_{bk}$ would be less.

Cadmium is one of elements for which there is little gain in AF signal at higher peak HCL currents (see Figure 26). The decrease in $(S/N)_{bk}$ for Cd with a fixed lap time of 80 ms is illustrated in Figure 28. Here the %DC is varied from 12.5 to 1.25% to increase the peak HCL current. The pulse width is decreased from 10 to 1 ms to keep the lap time constant. Above a peak HCL current of 330 mA, the loss in $(S/N)_{bk}$ is obvious. Above this current, the peak AF increases little but the background noise increases significantly due to a smaller pulse width.

Figure 28 shows the results for the same type of study with Co. With Co the log-log slope is 1.0 over the range of peak HCL current studied (Figure 26) so there is little change in $(S/N)_{bk}$ with HCL peak

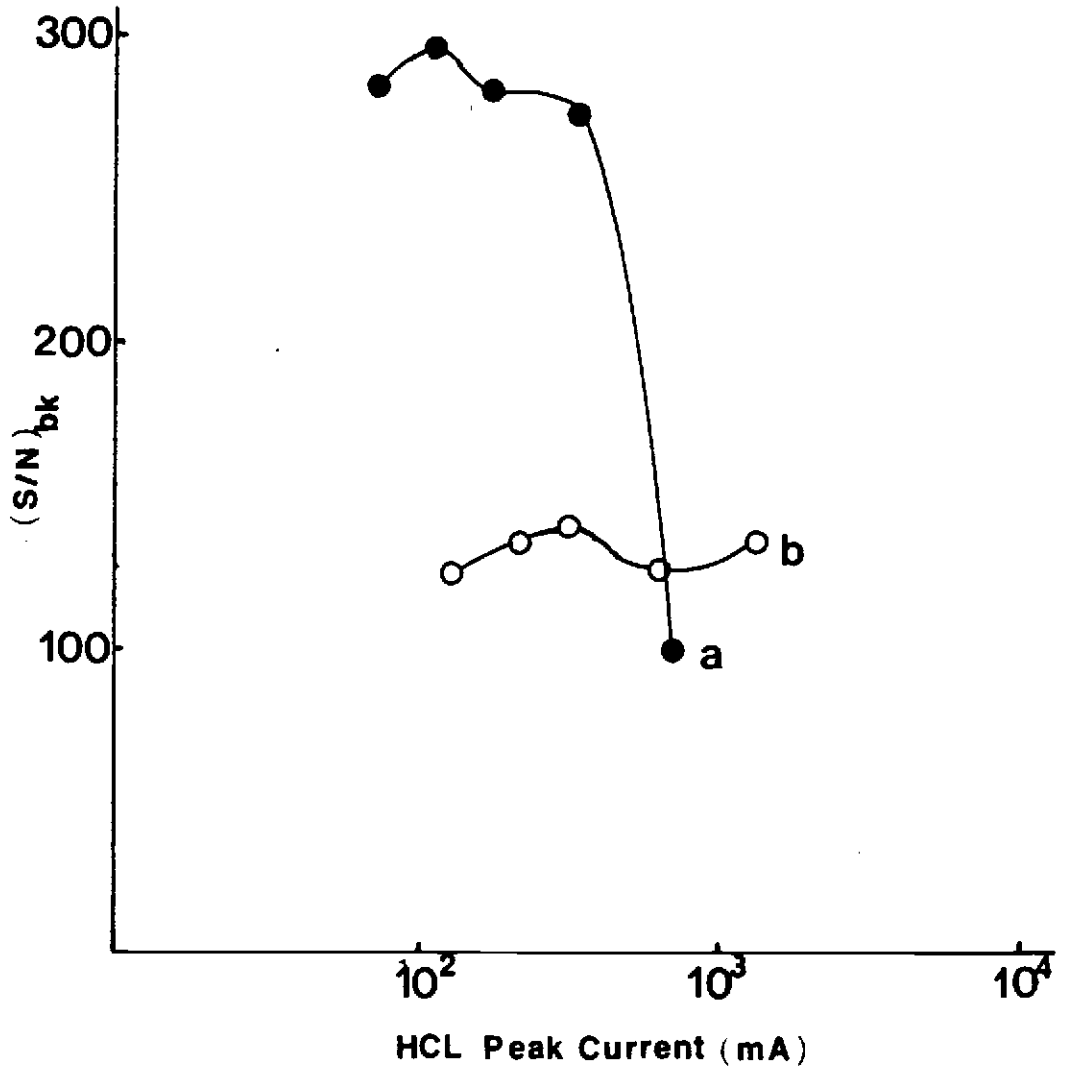

Figure 28. Dependence of $(S/N)_{bk}$ on HCL peak current for Cd and Co. a, Cd; b, Co; experimental conditions same as in Table XI except with a fixed lap time and $(i_{rms})_{HCL}$ of 15 mA for Co.

current.

At higher analyte concentrations, analyte fluorescence shot or flicker noise may be limiting. Under signal shot noise limiting conditions, the best S/N for a given pulse width is obtained at the highest HCL peak current. With the restriction of a fixed total measurement time, the S/N is proportional to $(E_f t_p)^{1/2}$. For many elements, the relative signal shot noise is less with a larger t_p and smaller $(i_p)_{HCL}$ because E_f is proportional to t_p^{-x} where x is smaller than 1.

Single Element Measurements

Detection limits

The information from the optimization studies was used to establish the conditions to measure the detection limits for the ten test elements in the single element mode (i.e. one slit open and one lamp pulsed at a time). With a lap time of 80 ms or total measurement time of 8 s for 100 laps, the %DC and pulse width were varied to find the values yielding the best detection limits. The optimum conditions and detection limits achieved are reported in Table XII.

For Au, Cd, Mg, Pb, and Zn the optimum pulse width is larger (i.e. 10 ms) and the optimum HCL peak current is smaller (i.e. 50 - 144 mA) than for the other elements. As previously noted for these elements, higher HCL peak currents provide little increase in the AF signal but a larger pulse width reduces the blank noise and improves the detection limit.

At the detection limit dark current noise is limiting or signifi-

Table XII. Single Element AF Detection Limits[a]

Element	Wavelength (nm)	DL (μg/L)	t_p (ms)	%DC	$(i_{rms})_{HCL}$ (ms)	i_p (mA)	H_2 Flow Rate (L/min)	k[b]	σ_{bft}[c]	σ_d[d]
Au	267	218	10	12.5	12	96	1.5	1.4	1.5	0.95
Cd	224	4.6	10	12.5	15	127	0.8	51	1.2	0.92
Co	241	26	2	2.5	15	614	3.7	4.1	5.3	3.0
Cu	325	3	2	2.5	15	614	0.8	480	7.5	2.9
Fe	248	50	2	2.5	16	652	4.6	21	5.3	4.0
Mg	285	0.8	10	12.5	16	136	3.7	2000	7.8	0.76
Mn	279	7	3.2	4	16	414	5.0	410	14	2.3
Ni	232	36	2	2.5	18	736	3.7	16	3.0	3.0
Pb	283	1030	10	12.5	6	52	0.8	0.47	2.4	0.84
Zn	214	21	10	12.5	13	111	2.3	12	1.3	1.0

[a]number of data points, 20; ℓ, 100; R_f, 1 MΩ; E_{PMT}, 1000 V; air flow rate, 4.8 L/min; Ar flow rate 3.8 - 4.2 L/min; # of runs, 1; flame height, 2.8 cm.

[b]calibration slope, peak photocathodic current signal x 10^{19} A/μg/L.

[c]photocathodic rms background noise x 10^{17} A.

[d]cathodic rms dark noise x 10^{17} A.

cant ($\sigma_{bft} \tilde{=} \sigma_{dt}$) for Au, Cd, Co, Fe, Ni, and Zn. For the other elements flame background emission noise limits the detection limit.

Calibration and precision curves

Five of the test elements, Cd, Co, Cu, Mg, and Zn were studied in more detail. All of these elements except Co were used by Salin (1) and in this research for multielement AF measurements. Repetitive measurements were made for each element in the single element mode over a large concentration range with a 1 ms pulse width. From this data the peak fluorescence signal (E_f), σ_{ft}, σ_{bft}, σ_{dt}, and σ_F were calculated. The results are presented in the form of calibration curves of E_f versus analyte concentration and of precision curves of the RSD in E_f (σ_F/E_f) versus analyte concentration. The total analyte emission noise (σ_{et}) was measured at high concentrations with the lamp off to determine if σ_{et} is a significant noise component. The shot noise in the analyte fluorescence signal was also calculated and compared to σ_{ft} to determine if fundamental shot noise is limiting at any concentrations.

All the calibration curves (Figure 29) exhibit typical behavior for AF measurements. The AF signal is linear with respect to analyte concentration at low analyte concentration. At moderate concentration negative deviation occurs. The AF signal is approximately 5% below the signal predected by extrapolation of the linear portion of the calibration curve at concentrations of 5, 50, 50, 25, and 25 mg/L for Cd, Co, Cu, Mg, and Zn, respectively. At high analyte concentrations, a plateau region is observed (Co) or the AF signal passes through a

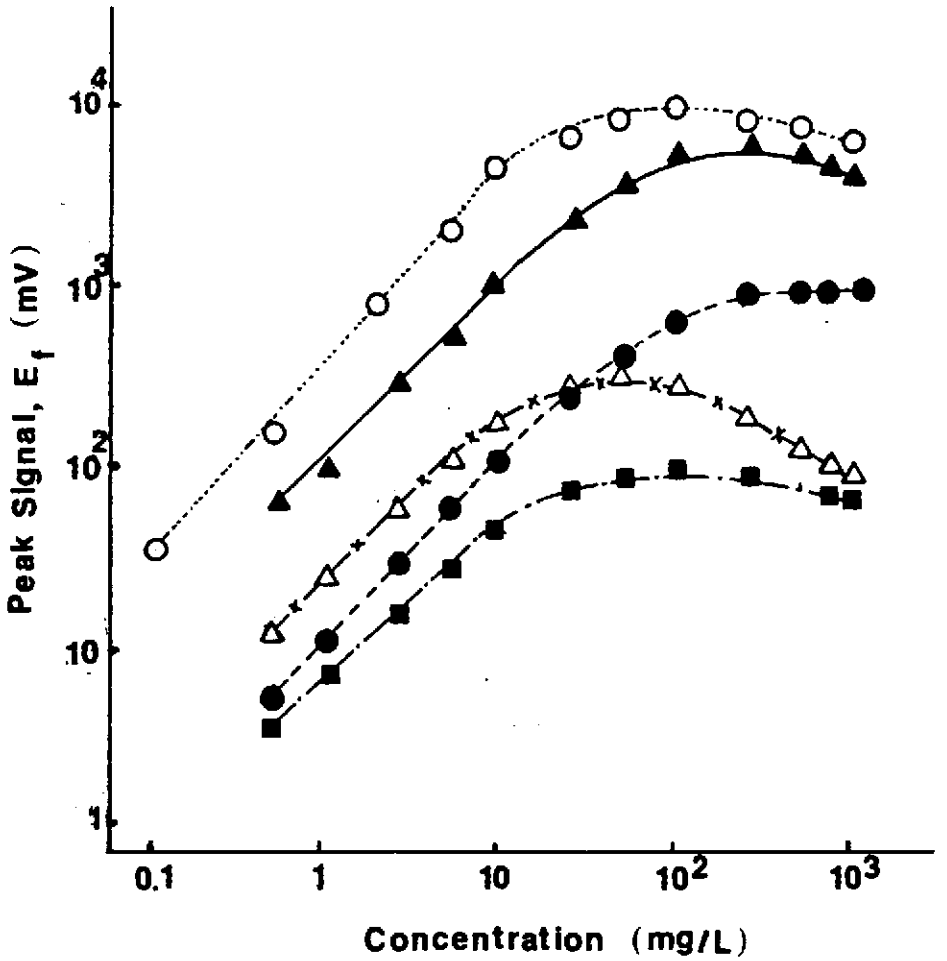

Figure 29. Single element calibration curves. △, Cd; ●, Co; ▲, Cu; ○, Mg; ■, Zn; conditions same as in Table XII except:

Element	%DC	$(i_{rms})_{HCL}$ (mA)	$(i_p)_{HCL}$ (mA)
Cd	4	8	211
Co	2	12	576
Cu	2	12	606
Mg	2	12	622
Zn	2	13	625

maximum and decreases at the highest concentrations (Cd, Cu, Mg, Zn).

The non-linear behavior is caused by several factors. Firstly, there is a inherent non-linear relationship between the fluorescence signal and concentration at high concentrations because the fraction of the source radiation absorbed at higher concentrations is not proportional to analyte concentration. Secondly, this effect is accentuated by source line broadening. The atomic absorption coefficient varies over the source profile. Thirdly, the prefilter or inner effect reduces the source intensity that reaches the viewed central part of the flame. Fourthly, the post filter effect or self-absorption results in attenuation of the fluorescence radiation. Fluorescence photons from the central viewed part of the flame are reabsorbed by analyte atoms in the outer part of the flame.

The degree of non-linearity caused by these affects increases with analyte concentration because the absorbance increases with analyte concentration. The prefilter effect causes the decrease in the AF signal at the highest concentrations. The concentration where the maximum in the calibration curve is reached varies with the element because the absorption coefficients and source profile widths of the elements are different.

The precision curves (Figure 30) all exhibit the same type of general behavior as noted for AF measurements of Cu by Bower and Ingle (84). At low concentrations, the precision improves as the concentration increases because the signal is increasing faster than the noise. The noise is relatively constant because the blank noise is dominant or significant and independent of the analyte concentration.

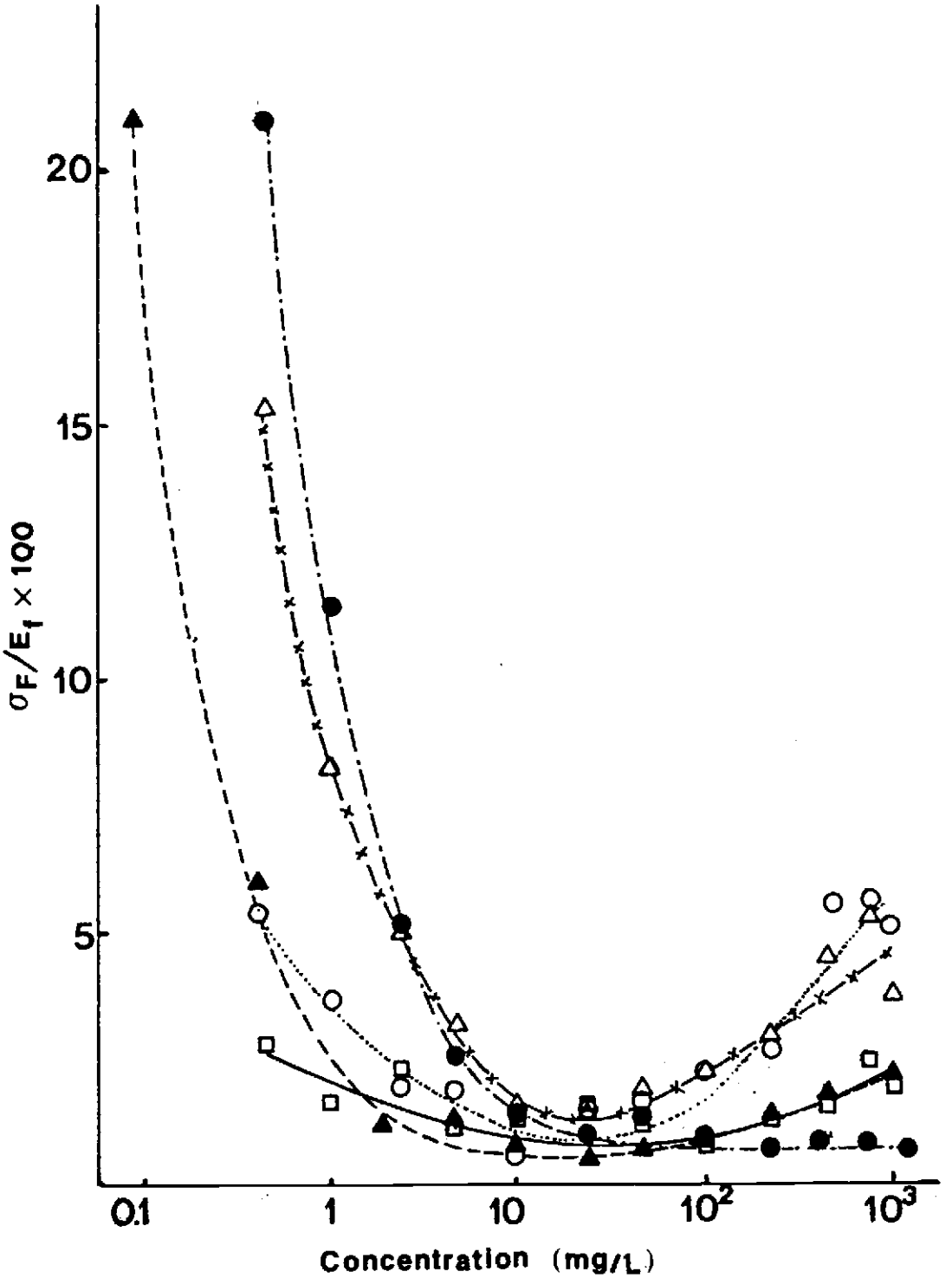

Figure 30. Single element precision curves. ○, Cd; ●, Co; □, Cu; ▲, Mg; △, Zn; conditions same as Figure 29.

In the moderate concentration range, the precision is relative constant (1 - 2% RSD). In this region, analyte fluorescence shot or flicker noise is dominant. At the highest concentrations (100 - 1000 mg/L) the precision decreases for all elements except Co. According to Bower and Ingle (84), this decrease in precision can be due to an increase in the analyte fluorescence flicker factor or in analyte emission noise.

Other measurements and calculations revealed more about the limiting noise sources. For Cd, Cu, and Zn the blank noise is primarily dark current or amplifier-readout noise ($\sigma_{dt} \cong \sigma_{bft}$). For Co and Mg, background emission is the limiting component of the blank noise ($\sigma_{bft} \cong 2\ \sigma_{dt}$ for Co and $\sigma_{bft} \cong 10\ \sigma_{dt}$ for Mg).

No significant analyte emission noise ($\sigma_{bft} > 0.5\ \sigma_{et}$) at the highest concentrations for Cd, Co, or Zn. For Cu and Mg, analyte emission is significant ($\sigma_{et} \cong 2\ \sigma_{bft}$) at the highest concentration. However the analyte emission noise is insignificant compared to the analyte fluorescence noise ($\sigma_{ft} >> \sigma_{et}$). Thus analyte emission noise does not account for the loss in precision at high concentrations observed for four of the elements.

Theoretical shot noise calculations were used to determine if fluorescence shot is significant in some cases. Since analyte fluorescence flicker and shot noise are proportional to the first power and square root of the fluorescence signal, respectively, signal shot noise is more likely to be significant for elements with a less intense fluorescence signal (smaller calibration sensitivity) and at lower concentrations. The calibration sensitivities for Mg and Cu are

the highest (see Figure 29). For Mg, analyte fluorescence shot noise is not limiting at any concentration and analyte fluorescence flicker noise is dominant ($\sigma_F > 3\,\sigma_{bft}$) at and above 5 mg/L. With Cu, analyte fluorescence flicker noise is dominant at and above 5 mg/L but significant between 0.5 and 2.5 mg/L.

The lower calibration sensitivities for Co, Zn, and Cd make it more likely that signal shot noise is dominant. Above 2.5 mg/L for Co, blank noise becomes insignificant and signal shot noise is limiting to the highest concentrations. The RSD becomes constant above 250 mg/L because the AF signal is relatively independent of concentration. For Cd and Zn, blank noise becomes insignificant above 1 and 2.5 mg/L, respectively, and signal shot noise is limiting or significant ($(\sigma_f)_S > 0.5\,\sigma_F$) up to 50 and 100 mg/L, respectively. Above these latter concentrations, analyte fluorescence flicker noise becomes dominant.

The difference in the limiting noise at high concentrations for Co compared to Cd or Zn can be explained in terms of the calibration curves. For Zn and especially Cd, the negative deviation in the calibration is worse at lower concentrations than for Co. Also the calibration curve goes through a maximum for Zn and Cd but not for Co. These calibration curves effects are caused by larger pre- and post absorption effects for these elements. The fluctuations in these absorption effects enhance the relative analyte fluorescence flicker noise as discussed by Bower and Ingle (84). Thus the absolute noise remains constant or even increases even though the AF signal is relatively constant or decreasing. The analyte fluorescence flicker fac-

tor (i.e. the ratio of the absolute analyte flicker noise to the AF signal) increases at higher concentrations. Thus the decrease in precision at high concentrations observed for Cd, and to a less extent for Cu, Zn, and Mg, is due to greater relative analyte fluorescence flicker noise at concentrations where inner filter and self-absorption effects are larger.

Multielement Measurements

Four elements, Cd, Cu, Mg, and Zn, were selected for multielement measurements. These four elements were picked from the 10 elements studied under single element conditions. The wavelengths for these four elements span the entire range of the exit slit mask (Zn at the lowest wavelength and Cu at the highest wavelength). The results of the single element studies showed that there is not a set of optimum conditions shared by all four elements. Thus it is necessary to choose and chase a compromise set of conditions for multielement measurements.

Optimization studies

For the multielement measurements, four slits were opened. Compared to single element measurements with one slit open, this change is expected to increase the total background emission signal and noise observed and possibly caused excess light problems (i.e. fluorescence of one element excited and observed when another element's HCL is pulsed on).

It was decided to use a 10 ms pulse width since this is optimum with an 8 s total measurement time for all four elements except Cu.

An extensive optimization study was carried out in which the AF signal and $(S/N)_{bk}$ for each element was determined in the multielement mode at H_2 flow rates of 0.8, 1.9, 3.7, 4.6, and 5.6 L/min with Ar flow rates of 0, 2.2, and 3.8 L/min at each H_2 flow rate. This measurement sequence was repeated at flame heights of 1, 2, 2.5, and 3.3 cm.

The results of these studies are essentially the same as obtained in the optimization studies for single element measurements. The highest $(S/N)_{bk}$'s and best detection limits are obtained with a flame height between 2 and 3 cm and an Ar flow rate of about 4 L/min. For Zn, Cu, and Cd, a low H_2 flow rate is optimal while a high H_2 flow rate is best for Mg.

An excess light problem was noted only for the Zn HCL. This lamp has a substantial Cu impurity. When the Zn HCL is pulsed on, Cu aspirating into the flame, fluorescence from Cu passes through the Cu slit and causes a falsely high Zn signal (approximately 50% for equivalent concentrations).

To eliminate this problem, an interference filter with central wavelength of 225.0 nm was placed in front of Zn HCL to eliminate Cu line from the Zn HCL. Unfortunately the Zn AF signal was severely attenuated too because this filter has a throughput of about 10%. Therefore, a filter was not used and an interference calibration curve was made for the AF signal that a given concentration of Cu would produce in the Zn channel. This interference calibration curve was used for the appropriate correction of the Zn AF data.

Calibration curves and detection limits

Because the H_2 flow rate is the most critical variable to optimize for

the four test elements, detection limits and calibration curves were determined at the H_2 flow rates of 0.8 and 3.7 L/min. The calibration curves are show in Figure 31 and the detection limit, noise, and calibration slope data are presented in Table XIII.

Table XIII. TMMS Multielement AF Detection Limits[a]

	0.8 L/min H_2 Flow Rate			3.7 L/min H_2 Flow Rate				
Element	DL (μg/L)	k[b]	σ_{bft}[c]	DL (μg/L)	k[b]	σ_{bft}[c]	DL[d] (μg/L)	DL[e] (μg/L)
Cd	10	4.3	2.2	51	3.7	9.6	90	4.6
Cu	4	17	3.8	9	21	8.9	50	3
Mg	150	0.37	3.2	1	160	10	100	0.8
Zn	110	0.54	2.9	245	0.53	6.5	200	21

[a] E_{PMT}, 1000 V; R_f, 1 MΩ; t_d, 0.5 ms; t_p, 10 ms; ℓ, 100; %DC, 12.5; Ar flow rate, 4 L/min; number of runs, 2; number of data points, 20; burner height 2.5 cm; air flow rate, 4.8 L/min; $(i_p)_{HCL}$'s (mA), Cd (119), Cu (127), Mg (127), Zn (110).

[b] calibration slope, peak photocathodic current signal x 10^{18} A/μg/L.

[c] photocathodic rms background noise x 10^{17} A.

[d] detection limits obtained by Salin under TMMS multielement AF mode (1).

[e] detection limits obtained under TMMS single element AF mode (Table XII).

For Cu, Zn, and Cd, the calibration curves and slopes are very similar at both H_2 flow rates and only the calibration curves for the lower H_2 flow rate is shown in Figure 31. The multielement detection limits for Cu, Zn, and Cd at the lower H_2 flow rate are only a factor

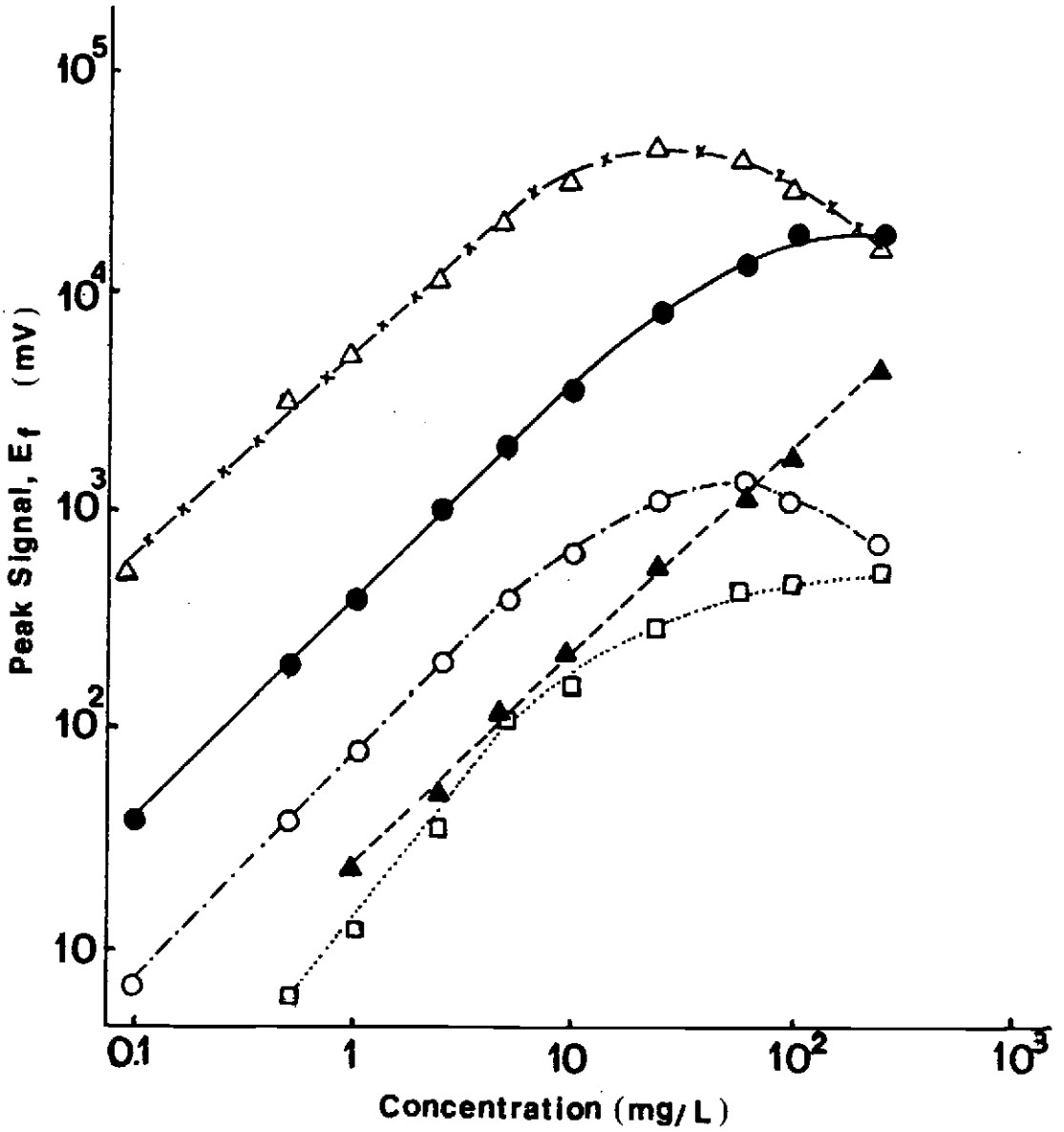

Figure 31. TMMS multielement calibration curves. ○, Cd; ●, Cu; ▲, Mg; □, Zn; △, Mg (H_2 flow rate 3.7 L/min); conditions same as in Table XIII, except t_p, 1 ms.

of 2 worse than the optimized single element detection limits. The worse detection limits are caused by the larger blank noise observed when more slits are open.

With the higher H_2 flow rate, the detection limits for Cu, Zn, and Cd are a factor of 2 - 5 worse than at the lower H_2 flow rate. This is caused primarily by the increased flame background emission noise in the richer flame.

The two calibration plots for Mg in Figure 31 show the dramatic effect of H_2 flow on the atomization efficiency for Mg. The detection limit for Mg at the higher H_2 flow rate is essentially the same as obtained under single element conditions but is a factor of 400 worse at the lower H_2 flow rate. The calibration curve for Mg in the richer flame starts to bend at a concentration of about 20 mg/L, but there is no evidence of bending in calibration curve in the leaner flame up to 250. This indicates that self absorption and inner filter effects are substantially less important in the leaner flame. Only a small fraction of the Mg is in the atomic form that can cause these effects.

Table XIII also shows that the multielement detection limits achieved in this study are significantly better than obtained by Salin (1) for Cd, Cu, and Zn at the low H_2 flow rate and for Mg at the higher H_2 flow rate. The multielement detection limits achieved in this work for Cd and Zn are also a factor of 2 and 5 better, respectively, than those reported by Palermo and Crouch (73) for multielement non-dispersive time multiplex AF measurements.

Air/acetylene flame results

The multielement determination on Cd, Cu, Mg, and Zn was briefly

studied with an air/acetylene flame as the atomizer. A different flame has different atomization, quenching and background emission characteristics.

The effect of acetylene flow rate and flame height were briefly studied to determine approximate optimum conditions. Argon sheathing was found to reduce the flame background emission noise by about a factor of 2. The calibration slope, blank and dark current noise and detection limit data are reported in Table XIV. The detection limits and calibration slopes obtained with the air/H_2 flame are also given for comparison purposes.

Table XIV. TMMS Multielement AF Air/C_2H_2 Flame Detection Limits[a]

Element	$(i_p)_{HCL}$ (mA)	DL (mg/L)	k[b]	σ_{bft}[c]	σ_d[d]	DL[e] (mg/L)	k[e]
Cd	119	0.8	3.7	1.4	1.5	0.05	3.7
Cu	128	0.1	26	1.7	1.8	0.009	21
Mg	128	0.02	158	1.4	2.0	0.001	160
Zn	110	4	0.77	1.7	1.7	0.25	0.53

[a] C_2H_2 flow rate, 0.8 L/min; air flow rate, 4.6 L/min; Ar flow rate, 4.3 L/min; R_f, 1 MΩ; PMT, 1000 V; t_p, 10 ms; τ, 0.1 ms; t_d, 0.5 ms; %DC, 12.5; burner height, 2.5 cm; ℓ, 100.

[b] calibration slope, peak photocathodic current x 10^{15} A/mg/L.

[c] photocathodic rms background noise x 10^{15} A.

[d] cathodic rms dark current noise x 10^{17} A.

[e] DL and calibration slope (peak photocathodic current x 10^{15} A/mg/L) for multielement measurements in H_2/air flame with 3.7 L/min H_2 flow rate (from Table XIII).

The detection limits are about 15 times higher with the air/C_2H_2 flame compared to those obtained with the fuel rich air/H_2 flame. This loss of detectability is the result of much higher background emission signal and noise with the hydrocarbon flame, primarily due to excitation of carbon containing molecules (e.g., CN and CO). The background emission noise is about 15 times greater with C_2H_2 rather than H_2 as the fuel and dark current noise is insignificant. The calibration slopes for a given element are approximately the same in both flames. This indicates that the atomization and quenching characteristics are similar for both flames.

Nondispersive AF Multielement Measurements

Multielement AF measurements of Cu, Mg, and Mn in an air/H_2 flame were briefly studied in the nondispersive mode. As described in the Experimental Section, interference filters, instead of the monochromators, are used to isolate the AF signals (see Figure 8 and Table I). The filter with a wavelength of maximum transmitance of 285.2 nm was used for Mg and Mn with resonance lines of 285.2 nm and 279.5 nm, respectively. The filter with a wavelength maximum of 322.5 nm was employed to isolate the Cu resonance line at 324.7 nm.

Optimization

Most experimental conditions were set to the optimum values determined from single element and multielement optimization studies in the TMMS mode. In particular, the H_2 flow rate must be high (e.g. 3-4 L/min) for Mn and Mg to ensure good atomization. The distances between the flame and entrance lens and between the filters and

entrance lens were optimized. The optimized distance between the flame and the entrance lens is 3 in., which is equal to focal length of entrance lens, and the distance between filters and lens is 0.25 in. This position of the entrance lens collimates the fluorescence radiation and ensures that both filters are filled with the collected radiation.

Calibration curves and detection limits

The calibration curves for all three elements under multielement measurements conditions with a 12.5% duty cycle are shown in Figure 32 (curves a-c). All the curves exhibit severe nonlinearity at high concentrations as previously noted with dispersive AF measurements. For Mn only, the AF signal passes through a maximum and decreases at the highest concentrations.

The detection limit, noise, and calibration slope data are presented in Table XV. All conditions are the same as used to obtain the calibration curves except that the PMT voltage is 800 V instead of 400 V. The detection limit, blank noise and calibration slope data obtained with the same flame under dispersive conditions are also given for comparison.

The data indicate that the detection limits for Cu and Mg are approximately a factor of 4 and 16 worse, respectively, in the TMMF mode compared to the TMMS mode. This occurs because the blank noise is about 40 times greater in the nondispersive mode. The bandpass of the filters is about 2.5 times greater than the spectral bandpass of the monochromator. Thus the background emission signal, and hence the background emission noise is much greater when filters are used. The

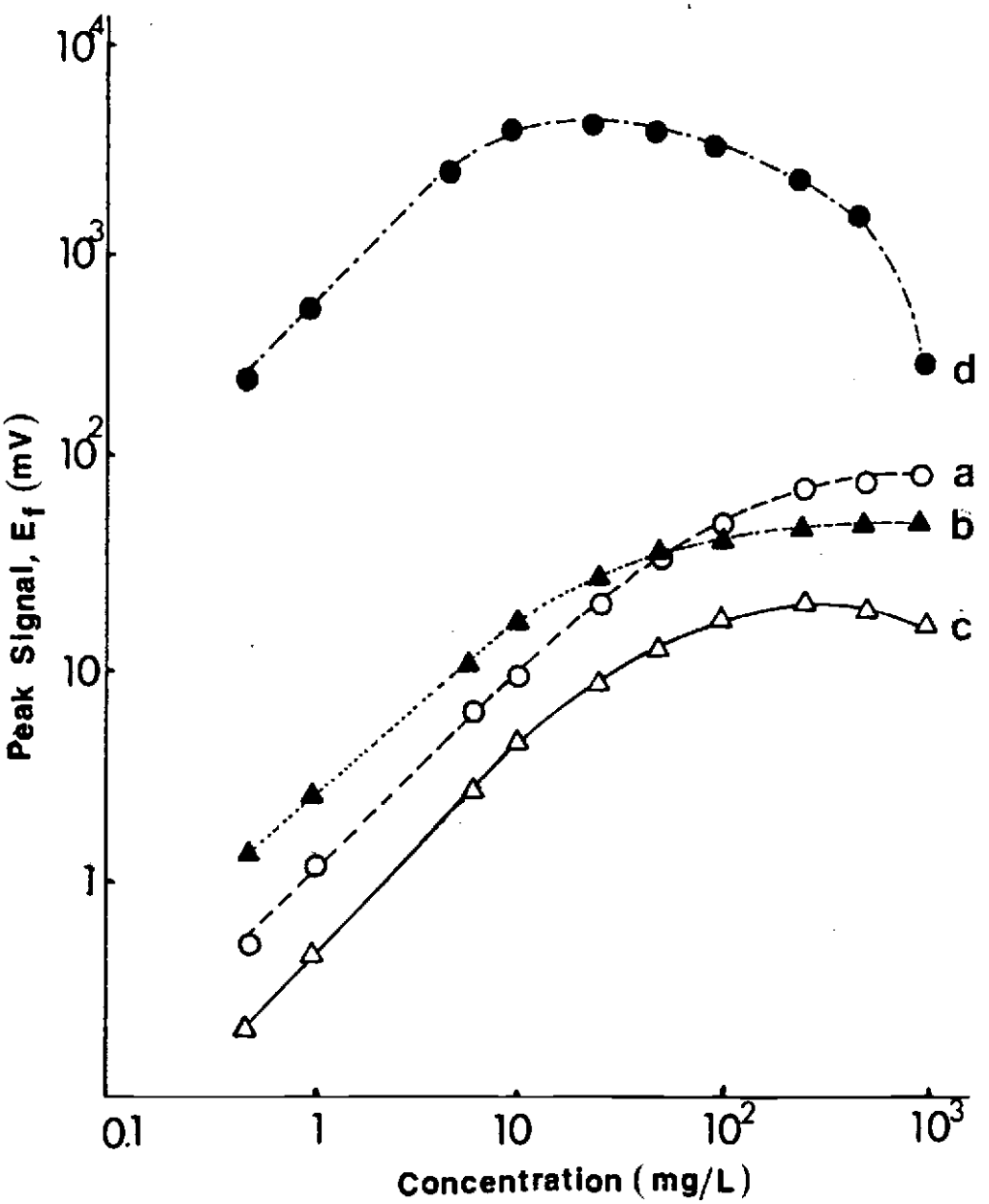

Figure 32. TMMF AF multielement calibration curves. a, Cu; b, Mg; c, Mn; d, Cu (%DC = 2.5); E_{PMT}, 400 V for curves a, b, and c and 800 V for curve d; R_f, 1 MΩ; %DC, 12.5; burner height, 2.5 cm; air flow rate, 4.7 L/min; Argon flow rate, 4.3 L/min; H_2 flow rate, 3.8 L/min; ℓ, 100; number of data points, 20; peak HCL currents, Cu (137 mA at 12.5 %DC and 614 mA at 2.5 %DC), Mg (137 mA), Mn (135 mA); t_p, 10 ms (2 ms for Cu with 2.5 %DC); number of runs, 1.

Table XV. TMMF Multielement AF Detection Limits[a]

Element	DL (μg/L)	k[b]	σ_{bft}[c]	σ_d[d]	DL[f]	k[f]	σ_{bft}[f]
Cu	33	2.4	4.0	4.2	9	0.21	0.089
Mg	16	4.8	3.7	5.7	1	1.6	0.10
Mn	76	0.99	3.8	3.3	-	-	-
Cu[e]	12	39	25	54	-	-	-

[a]conditions same as specified in caption of Figure 32 except E_{PMT}, 800 V.

[b]calibration slope, peak photocathodic current x 10^{16} A/μg/L.

[c]photocathodic rms background noise x 10^{15} A.

[d]cathodic rms dark current noise x 10^{17} A.

[e]measurements with t_p, 2 ms; %DC, 2.5; and $(i_p)_{HCL}$, 614 mA.

[f]DL, calibration slope (peak photocathodic current x 10^{16} A/μg/L), and blank noise (x 10^{15} A) for multielement TMMS measurements in H_2/air flame with 3.7 L/min H_2 flow rate (from Table XIII).

calibration slopes with the filters are about a factor of 10 and 3 greater for Cu and Mg, respectively. Thus the throughput or optical efficiency of the filter based system is greater than that of the monochromator based configuration. However, the increase in optical efficiency does not compensate for the greater increase in the blank noise. The enhancement in optical efficiency is less for Mg than Cu because the Mg filter has a smaller peak transmittance.

The precision curve for Cu is shown in Figure 33 (curve a). The RSD decreases with increasing concentration up to about 5 mg/L. Above

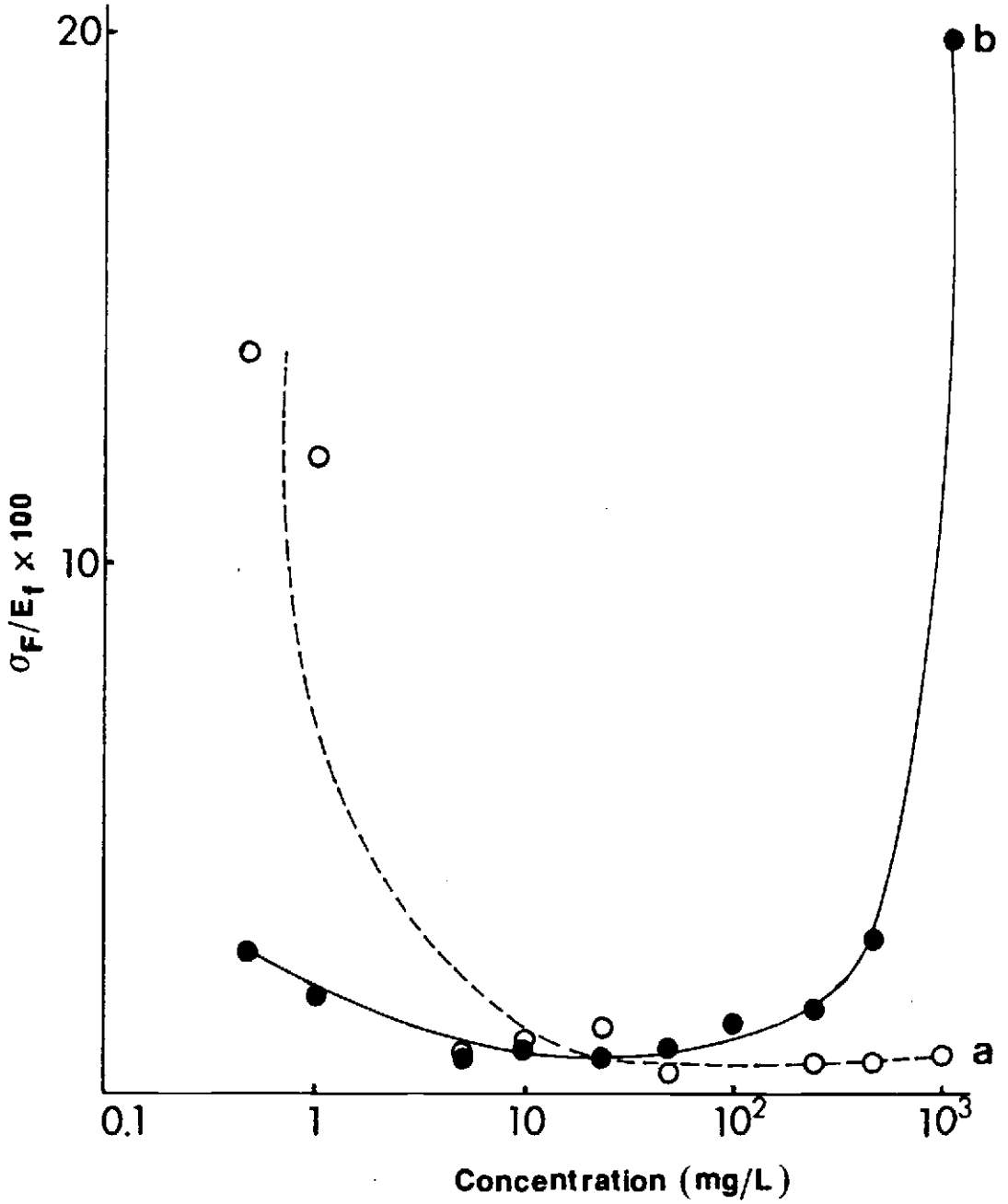

Figure 33. TMMF precision curves for Cu. a, Cu (%DC = 12.5); b, Cu (%DC = 2.5); other experimental conditions are the same as specified for Table XV.

this concentration, blank noise is not limiting and the RSD is independent of the concentration and typically 0.5 - 1.0%. Similar results were obtained for Mg and Mn although the concentration at which the RSD became independent of concentration is higher (10 and 25 mg/L, respectively). Theoretical shot noise calculations indicate that analyte fluoescence shot noise is not limiting at any concentration for any of the elements and suggest that analyte fluorescence flicker noise is limiting at high concentrations.

Separate measurements were made to determine the source of the blank noise. Dark current noise is insignificant compared to flame background emission noise. The noise with the flame on and the blank aspirating is about twice as great with the HCL's on as opposed to off. This increased noise can be attributed to noise in the signal due to reflected or scattered light. The scattering signal is expected to be more significant when using a filter instead of a monochromator because the large bandpass of the filters may pass both scattered resonance and nonresonance line radiation from the HCL's.

A separate experiment was carried out in which the only Cu HCL was pulsed at a peak current about five times higher than in the previous multielement TMMF experiment. The results are reported in the last row of Table XV and as curves d and b in Figures 32 and 33, respectively. The detection limit is improved about a factor of 3 by using a higher excitation intensity which produces a calibration slope about 16 times larger. As shown in Figure 32, the calibration curve for Cu changes significantly with HCL peak current. With a higher peak current (curve d), the maximum AF signal occurs at about 25 mg/L.

Above this concentration, the AF signal decreases significantly and the AF signals at 0.5 and 1000 mg/L are approximately equal. This would indicate that line broadening or self-reversal affects in the HCL emission line profile are very significant at higher currents which enhances nonlinearity due to prefilter effects.

The precision curves for Cu at the two HCL peak currents are also quite different as show in Figure 33. At moderate concentrations, the RSD's are comparable. However, with the higher HCL peak current (curve b), the RSD is lower at low concentrations but larger at higher concentrations. The precision is better at low concentrations because the Cu AF signal is larger relative to the blank noise. The decrease in precision at high concentrations relates to the negative slope of the calibration curve at high concentrations as previously noted in TMMS single element studies. Fluctuations in the large pre- or post filter absorption cause the relative analyte fluorescence noise to increase.

CONCLUSIONS

Numerous modifications and computerization of time multiplex multiple slit spectrometer has resulted in a powerful spectrometer for multielement AF measurements. Incorporation of a microcomputer with appropriate software greatly enhances the versatility and ease of use of the spectrometer. The user through the computer terminal can select the magnitude of numerous experimental variables. This allows the operator to examine different experimental conditions during optimization studies in a relatively very short period of time. Automated data acquisition, reporting of data and reporting of the results of complex calculations significantly reduces the post-analysis time. Useful calculation options include blank signal substraction, calculation of S/N's, detection limits, analyte fluorescence shot noise, and the concentration of the analyte in an unknown.

Modification of the HCL pulsing circuitry along with computer control allow critical parameters such as HCL peak current and width to be easily varied through software control. Use of feedback control for the HCL current circuitry was one of the more significant changes because it improved the stability of the HCL output signal by an order of magnitude. The system also measures and reports the actual HCL operating current so that the operator can confirm that the desired conditions were selected.

Control of the mode of data acquisition and of data acquisition parameters has proved to be very useful. Data can be digitized with a V/F converter and counter or with an ADC. The ADC mode was found to

be optimal for pulse widths of 4 ms or less because the readout resolution is better than in the V/F mode. Selection of the delay time after initiation of the HCL pulse before data acquisition is critical in S/N optimization. User selection of the number of pulses for which data are acquired and the number of repetitive runs is particularly useful for S/N optimization.

Several hardware changes improved the performance of the instrument. The new Meker burner head allows the use of an Ar gas sheathed flame. Argon gas sheathing can increase the AF signal by reducing the concentration of quenchers in the flame and reduce the flame background emission signal and noise. For many elements studied, the Ar sheathing improved detection limits by a factor of 2 - 4. An automated sampler allows computer controlled introduction of a blank or analyte solution. This option is particularily useful for optimization studies.

The improved design of the multielement AF instrument and ability to optimize lamp parameters such as pulse width and peak current provides excellent single element detection limits that are 3 - 7 better for 9 elements and 50 times better for Mg than achieved with the TMMS instrument designed by Salin (1). Of the many variables optimized, the H_2 flow rate and HCL peak current are the most critical. A fuel rich air/C_2H_2 flame is required for the best detection limits for more difficult to atomize elements like Ni, Fe, Mn, Pb, and Mg. For elements such as Au, Mg, Pb, Cd, and Zn the AF signal increases little above HCL peak currents of about 200 mA. With these elements and the restraint of a fixed total measurement time, the best detection limits

are achieved with smaller HCL peak currents and large pulse widths (larger duty cycles) because background noise is reduced to a greater extent than the peak AF signal is reduced.

The dependence of precision on analyte concentration for five elements was shown to follow the pattern described by Bower and Ingle (84) for Cu. In particular the precision decreases at high concentrations because the relative analyte flicker noise increases at high concentrations where the AF signal decreases due to large pre- and post-absorption effects. Other studies with Cu showed that the precision at high concentrations is worse with a higher HCL peak current because non-linearity effects are worse due to increased source emission profile broadening and self-reversal. For elements such as Co, Zn, and Cd, analyte fluorescence shot noise is limiting over a large range of concentrations. Thus the S/N could be improved with a higher intensity source.

Multielement AF measurements of Cd, Cu, Mg, and Zn demonstrated the compromises involved in multielement measurements. However, in general the multielement detection limits were improved significantly over those achieved by Salin (1). With a lean air/H_2 flame, the multielement detection limits are about a factor of 2 worse for Cd, Cu, and Zn and 400 times worse for Mg than for optimized single element measurements. In a fuel rich flame, the detection limits are a factor of 2 - 5 worse for Cd, Cu, and Zn but are equivalent for Mg compared to optimized single element detection limits. A fuel rich flame is needed to atomize efficiency Mg but this increases the background emission noise.

With the instrument designed, the same HCL pulse width must be used for all elements in the multielement mode. A smaller pulse width and higher HCL peak current would have improved the Cu detection limit. Clearly optimal multielement detection limits for a given group of elements can be achieved only if the single element detection limits for elements in the group are achieved with similar H_2 flow rates and HCL pulse widths.

The air/C_2H_2 flame is usually a better atomization source than the air/H_2 flame. However, for AF measurements, the detection limits were shown to be about 15 times worse with the hydrocarbon flame due to increased background emission noise.

Nondispersive AF measurements of Cu, Mg, and Mn indicated that the optical throughput of the AF signal is higher. However, the larger bandpass of the filters increases the flame background emission and scattering signals and noise observed. This results in a substantial decrease in detectability compared to dispersive AF measurements.

Today no commercial single or multielement flame AF spectrometer is available. This situation is unlikely to change even with the new information provided in this thesis. However, an AF instrument of the TMMS design could be useful for multielement analysis of a few easy to atomize elements in a routine analysis situation. In general AF detection limits for some elements are better than achieved with AA or plasma emission spectrometry only if a laser is used for the excitation source. However one commercial (Baird) AF spectrometer is now on the market which uses an ICP as the atomization source. It is based on a nondispersive time multiplex mode of operation using a

separate pulsed HCL and emission filter for each element. The information from this thesis on optimization of the HCl peak current, pulse width, and duty cycle and the data acquisition parameters could be used to optimize the performance of this commercial instrument.

BIBLIOGRAPHY

1. E. D. Salin, PhD Thesis, Oregon State Univ., 1978.
2. J. D. Winefordner J. J. Fitzgerald and N. Omenetto, Appl. Spec., 29, 369 (1975).
3. J. A. Decker, Jr., Anal. Chem., 44, 127A (1972).
4. R. P. Cooney, G. D. Boutilier and J. D. Winefordner, Anal. Chem., 49, 1048 (1977).
5. A. Gustavsson and F. Ingman, Spectrochim. Acta., 34B, 31 (1979).
6. K. W. Busch and G. H. Morrison, Anal. Chem., 45, 712A (1973).
7. H. L. Felkel, Jr. and H. L. Pardue, Clin. Chem., 24, 602 (1978).
8. H. L. Felkel, Jr. and H. L. Pardue, Anal. Chem., 50, 602 (1978).
9. A. H. Ullman, Prog. Anal. Atom. Spec., 3, 87 (1980).
10. G. Horlick and E. Codding, Appl. Spec., 29, 176 (1975).
11. D. G. Mitchell, K. W. Jackson and K. M. Aldous, Anal. Chem., 45, 1215A (1973).
12. H. L. Felkel and H. L. Pardue, Anal. Chem., 49, 1112, (1977).
13. T. L. Chester, H. Haraguchi, D. O. Knapp, J. D. Messman and J. D. Winefordner, Appl. Spec., 30, 410 (1976).
14. G. Horlick and E. G. Codding, Anal. Chem., 45, 1490 (1973).
15. E. G. Codding, J. D. Ingle, Jr. and A. J. Stratton, Anal. Chem., 52, 2133 (1980).
16. K. W. Busch, B. Malloy and Y. Talml, Anal. Chem., 51, 670 (1979).
17. G. Horlick, Appl. Spec., 30, 113 (1976).
18. A. T. Zander, T. C. O'Haver and P. N. Keliher, Anal. Chem., 49, 838 (1977).
19. Ibid, 48, 1166 (1976).
20. P. N. Keliher and C. C. Wohlers, Anal. Chem., 48, 140 (1976).
21. J. M. Harnley and T. C. O'Haver, Anal. Chem., 53, 1291 (1981).
22. R. Mavrodineau and R. C. Hughes, Appl. Optics., 17, 1281 (1968).

23. R. A. G. Rawson, (1973), Unpublished Work.

24. L. R. P. Butler and A. Strasheim, Spectrochim. Acta., 21B, 1207 (1965).

25. E. Lundberg and G. Johansson, Anal. Chem., 48, 1922 (1976).

26. O. Rose, Jr., W. R. Heineman, J. A. Caruso and F. L. Fricke, Analyst., 103, 113 (1978).

27. B. D. Pollard, A. H. Ullman and J. D. Winefordner, Anal. Chem., 53, 330 (1981).

28. F. Lipari and F. W. Plankey, Anal. Chem., 50, 386 (1978).

29. A. H. Ullman, B. D. Pollard, G. D. Boutilier, R. P. Bateh, P. Hanley and J. D. Winefordner, Anal. Chem., 51, 2382 (1979).

30. O. Rose, Jr. and J. A. Caruso, Appl. Spec. Reviews, 14, 145 (1978).

31. R. A. G. Dawson and D. J. Ellis, Spectrochim. Acta., 23B, 695 (1968).

32. T. W. Barnard, Anal. Chem., 51, 1172A (1979).

33. J. P. McCarthy, J. A. Caruso, K. A. Wolknik and F. L. Fricke, Anal. Chim. Acta., 147, 163 (1983).

34. S. S. Berman and J. W. McLaren, Appl. Spec., 32, 372 (1978).

35. K. J. Mulligan, M. H. Hahn, J. A. Caruso and F. L. Fricke, Anal. Chem., 51, 1935 (1979).

36. J. Burman, B. Johansson, B. Morefat, K. Narfeldt and L. Olsson, Anal. Chim. Acta., 133, 379 (1981).

37. O. Rose, Jr., D. W. Mincey, A. M. Yacynych, W. R. Heineman and J. A. Caruso, Analyst, 101, 753 (1976).

38. B. T. N. Newland, Proc. Anal. Div. Chem. Soc., 15, 309 (1978).

39. R. N. Savage and G. M. Hieftje, Anal. Chim. Acta., 123, 319 (1981).

40. G. A. Kobra and E. S. Yeung, Anal. Chim. Acta., 104, 209 (1979).

41. J. Van Loon, Anal. Chem., 53, 332 (1981).

42. N. Omenetto, G. D. Boulilier, S. J. Weeks, B. W. Smith and J. D. Winefordner, Anal. Chem., 49, 1076 (1977).

43. M. B. Denton and H. V. Malmstadt, Appl. Phys. Lett., 18, 485 (1971).

44. L. M. Fraser and J. D. Winefordner, Anal. Chem., 43, 1693 (1971).

45. S. J. Weeks, H. Haraguchi and J. D. Winefordner, Anal. Chem., 50, 360 (1978).

46. E. H. Piepmeier, Spectrochim. Acta., 27B, 431 (1972).

47. N. Omenetto, P. Benetti, L. P. Hart, J. D. Winefordner and C. Th. J. Alkemade, Spectrochim. Acta., 28B, 289 (1978).

48. N. Omenetto, P. Benetti, L. P. Hart, J. D. Winefordner and C. Th. J. Alkemade, Spectrochim. Acta., 28B, 301 (1973).

49. M. S. Epstein, J. Bradshaw, S. Bayer, J. Bower, E. Voigtman and J. D. Winefordner, Appl. Spec., 34, 372 (1980).

50. G. J. De Jong and E. H. Piepmeier, Spectrochim. Acta., 29B, 159 (1974).

51. E. R. Johnson, C. K. Mann and T. J. Vickers, Appl. Spec., 30, 415 (1976).

52. E. H. Piepmeier and L. De Galan, Spectrochim. Acta., 30B, 263 (1975).

53. E. H. Piepmeier and L. De Galan, Spectrochim. Acta., 30B, 211 (1975).

54. H. G. C. Human, Spectrosc. Lett., 6, 719 (1973).

55. E. Cordos and H. V. Malmstadt, Anal. Chem., 45, 27 (1973).

56. T. C. Wolfe and T. J. Vickers, Appl. Spec., 32, 265 (1978).

57. D. J. Johnson, F. W. Plankey and J. D. Winefordner, Anal. Chem., 46 1898 (1974).

58. D. G. Mitchell and A. Johansson, Spectrochim. Acta., 25B 175 (1970).

59. D. J. Johnson, F. W. Plankey and J. D. Winefordner, Anal. Chem., 47, 1739 (1975).

60. M. S. Epstein, S. Nikdel, N. Omenetto, R. Reeves, J. Bradshaw and J. D. Winefordner, Anal. Chem., 51, 2071 (1979).

61. M. S. Epstein, N. Omenetto, S. Nikdel, J. Bradshaw and J. D. Winefordner, Anal. Chem., 52, 284 (1980).

62. G. B. Marshall and T. S. West, Anal. Chim. Acta., 51, 179 (1970).

63. A. Fulton, K. C. Thompson and T. S. West, Anal. Chim. Acta., 51, 373 (1970).

64. M. S. Cresser and T. S. West, Anal. Chim. Acta., 51, 530 (1970).

65. J. D. Norris and T. S. West, Anal. Chim. Acta., 55, 359 (1971).

66. J. D. Norris and T. S. West, Anal. Chem., 45, 226 (1973).

67. J. D. Norris and T. S. West, Spectrosc. Lett., 11, 707 (1978).

68. H. V. Malmstadt and E. Cordos, Amer. Lab., 4, 35 (1972).

69. R. W. Spillman and H. V. Malmstadt, Anal. Chem., 48, 303 (1976).

70. R. W. Spillman and H. V. Malmstadt, Amer. Lab., 8(3), 89 (1976).

71. D. W. Brinkman, M. L. Whisman and J. W. Goetzinger, Appl. Spec., 33, 245 (1979).

72. D. G. Mitchell and A. Johansson, Spectrochim. Acta., 26B, 677 (1971).

73. E. F. Palermo, A. Montaser and S. R. Crouch, Anal. Chem., 46 2154 (1974).

74. J. Ip, Y. Thomassen, L. R. P. Butler, B. Radzivk and J. C. VanLoom, Anal. Chim. Acta., 110, 1 (1979).

75. D. R. Demers and C. D. Allem and, Paper No. 122, 31st Pittsburgh Conf. Anal. Chem., Atlantic City, N. J. (1981).

76. D. R. Demers and C. D. Allemand, Paper No. 123, 31st Pittsburgh Conf. Anal. Chem., Atlantic City, N. J. (1981).

77. D. R. Demers and C. D. Allemand, Anal. Chem., 53, 1915 (1981).

78. Heath Module EU-800-KC, Heath Company, Benton Harber, MI (1970).

79. K. M. Aldous, R. F. Brown, R. M. Dagnall and T. S. West, Anal. Chem., 42, 939 (1970).

80. SYM-1 REFERENCE MANUAL, Synertek Systems Corporation, P. O. Box 552, Santa Clara, CA, 95052 (1979).

81. J. C. Sinnett, SYM-physics, 3, 4, (1980).

82. J. W. Brown, "BROWN BASIC ENHANCEMENTS FOR SY-1/BAS-1 Manual", SYM-physis, SYM-1 Users' Group, P. O. Box 315, Chico, CA 95927.

83. D. Marino, PhD Thesis, Oregon State Univ. 1980.

84. N. W. Bower, PhD Thesis, Oregon State Univ. 1977.

APPENDICES

APPENDIX I

Complete Control Board

In Figure A1, the circled numbers refer to connections made to fingers 1 through 22 on the PC board. These fingers are connected to a female edge connector to which wires are connected to and from other devices as indicated in Table AI. The configuration and coding for the lap switches are shown in Figure A2 and Table AII. An H refers to high (+5 V) and GND to ground. The coding for the readout switches is detailed in Table AIII.

Figure A1. Control board schematic.

Component	Identification No. or Value	Description
IC1, IC9	SN7404	Hex inverter
IC2	SN74122	Monostable multivibrator (delay monostable)
IC3	SN7400	Quadruple 2-input positive NAND gate (delay and lap gate)
IC4, IC7	SN7493	4-bit binary counter (lap counter)
IC5	SN74221	Dual monostable multivibrator
IC6	SN74161	Synchronous 4-bit binary counter (counter demultiplexer)
IC8	SN7420	Dual 4-input positive NAND gate
IC10	SN7442	BCD-to-decimal decoder (lamp demultiplexer)
IC11	SN7442	BCD-to-decimal decoder (signal demultiplexer)
S1, S2, S3, S4,	8 keys	SPST switch
C1	100 pF	Capacitor
C2	10 μF	Capacitor
C3	0.022 μF	Capacitor
C4	0.22 mF	Capacitor
R1, R4	2.2 kΩ	Resistor
R2	10 kΩ	Resistor
R3	100 kΩ	Resistor

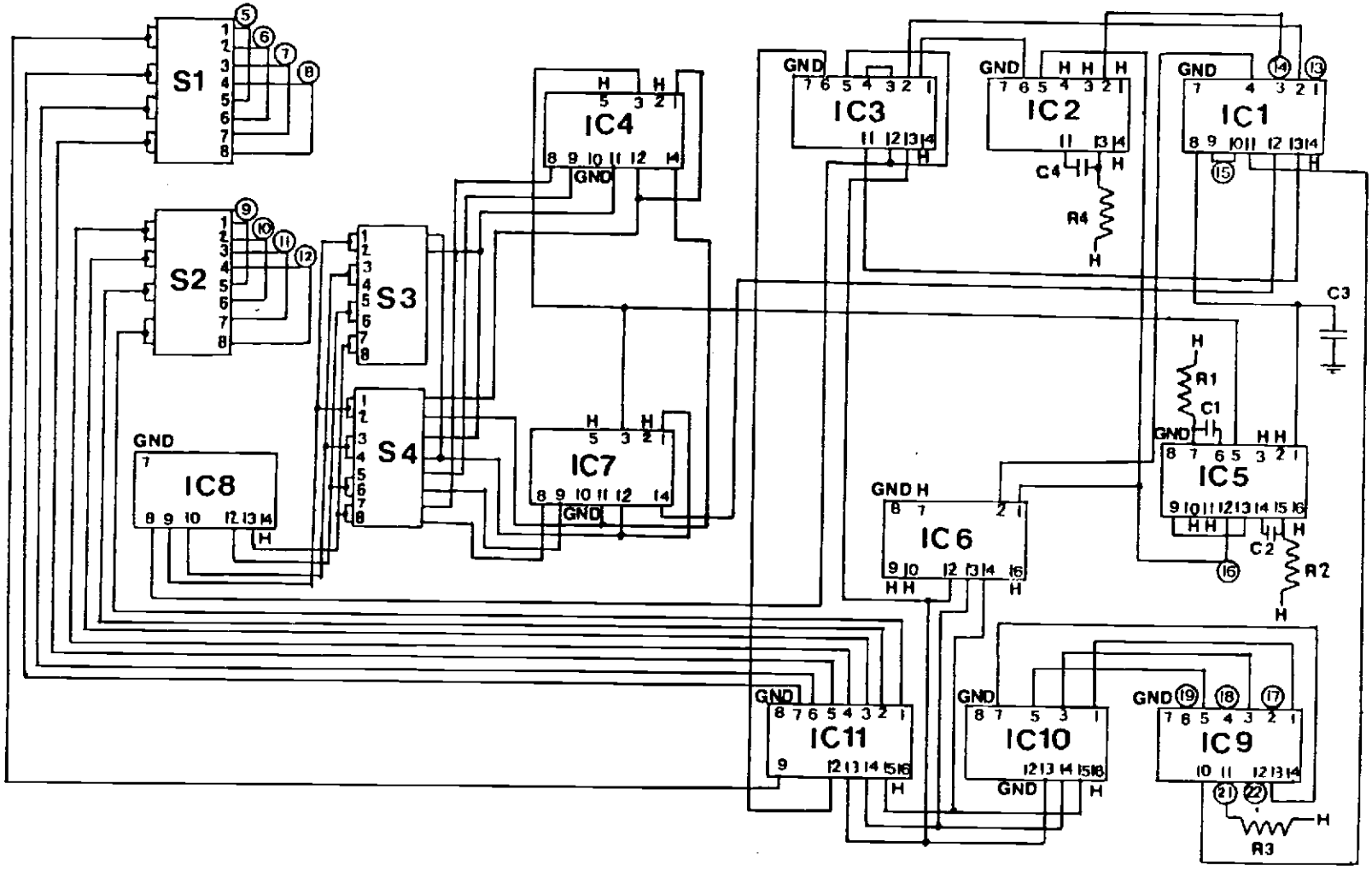
S1
S2
S3
S4
IC1
IC2
IC3
IC4
IC5
IC6
IC7
IC8
IC9
IC10
IC11
GND
H
C1
C2
C3
C4
R1
R2
R3
R4

Figure A1.

Table AI. Control Board Pin Description

Pin	Description
1.	GND (system and logic ground)
2.	N.C. (no connection)
3.	N.C.
4.	N.C.
5.	To pin 6 of counter 4 (down channel)
6.	To pin 6 of counter 3 (down channel)
7.	To pin 5 of counter 4 (up channel)
8.	To pin 5 of counter 3 (up channel)
9.	To pin 6 of counter 2 (down channel)
10.	To pin 6 of counter 1 (down channel)
11.	To pin 5 of counter 2 (up channel)
12.	To pin 5 of counter 1 (up channel)
13.	Input signal from V/F converter
14.	CLOCK, from clock PC board pin 10
15.	CLEAR, to all counter PC boards pin 4
16.	RESET, to clock reset, pin 21
17.	To pin 19 of control transistor PC board
18.	To pin 22 of control transistor PC board
19.	To pin 21 of control transistor PC board
20.	To pin 20 of control transistor PC board
21.	START, from variable timer PC board, pin 16, or manual start
22.	+5 V

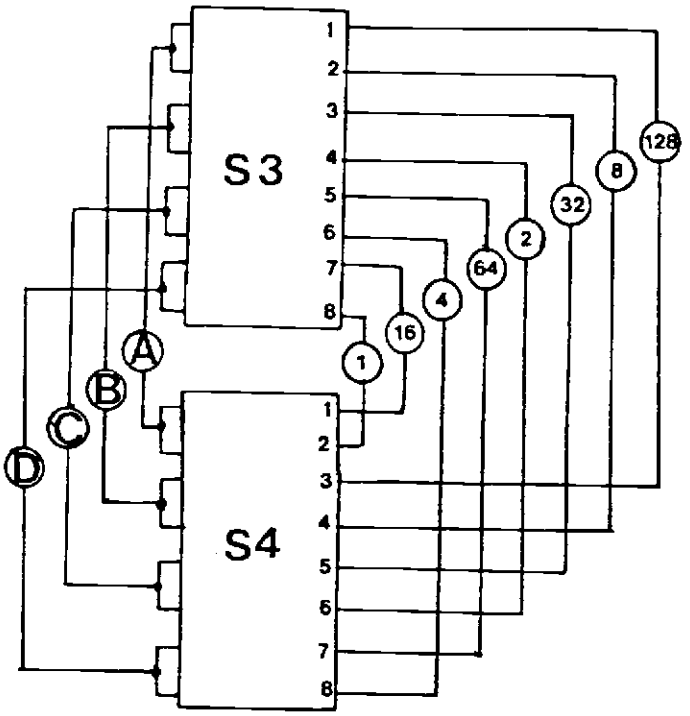

Figure A2. Configuration for lap switch. A, B, C, and D are inputs to NAND gate (IC8), and circled numbers are decimal representations of the binary outputs of the cascaded binary lap counters (IC4 and IC7).

Table AII. Selection of Number of Laps

No. of Laps	S3-Key No.[a]	S4-Key No.[a]	Input to IC8
10	2,4	---	A,B
25	7	2,4	D,A,B
50	3,7	6	B,D,C
100	3,5	8	B,C,D
150	1,4,6,7	---	A,B,C,D
200	1,5	4	A,C,B

[a]Refers to which keys to switch to the on position. Each input of the NAND gate may be connected to only one lap counter output.

Table AIII. Readout Switch Coding[a]

Channel No.	Counter No.	Switch No.	Key No.
1	1	2	8,6,3,1
2	2	2	8,6,3,1
3	3	1	8,6,3,1
4	4	1	8,6,3,1
1	2	2	7,5,4,2
2	1	2	7,5,4,2
3	4	1	7,5,4,2
4	3	1	7,5,4,2
1	1,2	2	8,7,6,5
2	1,2	2	4,3,2,1
3	3,4	1	8,7,6,5
4	3,4	1	4,3,2,1

[a]To send signal from HCL1 or channel 1 of signal demultiplexer (IC11) to up-down counter and readout system 1, keys 8, 6, 3, and 1 of switch no. S2 must be switched to the on position and keys 2, 4, 5, and 7 switched to the off position.

APPENDIX II

5-Digit Display Readout

IC1 - IC5 (N7447, BCD-to-seven segment decoder/driver) in Figure A3 are TTL monolithic devices consisting of the necessary logic to decode a BCD coded signal to seven segment readout plus selected signs. They provide open collector output transistors for directly driving LED displays IC6 - IC10 (MAN72, Monsanto LED display) through 200 Ω resistors R1 - R35. External connections to IC1 - IC5 are described in the caption for Figure A3.

Figure A3. 5-digit display readout schematic.

Pin	Description
4	C input - from least significant up-down counter
5	B input - from least significant up-down counter
8	C input - from 2nd up-down counter
9	B input - from 2nd up-down counter
12	C input - from 3rd up-down counter
13	B input - from 3rd up-down counter
16	C input - from 4th up-down counter
17	B input - from 4th up-down counter
20	C input - from most significant counter
21	B input - from most significant counter
22	+5 V
A	GND
B	A input - from least significant up-down counter
C	D input - from least significant up-down counter
F	A input - from 2nd up-down counter
H	D input - from 2nd up-down counter
L	A input - from 3rd up-down counter
M	D input - from 3rd up-down counter
R	A input - from 4th up-down counter
S	D input - from 4th up-down counter
V	A input - from most significant up-down counter
W	D input - from most significant up-down counter

All other pins are not connected.

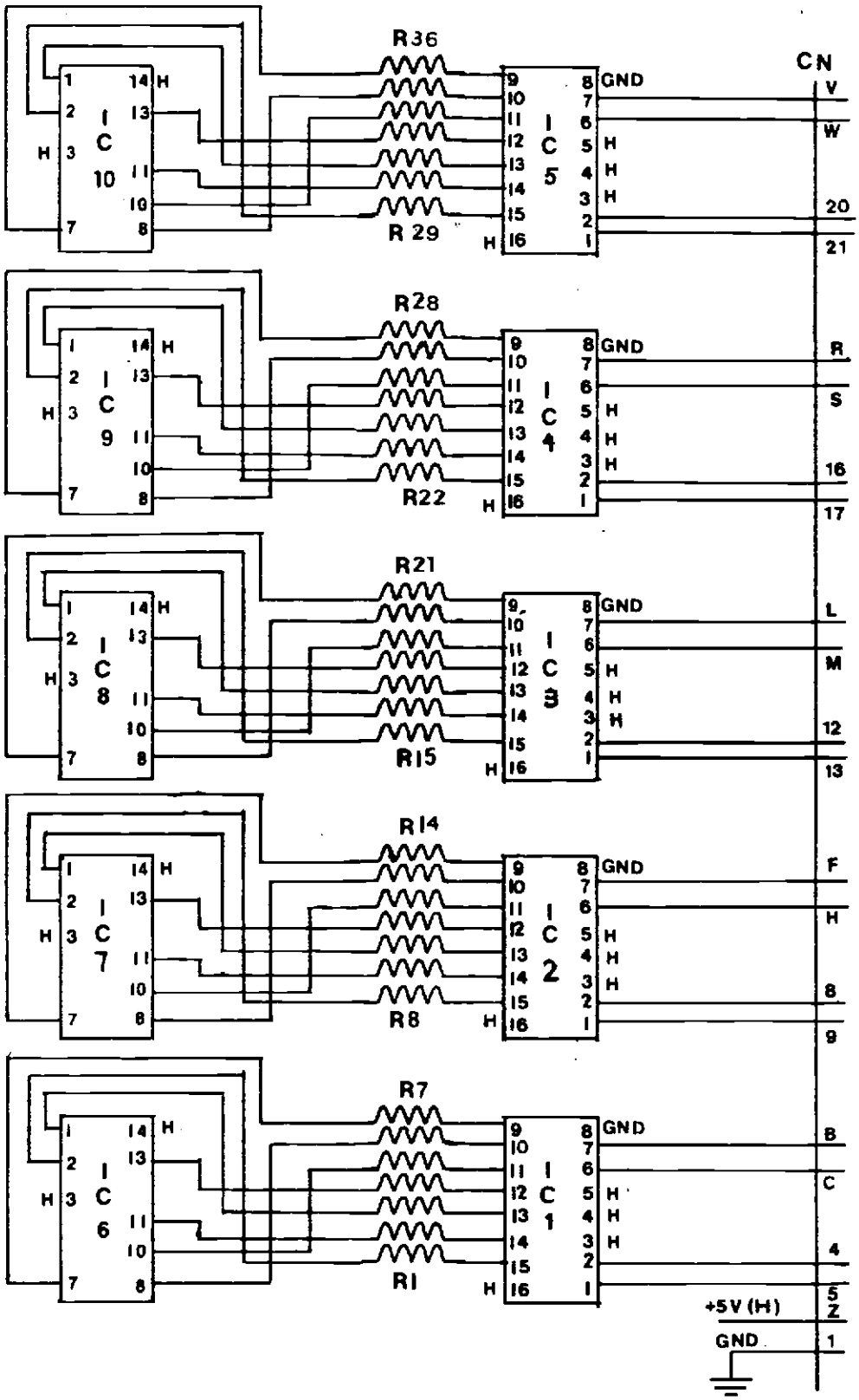
R36
R 29
R28
R22
R21
R15
R14
R8
R7
R1
IC 10
IC 9
IC 8
IC 7
IC 6
IC 5
IC 4
IC 3
IC 2
IC 1
GND
H
CN
V
W
20
21
R
S
16
17
L
M
12
13
F
H
8
9
B
C
4
5
Z
+5V (H)
GND
1

Figure A3.

APPENDIX III

1 MHz Crystal Clock Board

The 1 MHz resonant output frequency of the crystal is divided with decade counters to provide the frequencies from 10 Hz - 1 MHz. All the frequencies are accessible from separate pins of edge connector. Any one frequency at a time can be obtained from pin 12 as selected from a 7-key SPST switch (only one key must be in on position at a time) (Figure A4).

This clock is constructed on a PC board and located in the Vector cage. Pin 10 of this clock board is connected to pin 14 of control board to provide appropriate pulses. Also pin 12 is connected to pin 14 of the automated start switch board . RESET, pin 21 is an input from the CLEAR of control board. Pin 18 (INT) is oscillator output which is connected externally to pin 17 (EXT) which is the external oscillator input to the rest of the clock system.

Figure A4. 1 MHz crystal clock board schematic.

Component	Identification No. or Value	Description
F	1 MHz	Quartz crystal oscillator
IC1-IC5	SN7490	Decade counter
IC6-IC10	SN7400	Quadruple 2-input positive NAND gate
R1,R2	680 Ω	Resistor
R3	150 Ω	Resistor
R4	1 kΩ	Resistor
C1	5 pF	Capacitor
C2	10 pF	Capacitor

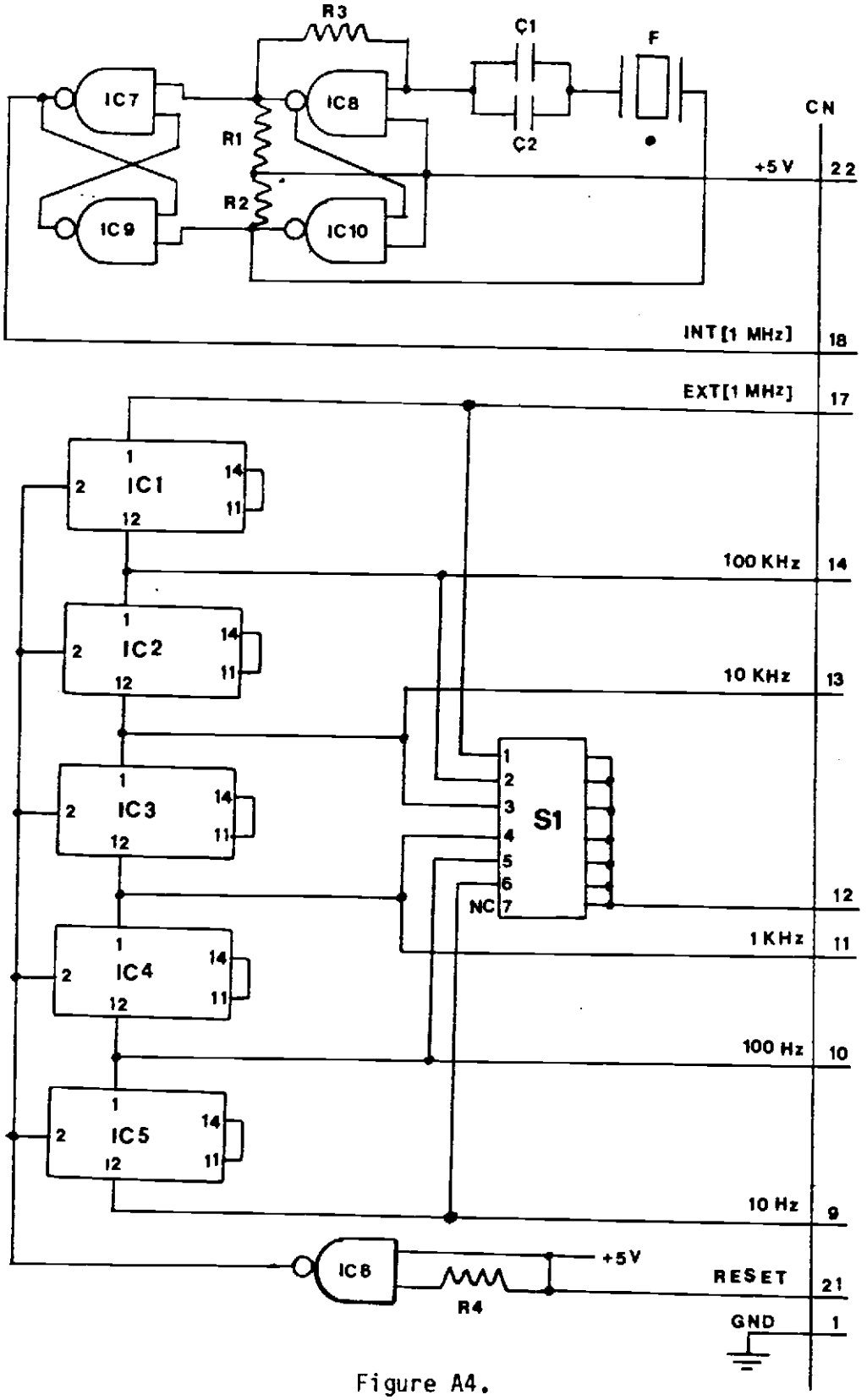
R3
C1
F
IC7
IC8
R1
C2
CN
+5V
22
R2
IC9
IC10
INT[1 MHz]
18
EXT[1 MHz]
17
IC1
100 KHz
14
IC2
10 KHz
13
IC3
S1
NC
12
IC4
1 KHz
11
100 Hz
10
IC5
10 Hz
9
IC6
+5V
RESET
21
R4
GND
1

Figure A4.

APPENDIX IV

Automated Start Switch

The automated start switch circuit is based on a 555 timer which operates in the one shot monostable mode. The circuit shown in Figure A5 was constructed on a PC board with a 22 pin finger edge connector. A logic 0 pulse from pin 12 of the clock board (10 Hz frequency) to the input of IC2 drives the output of IC2 to logic 1 (high). The circuit will remain in this state until the set time is elapsed. This period is given by $t = 1.1\ RC$ where C can be selected to be 1, 4.7 or 10 μF with switch S1 and R can be varied from 1.5 to 2.5 MΩ with potentiometer R1.

Also, a manual start switch is available which is basically a momentary push button switch connected to the back of the instrument which can generate a logic 0 pulse. The system can be switched between the manual or automated start mode through a SPDT switch installed on the front of the instrument (Figure A10). The start switch (manual or automated) output is connected to pin 21 of control board.

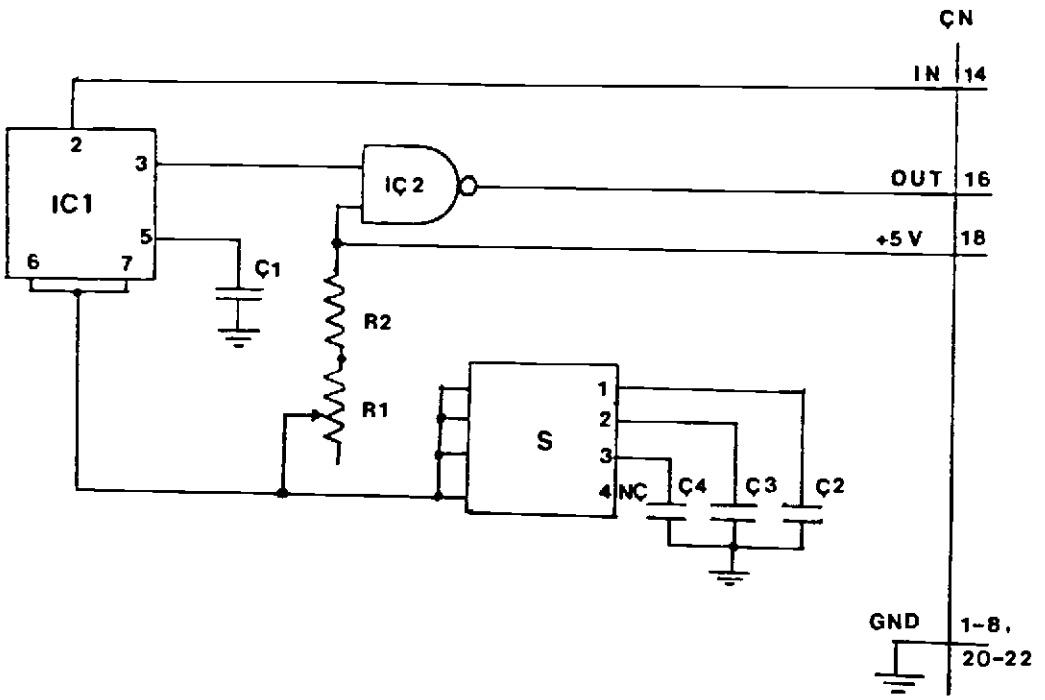

Figure A5. Automated start switch schematic. IN, timer input from pin 12 of the clock board; OUT, to control board pin 21 (START); IC1, NE555 Timer; IC2, SN7400, Quadruple 2-input positive NAND gate; S1, 4 key, SPST switch; C1, C2, C3, and C4 are 0.01, 10, 4.7, 1 μF capacitors, respectively; R1, 1 MΩ, 10 turn potentiometer; R2, 1.5 MΩ resistor; CN, connection edge.

APPENDIX V

Changes, Additions, and Expansion

In order to make SYM-1 more versatile according to our needs, the following changes were made:

A. Automated Log-on (80)

To log-on a current loop device like a TTY, a "Q" is entered at the device. To provide this option, the following jumpers on the SYM-1 were changed:

Jumpers CC-32 and BB-31

changed to CC-31 and BB-32

B. I/O Line Addition

To be able to use PB4-PB7 at AC00, the following changes were made on SYM-1:

Jumpers B-16 and A-2

changed to B-18 and A-3

C. Basic ROMs Addition

To install two-4Kx8 BASIC ROMs chips at locations C000 to CFFF and D000 to DFFF, the following jumpers have to be changed on SYM-1:

Jumpers B-2, C-2, F-5, G-5, K-11, L-12, and M-13 are removed.

Jumpers B-1, C-1, F-2, G-2, K-11, K-12, L-12, and L-13 are added.

D. Tape Recording Improvement

For better tape reliability (81), the following hardware

modification was made on SYM-1 board:

a) Changing R94, R95, and R96 to 100 Ω.

b) Removing R87 and R126.

c) Installing a 2.2 kΩ resistor from the right end of R94 to the right end of R126

d) Removing right end of CR28 and connecting it to left side of R87

e) Removing right end of CR29 and connecting it to left side of R94.

f) Installing R97 (1 kΩ) and C16 (0.22 μF).

E. EPROM Board Address Boundaries

Each 8K bank on EPROM board can be addressed separately. The switch at the right hand side corresponds to the upper 8K bank and the one at the left hand side to the lower 8K bank. Table AIV has the address boundaries and corresponding key (it can be used for both switches).

F. LBM Key Positioning

The proper position of the switches on the LBM board is indicated in Table AV.

G. RAM Board Addressing

Each 8K block of RAM board can be addressed separately through switches A and B. The RAM was located from 2000 to 5FFF with switches A and B in the positions given in Table AVI.

Table AIV. EPROM Board Address Boundaries

Key No.	Address Boundaries
1	0000-1FFF
2	2000-3FFF
3	4000-5FFF
4	6000-7FFF
5	8000-9FFF
6	A000-BFFF
7	C000-DFFF
8	E000-FFFF

Table AV. LBM Key Positioning

Key No.	Position	
1	X (no difference)	
2	Closed (monitor)	
3	X	
4	Closed (I/O)	
5	X	
6	Closed	8K Basic
7	Closed	
8	X	
9	X	
10	Closed	

Table AVI. Addressing RAM Board

Key No.	Switch A (2000-3FFF)	Switch B (4000-5FFF)
1	Closed	Open
2	Open	Closed
3	Open	Open
4	Closed	Closed
5	Closed	Closed
6	Closed	Closed

APPENDIX VI

Mode 2 and 3 I/O Port Connections

The I/O ports from connectors A, B, C, and D (Figure 10A) are connected to appropriate electronic parts of the instrument through a series of parallel ribbon cables. Table AVII describes the connection to each bit of the above I/O ports.

For mode 2 which the 2-byte up-down counter is used, there is a shortage of I/O ports. This problem was solved by using the two I/O ports from connector A for both the counter board and the ADC. In the mode 2, at the beginning of the program the ADC is needed for adjusting the HCL currents. When the actual measurements start, the ADC is not needed anymore, and instead the 2-byte up-down counter is needed to count the frequencies proportional to the signals. Therefore the two I/O ports from connector A is disconnected from the ADC and connected to counter board. At appropriate times, messages appear at the terminal to indicate that the user should change the connections. Connections between the 2-byte up-down counter and the I/O ports from connector A are shown in Table AVIII.

Table AVII. I/O Port Connections for Mode 2 and 3

Bit No.	Address	Description
	A000	To DAC
0		Strobe (STB)
1		Input, bit 9
2		10
3		11
4		12
5-7		N.C.
	A001	To DAC
0		Input, bit 1
1		2
2		3
3		4
4		5
5		6
6		7
7		8
	A800	To ADC
0		Start conversion
1		Conversion mode
2		Enable
3		Line select A0
4		A1
5		A2

Table AVII Continued

Bit No.	Address	Description
6		End conversion
7		N.C.
	A801	To ADC
0		Output, bit 5
1		6
2		7
3		8
4		9 and 1
5		10 and 2
6		11 and 3
7		12 and 4
	AC00	
0		To HCL, 1[a]
1		2
2		3
3		4
4		N.C.
5		HCL control to HCL pulser board
6		N.C.
7		Clock to control board
	AC01	
0		N.C.

Table AVII Continued

Bit No.	Address	Description
1		Automated sampler
2-7		N.C.

[a]These lines are actually connected to the input of the HCL's pulse control AND gates on HCL pulser board.

Table AVIII. Extra I/O Port Connections for Mode 2

Bit No.	Address	Description
	A800	To 2-byte up-down counter
0		Clear
1		Gate
2		Low control
3		High control
4		Up-down control
5-7		N.C.
	A801	To 2-byte up-down counter
0		Data bit, 1
1		2
2		3
3		4
4		5
5		6
6		7
7		8

APPENDIX VII

Mover Program

The following program is written in order to move BROWN'S BASIC ENHANCEMENT program (burned on two-2K EPROM) from location 6000 to location 0200 (original starting location of the program).

```
LINE # LOC      CODE      LINE

0002  0000              :  THIS PROGRAM MOVES BASIC ENHANCEMENTS
                            PROGRAM FROM 6000 TO
0003  0000              :
0004  0000                     *=6B00
0005  6B00  A9  00              LDA #$00
0006  6B02  85  50              STA $50       :STORE FOR LOW BYTE OF OLD
                                                 ADD.
0007  6B04  85  52              STA $52       :STORE FOR LOW BYTE OF NEW
                                                 ADD.
0008  6B06  A9  60              LDA #$60      :STORE HIGH BYTE OF OLD
                                                 ADD
0009  6B08  85  51              STA $51
0010  6B0A  A9  02              LDA #$02      :STORE HIGH BYTE OF NEW
                                                 ADD
0011  6B0C  85  53              STA $53
0012  6B0E  A0  00              LDY #$00      :COUNTER FOR LOW BYTE
0013  6B10  A2  0B              LDX #$0B      :11-K BLOCKS COUNTER
0014  6B12  B1  50      MOVE    LDA ($50),Y
0015  6B14  91  52              STA ($52),Y
0016  6B16  CB                  INY
0017  6B17  D0  F9              BNE MOVE      :1-K BLOCK STORED?
0018  6B19  CA                  DEX
0019  6B1A  F0  07              BEQ EXIT      :ALL THE BLOCKS MOVED?
0020  6B1C  E6  51              INC $51
0021  6B1E  E6  53              INC $53
0022  6B20  4C  12  6B          JNP MOVE
0023  6B23  4C  00  02 EXIT     JMP $0200     :START THE BASIC
                                                 ENHANCEMENTS.
0024  6B26                     .END
```

APPENDIX VIII

Baud Rate Generator

The baud rate generator circuit (Figure A6) was constructed on PC board and added to the keyboard/printer interface system. One of four output clock rates are selected with switch S3 as shown in Table AIX.

Table AIX. Output Clock Rate

Key Position[a]				Rate Select		Rate
1	2	3	4	B	A	
1	0	1	0	0	0	X1
1	0	0	1	0	1	X8
0	1	1	0	1	0	X16
0	1	0	1	1	1	X64

[a] 1 = Closed, 0 = Open

The MC14411 bit rate generator chip can generate a wide range of output frequencies as shown in Table AX. Any of these frequencies can be selected through switches S1 or S2. Normally keys 2 and 3 on switch S3, and key 5 on switch S2 are closed.

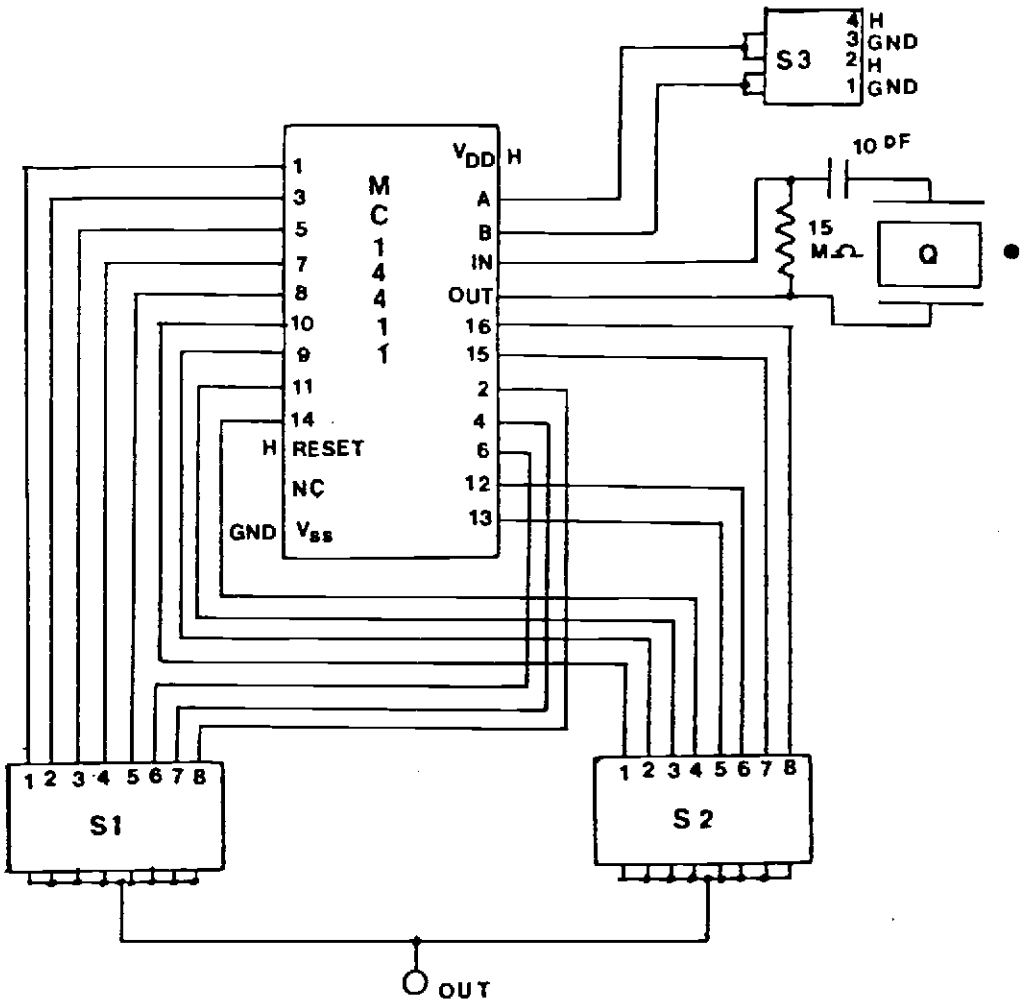

Figure A6. Baud rate generator. S1 and S2, 8 key SPST switch; S3, 4 key SPST switch; Q, 1.8432 MHz quartz crystal oscillator.

Table AX. Frequencies Generated by MC14411 Chip

Switch	Key No.	Output Rate (Hz)			
		X64	X16	X8	X1
S1	1	614.4k	153.6k	76.8k	9600
	2	460.8k	115.2k	57.6k	7200
	3	307.2k	76.8k	38.4k	4800
	4	230.4k	57.6k	28.8k	3600
	5	153.6k	38.4k	19.2k	2400
	6	115.2k	28.6k	14.4k	1800
	7	76.8k	19.2k	9600	1200
	8	38.4k	9600	4800	600
S2	1	19.2k	4800	2400	300
	2	12.8k	3200	1600	200
	3	9600	2400	1200	150
	4	8613.2	2153.3	1076.6	134.5
	5	7035.5	1758.8	879.4	109.9
	6	4800	1200	600	75
	7	921.6k	921.6k	921.6k	921.6k
	8	1.843M	1.843M	1.843M	1.843M

APPENDIX IX

2-Byte Multiplexed Up-Down Counter

The circuit (Figure A7) is built on PC board and placed in the Vector cage beside the other PC boards. The signal from I/V can be switched between this board and ADC through a SPDT switch in the switch box (Figure A10).

The data are transferred into the SYM-1 through eight I/O lines by employing TRI-STATE multiplexing of the data lines. IC5-IC8 are under the control of two SYM-1 I/O lines, Buss Control (BC) 1 and 2. When BC1 is high, IC7 and IC8 are enabled and data bits zero through seven are presented to the SYM-1 I/O port for transfer into memory, and when BC2 is high, IC5 and IC6 are enabled and bits eight through fifteen are presented.

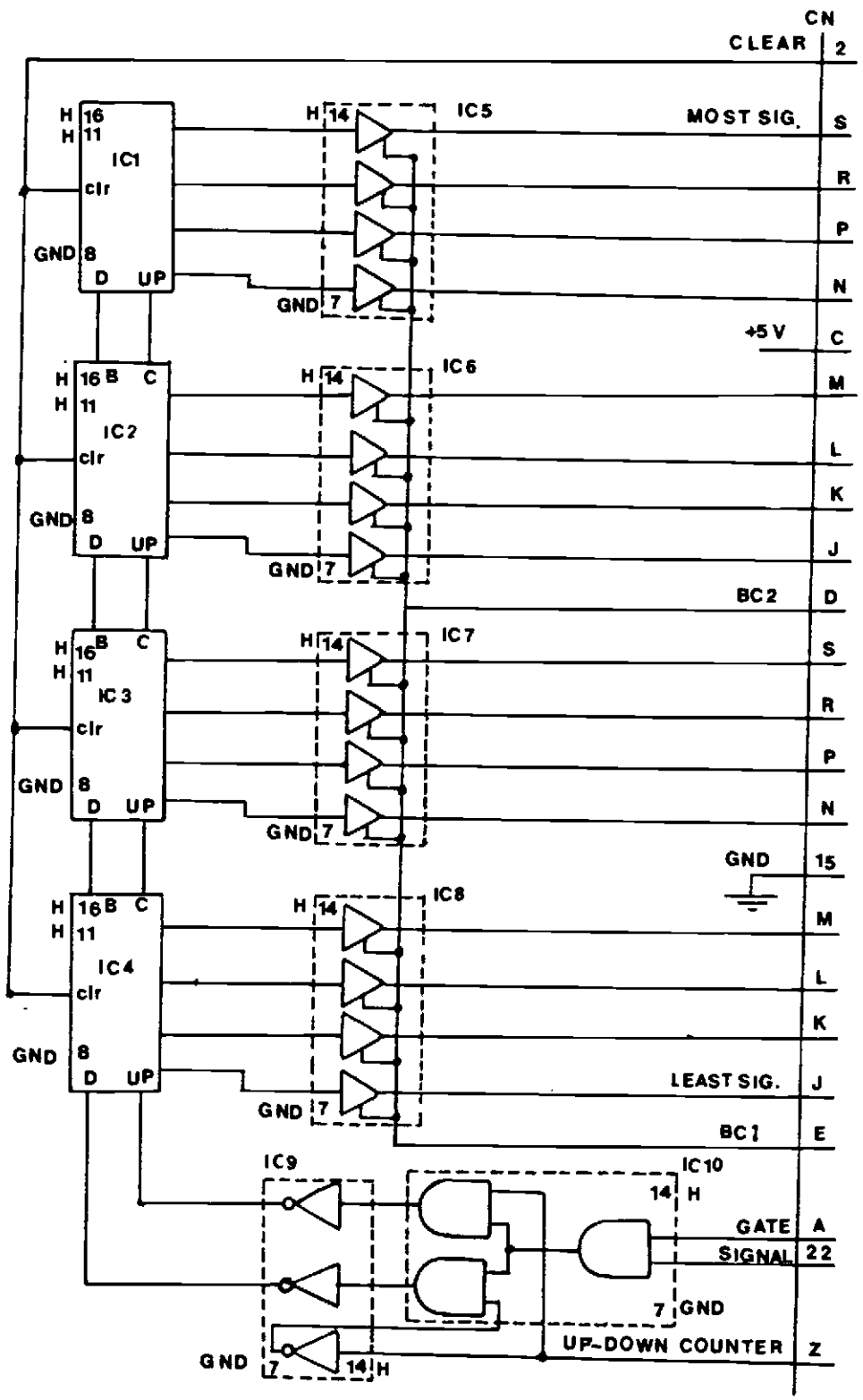

Figure A7. 2-byte multiplexed up-down counter. IC1-IC4, SN74193, synchronous 4-bit binary up-down counter; IC5-IC8, SN74126, tri-state quad buffer hex inverter; IC9, SN7404, quadruple 2-input positive AND gate; CN, connection edge.

APPENDIX X

HCL Pulser Board

A HCL pulser was constructed on PC board (Figure A8). The SYM-1 clock (from a 6522's (AC00) timer) is input to a 4-bit counter. The outputs of this counter go to a BCD-to-decimal decoder which decodes a four bit BCD number to one of ten outputs (the D input is kept low all the time). The decoder outputs (pins 1, 3, 5, and 7) are connected to a TRI-STATE HEX buffers which are controlled by the C. A logic zero signal to the control line allows the signals from the decoder to pass through buffers and this is denoted the free running mode. These signals are used to turn the HCL's on and off one at a time (up to four HCL's). The timer from the 6522 is programmed in a way that the pulse width of the decoder's outputs is the same as chosen pulse width for HCL's under software control. All four I/O lines (12, 14, 16, and 18, inputs of AND gates) are programmed high in the free running mode.

When software controls the pulsing through the four I/O lines (12, 14, 16, and 18), the control line (E) is set high to isolate the NAND gates from the inputs to the TRI-STATE buffers. This is the software control mode.

Figure A8. HCL pulser board schematic.

Pin	Description
A-D	GND
E	HCL pulsing control line from PB5 (AC00)
H	Sampler control in PA (AC01
J	Sampler control to front panel
K	+5 V
M	Clock from PB7 (AC00)
P	HCL 2 control line out to HCL current reg. board
S	HCL 1 control line out to HCL current reg. board
U	HCL 4 control line out to HCL current reg. board
W	HCL 3 control line out to HCL current reg. board
X-Z	GND
1-11	GND
12	HCL 1 control line in from PB0 (AC00)
14	HCL 2 control line in from PB1 (AC00)
16	HCL 3 control line in from PB2 (AC00)
18	HCL 4 control line in from PB3 (AC00)
19-22	GND

All other pins are not connected

Components: IC1, SN74161, synchronous 4-bit counter; IC2, SN7442, BCD-TO-decimal decoder; IC2-IC7, 74lS368, tri-state hex buffer; IC8-IC11, SN7408, quadruple 2-input positive AND gate; CN, connection edge.

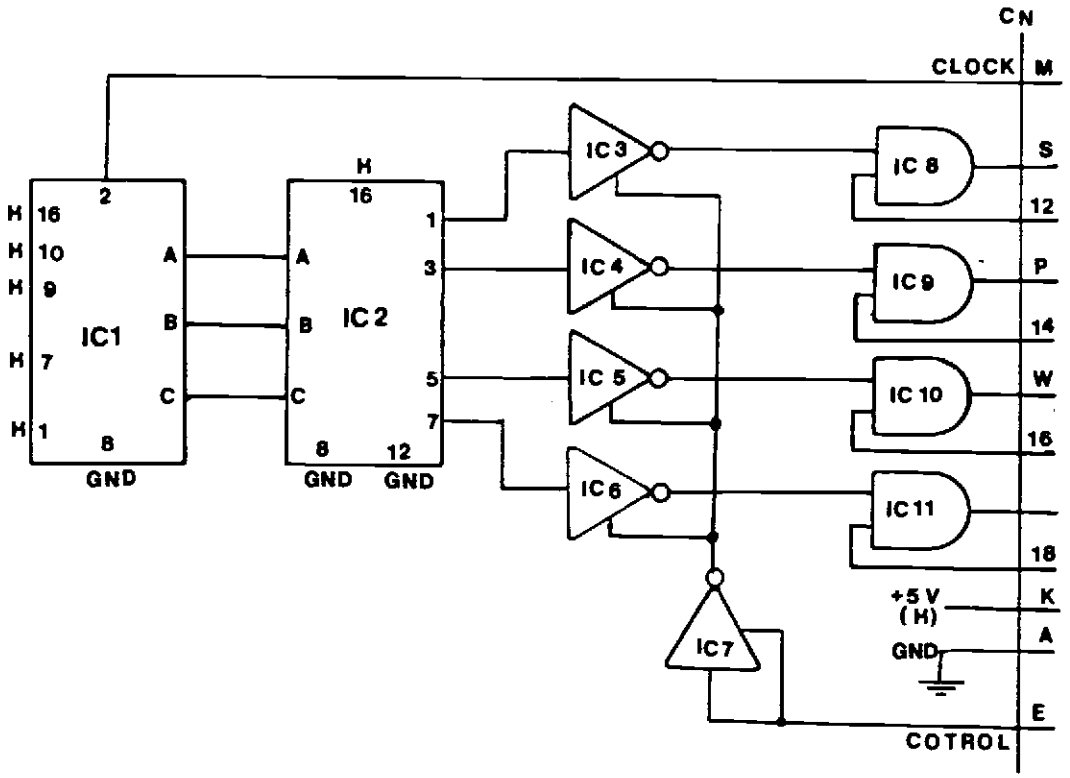
CN
CLOCK
M
IC1
IC2
IC3
IC4
IC5
IC6
IC7
IC8
IC9
IC10
IC11
S
P
W
K
A
E
12
14
16
18
+5 V
(H)
GND
COTROL

Figure A8.

APPENDIX XI

DAC Output Buffer

The circuit shown in Figure A9 was added to the previously designed DAC circuit (83) to improve the performance of DAC.

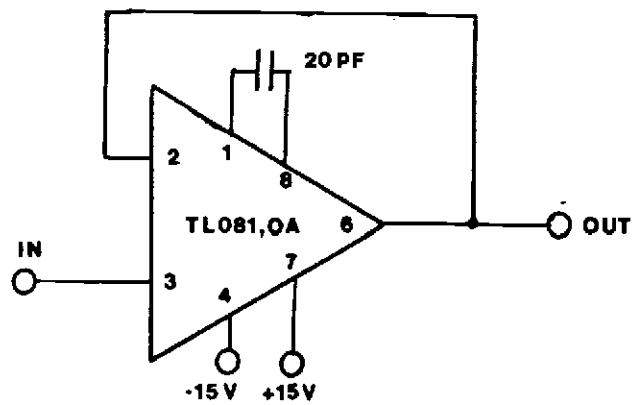

Figure A9. DAC output buffer. IN from pin 22 DAC 80 chip (Figure 14, (83), out; to pin Y (20) of DAC board connection edge.

APPENDIX XII

Mode Selection Switch Box

A set of seven switches were installed in front of the PC board's cage. Through these switches, three modes of operation are selected. Figure A10 shows the location of each switch on the box and each switch's function is described in Table AXI.

Table AXI. Switch Box Functions

Switch	Function
S1,S2	Switches the HCL pulse control between mode 1 (control board) and mode 2 or 3 (computer control).
S3	Disconnects the +5 V from unused PC boards (e.g. in mode 2 and 3 it disconnects clock, auto start, four up-down counters, four digital displays and control board).
S4	Switches V/F output signal between 2-byte multiplexed up-down counter and four up-down counters.
S5	Directs the I/V output to ADC or to V/F
S6	Switches between +5 V and DAC as input voltage for HCL pulsing current control.
S7	Selects between manual and automated start switch.

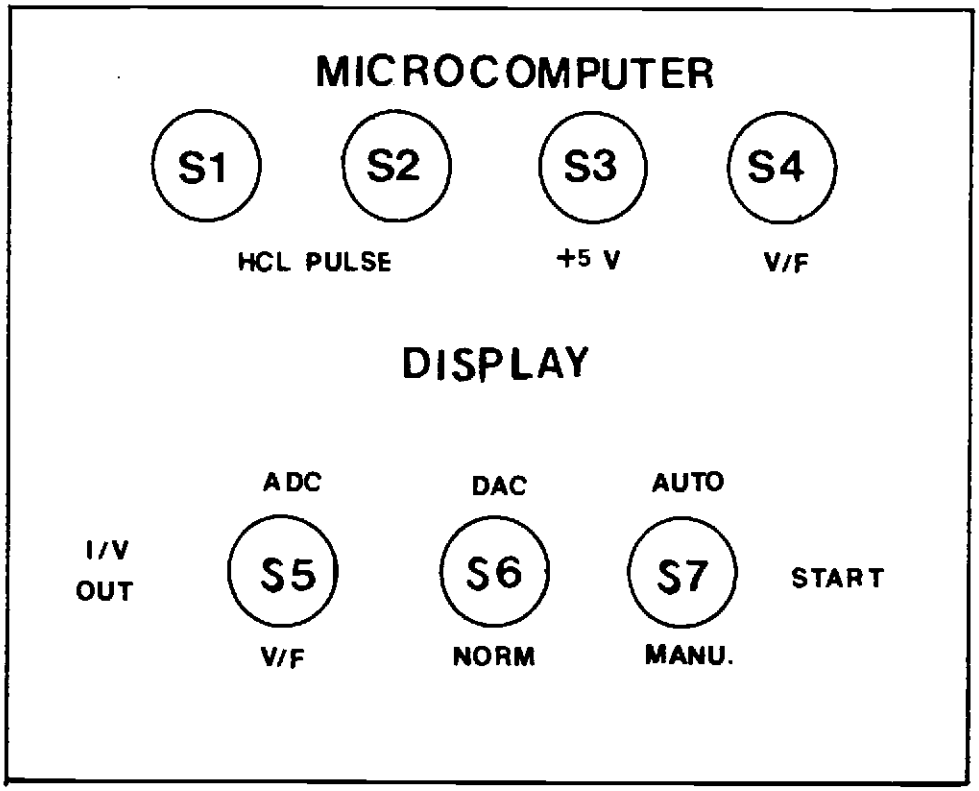

Figure A10. Switch box diagram. S1 and S2, DPDT switches, S3-S7 SPDT switches; for mode 1, all switches down (S7 can be up or down); for mode 2, S1-S4, and S6 up, and S5 down; for mode 3, all switches up.

APPENDIX XIII

Computer Program Operation

The programs for operation in both mode 2 and mode 3 are recorded on cassette tape. For each mode of operation there are two programs: 1) a BASIC program which handles operator input, calculations, and presentation of results 2) an assembly program for operations requiring higher speed such as data acquisition, pulsing of HCL's, HCL current control, DAC and ADC control, and clock programing. The assembly program is loaded first, with the μC in the monitor mode as described in SYM-1 manual (80). Next the BASIC program is loaded. This is done by first typing G 6B00 with the μC still in the monitor mode. The μC jumps to BASIC mode, and is ready to load the BASIC program as described in Brown's Basic Enhancement manual (82).

The programs used for mode 2 are "MULTI-VF" for the BASIC part of program and "3B" for the assembly part, and for mode 3, are "MULTI-AD" and "2B" for the BASIC and the assembly parts, respectively. The listings of the programs follow.

MULTI-VF

```
5 REM THIS PROG TAKES DATA FROM MEMORY, COMPUTES AVR., STD DIV & S/N
10 PRINT
15 DIM L1(35),L2(35),L3(35),L4(35),M1(20),M2(20),M3(20),M4(20),M5(20)
20 PRINT
25 PRINT "HC #1"
30 PRINT "HC #2"
35 PRINT "HC #3"
40 PRINT "HC #4"
45 REM TO START PULSING LAMPS.
50 PRINT
55 PRINT"CHANGE A800-CONNECTION FROM V/F TO A/D & PUSH (CR)"
60 Z=USR(&"8A58",00)
65 PRINT
70 PRINT" TIME ON"
75 INPUT" T1=";T1
80 POKE 20480,T1
85 PRINT
90 PRINT" %TIME ON"
95 INPUT" PC=";PC
100 PRINT
105 PRINT" # OF LAMP"
110 INPUT" LM=";LM
115 POKE 20481,LM
120 PRINT
125 REM RESISTOR USED FOR POWER TRANSISTOR (EMIT-GND)
130 PRINT" RESISTOR VALUE"
135 INPUT" R=";R
140 PRINT
145 T2=T1*((100/(PC*LM))-1)
150 POKE 20483,01
155 IF T2<255 THEN A=T2: GOTO 170
160 A=INT((T2/5)+.5)
165 POKE 20483.05
170 POKE 20482.A
175 IF T1>T2 THEN PRINT"LARGE %TIME ON": GOTO 50
180 CK=(T1*1000/2)-2
185 A=INT(CK/256)
190 POKE 20515,A
195 B=CK-(A*256)
200 POKE 20514,B
205 OF=T2-T1
210 POKE 20484.01
215 IF OF<255 THEN A=OF: GOTO 230
220 A=INT((OF/5)+.5)
```

```
225 POKE 20484,05
230 POKE 20485.A
235 ML=LM
240 PRINT"H.C. AVE. MAMP CURRENTS"
245 PRINT
250 C1=0
255 C2=0
260 C3=0
265 C4=0
270 PRINT" H.C.#1 CURRENT"
275 INPUT" C1=";C1
280 PRINT
285 REM CURRENT CORRECTION FOR RESISTOR VALUE.
290 H=(10-R)*PC/2.5
295 V1=(C1*4.2*R)-(H/C1)
300 REM LAMPS' CURRENT CORRECTION FOR PC NOT EQUAL TO 12.5%
305 MA=(V1*12.5)/PC
310 A=INT(MA/256)
315 IF A<=15 THEN 330
320 PRINT" NOT ACCEPTABLE, CHANGE C1 OR R VALUE": GOTO 53
325 PRINT
330 POKE 20486,A
335 B=MA-(A*256)
340 POKE 20487,B
345 IF ML-1=0 THEN 540
350 PRINT" H.C.# 2 CURRENT"
355 INPUT" C2=";C2
360 PRINT
365 V2=(C2*4.2*R)-(H/C2)
370 MA=(V2*12.5)/PC
375 A=INT(MA/256)
380 IF A<=15 THEN 395
385 PRINT" NOT ACCEPTABLE, CHANGE C2 OR R VALUE": GOTO 50
390 PRINT
395 POKE 20488,A
400 B=MA-(A*256)
405 POKE 20489,B
410 IF ML-2=0 THEN 540
415 PRINT" H.C.#3 CURRENT"
420 INPUT" C3=";C3
425 PRINT
430 V3=(C3*4.2*R)-(H/C3)
435 MA=(V3*12.5)/PC
440 A=INT(MA/256)
445 IF A<=15 THEN 460
450 PRINT" NOT ACCEPTABLE, CHANGE C3 OR R VALUE": GOTO 50
455 PRINT
460 POKE 20490,A
465 B=MA-(A*256)
470 POKE 20491,B
475 IF ML-3=0 THEN 540
```

```
480 PRINT" H.C.#4 CURRENT"
485 INPUT" C4=";C4
490 PRINT
495 V4=(C4*4.2*R)-(H/C4)
500 MA=(V4*12.5)/PC
505 A=INT(MA/256)
510 IF A<=15 THEN 525
515 PRINT" NOT ACCEPTABLE, CHANGE C4 OR R VALUE": GOTO 50
520 PRINT
525 POKE 20492,A
530 B=MA-(A*256)
535 POKE 20493,B
540 AV=(C1+C2+C3+C4)/LM
545 AV=(AV*4.2*R)-(H/AV)
550 A=INT(AV/256)
555 POKE 20494,A
560 B=AV-(A*256)
565 POKE 20495,B
570 PRINT
575 PRINT" T1=";T1,"PC=";PC,"LM=";LM,"R=";R
580 PRINT" C1=";C1,"C2=";C2,"C3=";C3,"C4=";C4
585 PRINT
590 PRINT" ARE THESE VALUES CORRECT? YES=1,NO=0"
595 INPUT" ANS=";Y
600 IF Y=0 THEN 50
605 PRINT
610 PRINT" READY TO READ CURRENT! PUSH (CR)."
615 Z=USR(&"4500",00)
620 REM CURRENT READING BY A/D ACROSS ABOVE RESISTOR
625 A=PEEK(20496)
630 B=PEEK(20497)
635 C=((B*256)+A)*10000/(4095*R)
640 D=INT(C+.5)
645 PRINT
650 PRINT" PEAK TO PEAK CURRENTS"
655 PRINT
660 PRINT" H.C.#1 CURRENT=";D;" MAMP"
665 A=PEEK(20498)
670 B=PEEK(20499)
675 C=((B*256)+A)*10000/(4095*R)
680 D=INT(C+.5)
685 PRINT" H.C.#2 CURRENT=";D;" MAMP"
690 A=PEEK(20500)
695 B=PEEK(20501)
700 C=((B*256)+A)*10000/(4095*R)
705 D=INT(C+.5)
710 PRINT" H.C.#3 CURRENT=";D;" MAMP"
715 A=PEEK(20502)
720 B=PEEK(20503)
725 C=((B*256)+A)*10000/(4095*R)
730 D=INT(C+.5)
```

```
735 PRINT" H.C.#4 CURRENT=";D;" MAMP"
740 PRINT
745 PRINT" READ MORE YES=1,NO=0"
750 INPUT" ANS=";Y
755 IF Y=0 THEN 790
760 PRINT
765 PRINT" ANY CHANGE YES=1,NO=0"
770 INPUT" ANS=";Y
775 PRINT
780 IF Y>0 THEN 235
785 IF Y=0 THEN 605
790 PRINT
795 PRINT"CHANGE A800-CONNECTION FROM A/D TO V/F & PUSH (CR)"
800 Z=USR(&"8A58",00)
805 PRINT
810 PRINT" # OF LAPS"
815 INPUT" LP=";LP
820 POKE 20504,LP
825 PRINT
830 PRINT" # OF POINT"
835 INPUT" PT=";PT
840 POKE 20505,PT
845 PRINT
850 PRINT" RF VALUE (M-OHM)"
855 INPUT" RF=";RF
860 PRINT
865 PRINT" CF VALUE (P-F)"
870 INPUT" CF=";CF
875 TM=INT((5*RF*CF/50)+.5)
880 DT=TM*.05
885 POKE 20516,TM
890 RD=1000*(T1-DT)
895 TT=T1-DT
900 POKE 20513,01
905 IF RD<=256 THEN A=RD: GOTO 940
910 FOR J=0 TO 251
915 B=5+J
920 A=INT((RD/B)+.5)
925 IF A<=256 THEN 935
930 NEXT
935 POKE 20513,B
940 POKE 20506,A
945 PRINT
950 PRINT" # OF RUNS"
955 INPUT" RN=";RN
960 PRINT
965 PRINT" PMT VOLTAGE"
970 INPUT" PM=";PM
975 PRINT
980 IF PM=400 THEN GM=2.75E03
985 IF PM=500 THEN GM=1.5E04
```

```
990 IF PM=600 THEN GM=6.8E04
995 IF PM=700 THEN GM=2.25E05
1000 IF PM=800 THEN GM=6.8E05
1005 IF PM=900 THEN GM=1.9E06
1010 IF PM=1000 THEN GM=5E06
1015 REM NOISE EQUIVALENT BANDPASS 1/S.
1020 DF=1000/(2*(T1-DT)*LP)
1025 G=(LOG(GM)/LOG(10))/9
1030 GA=10^G
1035 KK=2*1.6E-19*DF*(1+1/(GA-1))
1040 ZA=GM*RF*KK*(1E06)
1045 PRINT" CALIBRATION CURVE YES=1,NO=0"
1050 INPUT" ANS=";CC
1055 IF CC=1 THEN 2500
1060 PRINT
1065 REM ABOVE SECTION INITIALIZES USER DEFINED VARIABLES.
1070 REM THE NEXT SECTION COLLECTS BLANK DATA FROM MEMORY.
1075 Q=0
1080 REM FOR FIRST RUN
1085 PRINT
1090 POKE 44033,00
1095 REM TO START SAMPLER FOR BLANK.
1100 PRINT" DO YOU WANT DARK DATA? YES=1,NO=0"
1105 INPUT" DK=";DK
1110 IF DK=0 THEN 1170
1115 PRINT
1120 PRINT" COVER ENTRANCE SLIT & PUSH (CR)."
1125 PRINT
1130 Z=USR(&"8A58",00)
1135 PRINT" DARK DATA"
1140 PRINT"----------"
1145 Z=USR(&"56E6",00)
1150 GOSUB 1390
1155 PRINT" DARK AVE & STD DIV."
1160 PRINT
1165 GOSUB 1525
1170 PRINT
1175 PRINT" RUN BLANK PUSH (CR) TO START."
1180 Z=USR(&"8A58",00)
1185 PRINT
1190 PRINT "BLANK DATA"
1195 PRINT"----------"
1200 Z=USR(&"56E6",00)
1205 REM TO COLLECT BLANK DATA
1210 GOSUB 1390
1215 PRINT
1220 PRINT "BLANK AVE & STD DIV"
1225 PRINT
1230 GOSUB 1525
1235 PRINT
1240 POKE 44033,02
```

```
1245 REM TO START SAMPLER FOR SAMPLE.
1250 PRINT" RUN SAMPLE PUSH (CR) TO START."
1255 Z=USR(&"8A58",00)
1260 PRINT
1265 PRINT "SAMPLE DATA"
1270 PRINT"-----------"
1275 Z=USR(&"56E6",00)
1280 REM TO COLLECT SAMPLE DATA
1285 GOSUB 1390
1290 PRINT
1295 PRINT "TOTAL SIG AVER & STD DEV"
1300 PRINT
1305 POKE 44033.00
1310 GOSUB 1790
1315 IF CC=0 THEN 1325
1320 RETURN
1325 GOSUB 2150
1330 Q=Q+1
1335 IF Q<RN THEN 1085
1340 PRINT "EXTRA RUN YES=1 NO=0"
1345 INPUT" ANS=";Y
1350 IF Y=0 THEN 2940
1355 PRINT
1360 PRINT "CHANGE VARIABLES: UPPER SEC.=2, LOWER SEC.=1, NO=0"
1365 INPUT" ANS=";Y
1370 IF Y=0 THEN 1085
1375 IF Y=1 THEN 805
1380 IF Y=2 THEN 50
1385 PRINT
1390 REM THIS SUB TAKES DATA FROM MEMORY FOR EACH LAMP.
1395 N=PT-1
1400 FOR J=0 TO N
1405 A=PEEK(20550+J)
1410 B=PEEK(20600+J)
1415 C=PEEK(20650+J)
1420 REM A,B,C THREE BYTES WHICH CONTAIN THE JTH
1425 REM DATA POINT A THE LEAST SIG FIG. & C MOST SIG FIG.
1430 D=(C*256)+B
1435 L1(J)=(D*256)+A
1440 A=PEEK(20700+J)
1445 B=PEEK(20750+J)
1450 C=PEEK(20800+J)
1455 D=(C*256)+B
1460 L2(J)=(D*256)+A
1465 A=PEEK(20850+J)
1470 B=PEEK(20900+J)
1475 C=PEEK(20950+J)
1480 D=(C*256)+B
1485 L3(J)=(D*256)+A
1490 A=PEEK(21000+J)
1495 B=PEEK(21050+J)
```

```
1500 C=PEEK(21100+J)
1505 D=(C*256)+B
1510 L4(J)=(D*256)+A
1515 NEXT J
1520 RETURN
1525 REM THIS SUB. FINDS MEANS AND STD DIV. IN BLANK & DARK.
1530 K1=0
1535 K2=0
1540 K3=0
1545 K4=0
1550 N=PT-1
1555 FOR J=0 TO N
1560 K1= K1+L1(J)
1565 K2= K2+L2(J)
1570 K3= K3+L3(J)
1575 K4= K4+L4(J)
1580 NEXT J
1585 K1=K1/PT
1590 K2=K2/PT
1595 K3=K3/PT
1600 K4=K4/PT
1605 PRINT INT(K1+.5),INT(K2+.5),INT(K3+.5),INT(K4+.5)
1610 F1=0
1615 F2=0
1620 F3=0
1625 F4=0
1630 G1=0
1635 G2=0
1640 G3=0
1645 G4=0
1650 FOR J=0 TO N
1655 F1= L1(J)-K1
1660 G1=(F1*F1)+G1
1665 F2= L2(J)-K2
1670 G2=(F2*F2)+G2
1675 F3= L3(J)-K3
1680 G3=(F3*F3)+G3
1685 F4= L4(J)-K4
1690 G4=(F4*F4)+G4
1695 NEXT J
1700 S1= SQR(G1/N)
1705 S2= SQR(G2/N)
1710 S3= SQR(G3/N)
1715 S4= SQR(G4/N)
1720 A=INT(S1*100+.5)/100
1725 B=INT(S2*100+.5)/100
1730 C=INT(S3*100+.5)/100
1735 D=INT(S4*100+.5)/100
1740 PRINT A,B,C,D
1745 PRINT
1750 PRINT"PRINT DATA YES=1,NO=0"
```

```
1755 INPUT" ANS=";Y
1760 PRINT
1765 IF Y=0 THEN 1785
1770 FOR J=0 TO N
1775 PRINT INT(L1(J)+.5),INT(L2(J)+.5),INT(L3(J)+.5),INT(L4(J)+.5)
1780 NEXT J
1785 RETURN
1790 REM THIS SUB. FINDS MEAN & STD DIV. OF TOTAL SIGNAL.
1795 T1=0
1800 T2=0
1805 T3=0
1810 T4=0
1815 N=PT-1
1820 FOR J=0 TO N
1825 T1=L1(J)+T1
1830 T2=L2(J)+T2
1835 T3=L3(J)+T3
1840 T4=L4(J)+T4
1845 NEXT J
1850 T1=T1/PT
1855 T2=T2/PT
1860 T3=T3/PT
1865 T4=T4/PT
1870 PRINT INT(T1+.5),INT(T2+.5),INT(T3+.5),INT(T4+.5)
1875 Z1=ZA*T1/(TT*LP*1E05)
1880 Z2=ZA*T2/(TT*LP*1E05)
1885 Z3=ZA*T3/(TT*LP*1E05)
1890 Z4=ZA*T4/(TT*LP*1E05)
1895 IF Z1=<0 THEN ZA=0: GOTO 1905
1900 ZA=SQR(Z1)
1905 IF Z2=<0 THEN ZB=0: GOTO 1915
1910 ZB=SQR(Z2)
1915 IF Z3=<0 THEN ZC=0: GOTO 1925
1920 ZC=SQR(Z3)
1925 IF Z4=<0 THEN ZD=0: GOTO 1935
1930 ZD=SQR(Z4)
1935 H1=0
1940 N1=0
1945 H2=0
1950 N2=0
1955 H3=0
1960 N3=0
1965 H4=0
1970 N4=0
1975 FOR J=0 TO N
1980 H1=L1(J)-T1
1985 N1=(H1*H1)+N1
1990 H2=L2(J)-T2
1995 N2=(H2*H2)+N2
2000 H3=L3(J)-T3
2005 N3=(H3*H3)+N3
```

```
2010 H4=L4(J)-T4
2015 N4=(H4*H4)+N4
2020 NEXT J
2025 V1=SQR(N1/N)
2030 V2=SQR(N2/N)
2035 V3=SQR(N3/N)
2040 V4=SQR(N4/N)
2045 A=INT(V1*100+.5)/100
2050 B=INT(V2*100+.5)/100
2055 C=INT(V3*100+.5)/100
2060 D=INT(V4*100+.5)/100
2065 PRINT A,B,C,D
2070 GOSUB 1745
2075 PRINT
2080 PRINT" RMS SHOT NOISE (VOLTAGE)."
2085 PRINT
2090 PRINT ZA,ZB,ZC,ZD
2095 PRINT
2100 PRINT "NET SIGNAL"
2105 PRINT
2110 REM THIS SUBROUTINE FINDS THE NET SIGNAL.
2115 X1=T1-K1
2120 X2=T2-K2
2125 X3=T3-K3
2130 X4=T4-K4
2135 PRINT INT(X1+.5),INT(X2+.5),INT(X3+.5),INT(X4+.5)
2140 PRINT
2145 RETURN
2150 PRINT" NET SIGNAL/BLANK STD DIV."
2155 REM THIS SUBROUTINE FINDS RATIO OF NET SIGNAL TO
2160 REM BLANK NOISE & NET SIGNAL TO TOTAL NOISE.
2165 IF S1<=0 THEN 2175
2170 P1=X1/S1
2175 IF S2<=0 THEN 2185
2180 P2=X2/S2
2185 IF S3<=0 THEN 2195
2190 P3=X3/S3
2195 IF S4<=0 THEN 2205
2200 P4=X4/S4
2205 PRINT
2210 A=INT(P1*10+.5)/10
2215 B=INT(P2*10+.5)/10
2220 C=INT(P3*10+.5)/10
2225 D=INT(P4*10+.5)/10
2230 PRINT A,B,C,D
2235 PRINT
2240 PRINT" NET SIGNAL/TOTAL NOISE"
2245 Q1=SQR((S1*S1)+(V1*V1))
2250 Q2=SQR((S2*S2)+(V2*V2))
2255 Q3=SQR((S3*S3)+(V3*V3))
2260 Q4=SQR((S4*S4)+(V4*V4))
```

```
2265 IF Q1=0 THEN 2275
2270 W1=X1/Q1
2275 IF Q2=0 THEN 2285
2280 W2=X2/Q2
2285 IF Q3=0 THEN 2295
2290 W3=X3/Q3
2295 IF Q4=0 THEN 2305
2300 W4=X4/Q4
2305 PRINT
2310 A=INT(W1*10+.5)/10
2315 B=INT(W2*10+.5)/10
2320 C=INT(W3*10+.5)/10
2325 D=INT(W4*10+.5)/10
2330 PRINT A,B,C,D
2335 PRINT
2340 PRINT" CONC. OF SOLN. #1 (PPM)"
2345 INPUT" G1=";G1
2350 PRINT
2355 IF ML-1=0 THEN 2415
2360 PRINT" CONC. OF SOLN. #2 (PPM)"
2365 INPUT" G2=";G2
2370 PRINT
2375 IF ML-2=0 THEN 2415
2380 PRINT" CONC. OF SOLN. #3 (PPM)"
2385 INPUT" G3=";G3
2390 PRINT
2395 IF ML-3=0 THEN 2415
2400 PRINT" CONC. OF SOLN. #4 (PPM)"
2405 INPUT" G4=";G4
2410 PRINT
2415 IF P1=0 THEN Y1=0: GOTO 2430
2420 D1=2*G1/P1
2425 Y1=INT((D1*1000)+.5)/1000
2430 IF P2=0 THEN Y2=0: GOTO 2445
2435 D2=2*G2/P2
2440 Y2=INT((D2*1000)+.5)/1000
2445 IF P3=0 THEN Y3=0: GOTO 2460
2450 D3=2*G3/P3
2455 Y3=INT((D3*1000)+.5)/1000
2460 IF P4=0 THEN Y4=0: GOTO 2475
2465 D4=2*G4/P4
2470 Y4=INT((D4*1000)+.5)/1000
2475 PRINT" DETECTION LIMITS (PPM)"
2480 PRINT"------------------------"
2485 PRINT Y1,Y2,Y3,Y4
2490 PRINT
2495 RETURN
2500 REM THIS SUB. IS FOR CALIB. CURVE & UKN. CALCULATIONS.
2505 PRINT
2510 PRINT" # OF STANDARDS"
2515 INPUT" SD=";SD
```

```
2520 PRINT
2525 PRINT" INTER THE CONCENTRATION OF STANDARDS."
2530 PRINT
2535 F=SD-1
2540 FOR I=0 TO F
2545 PRINT I+1;
2550 INPUT J
2555 PRINT
2560 M5(I)=J
2565 NEXT I
2570 PRINT
2575 PRINT" CALIBRATION CURVE DATA"
2580 PRINT"-----------------------"
2585 FOR H=0 TO F
2590 A1=0:A2=0:A3=0:A4=0
2595 K=RN-1
2600 FOR I=0 TO K
2605 GOSUB 1060
2610 A1=A1+X1
2615 A2=A2+X2
2620 A3=A3+X3
2625 A4=A4+X4
2630 NEXT I
2635 M1(H)=A1/RN
2640 M2(H)=A2/RN
2645 M3(H)=A3/RN
2650 M4(H)=A4/RN
2655 NEXT H
2660 PRINT" CONC.          NET AVE. SIGNAL."
2665 FOR H=0 TO F
2670 PRINT
2675 PRINT M5(H),INT(M1(H)),INT(M2(H)),INT(M3(H)),INT(M4(H))
2680 NEXT H
2685 PRINT
2690 L=0
2695 PRINT" WHAT ARE THE 1ST & 2ND POINTS FOR THE SLOPE CALC."
2700 INPUT" 1ST=";N
2705 INPUT" 2ND=";K
2710 S1=0:S2=0:S3=0:S4=0
2715 N=N-1
2720 K=K-2
2725 FOR J=N TO K
2730 W=M5(J+1)-M5(J)
2735 S1=(M1(J+1)-M1(J))/W+S1
2740 S2=(M2(J+1)-M2(J))/W+S2
2745 S3=(M3(J+1)-M3(J))/W+S3
2750 S4=(M4(J+1)-M4(J))/W+S4
2755 NEXT J
2760 PRINT
2765 PRINT" SLOPES OF CALIB. CURVES"
2770 PRINT
```

```
 2775 PRINT INT(S1+.5),INT(S2+.5),INT(S3+.5),INT(S4+.5)
 2780 PRINT
 2785 IF L=1 THEN 2875
 2790 PRINT" DO YOU RUN UNKNOWN YES=1, NO=0"
 2795 INPUT" ANS=";Y
 2800 IF Y=0 THEN 2915
 2805 A1=0:A2=0:A3=0:A4=0
 2810 K=RN-1
 2815 FOR H=0 TO K
 2820 GOSUB 1060
 2825 A1=A1+(X1/RN)
 2830 A2=A2+(X2/RN)
 2835 A3=A3+(X3/RN)
 2840 A4=A4+(X4/RN)
 2845 NEXT H
 2850 PRINT
 2855 PRINT" NET UKN. SIGNAL."
 2860 PRINT
 2865 PRINT INT(A1+.5),INT(A2+.5),INT(A3+.5),INT(A4+.5)
 2870 PRINT
 2875 PRINT" CONCENTRATION OF UKN."
 2880 PRINT
 2885 IF S1=0 THEN A1/S1=0
 2890 IF S2=0 THEN A2/S2=0
 2895 IF S3=0 THEN A3/S3=0
 2900 IF S4=0 THEN A4/S4=0
 2905 PRINT A1/S1,A2/S2,A3/S3,A4/S4
 2910 PRINT
 2915 PRINT" CALCULATE THE SLOPE AGAIN YES=1, NO=0"
 2920 INPUT" ANS=";L
 2925 PRINT
 2930 IF L=1 THEN 2770
 2935 GOTO 1340
 2940 PRINT
 2945 PRINT"CHANGE A800-CONNECTION FROM V/F TO A/D"
 2950 END
OK
```

3B

```
.....PAGE 0001

LINE # LOC     CODE       LINE

0002  0000               ; THIS PROGRAM IS A PART OF A BASIC PROGRAM
0003  0000               ; WHICH RUNS TMMS INSTRUMENT & COLLECT DATA.
0004  0000               ;**************  I/O PORTS  ***************
0005  0000               ;
0006  0000               RBD=$A000         ;DAC'S STB. & 4 HIGH BITS.
0007  0000               RBDD=$A002
0008  0000               RAD=$A001         ;DAC'S 8 LOW BITS.
0009  0000               RADD=$A003
0010  0000               ORB=$A402
0011  0000               DRB=$A800         ;ADC'S CONTROL BITS.
0012  0000               DDRB=$A802         ;OR COUNTER CONTROLS.
0013  0000               DRA=$A801         ;ADC'S DATA BITS.
0014  0000               DDRA=$A803         ;OR COUNTER DATA OUTPUT.
0015  0000               PBD=$AC00         ;H.C. LAMP PULSING & CLOCK.
0016  0000               PBDD=$AC02
0017  0000               PAD=$AC01         ;SAMPLER CONTROL.
0018  0000               PADD=$AC03
0019  0000               T1LL=$AC04         ;LOW-ORDER LATCH TIMER-1.
0020  0000               T1CH=$AC05         ;HIGH-ORDER COUNTER.
0021  0000               ACR=$AC0B         ;AUXILIARY CONTROL REGISTER.
0022  0000               PW=$A414         ;1T (1 USEC)
0023  0000               SR=$A417         ;1024T (1 MSEC)
0024  0000               CRLF=$834D
0025  0000               ;
0026  0000               ;****RESERVED MEMORY LOCATIONS FOR VARIABLES****.
0027  0000                     *=$5000
0028  5000               ON     *=*+1
0029  5001               LAMP   *=*+1
0030  5002               DARK   *=*+1
0031  5003               TLOOP  *=*+1
0032  5004               TIMLOP *=*+1
0033  5005               OFF    *=*+1
0034  5006               CURH1  *=*+1
0035  5007               CURL1  *=*+1
0036  5008               CURH2  *=*+1
0037  5009               CURL2  *=*+1
0038  500A               CURH3  *=*+1
0039  500B               CURL3  *=*+1
0040  500C               CURH4  *=*+1
0041  500D               CURL4  *=*+1
0042  500E               AVCRH  *=*+1
0043  500F               AVCRL  *=*+1
```

```
0044  5010              CORL1   *=*+1
0045  5011              CORH1   *=*+1
0046  5012              CORL2   *=*+1
0047  5013              CORH2   *=*+1
0048  5014              CORL3   *=*+1
0049  5015              CORH3   *=*+1
0050  5016              CORL4   *=*+1
0051  5017              CORH4   *=*+1
0052  5018              LAP     *=*+1
0053  5019              POINT   *=*+1
0054  501A              RD      *=*+1
0055  501B              DACL    *=*+1
0056  501C              DACH    *=*+1

......PAGE 0002


LINE # LOC     CODE       LINE

0057  501D              ADCL    *=*+1
0058  501E              ADCH    *=*+1
0059  501F              LOP     *=*+1
0060  5020              LOMP    *=*+1
0061  5021              REED    *=*+1
0062  5022              CLOCK   *=*+2
0063  5024              TM      *=*+1
0064  5025              MT      *=*+1
0065  5026                      *=$00F6
0066  00F6              HOLDER  *=*+2
0067  00F8              ;
0068  00F8              ;***** MEMORY LOCATIONS RESERVED FOR DATA STORAGE **
0069  00F8              ;
0070  00F8              ARY11=$5046
0071  00F8              ARY12=$5078
0072  00F8              ARY13=$50AA
0073  00F8              ARY21=$50DC
0074  00F8              ARY22=$510E
0075  00F8              ARY23=$5140
0076  00F8              ARY31=$5172
0077  00F8              ARY32=$51A4
0078  00F8              ARY33=$51D6
0079  00F8              ARY41=$5208
0080  00F8              ARY42=$523A
0081  00F8              ARY43=$526C
0082  00F8              ;*** INITIALIZATION OF DATA DIRECTION ***
0083  00F8              ;
0084  00F8                      *=$5500
0085  5500  A9 FF               LDA #$FF        ;OUTPUT PORT FOR DAC
0086  5502  8D 03 A0           STA RADD
0087  5505  8D 02 A0           STA RBDD
0088  5508  A9 0F              LDA #$0F        ;LAMP PULSING I/O PORT
0089  550A  8D 02 AC           STA PBDD
0090  550D  8D 03 AC           STA PADD        ;SAMPLER I/O PORT
```

```
0091  5510  A9 00           LDA #$00        ;ADC DATA INPUT
0092  5512  8D 03 A8        STA DDRA
0093  5515  A9 3F           LDA #$3F        ;ADC CONTROL PORT
0094  5517  8D 02 A8        STA DDRB
0095  551A                 ;
0096  551A                 ;***** H.C. LAMP.S CURRENT READING *****
0097  551A                 ;
0098  551A  A9 00           LDA #$00        ;CLEAR ALL FOLLOWING LOC.
0099  551C  8D 10 50        STA CORL1
0100  551F  8D 11 50        STA CORH1
0101  5522  8D 12 50        STA CORL2
0102  5525  8D 13 50        STA CORH2
0103  5528  8D 14 50        STA CORL3
0104  552B  8D 15 50        STA CORH3
0105  552E  8D 16 50        STA CORL4
0106  5531  8D 17 50        STA CORH4
0107  5534  A9 59      LMP1  LDA #<RED1      ;LOAD LOW BYTE OF RED1 ADDR.
0108  5536  85 F6           STA HOLDER
0109  5538  A9 55           LDA #>RED1        ;LOAD HIGH BYTE OF ADDR.
0110  553A  85 F7           STA HOLDER+1
0111  553C  AD 01 50        LDA LAMP
```

.....PAGE 0003

```
LINE # LOC     CODE       LINE

0112  553F  8D 20 50        STA LOMP
0113  5542  AD 07 50        LDA CURL1       ;LOAD THE CURRENT FOR #1
0114  5545  8D 1B 50        STA DACL
0115  5548  AD 06 50        LDA CURH1
0116  554B  8D 1C 50        STA DACH
0117  554E  20 63 56        JSR DAK         ;CONVERT TO ANALOGE.
0118  5551  A9 01           LDA #$01        ;TURN LAMP #1 ON.
0119  5553  8D 00 AC        STA PBD
0120  5556  4C 7B 56        JMP KLOK
0121  5559  AD 1D 50   RED1  LDA ADCL        ;LOAD CURRENT READING BY A/D.
0122  555C  8D 10 50        STA CORL1
0123  555F  AD 1E 50        LDA ADCH
0124  5562  8D 11 50        STA CORH1
0125  5565  A9 00           LDA #$00        ;TURN OFF THE LAMP.
0126  5567  8D 00 AC        STA PBD
0127  556A  A9 71           LDA #<LMP2
0128  556C  85 F6           STA HOLDER      ;SAVE RETURNE ADDR.
0129  556E  4C 93 56        JMP TIMOFF
0130  5571  CE 20 50   LMP2  DEC LOMP
0131  5574  D0 03           BNE TWO
0132  5576  4C 34 55        JMP LMP1
0133  5579  AD 09 50   TWO   LDA CURL2
0134  557C  8D 1B 50        STA DACL
0135  557F  AD 08 50        LDA CURH2
```

```
0136  5582  8D 1C 50          STA DACH
0137  5585  20 63 56          JSR DAK
0138  5588  A9 02             LDA #$02        ;TURN LAMP #2 ON.
0139  558A  8D 00 AC          STA PBD
0140  558D  A9 94             LDA #<RED2
0141  558F  85 F6             STA HOLDER
0142  5591  4C 7B 56          JMP KLOK
0143  5594  AD 1D 50    RED2  LDA ADCL
0144  5597  8D 12 50          STA CORL2
0145  559A  AD 1E 50          LDA ADCH
0146  559D  8D 13 50          STA CORH2
0147  55A0  A9 00             LDA #$00
0148  55A2  8D 00 AC          STA PBD
0149  55A5  A9 AC             LDA #<LMP3
0150  55A7  85 F6             STA HOLDER
0151  55A9  4C 93 56          JMP TIMOFF
0152  55AC  CE 20 50    LMP3  DEC LOMP
0153  55AF  D0 03             BNE THREE
0154  55B1  4C 34 55          JMP LMP1
0155  55B4  AD 0B 50    THREE LDA CURL3
0156  55B7  8D 1B 50          STA DACL
0157  55BA  AD 0A 50          LDA CURH3
0158  55BD  8D 1C 50          STA DACH
0159  55C0  20 63 56          JSR DAK
0160  55C3  A9 04             LDA #$04        ;TURN LAMP #3 ON.
0161  55C5  8D 00 AC          STA PBD
0162  55C8  A9 CF             LDA #<RED3
0163  55CA  85 F6             STA HOLDER
0164  55CC  4C 7B 56          JMP KLOK
0165  55CF  AD 1D 50    RED3  LDA ADCL
0166  55D2  8D 14 50          STA CORL3
```

.....PAGE 0004

```
LINE # LOC     CODE       LINE

0167  55D5  AD 1E 50          LDA ADCH
0168  55D8  8D 15 50          STA CORH3
0169  55DB  A9 00             LDA #$00
0170  55DD  8D 00 AC          STA PBD
0171  55E0  A9 E7             LDA #<LMP4
0172  55E2  85 F6             STA HOLDER
0173  55E4  4C 93 56          JMP TIMOFF
0174  55E7  CE 20 50    LMP4  DEC LOMP
0175  55EA  D0 03             BNE FOUR
0176  55EC  4C 34 55          JMP LMP1
0177  55EF  AD 0D 50    FOUR  LDA CURL4
0178  55F2  8D 1B 50          STA DACL
0179  55F5  AD 0C 50          LDA CURH4
```

```
0180  55F8  8D 1C 50          STA DACH
0181  55FB  20 63 56          JSR DAK
0182  55FE  A9 08             LDA #$08        ;TURN LAMP #4 ON.
0183  5600  8D 00 AC          STA PBD
0184  5603  A9 0E             LDA #<RED4
0185  5605  85 F6             STA HOLDER
0186  5607  A9 56             LDA #>RED4
0187  5609  85 F7             STA HOLDER+1
0188  560B  4C 7B 56          JMP KLOK
0189  560E  AD 1D 50    RED4  LDA ADCL
0190  5611  8D 16 50          STA CORL4
0191  5614  AD 1E 50          LDA ADCH
0192  5617  8D 17 50          STA CORH4
0193  561A  A9 00             LDA #$00
0194  561C  8D 00 AC          STA PBD
0195  561F  A9 34             LDA #<LMP1
0196  5621  85 F6             STA HOLDER
0197  5623  A9 55             LDA #>LMP1
0198  5625  85 F7             STA HOLDER+1
0199  5627  4C 93 56          JMP TIMOFF
0200  562A  A9 00       PULS  LDA #$00        ;TURN THE LAMP OFF.
0201  562C  8D 00 AC          STA PBD
0202  562F  20 4D 83          JSR CRLF
0203  5632  A9 F0             LDA #$F0        ;LAMP PULSING I/O PORT.
0204  5634  8D 02 AC          STA PBDD
0205  5637  A9 C0             LDA #$C0        ;SET REGISTER FOR TIMER-1.
0206  5639  8D 0B AC          STA ACR
0207  563C  AD 22 50          LDA CLOCK       ;LOAD TIMER-1 LOW LATCH.
0208  563F  8D 04 AC          STA T1LL
0209  5642  AD 23 50          LDA CLOCK+1      ;LOAD TIMER-1 HIGH COUNTER.
0210  5645  8D 05 AC          STA T1CH
0211  5648  AD 0E 50          LDA AVCRH       ;LOAD AVE. CURRENT.
0212  564B  8D 1C 50          STA DACH
0213  564E  AD 0F 50          LDA AVCRL
0214  5651  8D 1B 50          STA DACL
0215  5654  20 63 56          JSR DAK
0216  5657  A9 00             LDA #$00        ;START PULSING.
0217  5659  8D 00 AC          STA PBD
0218  565C  8D 03 A8          STA DDRA        ;PROTECT THE PORTS.
0219  565F  8D 02 A8          STA DDRB
0220  5662  60                RTS
0221  5663  AD 1B 50    DAK   LDA DACL        ;LOAD LOW 8 BITS

.....PAGE 0005


LINE # LOC     CODE       LINE

0222  5666  49 FF             EOR #$FF        ;TWO'S COMPLEMENT
0223  5668  8D 01 A0          STA RAD
0224  566B  AD 1C 50          LDA DACH        ;LOAD HIGH 4 BITS
0225  566E  49 FF             EOR #$FF
```

```
0226  5670  0A             ASL A          ;SHIFT LEFT FOR STROBE BIT
0227  5671  8D 00 A0       STA ORB
022B  5674  EE 00 A0       INC ORB        ;STROBE DAC
0229  5677  CE 00 A0       DEC ORB
0230  567A  60             RTS
0231  567B  AD 00 50  KLOK  LDA ON         ;SET THE CLOCK.
0232  567E  8D 17 A4       STA SR
0233  5681  A9 80       WEET  LDA #$80
0234  5683  2C 02 A4       BIT ORB        ;TEST IF (CR) IS PUSHED.
0235  5686  D0 08           BNE CUT1
0236  5688  2C 17 A4       BIT SR         ;TEST IF IT IS DONE.
0237  568B  10 F4           BPL WEET
0238  568D  4C B4 56       JMP ADK
0239  5690  4C 2A 56  CUT1  JMP PULS
0240  5693  AE 03 50  TIMOFF LDX TLOOP
0241  5696  F0 16       LOOK  BEQ BACK
0242  5698  AD 02 50       LDA DARK
0243  569B  8D 17 A4       STA SR
0244  569E  A9 80       VEET  LDA #$80
0245  56A0  2C 02 A4       BIT ORB
0246  56A3  D0 0C           BNE CUT2
0247  56A5  2C 17 A4       BIT SR
0248  56A8  10 F4           BPL VEET
0249  56AA  CA             DEX
0250  56AB  4C 96 56       JMP LOOK
0251  56AE  6C F6 00  BACK  JMP (HOLDER)
0252  56B1  4C 2A 56  CUT2  JMP PULS
0253  56B4  A9 C5       ADK   LDA #$C5       ;USE INPUT #1 OF A/D.
0254  56B6  8D 00 A8       STA DRB
0255  56B9  CE 00 A8       DEC DRB        ;START CONVERSION
0256  56BC  EE 00 A8       INC DRB
0257  56BF  A9 40           LDA #$40
0258  56C1  2C 00 A8  TEST  BIT DRB        ;TEST FOR END OF CONV.
0259  56C4  D0 FB           BNE TEST
0260  56C6  AD 01 A8       LDA DRA        ;READ 8 HIGH BITS
0261  56C9  8D 1E 50       STA ADCH
0262  56CC  A9 C7           LDA #$C7       ;TRANSFER 4 LOW BITS
0263  56CE  8D 00 A8       STA DRB
0264  56D1  AD 01 A8       LDA DRA        ;READ 4 LOW BITS
0265  56D4  8D 1D 50       STA ADCL
0266  56D7  A2 04           LDX #$04       ;REARRANGE DATA
0267  56D9  18           GO    CLC
0268  56DA  4E 1E 50       LSR ADCH
0269  56DD  6E 1D 50       ROR ADCL
0270  56E0  CA             DEX
0271  56E1  D0 F6           BNE GO
0272  56E3  6C F6 00       JMP (HOLDER)
0273  56E6                 ;
0274  56E6                 ;***** THIS PORTION COLLECT & STORE DATA *****
0275  56E6                 ;
0276  56E6  A0 00           LDY #$00       ;SET Y AS COUNTER.
```

```
LINE #  LOC     CODE        LINE

0277  56E8  A9 00       CLEAR  LDA #$00        ;CLEAR ALL DATA STORAGES.
0278  56EA  99 46 50            STA ARY11,Y
0279  56ED  99 0E 51            STA ARY22,Y
0280  56F0  99 D6 51            STA ARY33,Y
0281  56F3  C8                   INY
0282  56F4  C0 C8               CPY #200
0283  56F6  D0 F0               BNE CLEAR
0284  56F8  A0 00               LDY #$00        ;SET Y AS POINT COUNTER.
0285  56FA  A9 0F       DATA   LDA #$0F        ;SET PBD AS OUTPUT.
0286  56FC  8D 02 AC            STA PBDD        ;FOR LAMP PULSING.
0287  56FF  A9 00               LDA #$00
0288  5701  8D 03 A8            STA DDRA        ;DATA PORT INPUT.
0289  5704  A9 FF               LDA #$FF
0290  5706  8D 02 A8            STA DDRB        ;CONTROL PORT OUTPUT.
0291  5709  AD 18 50    LUP    LDA LAP         ;SAVE # OF LAPS/POINT.
0292  570C  8D 1F 50            STA LOP
0293  570F  AD 01 50    LUMP   LDA LAMP        ;SAVE # OF LAMPS AT LOMP.
0294  5712  8D 20 50            STA LOMP        ;LAMP COUNTER.
0295  5715  AD 07 50            LDA CURL1
0296  5718  8D 1B 50            STA DACL
0297  571B  AD 06 50            LDA CURH1
0298  571E  8D 1C 50            STA DACH
0299  5721  20 63 56            JSR DAK
0300  5724  A9 00               LDA #$00
0301  5726  8D 00 AC            STA PBD
0302  5729  20 B9 58            JSR TIMOF
0303  572C  A9 01               LDA #$01        ;CLEAR THE COUNTERS.
0304  572E  8D 00 A8            STA DRB
0305  5731  A9 02               LDA #$02        ;OPEN THE GATE & COUNT DOWN.
0306  5733  8D 00 A8            STA DRB
0307  5736  20 E3 58            JSR CLOK        ;CONTINUE COUNTING.
0308  5739  A9 00               LDA #$00        ;STOP COUNTING.
0309  573B  8D 00 A8            STA DRB
0310  573E  A9 01               LDA #$01        ;LAMP #1 ON.
0311  5740  8D 00 AC            STA PBD
0312  5743  20 CD 58            JSR DELAY       ;WAIT FOR TIME CONSTANT.
0313  5746  A9 12               LDA #$12        ;OPEN THE GATE & COUNT UP.
0314  5748  8D 00 A8            STA DRB
0315  574B  20 E3 58            JSR CLOK
0316  574E  A9 04               LDA #$04        ;TRANSFER LOW BYTE DATA.
0317  5750  8D 00 A8            STA DRB
0318  5753  18                   CLC             ;CLEAR CARRY.
0319  5754  AD 01 A8            LDA DRA         ;LOAD LOW 8 BITS.
0320  5757  79 46 50            ADC ARY11,Y     ;ADD TO FIRST ARY.
0321  575A  99 46 50            STA ARY11,Y     ;SAVE IT IN FIRST ARY.
0322  575D  A9 08               LDA #$08        ;TRANSFER HIGH BYTE DATA.
0323  575F  8D 00 A8            STA DRB
```

```
0324  5762  AD 01 A8          LDA IRA          ;LOAD HIGH 8 BITS.
0325  5765  79 78 50          ADC ARY12,Y      ;ADD TO SECOND ARY.
0326  5768  99 78 50          STA ARY12,Y      ;SAVE IT IN SECOND ARY.
0327  576B  A9 00             LDA #$00
0328  576D  79 AA 50          ADC ARY13,Y      ;USE THIRD ARY FOR OVERFLOW.
0329  5770  99 AA 50          STA ARY13,Y
0330  5773  CE 20 50    NXT1  DEC LOMP         ;CHECK # OF LAMPS.
0331  5776  D0 03             BNE JMP1          ;NOT LAST ONE, GO TO NEXT.

......PAGE 0007

LINE # LOC     CODE       LINE

0332  5778  4C A5 5B          JMP OUT
0333  577B  AD 09 50    JMP1  LDA CURL2
0334  577E  8D 1B 50          STA DACL
0335  5781  AD 08 50          LDA CURH2
0336  5784  8D 1C 50          STA DACH
0337  5787  20 63 56          JSR DAK
0338  578A  A9 00             LDA #$00
0339  578C  8D 00 AC          STA PBD
0340  578F  20 B9 58          JSR TIMOF
0341  5792  A9 01             LDA #$01
0342  5794  8D 00 A8          STA ORB
0343  5797  A9 02             LDA #$02
0344  5799  8D 00 A8          STA ORB
0345  579C  20 E3 58          JSR CLOK
0346  579F  A9 00             LDA #$00
0347  57A1  8D 00 A8          STA ORB
0348  57A4  A9 02             LDA #$02         ;LAMP #2 ON
0349  57A6  8D 00 AC          STA PBD
0350  57A9  20 CD 58          JSR DELAY
0351  57AC  A9 12             LDA #$12
0352  57AE  8D 00 A8          STA ORB
0353  57B1  20 E3 58          JSR CLOK
0354  57B4  A9 04             LDA #$04
0355  57B6  8D 00 A8          STA ORB
0356  57B9  18                CLC
0357  57BA  AD 01 A8          LDA IRA
0358  57BD  79 DC 50          ADC ARY21,Y
0359  57C0  99 DC 50          STA ARY21,Y
0360  57C3  A9 08             LDA #$08
0361  57C5  8D 00 A8          STA ORB
0362  57C8  AD 01 A8          LDA IRA
0363  57CB  79 0E 51          ADC ARY22,Y
0364  57CE  99 0E 51          STA ARY22,Y
0365  57D1  A9 00             LDA #$00
0366  57D3  79 40 51          ADC ARY23,Y
0367  57D6  99 40 51          STA ARY23,Y
0368  57D9  CE 20 50    NXT2  DEC LOMP
0369  57DC  D0 03             BNE JMP2
```

```
0370  57DE  4C A5 58          JMP CUT
0371  57E1  AD 0B 50    JMP2  LDA CURL3
0372  57E4  8D 1B 50          STA DACL
0373  57E7  AD 0A 50          LDA CURH3
0374  57EA  8D 1C 50          STA DACH
0375  57ED  20 63 56          JSR DAK
0376  57F0  A9 00             LDA #$00
0377  57F2  8D 00 AC          STA PBD
0378  57F5  20 B9 58          JSR TIMOF
0379  57F8  A9 01             LDA #$01
0380  57FA  8D 00 A8          STA DRB
0381  57FD  A9 02             LDA #$02
0382  57FF  8D 00 A8          STA DRB
0383  5802  20 E3 58          JSR CLOK
0384  5805  A9 00             LDA #$00
0385  5807  8D 00 A8          STA DRB
0386  580A  A9 04             LDA #$04        ;LAMP #3 DN.
```

.....PAGE 0008

```
LINE # LOC     CODE       LINE

0387  580C  8D 00 AC          STA PBD
0388  580F  20 CD 58          JSR DELAY
0389  5812  A9 12             LDA #$12
0390  5814  8D 00 A8          STA DRB
0391  5817  20 E3 58          JSR CLOK
0392  581A  A9 04             LDA #$04
0393  581C  8D 00 A8          STA DRB
0394  581F  18                CLC
0395  5820  AD 01 A8          LDA DRA
0396  5823  79 72 51          ADC ARY31,Y
0397  5826  99 72 51          STA ARY31,Y
0398  5829  A9 08             LDA #$08
0399  582B  8D 00 A8          STA DRB
0400  582E  AD 01 A8          LDA DRA
0401  5831  79 A4 51          ADC ARY32,Y
0402  5834  99 A4 51          STA ARY32,Y
0403  5837  A9 00             LDA #$00
0404  5839  79 D6 51          ADC ARY33,Y
0405  583C  99 D6 51          STA ARY33,Y
0406  583F  CE 20 50    NXT3  DEC LOMP
0407  5842  D0 03             BNE JMP3
0408  5844  4C A5 58          JMP CUT
0409  5847  AD 0D 50    JMP3  LDA CURL4
0410  584A  8D 1B 50          STA DACL
0411  584D  AD 0C 50          LDA CURH4
0412  5850  8D 1C 50          STA DACH
0413  5853  20 63 56          JSR DAK
0414  5856  A9 00             LDA #$00
0415  5858  8D 00 AC          STA PBD
0416  585B  20 B9 58          JSR TIMOF
```

```
0417  585E  A9 01          LDA #$01
0418  5860  8D 00 A8       STA DRB
0419  5863  A9 02          LDA #$02
0420  5865  8D 00 A8       STA DRB
0421  5868  20 E3 58       JSR CLOK
0422  586B  A9 00          LDA #$00
0423  586D  8D 00 A8       STA DRB
0424  5870  A9 08          LDA #$08        ;LAMP #4 ON
0425  5872  8D 00 AC       STA PBD
0426  5875  20 CD 58       JSR DELAY
0427  5878  A9 12          LDA #$12
0428  587A  8D 00 A8       STA DRB
0429  587D  20 E3 58       JSR CLOK
0430  5880  A9 04          LDA #$04
0431  5882  8D 00 A8       STA DRB
0432  5885  18             CLC
0433  5886  AD 01 A8       LDA DRA
0434  5889  79 08 52       ADC ARY41,Y
0435  588C  99 08 52       STA ARY41,Y
0436  588F  A9 08          LDA #$08
0437  5891  8D 00 A8       STA DRB
0438  5894  AD 01 A8       LDA DRA
0439  5897  79 3A 52       ADC ARY42,Y
0440  589A  99 3A 52       STA ARY42,Y
0441  589D  A9 00          LDA #$00

......PAGE 0009


LINE # LOC     CODE       LINE

0442  589F  79 6C 52          ADC ARY43,Y
0443  58A2  99 6C 52          STA ARY43,Y
0444  58A5  CE 1F 50    CUT   DEC LOP         ;ALL LAPS DONE?
0445  58A8  F0 03             BEQ GETOT       ;YES, GO FOR NEXT POINT.
0446  58AA  4C 0F 57          JMP LUMP        ;NO, START AGAIN.
0447  58AD  C8          GETOT INY
0448  58AE  CC 19 50          CPY POINT       ;ALL THE POINTS COLLECTED!
0449  58B1  F0 03             BEQ OUT         ;YES, GO OUT.
0450  58B3  4C 09 57          JMP LUP         ;NO, DO THE NEXT.
0451  58B6  4C 2A 56    OUT   JMP PULS
0452  58B9  AE 04 50    TIMOF LDX TIMLOP      ;# OF TIME LOOP(1 OR 5)
0453  58BC  F0 0F       DOIT  BEQ DELAY
0454  58BE  AD 05 50          LDA OFF
0455  58C1  8D 17 A4          STA SR
0456  58C4  2C 17 A4    VAIT  BIT SR
0457  58C7  10 FB             BPL VAIT
0458  58C9  CA                DEX
0459  58CA  4C BC 58          JMP DOIT
0460  58CD  AD 24 50    DELAY LDA TM
0461  58D0  8D 25 50          STA MT
0462  58D3  A9 32       DLAY  LDA #50          ;DELAY TIME FOR TIME CONSTANT
```

```
0463  58D5  8D 14 A4          STA PW
0464  58D8  2C 17 A4   WAIT   BIT SR
0465  58DB  10 FB             BPL WAIT
0466  58DD  CE 25 50          DEC MT
0467  58E0  D0 F1             BNE DLAY
0468  58E2  60                RTS
0469  58E3  AE 21 50   CLOK   LDX REED
0470  58E6  F0 0F      WATCH  BEQ STUP
0471  58E8  AD 1A 50          LDA RD
0472  58EB  8D 14 A4          STA PW
0473  58EE  2C 17 A4   LOOP   BIT SR
0474  58F1  10 FB             BPL LOOP
0475  58F3  CA                DEX
0476  58F4  4C E6 58          JMP WATCH
0477  58F7  60         STUP   RTS
0478  58F8                    .END
```

SYMBOL TABLE

SYMBOL VALUE

ACR	AC0B	ADCH	501E	ADCL	501D	ADK	56B4
ARY11	5046	ARY12	5078	ARY13	50AA	ARY21	50DC
ARY22	510E	ARY23	5140	ARY31	5172	ARY32	51A4
ARY33	51D6	ARY41	5208	ARY42	523A	ARY43	526C
AVCRH	500E	AVCRL	500F	BACK	56AE	CLEAR	56E8
CLOCK	5022	CLOK	58E3	CORH1	5011	CORH2	5013
CORH3	5015	CORH4	5017	CORL1	5010	CORL2	5012
CORL3	5014	CORL4	5016	CRLF	834D	CURH1	5006
CURH2	5008	CURH3	500A	CURH4	500C	CURL1	5007
CURL2	5009	CURL3	500B	CURL4	500D	CUT	58A5
CUT1	5690	CUT2	56B1	DACH	501C	DACL	501B
DAK	5663	DARK	5002	DATA	56FA	DDRA	A803
DDRB	A802	DELAY	58CD	DLAY	58D3	DOIT	58BC
DRA	A801	DRB	A800	FOUR	55EF	GETOT	58AD
GO	56D9	HOLDER	00F6	JMP1	577B	JMP2	57E1
JMP3	5847	KLOK	567B	LAMP	5001	LAP	5018
LMP1	5534	LMP2	5571	LMP3	55AC	LMP4	55E7
LOMP	5020	LOOK	5696	LOOP	58EE	LOP	501F
LUMP	570F	LUP	5709	MT	5025	NXT1	5773
NXT2	57D9	NXT3	583F	OFF	5005	ON	5000
ORB	A402	OUT	58B6	PAD	AC01	PADD	AC03
PBD	AC00	PBDD	AC02	POINT	5019	PULS	562A
PW	A414	RAD	A001	RADD	A003	RBD	A000
RBDD	A002	RD	501A	RED1	5559	RED2	5594
RED3	55CF	RED4	560E	REED	5021	SR	A417
STUP	58F7	T1CH	AC05	T1LL	AC04	TEST	56C1
THREE	55B4	TIMLOP	5004	TIMOF	58B9	TIMOFF	5693
TLOOP	5003	TM	5024	TWO	5579	VAIT	58C4
VEET	569E	WAIT	58D8	WATCH	58E6	WEET	5681

END OF ASSEMBLY

MULTI-AD

```
5 REM THIS PROG TAKES DATA FROM MEMORY, COMPUTES AVR., STD DIV & S/N
10 PRINT
15 DIM L1(35),L2(35),L3(35),L4(35),M1(20),M2(20),M3(20),M4(20),M5(20)
20 PRINT
25 PRINT "HC #1"
30 PRINT "HC #2"
35 PRINT "HC #3"
40 PRINT "HC #4"
45 REM TO START PULSING LAMPS.
50 PRINT
55 PRINT" TIME ON"
60 INPUT" T1=";T1
65 POKE 20480,T1
70 PRINT
75 PRINT" %TIME ON"
80 INPUT" PC=";PC
85 PRINT
90 PRINT" # OF LAMP"
95 INPUT" LM=";LM
100 POKE 20481,LM
105 PRINT
110 REM RESISTOR USED FOR POWER TRANSISTOR (EMIT-GND)
115 PRINT" RESISTOR VALUE"
120 INPUT" R=";R
125 PRINT
130 T2=T1*((100/(PC*LM))-1)
135 POKE 20483,01
140 IF T2<255 THEN A=T2: GOTO 155
145 A=INT((T2/5)+.5)
150 POKE 20483,05
155 POKE 20482,A
160 IF T1>T2 THEN PRINT"LARGE %TIME ON": GOTO 50
165 CK=(T1*1000/2)-2
170 A=INT(CK/256)
175 POKE 20515,A
180 B=CK-(A*256)
185 POKE 20514,B
190 OF=T2-T1
195 POKE 20484,01
200 IF OF<255 THEN A=OF: GOTO 215
205 A=INT((OF/5)+.5)
210 POKE 20484,05
215 POKE 20485,A
220 ML=LM
225 PRINT"H.C. AVE. MAMP CURRENTS"
```

```
230 PRINT
235 C1=0
240 C2=0
245 C3=0
250 C4=0
255 PRINT" H.C.#1 CURRENT"
260 INPUT" C1=";C1
265 PRINT
270 REM CURRENT CORRECTION FOR RESISTOR VALUE.
275 H=(10-R)*PC/2.5
280 V1=(C1*4.2*R)-(H/C1)
285 REM LAMPS' CURRENT CORRECTION FOR PC NOT EQUAL TO 12.5%
290 MA=(V1*12.5)/PC
295 A=INT(MA/256)
300 IF A<=15 THEN 315
305 PRINT" NOT ACCEPTABLE, CHANGE C1 OR R VALUE": GOTO 50
310 PRINT
315 POKE 20486,A
320 B=MA-(A*256)
325 POKE 20487,B
330 IF ML-1=0 THEN 525
335 PRINT" H.C.# 2 CURRENT"
340 INPUT" C2=";C2
345 PRINT
350 V2=(C2*4.2*R)-(H/C2)
355 MA=(V2*12.5)/PC
360 A=INT(MA/256)
365 IF A<=15 THEN 380
370 PRINT" NOT ACCEPTABLE, CHANGE C2 OR R VALUE": GOTO 50
375 PRINT
380 POKE 20488,A
385 B=MA-(A*256)
390 POKE 20489,B
395 IF ML-2=0 THEN 525
400 PRINT" H.C.#3 CURRENT"
405 INPUT" C3=";C3
410 PRINT
415 V3=(C3*4.2*R)-(H/C3)
420 MA=(V3*12.5)/PC
425 A=INT(MA/256)
430 IF A<=15 THEN 445
435 PRINT" NOT ACCEPTABLE, CHANGE C3 OR R VALUE": GOTO 50
440 PRINT
445 POKE 20490,A
450 B=MA-(A*256)
455 POKE 20491,B
460 IF ML-3=0 THEN 525
465 PRINT" H.C.#4 CURRENT"
470 INPUT" C4=";C4
475 PRINT
480 V4=(C4*4.2*R)-(H/C4)
```

```
485 MA=(V4*12.5)/PC
490 A=INT(MA/256)
495 IF A<=15 THEN 510
500 PRINT" NOT ACCEPTABLE, CHANGE C4 OR R VALUE": GOTO 50
505 PRINT
510 POKE 20492,A
515 B=MA-(A*256)
520 POKE 20493,B
525 AV=(C1+C2+C3+C4)/LM
530 AV=(AV*4.2*R)-(H/AV)
535 A=INT(AV/256)
540 POKE 20494,A
545 B=AV-(A*256)
550 POKE 20495,B
555 PRINT
560 PRINT" T1=";T1,"PC=";PC,"LM=";LM,"R=";R
565 PRINT" C1=";C1,"C2=";C2,"C3=";C3,"C4=";C4
570 PRINT
575 PRINT" ARE THESE VALUES CORRECT? YES=1,NO=0"
580 INPUT" ANS=";Y
585 IF Y=0 THEN 50
590 PRINT
595 PRINT" READY TO READ CURRENT! PUSH (CR)."
600 Z=USR(&"4500",00)
605 REM CURRENT READING BY A/D ACROSS ABOVE RESISTOR
610 A=PEEK(20496)
615 B=PEEK(20497)
620 C=((B*256)+A)*10000/(4095*R)
625 D=INT(C+.5)
630 PRINT
635 PRINT" PEAK TO PEAK CURRENTS"
640 PRINT
645 PRINT" H.C.#1 CURRENT=";D;" MAMP"
650 A=PEEK(20498)
655 B=PEEK(20499)
660 C=((B*256)+A)*10000/(4095*R)
665 D=INT(C+.5)
670 PRINT" H.C.#2 CURRENT=";D;" MAMP"
675 A=PEEK(20500)
680 B=PEEK(20501)
685 C=((B*256)+A)*10000/(4095*R)
690 D=INT(C+.5)
695 PRINT" H.C.#3 CURRENT=";D;" MAMP"
700 A=PEEK(20502)
705 B=PEEK(20503)
710 C=((B*256)+A)*10000/(4095*R)
715 D=INT(C+.5)
720 PRINT" H.C.#4 CURRENT=";D;" MAMP"
725 PRINT
730 PRINT" READ MORE YES=1,NO=0"
735 INPUT" ANS=";Y
```

```
740 IF Y=0 THEN 775
745 PRINT
750 PRINT" ANY CHANGE YES=1,NO=0"
755 INPUT" ANS=";Y
760 PRINT
765 IF Y>0 THEN 220
770 IF Y=0 THEN 590
775 PRINT
780 PRINT" # OF LAPS"
785 INPUT" LP=";LP
790 POKE 20504,LP
795 PRINT
800 PRINT" # OF POINT"
805 INPUT" PT=";PT
810 POKE 20505,PT
815 PRINT
820 PRINT" RF VALUE (M-OHM)"
825 INPUT" RF=";RF
830 PRINT
835 PRINT" CF VALUE (P-F)"
840 INPUT" CF=";CF
845 TM=INT((5*RF*CF/50)+.5)
850 DT=TM*.05
855 POKE 20516,TM
860 OF=T2-T1
865 POKE 16388,01
870 IF OF<255 THEN A=OF: GOTO 885
875 A=INT((OF/5)+.5)
880 POKE 16388,05
885 POKE 16389,A
890 RD=INT(((T1-DT)/.2)+.5)
895 POKE 20506,RD
900 PRINT
905 PRINT" # OF RUNS"
910 INPUT" RN=";RN
915 PRINT
920 PRINT" PMT VOLTAGE"
925 INPUT" PM=";PM
930 PRINT
935 IF PM=400 THEN GM=2.75E03
940 IF PM=500 THEN GM=1.5E04
945 IF PM=600 THEN GM=6.8E04
950 IF PM=700 THEN GM=2.25E05
955 IF PM=800 THEN GM=6.8E05
960 IF PM=900 THEN GM=1.9E06
965 IF PM=1000 THEN GM=5E06
970 REM NOISE EQUIVALENT BANDPASS 1/S.
975 DF=1000/(2*(T1-DT)*LP)
980 G=(LOG(GM)/LOG(10))/9
985 GA=10^G
990 KK=2*1.6E-19*DF*(1+1/(GA-1))
```

```
995 ZA=GM*RF*KK*(1E06)
1000 PRINT" CALIBRATION CURVE YES=1, NO=0."
1005 INPUT" ANS=";CC
1010 IF CC=1 THEN 2565
1015 PRINT
1020 REM ABOVE SECTION INITIALIZES USER DEFINED VARIABLES.
1025 REM THE NEXT SECTION COLLECTS BLANK DATA FROM MEMORY.
1030 D=0
1035 REM FOR FIRST RUN
1040 PRINT
1045 POKE 44033,00
1050 REM TO START SAMPLER FOR BLANK.
1055 PRINT" DO YOU WANT DARK DATA? YES=1,NO=0"
1060 INPUT" DK=";DK
1065 IF DK=0 THEN 1125
1070 PRINT
1075 PRINT" COVER ENTRANCE SLIT & PUSH (CR)."
1080 PRINT
1085 Z=USR(&"8A58",00)
1090 PRINT" DARK DATA"
1095 PRINT"----------"
1100 Z=USR(&"56E0",00)
1105 GOSUB 1335
1110 PRINT" DARK AVE & STD DIV."
1115 PRINT
1120 GOSUB 1590
1125 PRINT
1130 PRINT" RUN BLANK PUSH (CR) TO START."
1135 Z=USR(&"8A58",00)
1140 PRINT
1145 PRINT"BLANK DATA"
1150 PRINT"----------"
1155 Z=USR(&"56E0",00)
1160 REM TO COLLECT BLANK DATA
1165 GOSUB 1335
1170 PRINT "BLANK AVE & STD DIV"
1175 PRINT
1180 GOSUB 1590
1185 PRINT
1190 POKE 44033,02
1195 REM TO START SAMPLER FOR SAMPLE.
1200 PRINT" RUN SAMPLE PUSH (CR) TO START."
1205 Z=USR(&"8A58",00)
1210 PRINT
1215 PRINT"SAMPLE DATA"
1220 PRINT"-----------"
1225 Z=USR(&"56E0",00)
1230 REM TO COLLECT SAMPLE DATA
1235 GOSUB 1335
1240 PRINT "TOTAL SIG AVER & STD DEV"
1245 PRINT
```

```
1250 POKE 44033,00
1255 GOSUB 1855
1260 IF CC=0 THEN 1270
1265 RETURN
1270 GOSUB 2215
1275 Q=Q+1
1280 IF Q<RN THEN 1040
1285 PRINT "EXTRA RUN YES=1 NO=0"
1290 INPUT" ANS=";Y
1295 IF Y=0 THEN 3020
1300 PRINT
1305 PRINT "CHANGE VARIABLES: UPPER SEC.=2, LOWER SEC.=1, NO=0"
1310 INPUT" ANS=";Y
1315 IF Y=0 THEN 1040
1320 IF Y=1 THEN 775
1325 IF Y=2 THEN 50
1330 PRINT
1335 REM THIS SUB TAKES DATA FROM MEMORY FOR EACH LAMP.
1340 N=PT-1
1345 FOR J=0 TO N
1350 A=PEEK(20550+J)
1355 B=PEEK(20600+J)
1360 C=PEEK(20650+J)
1365 REM A,B,C THREE BYTES WHICH CONTAIN THE JTH
1370 REM DATA POINT A THE LEAST SIG FIG. & C MOST SIG FIG.
1375 D=(C*256)+B
1380 C=(D*256)+A
1385 A=PEEK(20700+J)
1390 B=PEEK(20750+J)
1395 D=PEEK(20800+J)
1400 E=(D*256)+B
1405 D=(E*256)+A
1410 L1(J)=(10000*(C-D))/(RD*4095)
1415 A=PEEK(20850+J)
1420 B=PEEK(20900+J)
1425 C=PEEK(20950+J)
1430 D=(C*256)+B
1435 C=(D*256)+A
1440 A=PEEK(21000+J)
1445 B=PEEK(21050+J)
1450 D=PEEK(21100+J)
1455 E=(D*256)+B
1460 D=(E*256)+A
1465 L2(J)=(10000*(C-D))/(RD*4095)
1470 A=PEEK(21150+J)
1475 B=PEEK(21200+J)
1480 C=PEEK(21250+J)
1485 D=(C*256)+B
1490 C=(D*256)+A
1495 A=PEEK(21300+J)
1500 B=PEEK(21350+J)
```

```
1505 D=PEEK(21400+J)
1510 E=(D*256)+B
1515 D=(E*256)+A
1520 L3(J)=(10000*(C-D))/(RD*4095)
1525 A=PEEK(21450+J)
1530 B=PEEK(21500+J)
1535 C=PEEK(21550+J)
1540 D=(C*256)+B
1545 C=(D*256)+A
1550 A=PEEK(21600+J)
1555 B=PEEK(21650+J)
1560 D=PEEK(21700+J)
1565 E=(D*256)+B
1570 D=(E*256)+A
1575 L4(J)=(10000*(C-D))/(RD*4095)
1580 NEXT J
1585 RETURN
1590 REM THIS SUB. FINDS MEANS AND STD DIV. IN BLANK & DARK.
1595 K1=0
1600 K2=0
1605 K3=0
1610 K4=0
1615 N=PT-1
1620 FOR J=0 TO N
1625 K1= K1+L1(J)
1630 K2= K2+L2(J)
1635 K3= K3+L3(J)
1640 K4= K4+L4(J)
1645 NEXT J
1650 K1=K1/PT
1655 K2=K2/PT
1660 K3=K3/PT
1665 K4=K4/PT
1670 PRINT INT(K1+.5),INT(K2+.5),INT(K3+.5),INT(K4+.5)
1675 F1=0
1680 F2=0
1685 F3=0
1690 F4=0
1695 G1=0
1700 G2=0
1705 G3=0
1710 G4=0
1715 FOR J=0 TO N
1720 F1= L1(J)-K1
1725 G1=(F1*F1)+G1
1730 F2= L2(J)-K2
1735 G2=(F2*F2)+G2
1740 F3= L3(J)-K3
1745 G3=(F3*F3)+G3
1750 F4= L4(J)-K4
1755 G4=(F4*F4)+G4
```

```
1760 NEXT J
1765 S1= SQR(G1/N)
1770 S2= SQR(G2/N)
1775 S3= SQR(G3/N)
1780 S4= SQR(G4/N)
1785 A=INT(S1*100+.5)/100
1790 B=INT(S2*100+.5)/100
1795 C=INT(S3*100+.5)/100
1800 D=INT(S4*100+.5)/100
1805 PRINT A,B,C,D
1810 PRINT
1815 PRINT"PRINT DATA YES=1,NO=0"
1820 INPUT" ANS=";Y
1825 PRINT
1830 IF Y=0 THEN 1850
1835 FOR J=0 TO N
1840 PRINT INT(L1(J)+.5),INT(L2(J)+.5),INT(L3(J)+.5),INT(L4(J)+.5)
1845 NEXT J
1850 RETURN
1855 REM THIS SUB. FINDS MEAN & STD DIV. OF TOTAL SIGNAL.
1860 T1=0
1865 T2=0
1870 T3=0
1875 T4=0
1880 N=PT-1
1885 FOR J=0 TO N
1890 T1=L1(J)+T1
1895 T2=L2(J)+T2
1900 T3=L3(J)+T3
1905 T4=L4(J)+T4
1910 NEXT J
1915 T1=T1/PT
1920 T2=T2/PT
1925 T3=T3/PT
1930 T4=T4/PT
1935 PRINT INT(T1+.5),INT(T2+.5),INT(T3+.5),INT(T4+.5)
1940 Z1=ZA*T1/1000
1945 Z2=ZA*T2/1000
1950 Z3=ZA*T3/1000
1955 Z4=ZA*T4/1000
1960 IF Z1=<0 THEN ZA=0: GOTO 1970
1965 ZA=SQR(Z1)
1970 IF Z2=<0 THEN ZB=0: GOTO 1980
1975 ZB=SQR(Z2)
1980 IF Z3=<0 THEN ZC=0: GOTO 1990
1985 ZC=SQR(Z3)
1990 IF Z4=<0 THEN ZD=0: GOTO 2000
1995 ZD=SQR(Z4)
2000 H1=0
2005 N1=0
2010 H2=0
```

```
2015 N2=0
2020 M3=0
2025 N3=0
2030 M4=0
2035 N4=0
2040 FOR J=0 TO N
2045 M1=L1(J)-T1
2050 N1=(M1*M1)+N1
2055 M2=L2(J)-T2
2060 N2=(M2*M2)+N2
2065 M3=L3(J)-T3
2070 N3=(M3*M3)+N3
2075 M4=L4(J)-T4
2080 N4=(M4*M4)+N4
2085 NEXT J
2090 V1=SQR(N1/N)
2095 V2=SQR(N2/N)
2100 V3=SQR(N3/N)
2105 V4=SQR(N4/N)
2110 A=INT(V1*100+.5)/100
2115 B=INT(V2*100+.5)/100
2120 C=INT(V3*100+.5)/100
2125 D=INT(V4*100+.5)/100
2130 PRINT A,B,C,D
2135 GOSUB 1810
2140 PRINT
2145 PRINT" RMS SHOT NOISE (VOLTAGE)"
2150 PRINT
2155 PRINT ZA,ZB,ZC,ZD
2160 PRINT
2165 PRINT "NET SIGNAL"
2170 PRINT
2175 REM THIS SUBROUTINE FINDS THE NET SIGNAL.
2180 X1=T1-K1
2185 X2=T2-K2
2190 X3=T3-K3
2195 X4=T4-K4
2200 PRINT INT(X1+.5),INT(X2+.5),INT(X3+.5),INT(X4+.5)
2205 PRINT
2210 RETURN
2215 PRINT" NET SIGNAL/BLANK STD DIV."
2220 REM THIS SUBROUTINE FINDS RATIO OF NET SIGNAL TO
2225 REM BLANK NOISE & NET SIGNAL TO TOTAL NOISE.
2230 IF S1<=0 THEN 2240
2235 P1=X1/S1
2240 IF S2<=0 THEN 2250
2245 P2=X2/S2
2250 IF S3<=0 THEN 2260
2255 P3=X3/S3
2260 IF S4<=0 THEN 2270
2265 P4=X4/S4
```

```
2270 PRINT
2275 A=INT(P1*10+.5)/10
2280 B=INT(P2*10+.5)/10
2285 C=INT(P3*10+.5)/10
2290 D=INT(P4*10+.5)/10
2295 PRINT A,B,C,D
2300 PRINT
2305 PRINT" NET SIGNAL/TOTAL NOISE"
2310 Q1=SQR((S1*S1)+(V1*V1))
2315 Q2=SQR((S2*S2)+(V2*V2))
2320 Q3=SQR((S3*S3)+(V3*V3))
2325 Q4=SQR((S4*S4)+(V4*V4))
2330 IF Q1=0 THEN 2340
2335 W1=X1/Q1
2340 IF Q2=0 THEN 2350
2345 W2=X2/Q2
2350 IF Q3=0 THEN 2360
2355 W3=X3/Q3
2360 IF Q4=0 THEN 2370
2365 W4=X4/Q4
2370 PRINT
2375 A=INT(W1*10+.5)/10
2380 B=INT(W2*10+.5)/10
2385 C=INT(W3*10+.5)/10
2390 D=INT(W4*10+.5)/10
2395 PRINT A,B,C,D
2400 PRINT
2405 PRINT" CONC. OF SOLN. #1 (PPM)"
2410 INPUT" G1=";G1
2415 PRINT
2420 IF ML-1=0 THEN 2480
2425 PRINT" CONC. OF SOLN. #2 (PPM)"
2430 INPUT" G2=";G2
2435 PRINT
2440 IF ML-2=0 THEN 2480
2445 PRINT" CONC. OF SOLN. #3 (PPM)"
2450 INPUT" G3=";G3
2455 PRINT
2460 IF ML-3=0 THEN 2480
2465 PRINT" CONC. OF SOLN. #4 (PPM)"
2470 INPUT" G4=";G4
2475 PRINT
2480 IF P1=0 THEN Y1=0: GOTO 2495
2485 D1=2*G1/P1
2490 Y1=INT((D1*1000)+.5)/1000
2495 IF P2=0 THEN Y2=0: GOTO 2510
2500 D2=2*G2/P2
2505 Y2=INT((D2*1000)+.5)/1000
2510 IF P3=0 THEN Y3=0: GOTO 2525
2515 D3=2*G3/P3
2520 Y3=INT((D3*1000)+.5)/1000
```

```
2525 IF P4=0 THEN Y4=0: GOTO 2540
2530 D4=2*G4/P4
2535 Y4=INT((D4*1000)+.5)/1000
2540 PRINT" DETECTION LIMITS (PPM)"
2545 PRINT"------------------------"
2550 PRINT Y1,Y2,Y3,Y4
2555 PRINT
2560 RETURN
2565 REM THIS SUB. IS FOR CALIB. CURVE & UNK. CALCULATIONS.
2570 PRINT
2575 PRINT" # OF STANDARDS"
2580 INPUT" SD=";SD
2585 PRINT
2590 PRINT" INTER THE CONCENTRATION OF STANDARDS."
2595 PRINT
2600 F=SD-1
2605 FOR I=0 TO F
2610 PRINT I+1;
2615 INPUT J
2620 PRINT
2625 M5(I)=J
2630 NEXT I
2635 PRINT
2640 PRINT" # OF RUNS PER SAMPLE"
2645 INPUT" RN=";RN
2650 PRINT
2655 PRINT" CALIBRATION CURVE DATA."
2660 PRINT"----------------------"
2665 FOR H=0 TO F
2670 A1=0:A2=0:A3=0:A4=0
2675 K=RN-1
2680 FOR I=0 TO K
2685 GOSUB 1015
2690 A1=A1+X1
2695 A2=A2+X2
2700 A3=A3+X3
2705 A4=A4+X4
2710 NEXT I
2715 M1(H)=A1/RN
2720 M2(H)=A2/RN
2725 M3(H)=A3/RN
2730 M4(H)=A4/RN
2735 NEXT H
2740 PRINT" CONC.          NET AVE. SIGNAL."
2745 FOR H=0 TO F
2750 PRINT
2755 PRINT M5(H),INT(M1(H)),INT(M2(H)),INT(M3(H)),INT(M4(H))
2760 NEXT H
2765 PRINT
2770 L=0
2775 PRINT" WHAT ARE THE 1ST & 2ND POINTS FOR THE SLOPE CALC."
```

```
2780 INPUT" 1ST=";N
2785 INPUT" 2ND=";K
2790 S1=0:S2=0:S3=0:S4=0
2795 N=N-1
2800 K=K-2
2805 FOR J=N TO K
2810 W=M5(J+1)-M5(J)
2815 S1=(M1(J+1)-M1(J))/W+S1
2820 S2=(M2(J+1)-M2(J))/W+S2
2825 S3=(M3(J+1)-M3(J))/W+S3
2830 S4=(M4(J+1)-M4(J))/W+S4
2835 NEXT J
2840 PRINT
2845 PRINT"  SLOPES OF CALIB. CURVES"
2850 PRINT
2855 PRINT INT(S1+.5),INT(S2+.5),INT(S3+.5),INT(S4+.5)
2860 PRINT
2865 IF L=1 THEN 2955
2870 PRINT "DO YOU RUN UNKNOWN YES=1, NO=0"
2875 INPUT" ANS=";Y
2880 IF Y=0 THEN 2995
2885 A1=0:A2=0:A3=0:A4=0
2890 K=RN-1
2895 FOR H=0 TO K
2900 GOSUB 1015
2905 A1=A1+(X1/RN)
2910 A2=A2+(X2/RN)
2915 A3=A3+(X3/RN)
2920 A4=A4+(X4/RN)
2925 NEXT H
2930 PRINT
2935 PRINT"  NET UNK. SIGNAL."
2940 PRINT
2945 PRINT INT(A1+.5),INT(A2+.5),INT(A3+.5),INT(A4+.5)
2950 PRINT
2955 PRINT" CONCENTRATION OF UNK."
2960 PRINT
2965 IF S1=0 THEN A1/S1=0
2970 IF S2=0 THEN A2/S2=0
2975 IF S3=0 THEN A3/S3=0
2980 IF S4=0 THEN A4/S4=0
2985 PRINT A1/S1,A2/S2,A3/S3,A4/S4
2990 PRINT
2995 PRINT" CALCULATE THE SLOPE AGAIN YES=1, NO=0"
3000 INPUT" ANS=";L
3005 PRINT
3010 IF L=1 THEN 2775
3015 GOTO 1285
3020 END
OK
```

2B

```
.....PAGE 0001

LINE # LOC     CODE       LINE

0002  0000              : THIS PROGRAM IS A PART OF A BASIC PROGRAM
0003  0000              : WHICH RUNS TMHS INSTRUMENT & COLLECT DATA.
0004  0000              ;*************  I/O PORTS  ***************
0005  0000              ;
0006  0000              RBD=$A000         ;DAC'S STB. & 4 HIGH BITS.
0007  0000              RBDD=$A002
0008  0000              RAD=$A001         ;DAC'S 8 LOW BITS.
0009  0000              RADD=$A003
0010  0000              DRB=$A402
0011  0000              DRB=$A800         ;ADC'S CONTROL BITS.
0012  0000              DDRB=$A802
0013  0000              DRA=$A801         ;ADC'S DATA BITS.
0014  0000              DDRA=$A803
0015  0000              PBD=$AC00         ;H.C. LAMP PULSING & CLOCK.
0016  0000              PBDD=$AC02
0017  0000              PAD=$AC01         ;SAMPLER CONTROL.
0018  0000              PADD=$AC03
0019  0000              T1LL=$AC04         ;LOW-ORDER LATCH TIMER-1.
0020  0000              T1CH=$AC05         ;HIGH-ORDER COUNTER.
0021  0000              ACR=$AC0B         ;AUXILIARY CONTROL REGISTER.
0022  0000              PW=$A414         ;1T (1 USEC)
0023  0000              SR=$A417         ;1024T (1 MSEC)
0024  0000              CRLF=$834D
0025  0000              ;
0026  0000              ;****RESERVED MEMORY LOCATIONS FOR VARIABLES****.
0027  0000                    *=$5000
0028  5000              ON      *=*+1
0029  5001              LAMP    *=*+1
0030  5002              DARK    *=*+1
0031  5003              TLOOP   *=*+1
0032  5004              TIMLOP  *=*+1
0033  5005              OFF     *=*+1
0034  5006              CURH1   *=*+1
0035  5007              CURL1   *=*+1
0036  5008              CURH2   *=*+1
0037  5009              CURL2   *=*+1
0038  500A              CURH3   *=*+1
0039  500B              CURL3   *=*+1
0040  500C              CURH4   *=*+1
0041  500D              CURL4   *=*+1
0042  500E              AVCRH   *=*+1
```

```
0043  500F              AVCRL   *=*+1
0044  5010              CORL1   *=*+1
0045  5011              CORH1   *=*+1
0046  5012              CORL2   *=*+1
0047  5013              CORH2   *=*+1
0048  5014              CORL3   *=*+1
0049  5015              CORH3   *=*+1
0050  5016              CORL4   *=*+1
0051  5017              CORH4   *=*+1
0052  5018              LAP     *=*+1
0053  5019              POINT   *=*+1
0054  501A              READ    *=*+1
0055  501B              DACL    *=*+1
0056  501C              DACH    *=*+1
```



```
LINE # LOC     CODE       LINE

0057  501D              ADCL    *=*+1
0058  501E              ADCH    *=*+1
0059  501F              LOP     *=*+1
0060  5020              LOMP    *=*+1
0061  5021              REED    *=*+1
0062  5022              CLOCK   *=*+2
0063  5024              TM      *=*+1
0064  5025              MT      *=*+1
0065  5026                      *=$00F6
0066  00F6              HOLDER  *=*+2
0067  00F8              ;
0068  00F8              ;***** MEMORY LOCATIONS RESERVED FOR DATA STORAGE ***
0069  00F8              ;
0070  00F8              ARY11=$5046
0071  00F8              ARY12=$5078
0072  00F8              ARY13=$50AA
0073  00F8              ARY1A=$50DC
0074  00F8              ARY1B=$510E
0075  00F8              ARY1C=$5140
0076  00F8              ARY21=$5172
0077  00F8              ARY22=$51A4
0078  00F8              ARY23=$51D6
0079  00F8              ARY2A=$5208
0080  00F8              ARY2B=$523A
0081  00F8              ARY2C=$526C
0082  00F8              ARY31=$529E
0083  00F8              ARY32=$52D0
0084  00F8              ARY33=$5302
0085  00F8              ARY3A=$5334
0086  00F8              ARY3B=$5366
0087  00F8              ARY3C=$5398
0088  00F8              ARY41=$53CA
```

```
0089  00F8                ARY42=$53FC
0090  00F8                ARY43=$542E
0091  00F8                ARY4A=$5460
0092  00F8                ARY4B=$5492
0093  00F8                ARY4C=$54C4
0094  00F8                ;*** INITIALIZATION OF DATA DIRECTION ***
0095  00F8                ;
0096  00F8                      *=$5500
0097  5500  A9 FF              LDA #$FF        ;OUTPUT PORT FOR DAC
0098  5502  8D 03 A0           STA RADD
0099  5505  8D 02 A0           STA RBDD
0100  5508  A9 0F              LDA #$0F        ;LAMP PULSING I/O PORT
0101  550A  8D 02 AC           STA PBDD
0102  550D  8D 03 AC           STA PADD        ;SAMPLER I/O PORT
0103  5510  A9 00              LDA #$00        ;ADC DATA INPUT
0104  5512  8D 03 A8           STA DDRA
0105  5515  A9 3F              LDA #$3F        ;ADC CONTROL PORT
0106  5517  8D 02 A8           STA DDRB
0107  551A                ;
0108  551A                ;***** H.C. LAMP,S CURRENT READING *****
0109  551A                ;
0110  551A  A9 00              LDA #$00        ;CLEAR ALL FOLLOWING LOC.
0111  551C  8D 10 50           STA CORL1

.....PAGE 0003

LINE # LOC     CODE       LINE

0112  551F  8D 11 50           STA CORH1
0113  5522  8D 12 50           STA CORL2
0114  5525  8D 13 50           STA CORH2
0115  5528  8D 14 50           STA CORL3
0116  552B  8D 15 50           STA CORH3
0117  552E  8D 16 50           STA CORL4
0118  5531  8D 17 50           STA CORH4
0119  5534  A9 59        LMP1  LDA #<RED1      ;LOAD LOW BYTE OF RED1 ADDR.
0120  5536  85 F6              STA HOLDER
0121  5538  A9 55              LDA #>RED1        ;LOAD HIGH BYTE OF ADDR.
0122  553A  85 F7              STA HOLDER+1
0123  553C  AD 01 50           LDA LAMP
0124  553F  8D 20 50           STA LOMP
0125  5542  AD 07 50           LDA CURL1        ;LOAD THE CURRENT FOR #1
0126  5545  8D 1B 50           STA DACL
0127  5548  AD 06 50           LDA CURH1
0128  554B  8D 1C 50           STA DACH
0129  554E  20 5D 56           JSR DAK         ;CONVERT TO ANALOGE.
0130  5551  A9 01              LDA #$01        ;TURN LAMP #1 ON.
0131  5553  8D 00 AC           STA PBD
0132  5556  4C 75 56           JMP KLOK
0133  5559  AD 1D 50     RED1  LDA ADCL        ;LOAD CURRENT READING BY A/D.
0134  555C  8D 10 50           STA CORL1
0135  555F  AD 1E 50           LDA ADCH
```

```
0136  5562  8D 11 50          STA CORH1
0137  5565  A9 00             LDA #$00        ;TURN OFF THE LAMP.
0138  5567  8D 00 AC          STA PBD
0139  556A  A9 71             LDA #<LMP2
0140  556C  85 F6             STA HOLDER      ;SAVE RETURNE ADDR.
0141  556E  4C 8D 56          JMP TIMOFF
0142  5571  CE 20 50    LMP2  DEC LOMP
0143  5574  D0 03             BNE TWO
0144  5576  4C 34 55          JMP LMP1
0145  5579  AD 09 50    TWO   LDA CURL2
0146  557C  8D 1B 50          STA DACL
0147  557F  AD 08 50          LDA CURH2
0148  5582  8D 1C 50          STA DACH
0149  5585  20 5D 56          JSR DAK
0150  5588  A9 02             LDA #$02        ;TURN LAMP #2 ON.
0151  558A  8D 00 AC          STA PBD
0152  558D  A9 94             LDA #<RED2
0153  558F  85 F6             STA HOLDER
0154  5591  4C 75 56          JMP KLOK
0155  5594  AD 1D 50    RED2  LDA ADCL
0156  5597  8D 12 50          STA CORL2
0157  559A  AD 1E 50          LDA ADCH
0158  559D  8D 13 50          STA CORH2
0159  55A0  A9 00             LDA #$00
0160  55A2  8D 00 AC          STA PBD
0161  55A5  A9 AC             LDA #<LMP3
0162  55A7  85 F6             STA HOLDER
0163  55A9  4C 8D 56          JMP TIMOFF
0164  55AC  CE 20 50    LMP3  DEC LOMP
0165  55AF  D0 03             BNE THREE
0166  55B1  4C 34 55          JMP LMP1

......PAGE 0004

LINE # LOC     CODE       LINE

0167  55B4  AD 0B 50    THREE LDA CURL3
0168  55B7  8D 1B 50          STA DACL
0169  55BA  AD 0A 50          LDA CURH3
0170  55BD  8D 1C 50          STA DACH
0171  55C0  20 5D 56          JSR DAK
0172  55C3  A9 04             LDA #$04        ;TURN LAMP #3 ON.
0173  55C5  8D 00 AC          STA PBD
0174  55C8  A9 CF             LDA #<RED3
0175  55CA  85 F6             STA HOLDER
0176  55CC  4C 75 56          JMP KLOK
0177  55CF  AD 1D 50    RED3  LDA ADCL
0178  55D2  8D 14 50          STA CORL3
0179  55D5  AD 1E 50          LDA ADCH
0180  55D8  8D 15 50          STA CORH3
0181  55DB  A9 00             LDA #$00
```

```
0182  55DD  8D 00 AC          STA PBD
0183  55E0  A9 E7             LDA #<LMP4
0184  55E2  85 F6             STA HOLDER
0185  55E4  4C 8D 56          JMP TIMOFF
0186  55E7  CE 20 50    LMP4  DEC LOMP
0187  55EA  D0 03             BNE FOUR
0188  55EC  4C 34 55          JMP LMP1
0189  55EF  AD 0D 50    FOUR  LDA CURL4
0190  55F2  8D 1B 50          STA DACL
0191  55F5  AD 0C 50          LDA CURH4
0192  55F8  8D 1C 50          STA DACH
0193  55FB  20 5D 56          JSR DAK
0194  55FE  A9 08             LDA #$08        ;TURN LAMP #4 ON.
0195  5600  8D 00 AC          STA PBD
0196  5603  A9 0E             LDA #<RED4
0197  5605  85 F6             STA HOLDER
0198  5607  A9 56             LDA #>RED4
0199  5609  85 F7             STA HOLDER+1
0200  560B  4C 75 56          JMP KLOK
0201  560E  AD 1D 50    RED4  LDA ADCL
0202  5611  8D 16 50          STA CORL4
0203  5614  AD 1E 50          LDA ADCH
0204  5617  8D 17 50          STA CORH4
0205  561A  A9 00             LDA #$00
0206  561C  8D 00 AC          STA PBD
0207  561F  A9 34             LDA #<LMP1
0208  5621  85 F6             STA HOLDER
0209  5623  A9 55             LDA #>LMP1
0210  5625  85 F7             STA HOLDER+1
0211  5627  4C 8D 56          JMP TIMOFF
0212  562A  A9 00       PULS  LDA #$00        ;TURN THE LAMP OFF.
0213  562C  8D 00 AC          STA PBD
0214  562F  20 4D 83          JSR CRLF
0215  5632  A9 F0             LDA #$F0        ;LAMP PULSING I/O PORT.
0216  5634  8D 02 AC          STA PBDD
0217  5637  A9 C0             LDA #$C0        ;SET REGISTER FOR TIMER-1.
0218  5639  8D 0B AC          STA ACR
0219  563C  AD 22 50          LDA CLOCK       ;LOAD TIMER-1 LOW LATCH.
0220  563F  8D 04 AC          STA T1LL
0221  5642  AD 23 50          LDA CLOCK+1      ;LOAD TIMER-1 HIGH COUNTER.

.....PAGE 0005


LINE # LOC     CODE       LINE

0222  5645  8D 05 AC          STA T1CH
0223  5648  AD 0E 50          LDA AVCRH       ;LOAD AVE. CURRENT.
0224  564B  8D 1C 50          STA DACH
0225  564E  AD 0F 50          LDA AVCRL
0226  5651  8D 1B 50          STA DACL
0227  5654  20 5D 56          JSR DAK
0228  5657  A9 00             LDA #$00        ;START PULSING.
```

```
0229  5659  8D 00 A0          STA PBD
0230  565C  60                RTS
0231  565D  AD 1B 50    DAK   LDA DACL        ;LOAD LOW 8 BITS
0232  5660  49 FF             EOR #$FF        ;TWO'S COMPLEMENT
0233  5662  8D 01 A0          STA RAD
0234  5665  AD 1C 50          LDA DACH        ;LOAD HIGH 4 BITS
0235  5668  49 FF             EOR #$FF
0236  566A  0A                ASL A           ;SHIFT LEFT FOR STROBE BIT
0237  566B  8D 00 A0          STA RBD
0238  566E  EE 00 A0          INC RBD         ;STROBE DAC
0239  5671  CE 00 A0          DEC RBD
0240  5674  60                RTS
0241  5675  AD 00 50    KLOK  LDA ON          ;SET THE CLOCK.
0242  5678  8D 17 A4          STA SR
0243  567B  A9 80       WEET  LDA #$80
0244  567D  2C 02 A4          BIT ORB         ;TEST IF (CR) IS PUSHED.
0245  5680  D0 08             BNE CUT1
0246  5682  2C 17 A4          BIT SR          ;TEST IF IT IS DONE.
0247  5685  10 F4             BPL WEET
0248  5687  4C AE 56          JMP ADK
0249  568A  4C 2A 56    CUT1  JMP PULS
0250  568D  AE 03 50    TIMOFF LDX TLOOP
0251  5690  F0 16       LOOK  BEQ BACK
0252  5692  AD 02 50          LDA DARK
0253  5695  8D 17 A4          STA SR
0254  5698  A9 80       VEET  LDA #$80
0255  569A  2C 02 A4          BIT ORB
0256  569D  D0 0C             BNE CUT2
0257  569F  2C 17 A4          BIT SR
0258  56A2  10 F4             BPL VEET
0259  56A4  CA                DEX
0260  56A5  4C 90 56          JMP LOOK
0261  56A8  6C F6 00    BACK  JMP (HOLDER)
0262  56AB  4C 2A 56    CUT2  JMP PULS
0263  56AE  A9 C5       ADK   LDA #$C5        ;USE INPUT #1 OF A/D.
0264  56B0  8D 00 A8          STA DRB
0265  56B3  CE 00 A8          DEC DRB         ;START CONVERSION
0266  56B6  EE 00 A8          INC DRB
0267  56B9  A9 40             LDA #$40
0268  56BB  2C 00 A8    TEST  BIT DRB         ;TEST FOR END OF CONV.
0269  56BE  D0 FB             BNE TEST
0270  56C0  AD 01 A8          LDA DRA         ;READ 8 HIGH BITS
0271  56C3  8D 1E 50          STA ADCH
0272  56C6  A9 C7             LDA #$C7        ;TRANSFER 4 LOW BITS
0273  56C8  8D 00 A8          STA DRB
0274  56CB  AD 01 A8          LDA DRA         ;READ 4 LOW BITS
0275  56CE  8D 1D 50          STA ADCL
0276  56D1  A2 04             LDX #$04        ;REARRANGE DATA

.....PAGE 0006

LINE # LOC     CODE       LINE
```

```
0277  56D3  18          GO      CLC
0278  56D4  4E 1E 50            LSR ADCH
0279  56D7  6E 1D 50            ROR ADCL
0280  56DA  CA                  DEX
0281  56DB  D0 F6               BNE GO
0282  56DD  6C F6 00            JMP (HOLDER)
0283  56E0                ;
0284  56E0                ;***** THIS PORTION COLLECT & STORE DATA *****
0285  56E0                ;
0286  56E0  A0 00               LDY #$00          ;SET Y AS COUNTER.
0287  56E2  A9 00          CLEAR LDA #$00          ;CLEAR ALL DATA STORAGES.
0288  56E4  99 46 50            STA ARY11,Y
0289  56E7  99 0E 51            STA ARY1B,Y
0290  56EA  99 D6 51            STA ARY23,Y
0291  56ED  99 9E 52            STA ARY31,Y
0292  56F0  99 66 53            STA ARY3B,Y
0293  56F3  99 2E 54            STA ARY43,Y
0294  56F6  C8                  INY
0295  56F7  C0 C8               CPY #200
0296  56F9  D0 E7               BNE CLEAR
0297  56FB  A0 00               LDY #$00          ;SET Y AS POINT COUNTER.
0298  56FD  A9 0F          DATA  LDA #$0F          ;SET PBD AS OUTPUT.
0299  56FF  8D 02 AC            STA PBDD          ;FOR LAMP PULSING.
0300  5702  AD 18 50     LUP    LDA LAP           ;SAVE # OF LAPS/POINT.
0301  5705  8D 1F 50            STA LOP
0302  5708  AD 01 50     LUMP   LDA LAMP          ;SAVE # OF LAMPS AT LOMP.
0303  570B  8D 20 50            STA LOMP          ;LAMP COUNTER.
0304  570E  AD 1A 50     SOR1   LDA READ          ;SAVE # OF READING/PULSE.
0305  5711  8D 21 50            STA REED          ;READ COUNTER.
0306  5714  AD 07 50            LDA CURL1
0307  5717  8D 1B 50            STA DACL
0308  571A  AD 06 50            LDA CURH1
0309  571D  8D 1C 50            STA DACH
0310  5720  20 5D 56            JSR DAK
0311  5723  A9 00               LDA #$00
0312  5725  8D 00 AC            STA PBD
0313  5728  20 46 59            JSR TIMOF
0314  572B  20 16 59     AGAN1  JSR ATDC
0315  572E  18                  CLC
0316  572F  AD 1D 50            LDA ADCL
0317  5732  79 DC 50            ADC ARY1A,Y
0318  5735  99 DC 50            STA ARY1A,Y
0319  5738  AD 1E 50            LDA ADCH
0320  573B  79 0E 51            ADC ARY1B,Y
0321  573E  99 0E 51            STA ARY1B,Y
0322  5741  A9 00               LDA #$00
0323  5743  79 40 51            ADC ARY1C,Y
0324  5746  99 40 51            STA ARY1C,Y
0325  5749  CE 21 50            DEC REED
0326  574C  F0 03               BEQ ADD1
0327  574E  4C 2B 57            JMP AGAN1
0328  5751  AD 1A 50     ADD1   LDA READ
0329  5754  8D 21 50            STA REED
```

```
0330  5757  A9 01           LDA #$01
0331  5759  8D 00 AC        STA PBD

.....PAGE 0007


LINE # LOC     CODE       LINE

0332  575C  20 5A 59        JSR DELAY       ;WAIT FOR TIME CONSTANT.
0333  575F  20 16 59  AGIN1  JSR ATDC
0334  5762  18              CLC             ;CLEAR CARRY.
0335  5763  AD 1D 50        LDA ADCL        ;LOAD LOW 8 BITS.
0336  5766  79 46 50        ADC ARY11,Y     ;ADD TO FIRST ARY.
0337  5769  99 46 50        STA ARY11,Y     ;SAVE IT IN FIRST ARY.
0338  576C  AD 1E 50        LDA ADCH        ;LOAD HIGH 8 BITS.
0339  576F  79 78 50        ADC ARY12,Y     ;ADD TO SECOND ARY.
0340  5772  99 78 50        STA ARY12,Y     ;SAVE IT IN SECOND ARY.
0341  5775  A9 00           LDA #$00
0342  5777  79 AA 50        ADC ARY13,Y     ;USE THIRD ARY FOR OVERFLOW.
0343  577A  99 AA 50        STA ARY13,Y
0344  577D  CE 21 50        DEC REED
0345  5780  F0 03           BEQ NXT1        ;ALL DONE GO TO NEXT POSITION.
0346  5782  4C 5F 57        JMP AGIN1       ;NOT DONE, DO THE NEXT.
0347  5785  CE 20 50  NXT1  DEC LOMP        ;CHECK # OF LAMPS.
0348  5788  D0 03           BNE SOB2         ;NOT LAST ONE, GO TO NEXT.
0349  578A  4C 02 59        JMP CUT
0350  578D  AD 1A 50  SOB2  LDA READ
0351  5790  8D 21 50        STA REED
0352  5793  AD 09 50        LDA CURL2
0353  5796  8D 1B 50        STA DACL
0354  5799  AD 08 50        LDA CURH2
0355  579C  8D 1C 50        STA DACH
0356  579F  20 5D 56        JSR DAK
0357  57A2  A9 00           LDA #$00
0358  57A4  8D 00 AC        STA PBD
0359  57A7  20 46 59        JSR TIMOF
0360  57AA  20 16 59  AGAN2 JSR ATDC
0361  57AD  18              CLC
0362  57AE  AD 1D 50        LDA ADCL
0363  57B1  79 08 52        ADC ARY2A,Y
0364  57B4  99 08 52        STA ARY2A,Y
0365  57B7  AD 1E 50        LDA ADCH
0366  57BA  79 3A 52        ADC ARY2B,Y
0367  57BD  99 3A 52        STA ARY2B,Y
0368  57C0  A9 00           LDA #$00
0369  57C2  79 6C 52        ADC ARY2C,Y
0370  57C5  99 6C 52        STA ARY2C,Y
0371  57C8  CE 21 50        DEC REED
0372  57CB  F0 03           BEQ ADD2
0373  57CD  4C AA 57        JMP AGAN2
0374  57D0  AD 1A 50  ADD2  LDA READ
0375  57D3  8D 21 50        STA REED
```

```
0376  57D6  A9 02           LDA #$02        ;LAMP #2 ON
0377  57D8  8D 00 AC        STA PBD
0378  57DB  20 5A 59        JSR DELAY
0379  57DE  20 16 59  AGIN2 JSR ATDC
0380  57E1  18              CLC
0381  57E2  AD 1D 50        LDA ADCL
0382  57E5  79 72 51        ADC ARY21,Y
0383  57E8  99 72 51        STA ARY21,Y
0384  57EB  AD 1E 50        LDA ADCH
0385  57EE  79 A4 51        ADC ARY22,Y
0386  57F1  99 A4 51        STA ARY22,Y
```

.....PAGE 0008

```
LINE # LOC     CODE       LINE

0387  57F4  A9 00           LDA #$00
0388  57F6  79 D6 51        ADC ARY23,Y
0389  57F9  99 D6 51        STA ARY23,Y
0390  57FC  CE 21 50        DEC REED
0391  57FF  F0 03           BEQ NXT2
0392  5801  4C DE 57        JMP AGIN2
0393  5804  CE 20 50  NXT2  DEC LOMP
0394  5807  D0 03           BNE SOB3
0395  5809  4C 02 59        JMP CUT
0396  580C  AD 1A 50  SOB3  LDA READ
0397  580F  8D 21 50        STA REED
0398  5812  AD 0B 50        LDA CURL3
0399  5815  8D 1B 50        STA DACL
0400  5818  AD 0A 50        LDA CURH3
0401  581B  8D 1C 50        STA DACH
0402  581E  20 5D 56        JSR DAK
0403  5821  A9 00           LDA #$00
0404  5823  8D 00 AC        STA PBD
0405  5826  20 46 59        JSR TIMOF
0406  5829  20 16 59  AGAN3 JSR ATDC
0407  582C  18              CLC
0408  582D  AD 1D 50        LDA ADCL
0409  5830  79 34 53        ADC ARY3A,Y
0410  5833  99 34 53        STA ARY3A,Y
0411  5836  AD 1E 50        LDA ADCH
0412  5839  79 66 53        ADC ARY3B,Y
0413  583C  99 66 53        STA ARY3B,Y
0414  583F  A9 00           LDA #$00
0415  5841  79 98 53        ADC ARY3C,Y
0416  5844  99 98 53        STA ARY3C,Y
0417  5847  CE 21 50        DEC REED
0418  584A  F0 03           BEQ ADD3
0419  584C  4C 29 58        JMP AGAN3
0420  584F  AD 1A 50  ADD3  LDA READ
0421  5852  8D 21 50        STA REED
0422  5855  A9 04           LDA #$04        ;LAMP #3 ON.
```

```
0423  5857  8D 00 AC          STA PBD
0424  585A  20 5A 59          JSR DELAY
0425  585D  20 16 59    AGIN3 JSR ATDC
0426  5860  18                CLC
0427  5861  AD 1D 50          LDA ADCL
0428  5864  79 9E 52          ADC ARY31,Y
0429  5867  99 9E 52          STA ARY31,Y
0430  586A  AD 1E 50          LDA ADCH
0431  586D  79 D0 52          ADC ARY32,Y
0432  5870  99 D0 52          STA ARY32,Y
0433  5873  A9 00             LDA #$00
0434  5875  79 02 53          ADC ARY33,Y
0435  5878  99 02 53          STA ARY33,Y
0436  587B  CE 21 50          DEC REED
0437  587E  F0 03             BEQ NXT3
0438  5880  4C 5D 58          JMP AGIN3
0439  5883  CE 20 50    NXT3  DEC LOMP
0440  5886  D0 03             BNE SOR4
0441  5888  4C 02 59          JMP CUT
```

.....PAGE 0009

```
LINE # LOC     CODE       LINE

0442  588B  AD 1A 50    SOR4  LDA READ
0443  588E  8D 21 50          STA REED
0444  5891  AD 0D 50          LDA CURL4
0445  5894  8D 1B 50          STA DACL
0446  5897  AD 0C 50          LDA CURH4
0447  589A  8D 1C 50          STA DACH
0448  589D  20 5D 56          JSR DAK
0449  58A0  A9 00             LDA #$00
0450  58A2  8D 00 AC          STA PBD
0451  58A5  20 46 59          JSR TIMOF
0452  58A8  20 16 59    AGAN4 JSR ATDC
0453  58AB  18                CLC
0454  58AC  AD 1D 50          LDA ADCL
0455  58AF  79 60 54          ADC ARY4A,Y
0456  58B2  99 60 54          STA ARY4A,Y
0457  58B5  AD 1E 50          LDA ADCH
0458  58B8  79 92 54          ADC ARY4B,Y
0459  58BB  99 92 54          STA ARY4B,Y
0460  58BE  A9 00             LDA #$00
0461  58C0  79 C4 54          ADC ARY4C,Y
0462  58C3  99 C4 54          STA ARY4C,Y
0463  58C6  CE 21 50          DEC REED
0464  58C9  F0 03             BEQ ADD4
0465  58CB  4C A8 58          JMP AGAN4
0466  58CE  AD 1A 50    ADD4  LDA READ
0467  58D1  8D 21 50          STA REED
0468  58D4  A9 08             LDA #$08          ;LAMP #4 ON
0469  58D6  8D 00 AC          STA PBD
```

```
0470  58D9  20 5A 59          JSR DELAY
0471  58DC  20 16 59    AGIN4 JSR ATDC
0472  58DF  18                CLC
0473  58E0  AD 1D 50          LDA ADCL
0474  58E3  79 CA 53          ADC ARY41,Y
0475  58E6  99 CA 53          STA ARY41,Y
0476  58E9  AD 1E 50          LDA ADCH
0477  58EC  79 FC 53          ADC ARY42,Y
0478  58EF  99 FC 53          STA ARY42,Y
0479  58F2  A9 00             LDA #$00
0480  58F4  79 2E 54          ADC ARY43,Y
0481  58F7  99 2E 54          STA ARY43,Y
0482  58FA  CE 21 50          DEC REED
0483  58FD  F0 03             BEQ CUT
0484  58FF  4C DC 58          JMP AGIN4
0485  5902  CE 1F 50    CUT   DEC LOP          ;ALL LAPS DONE?
0486  5905  F0 03             BEQ GETOT        ;YES, GO FOR NEXT POINT.
0487  5907  4C 08 57          JMP LUMP         ;NO, START AGAIN.
0488  590A  C8          GETOT INY
0489  590B  CC 19 50          CPY POINT        ;ALL THE POINTS COLLECTED!
0490  590E  F0 03             BEQ OUT          ;YES, GO OUT.
0491  5910  4C 02 57          JMP LUP          ;NO, DO THE NEXT.
0492  5913  4C 2A 56    OUT   JMP PULS
0493  5916  A9 E5       ATDC  LDA #$E5           ;USE INPUT #5 OF A/D.
0494  5918  8D 00 A8          STA DRB
0495  591B  CE 00 A8          DEC DRB
0496  591E  EE 00 A8          INC DRB

.....PAGE 0010


LINE # LOC     CODE       LINE

0497  5921  A9 40             LDA #$40
0498  5923  2C 00 A8    CHEK  BIT DRB
0499  5926  D0 FB             BNE CHEK
0500  5928  AD 01 A8          LDA DRA
0501  592B  8D 1E 50          STA ADCH
0502  592E  A9 E7             LDA #$E7
0503  5930  8D 00 A8          STA DRB
0504  5933  AD 01 A8          LDA DRA
0505  5936  8D 1D 50          STA ADCL
0506  5939  A2 04             LDX #$04
0507  593B  18          NXTGO CLC
0508  593C  4E 1E 50          LSR ADCH
0509  593F  6E 1D 50          ROR ADCL
0510  5942  CA                DEX
0511  5943  D0 F6             BNE NXTGO
0512  5945  60                RTS
0513  5946  AE 04 50    TIMOF LDX TIMLOP       ;# OF TIME LOOP (1 OR 5).
0514  5949  F0 0F       DOIT  BEQ DELAY
0515  594B  AD 05 50          LDA OFF
0516  594E  8D 17 A4          STA SR
```

```
0517  5951  2C 17 A4    VAIT   BIT SR
0518  5954  10 FB              BPL VAIT
0519  5956  CA                 DEX
0520  5957  4C 49 59           JMP DOIT
0521  595A  AD 24 50    DELAY  LDA TM
0522  595D  8D 25 50           STA MT
0523  5960  A9 32        DLAY   LDA #50        ;DELAY TIME FOR TIME CONSTANT.
0524  5962  8D 14 A4           STA PW
0525  5965  2C 17 A4    WAIT   BIT SR
0526  5968  10 FB              BPL WAIT
0527  596A  CE 25 50           DEC MT
0528  596D  D0 F1              BNE DLAY
0529  596F  60                 RTS
0530  5970                     .END
```

SYMBOL TABLE

SYMBOL	VALUE						
ACR	AC0B	ADCH	501E	ADCL	501D	ADD1	5751
ADD2	57D0	ADD3	584F	ADD4	58CE	ADK	56AE
AGAN1	572B	AGAN2	57AA	AGAN3	5829	AGAN4	58A8
AGIN1	575F	AGIN2	57DE	AGIN3	5B5D	AGIN4	5BDC
ARY11	5046	ARY12	5078	ARY13	50AA	ARY1A	50DC
ARY1B	510E	ARY1C	5140	ARY21	5172	ARY22	51A4
ARY23	51D6	ARY2A	5208	ARY2B	523A	ARY2C	526C
ARY31	529E	ARY32	52D0	ARY33	5302	ARY3A	5334
ARY3B	5366	ARY3C	5398	ARY41	53CA	ARY42	53FC
ARY43	542E	ARY4A	5460	ARY4B	5492	ARY4C	54C4
ATDC	5916	AVCRH	500E	AVCRL	500F	BACK	5648
CHEK	5923	CLEAR	56E2	CLOCK	5022	CORH1	5011
CORH2	5013	CORH3	5015	CORH4	5017	CORL1	5010
CORL2	5012	CORL3	5014	CORL4	5016	CRLF	B34D
CURH1	5006	CURH2	5008	CURH3	500A	CURH4	500C
CURL1	5007	CURL2	5009	CURL3	500B	CURL4	500D
CUT	5902	CUT1	568A	CUT2	56AB	DACH	501C
DACL	501B	DAK	565D	DARK	5002	DATA	56FD
DDRA	A803	DDRB	A802	DELAY	595A	DLAY	5960
DOIT	5949	DRA	A801	DRB	A800	FOUR	55EF
GETDT	590A	GO	56D3	HOLDER	00F6	KLOK	5675
LAMP	5001	LAP	5018	LMP1	5534	LMP2	5571
LMP3	55AC	LMP4	55E7	LOMP	5020	LOOK	5690
LOP	501F	LUMP	5708	LUP	5702	MT	5025
NXT1	5785	NXT2	5804	NXT3	5883	NXTGO	593B
OFF	5005	ON	5000	ORB	A402	OUT	5913
PAD	AC01	PADD	AC03	PBD	AC00	PBDD	AC02
POINT	5019	PULS	562A	PW	A414	RAD	A001
RADD	A003	RBD	A000	RBDD	A002	READ	501A
RED1	5559	RED2	5594	RED3	55CF	RED4	560E
REED	5021	SOB1	570E	SOB2	578D	SOB3	580C
SOB4	588B	SR	A417	T1CH	AC05	T1LL	AC04
TEST	56BB	THREE	55B4	TIMLOP	5004	TIMOF	5946
TIMOFF	568D	TLOOP	5003	TM	5024	TWO	5579
VAIT	5951	VEET	5698	WAIT	5965	WEET	567B